TRPM2- und TRPM8-vermittelte Radioresistenz in malignen Tumoren

Dissertation

der Mathematisch-Naturwissenschaftlichen Fakultät
der Eberhard Karls Universität Tübingen
zur Erlangung des Grades eines
Doktors der Naturwissenschaften
(Dr. rer. nat.)

vorgelegt von
Dominik Klumpp
aus Gernsbach

Tübingen
2016

Gedruckt mit Genehmigung der Mathematisch-Naturwissenschaftlichen Fakultät der Eberhard Karls Universität Tübingen.

Tag der mündlichen Qualifikation: 08.06.2016
Dekan: Prof. Dr. Wolfgang Rosenstiel
1. Berichterstatter: Prof. Dr. Stephan Huber
2. Berichterstatter: Prof. Dr. Peter Ruth

Inhaltsverzeichnis

Abkürzungsverzeichnis

$\Delta\Psi_m$	Potential der inneren Mitochondrienmembran
$[Ca^{2+}]_i$	freie intrazelluläre Ca^{2+}-Konzentration
ACA	N-(p-amylcinnamoyl)anthranilic, TRPM2-Inhibitor
ADP	Adenosindiphosphat
ADPR	Adenosindiphosphat-Ribose
ATP	Adenosintriphosphat
Bcl-2	„B-cell lymphoma 2“, anti-apoptotisches Protein
BK	“Big conductance potassium channel“
Ca^{2+}	Calciumion
CaMKII	“Ca^{2+}/Calmodulin-dependent protein kinase II“
cdc2	“Cell division cycle protein 2 homolog“
cdc25b	„Cell division cycle 25b“
CXCR4	CXC-Motiv-Chemokinrezeptor 4
DNA	„Desoxyribonucleic acid“
EdU	5-Ethynyl-2’-Deoxyuridine
ER	Endoplasmatisches Retikulum
fluo-3	Fluoreszensfarbstoff für Ca^{2+}
Fura-2	ratiometrischer Fluoreszenzfarbstoff für freies Ca^{2+}
Gy	Gray, pro Masse absorbierte Energie
h	Stunde
H_2O_2	Wasserstoffperoxid
IDH1	Isocitratdehydrogenase
IK	“Intermediate conductance potassium channel“
IP_3	Inositol-3-Phosphat
IP_3R	Inositol-3-Phosphat-Rezeptor
IR	“Ionizing radiation“
K^+	Kaliumion
$K_v3.4$	“Potassium voltage-gated channel, Shaw-related subfamily, member 4”
Mg^{2+}	Magnesiumion
MitoSOX	Superoxid-sensitiver Farbstoff
mM	Millimolar
MPF	“mitosis promoting factor“

mRNA	Messenger RNA
MSI1	“Musashi“, mRNA-Bindeprotein
Na^+	Natriumion
NCX	Na^+/Ca^{2+}-Austauscher
$NMDG^+$	N-Methyl-D-glucamin, nicht membrangängiger Na^+-Ersatzstoff
p53	humanes Tumorsuppressorprotein
PARP	Poly-ADP-Ribose-Polymerase
pH	*potentia hydrogenii*, Maßzahl für die Wasserstoffionenkonzentration
PI3K	Phosphoinositid-Kinase 3
PIP_2	Phosphatidylinositoldiphosphat
PLA_2	Phospholipase A_2
PMCA	“Plasma membrane calcium ATPase”
ROC	“Rezeptor-operated channels”
ROS	„reactive oxygen species“
RT-PCR	Reverse Transkriptase-Polymerase-Kettenreaktion
RYR	Ryanodin-Rezeptor
SERCA	“Sarcoplasmic/endoplasmic reticulum calcium ATPase”
SH2	“Src-homology 2“
siRNA	“small interfering RNA”
SMOC	“Second messenger-operated channels”
SOC	“Store-operated channels”
SPCA	“Secretory pathway calcium ATPase”
TMRE	Tetramethylrhodamin Etylester
TRP	“Transient receptor potential”
TRPA	ANTKTM1-Unterfamilie der TRP-Kanäle
TRPC	klassische Unterfamilie der TRP-Kanäle
TRPM	Melastatain-Unterfamilie der TRP-Kanäle
TRPML	Mucolipin-Unterfamilie der TRP-Kanäle
TRPP	Polycystin-Unterfamilie der TRP-Kanäle
TRPV	Vanilloid-Rezeptor-Unterfamilie der TRP-Kanäle
VOC	“Voltage-operated channels“

Zusammenfassung

Die Strahlentherapie stellt eine der wichtigsten Säulen dar, auf die sich die moderne Behandlung von Krebserkrankungen stützt. Die Resistenz der Tumorzellen gegenüber dieser Behandlung stellt hierbei trotz immer fortschrittlicherer Behandlungsstrategien ein großes Problem dar. Insbesondere die durch Bestrahlung veränderte Regulation des zellulären Ca^{2+}-Signalosoms scheint hier von großer Bedeutung zu sein. Ca^{2+}-Signale werden unter anderem von in der Plasmamembran lokalisierten Kationenkanälen generiert. Dabei konnte bereits mehrfach gezeigt werden, dass Kationenkanäle der Melastatin-Familie (TRPM) insbesondere die Resistenz und Malignizität von Tumoren beeinflussen, weshalb sie immer weiter in den Fokus der Krebsforschung rücken. Welche Rolle zwei ausgewählten Mitgliedern der TRPM-Familie bei der Radioresistenz maligner Tumore zukommt und wie sich diese Erkenntnis auf eine Strahlentherapie auswirken könnte, wurde in dieser Arbeit näher analysiert.

Im ersten Teil dieser Arbeit wurde die Interaktion von TRPM2 mit dem anti-apoptotischen Protein Bcl-2 in T-Zell Leukämiezellen untersucht. Insbesondere Bcl-2 ist nachweislich an der Therapieresistenz verschiedener Tumorentitäten beteiligt. Um dieses Zusammenspiel näher zu charakterisieren, wurden Jurkat Zellen mit ionisierender Strahlung behandelt und anschließend der Zellzyklus sowie das TRPM2-vermittelte Ca^{2+}-Signaling analysiert. Hierbei konnte gezeigt werden, dass Bestrahlung vor allem in Bcl-2 überexprimierenden Zellen einen Ca^{2+}-Einstrom induzierte, der nach pharmakologischer Inhibition von TRPM2 stark vermindert war. In Kontrollzellen führte dieser erhöhte Ca^{2+}-Einstrom zur Produktion von reaktiven Sauerstoffspezies. Bcl-2 überexprimierende Jurkat Zellen waren jedoch in der Lage, im Gegensatz zu Kontrollzellen, diese letale Ca^{2+}-Dosis zu tolerieren. Weiter führte der TRPM2-vermittelte Einstrom zu einem G_2/M-Arrest, der durch Inhibition der TRPM2-Kanäle verhindert wurde, was zu einer erhöhten Apoptoserate führte.

Im zweiten Teil dieser Arbeit wurde die Strahlenresistenz von Glioblastomen untersucht. Im Gegensatz zu benignem Hirngewebe ist der Kälterezeptor TRPM8 im Glioblastom stark überexprimiert. Der retrospektive Vergleich von mRNA-Daten zeigte, dass eine erhöhte Expression von TRPM8 im low-grade Gliom mit einer geringeren Lebenserwartung korreliert. In nachfolgenden *in vitro* Experimenten konnte diese Erkenntnis bestätigt werden: Eine siRNA-vermittelte Inhibition von

TRPM8 führte zu einem geringeren klonogenen Überleben. Die Kombination von Bestrahlung und Inhibition zeigte weiter sowohl eine erhöhte Caspasen-Aktivität als auch eine gestörte Proliferation.

Zusammenfassend legen diese Ergebnisse nahe, dass die beiden Kanäle TRPM2 und TRPM8 in den untersuchten Tumorentitäten eine wichtige Rolle in der Radioresistenz spielen. Weiter zeigen die Untersuchungen, dass diese beiden Kationenkanäle als mögliche Targets, einzeln oder in Kombination, zukünftiger Behandlungen in Frage kommen und somit neue Strategien in der Krebstherapie eröffnet werden.

Summary

Radiotherapy plays a major role in modern cancer treatment. Despite steadily improving therapy strategies the resistance of cancer cells against ionizing radiation often results in therapy failure. In particular, the altered regulation of the cellular Ca^{2+} signalosome seems to be of great importance. Amongst others, Ca^{2+} signals are generated by cation channels localized in the plasma membrane. In this context special TRP cation channels are getting more and more into the focus of oncologists. It has been shown that TRP channels from the melastatin family play an important role especially in the resistance and the malignancy of tumors. This work focuses on two members of the melastatin family and their role in radioresistance of malignant tumors.

The first part of this work analyzes the interaction between TRPM2 and the anti-apoptotic protein Bcl-2 in T-cell leukemia. Notably, Bcl-2 has been shown to be involved in the therapy resistance of different tumors. To characterize this interaction in more detail, Jurkat cells were treated with ionizing radiation. Thereafter, the cell cycle as well as TRPM2-mediated Ca^{2+} signals were analyzed. Especially in Bcl-2 overexpressing cells, irradiation induced a Ca^{2+} influx which was decreased after pharmacological inhibition of TRPM2. In control cells, this increased Ca^{2+} influx resulted in production of reactive oxygen species (ROS). In contrast, Bcl-2 overexpressing Jurkat cells were able to tolerate this increased channel activity without risking a hazardous ROS production and Ca^{2+} overload. Further, this TRPM2-mediated Ca^{2+} influx led to a G_2/M arrest which was overriden by inhibition of TRPM2 resulting in apoptotic cell death.

The second part of this work addressed the radioresistance of glioblastoma cells. Contrary to benign brain tissue the cold receptor TRPM8 of the melastatin family is highly expressed in glioma. The retrospective analysis of mRNA data revealed that an increased expression of TRPM8 in low grade glioma correlates with poor prognosis. In subsequent *in vitro* experiments these findings could be confirmed. TRPM8 knock-down led to a decreased clonogenic survival in human glioblastoma cell lines. Moreover, the combination of irradiation and TRPM8 inhibition resulted in both, a higher caspase activity and an impaired cell cycle regulation of glioblastoma cells.

Together, these results suggest an important role of TRPM2 and TRPM8 in the radioresistance of leukemia and glioblastoma cells. Therefore, TRPM8 and TRPM2 might represent promising targets of future anti-cancer therapy.

EBERHARD KARLS
UNIVERSITÄT
TÜBINGEN

Mathematisch-Naturwissenschaftliche Fakultät

Erklärung nach § 5 Abs. 2 Nr. 7 der Promotionsordnung der Math.-Nat. Fakultät
-Anteil an gemeinschaftlichen Veröffentlichungen-

Name: **Dominik Klumpp**

Liste der Publikationen

1. **Stegen, B., L. Klumpp, M. Misovic, L. Edalat, M. Eckert, D. Klumpp, P. Ruth, SM. Huber (2016)** K^+ channels signaling in irradiated tumor cells (submitted)

2. **Klumpp, D., SC. Frank, L. Klumpp, M. Eckert, L. Edalat, M. Bastmeyer, P. Ruth, SM. Huber (2016b).** "TRPM8-mediated Ca^{2+}-signaling confers radioresistance and promotes migration of glioblastoma cells." Radiotherapy and Oncology (submitted)

3. **Klumpp, D., M. Misovic, K. Szteyn, E. Shumilina, J. Rudner and S. M. Huber (2016a)**. "Targeting Trpm2 Channels Impairs Radiation-Induced Cell Cycle Arrest and Fosters Cell Death of T Cell Leukemia Cells in a Bcl-2-Dependent Manner." Oxidative Medicine and Cellular Longevity (in press).

4. **Braun, N., D. Klumpp, J. Hennenlotter, J. Bedke, C. Duranton, M. Bleif, SM. Huber (2015).** "UCP-3 uncoupling protein confers hypoxia resistance to renal epithelial cells and is upregulated in renal cell carcinoma." Sci. Rep. 5: 13450.

5. **Huber, SM., L. Butz, B. Stegen, L. Klumpp, D. Klumpp, F. Eckert (2014).** “Role of ion channels in ionizing radiation-induced cell death.” Biochim Biophys Acta. 1848: 2657-64

6. **Huber, S. M., L. Butz, B. Stegen, D. Klumpp, N. Braun, P. Ruth and F. Eckert (2013)**. "Ionizing Radiation, Ion Transports, and Radioresistance of Cancer Cells." Front Physiol 4: 212.

7. **Palme, D., M. Misovic, E. Schmid, D. Klumpp, H. R. Salih, J. Rudner and S. M. Huber (2013)**. "Kv3.4 Potassium Channel-Mediated Electrosignaling Controls Cell Cycle and Survival of Irradiated Leukemia Cells." Pflugers Arch 465(8): 1209-1221.

Nr.	Accepted for publication yes/no	Number of all authors	Position of the candidate in list of authors	Scientific ideas of candidate (%)	Data generation by candidate (%)	Analysis and interpretation by candidate (%)	Paper writing by candidate (%)
1.	No	8	6	10			10
2.	No	8	1	80	70	80	60
3.	Yes	6	1	60	50	60	50
4.	Yes	7	2	10	30	30	10
5.	Yes	6	5	10			10
6.	Yes	7	4	10			10
7.	Yes	7	4	10	20	20	10

I certify that the above statement is correct.

_____

Date, Signature of the candidate

I/We certify that the above statement is correct.

_____

Date, Signature of the doctoral committee or at least of one of the supervisors

EBERHARD KARLS
UNIVERSITÄT
TÜBINGEN

Mathematisch-Naturwissenschaftliche Fakultät

Erklärung zum Eigenanteil der Dissertation

Die Arbeit wurde am Universitätsklinikum Tübingen, Abteilung Experimentelle Radioonkologie unter Betreuung von Prof. Dr. Stephan Huber und Prof. Dr. Peter Ruth durchgeführt. Sämtliche Versuche wurden nach Einarbeitung durch Prof. Dr. Stephan Huber, Heidrun Faltin und Ilka Müller von mir eigenständig, teils mit Unterstützung durch Heidrun Faltin und Ilka Müller durchgeführt. Die statistische Auswertung erfolgte eigenständig, nach Anleitung durch Prof. Dr. Stephan Huber.

Ich versichere, das Manuskript selbständig unter Mithilfe von Prof. Dr. Stephan Huber verfasst und keine weiteren als die von mir angegebenen Quellen verwendet zu haben.

Tübingen, den

[Dominik Klumpp]

Einleitung

Ionenkanäle in der Krebstherapie

Vieles deutet darauf hin, dass der Transport von Ionen über biologische Membranen eine wesentlich größere Rolle in der Medizin spielt als bisher angenommen. So sind Ionenkanäle nicht nur, wie in der klassischen Physiologie beschrieben, am epithelialen Transport von geladenen Teilchen oder an der Erregung von Muskel- und Nervenzellen beteiligt. Vielmehr nehmen sie Einfluss auf nahezu alle zellbiologischen Prozesse (Huber et al. 2013). In den letzten zwei Jahrzehnten rückten Ionenkanäle zudem immer weiter in den Fokus der Krebsforschung, da sie direkt an der neoplastischen Transformation, der malignen Progression, der Gewebsinfiltration sowie der Metastasierung beteiligt sind (Huber 2013). Neben den Schritten der Karzinogenese stehen Ionenkanäle auch in Zusammenhang mit der Resistenzentwicklung von Tumorzellen gegenüber gängigen Therapiemethoden. Die Strahlentherapie stellt eine dieser Methoden dar, auf die sich die moderne Krebstherapie stützt. Neben dieser Art der Tumorbehandlung zählen auch die chirurgische Resektion des Tumors, die Chemotherapie sowie neuerdings die Immuntherapie zu den gängigen Behandlungsmethoden. Umso wichtiger ist es daher, die Entwicklung von Resistenzen gegen eine oder mehrere dieser Therapieformen zu verhindern. Bemerkenswerterweise wurde im Jahr 2010 gezeigt, dass Ionenkanäle bei allen sogenannten „*Hallmarks of Cancer*“ eine bedeutende Rolle spielen (Prevarskaya et al. 2010). Insbesondere die veränderte Regulation des Ca^{2+}-Signalosoms scheint hier von essentieller Bedeutung zu sein (Stewart et al. 2014).

Tumor-assoziierte Veränderungen des Ca^{2+}-Signalosoms

Um elementare Funktionen in der Zelle korrekt auszuführen, sind präzise zeitlich und räumlich koordinierte Ca^{2+}-Signale zwingend notwendig. Neben der Zellteilung, der Migration und der Transkription wird unter anderem auch der Zelltod durch Ca^{2+} reguliert (Steinhardt and Alderton 1988; Berridge et al. 2000; Berridge et al. 2003;

Taylor et al. 2008). Ca^{2+} dient in der Zelle als Signalmolekül und hat hier eine Vielzahl an potentiellen Bindungspartnern, unter anderem Calmodulin.

Änderungen in der freien intrazellulären Ca^{2+}-Konzentration $[Ca^{2+}]_i$ können hierbei sehr vielfältig sein. Diese reichen von genau lokalisierten Ca^{2+}-*Peaks*, die räumlich und zeitlich begrenzt sind, bis hin zu einzelnen Ca^{2+}-Wellen oder -Oszillationen (Berridge et al. 2003; Parkash and Asotra 2010). Durch die „Dekodierung“ dieser komplexen Änderungen ist die Zelle in der Lage, viele verschiedene Ca^{2+}-Signale zu interpretieren und spezifische zelluläre Prozesse zu steuern (Berridge et al. 2000; Berridge et al. 2003).

Im Ruhezustand herrscht ein Gleichgewicht zwischen $[Ca^{2+}]_i$, die im Bereich von etwa 50-100 nM liegt, und der deutlich höheren extrazellulären Ca^{2+}-Konzentration $[Ca^{2+}]_e$, welche ungefähr 10.000 mal so hoch ist. Dieser Gradient wird mit Hilfe von Ca^{2+}-pumpen, Na^+/Ca^{2+}-Antiporteren und speziellen Ca^{2+}-Bindeproteinen aufrechterhalten (Berridge et al. 2000; Berridge et al. 2003).

Die Stabilisierung dieses Gleichgewichtes wird auch Ca^{2+}-Homöostase genannt. Hierzu bedarf es Prozesse, welche sowohl das Ansteigen der $[Ca^{2+}]_i$ verhindern, als auch dem zu starken Konzentrationsabfall entgegenwirken (Abb. 1). Die vier wichtigsten Transportmechanismen, die einer $[Ca^{2+}]_i$-Erhöhung entgegenwirken sind die Plasmamembran-Ca^{2+}-ATPase (PMCA), der Na^+/Ca^{2+}-Austauscher (NCX), die Ca^{2+}-Pumpe des sarkoplasmatischen und endoplasmatischen Retikulums (SERCA) und der mitochondriale Uniporter (Volpe et al. 1990; Blaustein and Lederer 1999; Hussain and Inesi 1999). Dem gegenüber steht die Erhöhung der $[Ca^{2+}]_i$ durch die Freisetzung von Ca^{2+} aus den internen Speichern und dem Einstrom aus dem Extrazellularraum über die Plasmamembran. Verantwortlich hierfür sind verschiedene Ionenkanäle, die aufgrund ihrer Aktivierungsmechanismen in unterschiedliche Gruppen eingeteilt werden können: Die Liganden-abhängigen Ca^{2+}-Kanäle wie der Inositol-1,4,5-Trisphosphat (IP_3)-Rezeptor bzw. der Ryanodin (RY)-Rezeptor sorgen für einen schnellen Anstieg der $[Ca^{2+}]_i$-Konzentration über die Ca^{2+}-Freisetzung aus den internen Speichern. Darüber hinaus gibt es die Ca^{2+}-permeablen Ionenkanäle in der Plasmamembran, die

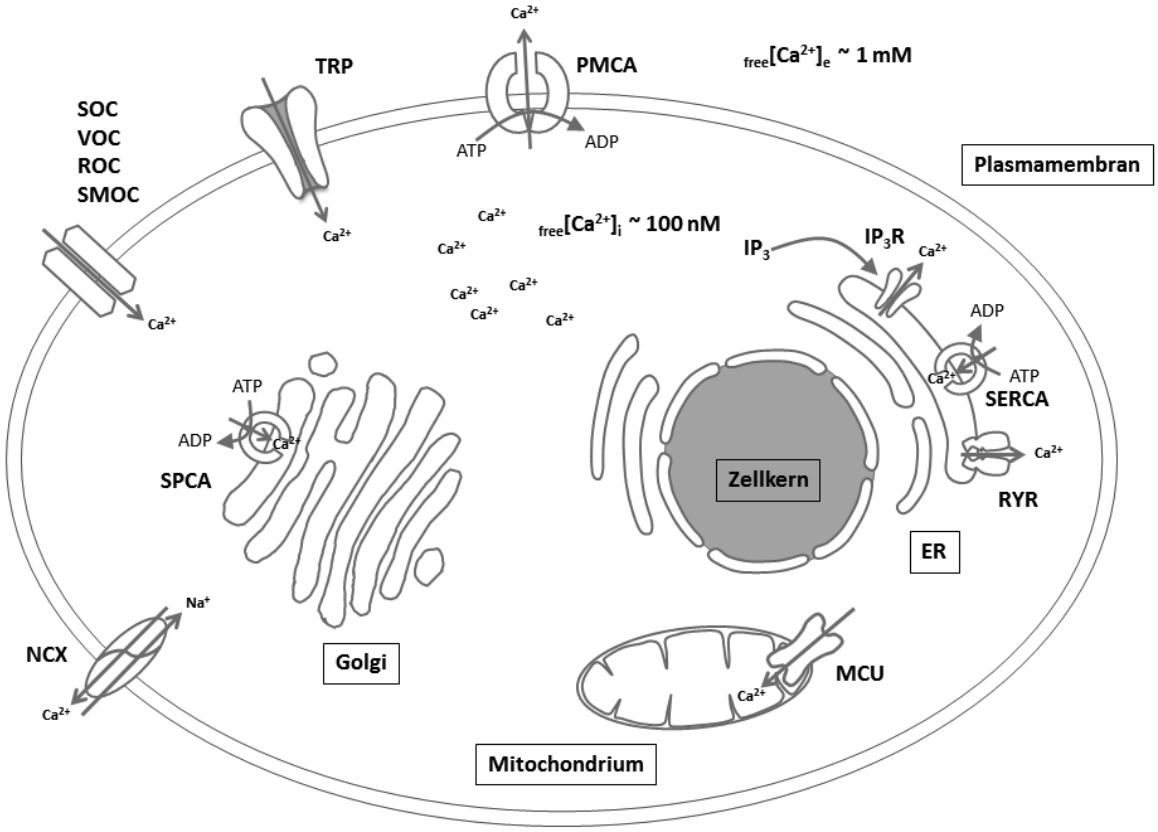

Abbildung 1

Schematische Darstellung der Hauptmechanismen zur Aufrechterhaltung des intrazellulären Ca^{2+}-Gleichgewichtes. Membranständige Kanäle, zu denen neben den spannungs-, speicher- und ligandengesteuerten Kanälen (SOC, VOC, ROC, SMOC) auch die TRP-Kanäle zählen, sind maßgeblich an der langsamen Erhöhung des intrazellulären Ca^{2+} über die Membran beteiligt. Der IP_3-Rezeptor (IP_3R), ebenso wie der Ryanoid-Rezeptor (RYR), regulieren die schnelle Freisetzung von Ca^{2+} aus dem Endoplasmatischen Retikulum (ER). Um die Ca^{2+}-Konzentration zu verringern, gibt es verschiedene ATPasen die das Ca^{2+} sowohl in den Extrazellularraum (PMCA) als auch in Organellen wie den Golgi (SPCA) oder das ER (SERCA) transportieren. Weitere Mechanismen sind der mitochondriale Uniporter, der die Ca^{2+}-Aufnahme in die Mitochondrien gewährleistet, und der Na^+/Ca^{2+}-Austauscher, welcher im Austausch für ein aus der Zelle transportiertes Ca^{2+}-Ion drei Na^+-Ionen in die Zelle einschleust.

unterteilt werden in Speicher-regulierte Ca^{2+}-Kanäle (*store-operated-channels*, SOCs), spannungsgesteuerte Ca^{2+}-Kanäle (*voltage-operated-channels*, VOCs), rezeptorgesteuerte Ca^{2+}-Kanäle (*receptor-operated-channels*, ROCs) und Kanäle, die über intrazelluläre Botenstoffe aktiviert werden (*second-messenger-operated-channels*, SMOCs) (Craven and Zagotta 2006; Watanabe et al. 2008). Die Familie der TRP-Kanäle zählt zur letzten Gruppe Ca^{2+}-permeabler Kanäle, die anhand ihrer

Aktivierung nur schwer einzuteilen sind. TRP-Kanäle stehen auch im Fokus dieser Arbeit steht. Diese Kanäle reagieren sensitiv auf Reize wie Temperatur, Osmolarität, pH-Wert und andere physiologische Veränderungen der Umgebung (Harteneck et al. 2000; Nilius and Voets 2004; Tominaga and Caterina 2004; Vennekens et al. 2008; Gees et al. 2010; Wu et al. 2010; Vay et al. 2012)

TRP-Kanäle

Die *Transient Receptor Potential* (TRP) Kationenkanal Superfamilie besteht aus einer Reihe spannungsabhängiger und Ca^{2+}-permeabler Kanäle, die ein weites Spektrum an zellulären Funktionen besitzen. Neben ihrer Aufgabe als multifunktionale Sensoren spielen sie auch eine wichtige Rolle bei der Zellkontraktilität, der Zellteilung und der Apoptose. Bisher wurden in Säugetieren 28 verschiedene Kanäle beschrieben, die ubiquitär exprimiert sind und ihrerseits in sechs Familien unterteilt werden: TRP**C** (classic/canonical), TRP**V** (vanilloid), TRP**M** (melastatin), TRP**P** (polycystein), TRP**ML** (mucolipin) und TRP**A** (ankyrin) (Clapham et al. 2005; Montell 2005; Nilius and Owsianik 2011). Alle TRP-Kanäle besitzen eine ähnliche Grundstruktur, welche mit der von spannungsaktivierten K^+-Kanälen vergleichbar ist. Sie besteht aus sechs Transmembrandomänen (S1-S6), die um eine Porenregion (S5-S6) angeordnet sind. Die Kanäle sind meist als Homo- beziehungsweise Heterotetramere angeordnet, wobei sich die C- und N-Termini stets intrazellulär befinden (Gaudet 2008; 2009; Wu et al. 2010). Die Länge und Funktion der zytoplasmatischen Regionen variiert dabei stark zwischen den einzelnen Familien. Während Mitglieder der TRPC und TRPV Familie drei bis vier intrazelluläre Ankyrin-*Repeat*-Domänen besitzen, sind es bei TRPA1 bis zu 14 *Repeats* am N-Terminus. In den anderen Familien sind diese Domänen nicht vorhanden. Eine Gemeinsamkeit der TRPC-, TRPM- und TRPV-Kanäle ist die sogenannte TRP-Domäne. Sie ist ein aus 25 Aminosäuren bestehender, konservierter Abschnitt am C-Terminus, beginnend mit einer TRP-Box, welche unter anderem als Bindestelle für das Membran-Phospholipid $PI(4,5)P_2$ dient (Rohacs and Nilius 2007; Nilius and Szallasi 2014). Weitere Interaktionsstellen konnten auch in anderen TRP-Kanälen funktionell nachgewiesen werden. So wurden bisher mehrere

Phosphorylierungsstellen für die Proteinkinasen A und C identifiziert, ebenso wie eine SH2-Erkennungssequenz der PI3-Kinase (Watanabe et al. 2008).

An der Regulierung der intrazellulären Ca^{2+}-Konzentration sind alle TRP-Kanäle auf unterschiedliche Arten beteiligt. Sie können direkt als Ca^{2+}-Kanäle in der Plasmamembran und den Organellen fungieren oder indirekt die Membranspannung verändern, so dass die Aktivität anderer Kanäle beziehungsweise das elektrochemische Gefälle für Ca^{2+} moduliert wird. Bis auf TRPM4 und TRPM5, die nur für monovalente Kationen durchlässig sind, besitzen alle anderen TRP Kanäle eine Ca^{2+}-Permeabilität. Sie unterscheiden sich lediglich in ihrer Permselektivitäts-Rangfolge für bestimmte Kationen. So sind TRPV5 und TRPV6 hochpermeabel für Ca^{2+}, TRPM6 und TRPM7 hochpermeabel für Mg^{2+} und TRPV1 sowie TRPML1 und TRPP3 hochpermeabel für H^{+}-Ionen (Nilius et al. 2007).

TRPM-Familie

Die Melastatin Familie der TRP-Kanäle umfasst acht Mitglieder, die aufgrund von Sequenzhomologien in vier Untergruppen eingeteilt werden. TRPM1/3, TRPM4/5, TRPM6/7 und TRPM2/8, wobei Letztere nur eine geringe Ähnlichkeit in ihren Sequenzen aufweisen (Harteneck 2005). Benannt ist die Familie nach dem ersten beschriebenen Mitglied TRPM1, welches als Tumorsupressor (Melastatin) im Zusammenhang mit metastasierenden Melanomen identifiziert wurde (Duncan et al. 1998; Hunter et al. 1998). Drei Mitglieder dieser Familie sind Träger eines funktionellen Enzyms an ihrer Carboxyl-Gruppe: TRPM2 besitzt eine NUDT9-Homologie-Region mit Adenosindiphosphat-Ribose(ADPR)-Pyrophosphatase-Aktivität und TRPM6 sowie TRPM7 eine funktionelle Serin/Threonin-Kinase (Clark et al. 2008). Alle Mitglieder der TRPM-Familie werden mit unterschiedlichen Erkrankungen, wie zum Beispiel Amyotrophe Lateralsklerose, in Verbindung gebracht. Dies wurde entweder in funktionellen Studien in der Maus oder durch humangenetische Analysen gezeigt (Hara et al. 2002; Clapham 2003; Naziroglu et al. 2007; Nilius et al. 2007; Naziroglu and Luckhoff 2008).

Die Mitglieder TRPM2 und TRPM8 der Melastatin Familie

In dieser Dissertation liegt der Fokus auf den Mitgliedern TRPM2 und TRPM8 aus der Melastatin Familie. TRPM2, ehemals bekannt als TRPC2 und LTRPC2 wurde erstmals 1998 beschrieben (Nagamine et al. 1998) und später in die Familie der TRPM-Kanäle eingeordnet. Die Aktivierung von TRPM2 erfolgt unter anderem durch reaktive Sauerstoffspezies (ROS). Zu diesen zählen die Superoxidanionen ($O_2^{\bullet -}$), Wasserstoffperoxid (H_2O_2) und andere Sauerstoffradikale, welche als intrazelluläre Messenger in Prozessen wie der mitogenen Signalweiterleitung, Genexpression und Regulierung der Zellteilung fungieren (Naziroglu 2007). Eine verstärkte Produktion von ROS, beziehungsweise die Inhibition des enzymatischen und nicht-enzymatischen Abbaus dergleichen, kann zu einer Schädigung der Zellen bis hin zum Zelltod führen (Halliwell 2006). Oxidativer Stress - im Experiment mit H_2O_2 simuliert - induziert TRPM2-Ströme und erhöht so $[Ca^{2+}]_i$ in mit TRPM2 transfizierten Zellen (Naziroglu and Luckhoff 2008), β-Zellen (Inamura et al. 2003), neutrophilen Granulozyten (Heiner et al. 2003) und U937 Monozyten (Perraud et al. 2001). Erhöhtes $[Ca^{2+}]_i$ wiederum steigert die Anfälligkeit für den programmierten Zelltod, so dass von einer proapoptotischen Funktion der TRPM2-Kanäle auszugehen ist.

TRPM8 ist ein Ca^{2+}-permeabler Kationenkanal der Melastatin Familie, der durch Membrandepolarisation, Kälte und kältesimulierende Stoffe wie Menthol oder Icilin aktiviert und unter anderem durch die Ca^{2+}-unabhängige Phospholipase A_2 ($iPLA_2$) reguliert wird. Die Endprodukte der enzymatischen Spaltung von Membranlipiden, sogenannte Lysophospholipide (Lysophosphatidylcholin, Lysophosphatidylinositol und Lysophosphatidylserin), stabilisieren die Offen-Konformation von TRPM8 (Vanden Abeele et al. 2006). Diese erhöhte Offenwahrscheinlichkeit wird dadurch erreicht, dass die Temperaturschwelle zur Aktivierung von TRPM8 dahingehend erhöht wird, dass der Kanal bereits bei regulärer Körpertemperatur aktiv ist. Die Modulation durch Lysophospholipide liefert somit einen physiologischen Mechanismus, den Kanal bei normaler Körpertemperatur zu aktivieren (Andersson et al. 2007). Mehrfach ungesättigte Fettsäuren, wie zum Beispiel die Arachidonsäure, sind in der Lage, TRPM8 in Gegenwart von Kälte, Menthol oder Icilin zu hemmen

(Bavencoffe et al. 2011). Neben ungesättigten Fettsäuren kann die Aktivität von TRPM8 durch eine Proteinkinase A-abhängige Phosphorylierung von Serin-9 und Threonin-17 inhibiert werden (Bavencoffe et al. 2010). Zusätzlich wurde beschrieben, dass zwei Spleißvarianten von TRPM8 (*short TRPM8 α* und *short TRPM8 β*) die geschlossene Konformation von TRPM8 stabilisieren und dadurch die Kältesensibilität sowie die Aktivität vermindern (Bidaux et al. 2012).

TRPM2 in Leukämie

TRPM2 wird, wie oben bereits beschrieben, durch den kanalvermittelten Ca^{2+}-Einstrom und die daraus resultierende Erhöhung von $[Ca^{2+}]_i$ in Verbindung mit dem programmierten Zelltod gebracht und wird deshalb auch als „Todeskanal“ bezeichnet. Dies wurde durch heterologe Expressionsstudien von TRPM2 in humanen embryonalen Nierenzellen und A172 Glioblastomzellen bestätigt, die zu einem durch oxidativen Stress verursachten Zelltod führten (Fonfria et al. 2004; Ishii et al. 2007). TRPM2 wird in mehreren Tumorentitäten, unter anderem in Leukämie, exprimiert und ist dabei ebenfalls nachweislich am Zelltod beteiligt (Inamura et al. 2003; Zhang et al. 2003; Zhang et al. 2006; Orfanelli et al. 2008; Zeng et al. 2010; Adachi et al. 2014). Die ROS-induzierte Aktivierung von TRPM2 verläuft dabei möglicherweise indirekt über ADPR (Perraud et al. 2005).

DNA-Schäden, speziell DNA-Doppelstrangbrüche, können auf vielerlei Arten, beispielsweise durch Bestrahlung, entstehen. Die meiste Energie ionisierender Strahlung wird hierbei durch das intrazelluläre Wasser absorbiert und resultiert in der Bildung von Hydroxyl-Radikalen ($OH^{\bullet}$) (Huber et al. 2013). Im Zuge der DNA-Schädigung werden durch Poly-ADP-Ribose-Polymerasen (PARPs) vermehrt ADPR-Polymere gebildet, welche bei der DNA-Reparatur durch Glycohydrolasen wieder in ADPR-Monomere gespalten werden (Fonfria et al. 2004; Eisfeld and Luckhoff 2007). Die Folge ist eine Freisetzung von ADPR, was zu einer Aktivierung von TRPM2 und einer $[Ca^{2+}]_i$ Veränderung führt. Diese Veränderung in der Ca^{2+}-Konzentration wiederum steht unter der Kontrolle von Bcl-2. Das anti-apoptotische Protein Bcl-2 ist ein wichtiger Regulator in der Ca^{2+}-Homöostase, da es unter anderem ein unkontrolliertes Fluten der Zelle mit Ca^{2+} verhindert (Rudner et al. 2002; Oakes et al.

2003; Pinton and Rizzuto 2006; Monaco et al. 2013). Eine weitere wichtige Quelle für ADPR-Monomere stellen die Mitochondrien dar (Dolle et al. 2013).

TRPM8 im Glioblastom

Neben der Expression von TRPM8 in sensorischen Neuronen, wo der Kanal an der Perzeption von Kälte und Schmerz beteiligt ist, wird TRPM8 normalerweise nur in Prostatagewebe, der Lunge und in der Blase exprimiert. In vielen malignen Tumorentitäten konnte jedoch gezeigt werden, dass TRPM8 stark überexprimiert wird. Beispiele hierfür sind: Prostatakarzinom (Tsavaler et al. 2001; Zhang and Barritt 2004; Bidaux et al. 2007), Bauchspeicheldrüsenkrebs (Yee et al. 2010; Yee et al. 2012), Brustkrebs (Chodon et al. 2010; Dhennin-Duthille et al. 2011), Blasenkrebs (Li et al. 2009), Glioblastom (Wondergem et al. 2008), Krebs der Mundhöhle (Okamoto et al. 2012), neuroendokrinen Tumoren (Mergler et al. 2007) und Melanomen (Yamamura et al. 2008).

Während die funktionelle Aufgabe von TRPM8 in sensorischen Neuronen bereits identifiziert wurde (Bautista et al. 2007), ist dies in Krebszellen bislang noch nicht vollständig geklärt (Zhang and Barritt 2004). Im Glioblastom konnte gezeigt werden, dass die Überexpression von TRPM8 an der Invasion und Metastasierung im Gehirn beteiligt ist (Wondergem et al. 2008; Alptekin et al. 2015). Dies kann möglicherweise mit der Regulation des BK (big conductance) K^+-Kanals durch Ca^{2+} erklärt werden. Spezielle Spleißvarianten des BK K^+-Kanals sind ebenfalls im Glioblastom überexprimiert und besonders Ca^{2+}-sensitiv (Ransom and Sontheimer 2001; Liu et al. 2002; Ransom et al. 2002). Da der BK Kanal nachweislich an der Migration von Glioblastomzellen und somit an der schlechten Prognose für diesen Tumor beteiligt zu sein scheint, ist es von essentieller Bedeutung, den zugrundeliegenden Regulierungsmechanismus über TRPM8 näher zu untersuchen (Wondergem and Bartley 2009; Steinle et al. 2011).

Zielsetzung

Diese Arbeit soll eine mögliche Funktion zweier Mitglieder - TRPM2 und TRPM8 - der Melastatin-TRP-Kanalfamilie bei der Radioresistenz von Tumoren identifizieren. Dazu wurden die beiden Tumorentitäten T-Zell-Lymphom und Glioblastom ausgewählt, die TRPM2 bzw. TRPM8 sehr stark exprimieren und eine besonders maligne Form von Tumoren darstellen. Mit Hilfe verschiedenster zellphysiologischer und molekularbiologischer Methoden wurden die Zellen untersucht und der Einfluss von Bestrahlung sowie unterschiedlicher pharmakologischer Agonisten und Antagonisten in *in vitro* Experimenten bestimmt. Insbesondere wurde der Effekt von Inhibition und *knock-down* von TRPM2 auf die Membranströme, das Ca^{2+}-Signaling, die mitochondriale Superoxid-Produktion sowie auf den Zellzyklus untersucht und die Ergebnisse von bestrahlten und unbestrahlten T-Zell-Leukämiezellen verglichen. In den untersuchten Glioblastomzelllinien wurde besonderes Augenmerk auf die Kanalaktivität von TRPM8, das daraus resultierende Ca^{2+}-Signaling, die Zellmigration und das klonogenem Überleben gelegt. Zusammen sollen diese Daten für ein besseres Verständnis der durch Ca^{2+}-Signale induzierten Resistenz gegenüber Bestrahlung sorgen und mögliche Strategien für zukünftige Krebstherapien eröffnen.

Ergebnisse TRPM2

Die Inhibition von TRPM2 stört den strahlungsinduzierten Zellzyklus Arrest und erhöht die Apoptoserate von T-Zell-Leukämie in Abhängigkeit von Bcl-2

Um die Kanalaktivität unter Einfluss von ionisierender Strahlung zu ermitteln, wurden Jurkat Zellen (T-Zell-Leukämie) mit einer Dosis von 10 Gy bestrahlt und anschließend die *Whole-Cell*-Ströme mit Hilfe der *Patch-Clamp*-Methode gemessen. Es konnte gezeigt werden, dass die strahlungsinduzierte Erhöhung der *Whole-Cell*-Ströme 2-6 h nach Applikation am stärksten ausgeprägt war und anschließend abflachte (Klumpp *et al.*, 2016a; Abb. 1A-B). Des Weiteren wurde durch das Austauschen von Na^+ in der Badlösung durch Ca^{2+} beziehungsweise $NMDG^+$ sowohl eine Kationenselektivität als auch die Ca^{2+}-Permeabilität der strahlungsinduzierten Ströme nachgewiesen (Klumpp *et al.*, 2016a; Abb. 1C-E).
Anschließend wurde die aus der Literatur beschriebene Korrelation zwischen der Bcl-2 und TRPM2-Expression mittels *Immunoblotting* analysiert. Im Gegensatz zu den mRNA Daten der *Broad-Novartis Cancer Cell Line Encyclopedia (CCLE)* (Klumpp et al., 2016a; Abb. 2A), konnte die Korrelation im Jurkat Zellmodell nicht bestätigt werden. Die TRPM2-Proteinmenge war in den Bcl-2 überexprimierenden Zellen sogar etwas geringer als in den Kontrollzellen (Klumpp *et al.*, 2016a; Abb. 2B). Die Bestrahlung der Zellen nahm dabei auf die Menge des Proteins keinen Einfluss (Klumpp *et al.*, 2016a; Abb. 2B).
Um nun die funktionelle Expression von TRPM2 im Jurkat-Zellmodell nachzuweisen, wurden ungepaarte *Patch-Clamp*-Versuche, jeweils in An- und Abwesenheit des spezifischen TRPM2-Agonisten ADP-Ribose in der Pipette, durchgeführt. Intrazelluläre ADP-Ribose stimulierte in den Experimenten eine Stromfraktion, welche durch den unspezifischen TRPM2-Inhibitor ACA (N-(p-amylcinnamoyl)anthranilic) (Kraft et al. 2006) gehemmt werden konnte (Klumpp *et al.*, 2016a; Abb. 2C-D). Die einzigartige Charakteristik der analysierten Ströme bestätigte die Annahme, dass es sich bei dem in den Versuchen gemessenen Kanal tatsächlich um TRPM2 handelt und dieser in Jurkat Zellen funktionell exprimiert wird (Klumpp *et al*., 2016a; Abb. 2E).
Im darauf folgenden Experiment wurde der Zusammenhang zwischen TRPM2 und der mitochondrialen Superoxid-Produktion untersucht. Hierzu wurden *Empty Vector*

und Bcl-2 überexprimierende Jurkat Zellen bestrahlt (0 bzw. 10 Gy), für 6 h kultiviert und im Anschluss 10 min mit dem Superoxid-sensitiven Fluoreszenzfarbstoff MitoSOX behandelt. Zusätzlich wurden die Zellen während der Färbung in An- und Abwesenheit des TRPM2-Inhibitors ACA inkubiert. Wie in Abb. 3 A-B (Klumpp *et al.*, 2016a) zu sehen ist, ergab die Auswertung drei unterschiedliche Populationen: jeweils eine Population mit einer niedrigen, eine mit einer mittleren und eine mit einer hohen MitoSOX Fluoreszenz. Hierbei wiesen die beiden letzteren eine deutlich geringere Zellgröße verglichen mit jenen, die eine niedrigere Fluoreszenz zeigten, auf. Dies könnte auf eine durch die Superoxid-Produktion verursachte Zellschrumpfung zurückzuführen sein. Parallel durchgeführte Experimente, bei welchen das Potential der inneren Mitochondrienmembran ($\Delta\Psi_m$) mit einem spezifischen Farbstoff (Tetramethylrhodamin Etylester - TMRE) bestimmt wurde, konnten zeigen, dass bei den meisten geschrumpften Zellen $\Delta\Psi_m$ bereits zusammengebrochen war. Daraus lässt sich folgern, dass bei einem Großteil der Zellen mit einer mittleren und einer hohen MitoSOX Fluoreszenz die Apoptose bereits eingeleitet wurde. Zellen mit einer geringen Fluoreszenz stellten den größten Anteil der gemessenen Population dar. Hier zeigten die Bcl-2 überexprimierenden Jurkat Zellen eine signifikant niedrigere Superoxid-Produktion, verglichen mit den Jurkat *vector* Zellen (Klumpp *et al*., 2016a; Abb. 3 C-D, links). Die Bestrahlung führte bei den gering-fluoreszierenden Populationen nur in den Jurkat Bcl-2 Zellen zu einer Erhöhung der Superoxid-Formation, wobei diese weiterhin unter dem Level der Jurkat *vector* Zellen lag (Klumpp *et al*., 2016a; Abb. 3 C). Wie die Behandlung mit ionisierenden Strahlen hat auch der TRPM2-Inhibitor ACA einen, wenn auch nur geringen, hemmenden Effekt einzig auf die Jurkat Bcl-2 Zellen. Diese Reduktion der Superoxid-Produktion ist sowohl bei den bestrahlten als auch bei den unbestrahlten Zellen signifikant (Daten nicht gezeigt). Auf die Populationen mit einer mittleren und hohen MitoSOX Fluoreszenz hat Bestrahlung keinerlei Einfluss (Klumpp *et al*., 2016a; Abb. 3 A). Während der Effekt von ACA in den gering-fluoreszierenden Populationen schwach ausfiel, verschwand unter ACA-Behandlung jener Teil der Zellen mit einer hohen Superoxid-Produktion komplett, sowohl bei den bestrahlten als auch bei den unbestrahlten Jurkat *vector* und Jurkat Bcl-2 Zellen (Klumpp *et al*., 2016a; Abb. 3 E).

Zusammenfassend lässt sich sagen, dass Bcl-2 überexprimierende Jurkat Zellen eine deutlich niedrigere mitochondriale Superoxid-Produktion aufwiesen als die

vector Zellen und auch nur in den Jurkat Bcl-2 Zellen eine Steigerung der Produktion nach Bestrahlung detektierbar war. Im Gegenzug hat ACA einen inhibitorischen Effekt auf die Superoxid-Formation, unabhängig vom Zelltyp oder der Behandlung. All dies lässt auf ein Zusammenspiel von einem TRPM2-vermittelten Ca^{2+}-Einstrom und der Bildung reaktiver Sauerstoffspezies schließen.

Um festzustellen, inwieweit Bestrahlung die Kanalaktivität von TRPM2 modifiziert, wurden beide Jurkat Zelltypen bestrahlt (0 und 5 Gy) und *Whole-Cell*-Messungen, in An- und Abwesenheit des TRPM2-Inhibitors, durchgeführt (Klumpp *et al*., 2016a; Abb. 4 A-C). Die ACA-sensitive Stromfraktion der unbestrahlten Gruppe zeigte sich in den Jurkat *vector* Zellen deutlich größer als in den Bcl-2 überexprimierenden Zellen (Klumpp *et al*., 2016a; Abb. 4 C). Dies lässt sich auch mit der unterschiedlichen TRPM2-Proteinkonzentration erklären und spiegelt die gewonnenen Erkenntnisse der Superoxid-Formation wider. Die strahlungsinduzierte Erhöhung der ACA-sensitiven Ströme trat dagegen in den Jurkat Bcl-2 Zellen deutlich ausgeprägter auf als in den Jurkat *vector* Zellen, was sich ebenfalls mit der Strahlensensibilität der Jurkat Bcl-2 Zellen, gemessen an der ROS-Produktion, deckt.

Ob eine durch Bestrahlung induzierte Steigerung der TRPM2-Aktivität einen Einfluss auf den Ca^{2+}-Einstrom hat, wurde mittels Fura-2 Ca^{2+}-Messungen in An- und Abwesenheit von ACA mit einem definierten Ca^{2+}-*Depletion/-Repletion* Protokoll bestimmt. Im Gegensatz zu den basalen ACA-sensitiven *Whole-Cell*-Strömen (Klumpp *et al*., 2016a; Abb. 4 B) war der basale ACA-sensitive Ca^{2+}-Einstrom in Bcl-2 überexprimierenden Zellen höher als in den Jurkat *vector* Zellen (Klumpp *et al*., 2016a; Abb. 4 E). Ebenso wie bei den *Whole-Cell*-Strömen stimulierte eine Bestrahlung bei den Jurkat Bcl-2 Zellen einen größeren Ca^{2+}-Einstrom als bei den Kontrollzellen (Klumpp *et al*., 2016a; Abb. 4 E). In Anwesenheit von ACA in der Badlösung, konnte kein Unterschied im Ca^{2+}-Anstieg zwischen bestrahlten *vector* und Bcl-2 Jurkat Zellen festgestellt werden (Klumpp *et al*., 2016a; Abb. 4 E). Zusammenfassend lässt sich sagen, dass die Bestrahlung einen durch Bcl-2 regulierten und möglicherweise TRPM2-vermittelten Anstieg der Ca^{2+}-Konzentration in Jurkat Zellen induziert.

Ein stetiger Anstieg der intrazellulären Ca^{2+}-Konzentration kann jedoch neben den überlebensnotwendigen Signalen durchaus auch negative Konsequenzen für die Zelle haben. So kann es passieren, dass sie bei einem stetigen Einstrom mit Ca^{2+} überflutet wird, was letztendlich zum Tod der Zelle führt. Tatsächlich konnte in dieser

Arbeit gezeigt werden, dass 24 h nach Bestrahlung (10 Gy) der Anteil der Jurkat Zellen mit einer stark erhöhten $[Ca^{2+}]_i$ auf ca. 25% anstieg (Klumpp *et al*., 2016a; Abb. 5 A-B).

Die Bestrahlung mit 5 Gy stimulierte die Autophosphorylierung und damit die Aktivierung von Isoformen der Ca^{2+}/Calmodulin-abhängigen Proteinkinase II (CaMK II) sowie die Phosphoylierungs-abhängige Inaktivierung des CaMKII Zielproteins cdc25b (Klumpp et al., 2016a; Abb. 5 C). Die strahlungsinduzierte Inaktivierung der Phosphatase cdc25b verhindert die Dephosphorylierung und somit die Aktivierung des *mitose-promoting-factors* cdc-2, was wiederum zu einer Blockade des Zellzyklus führt (Klumpp *et al*., 2016a; Abb. 5 C). Aus diesen Erkenntnissen lässt sich ein Zusammenhang zwischen Ca^{2+}-Effektorproteinen wie CaMKII und dem Auftreten eines G_2/M-Arrestes 24 h nach Bestrahlung folgern (Klumpp *et al*., 2016a; Abb. 5 D).
Um eine Beteiligung von TRPM2 und CaMKII an der Stressantwort nach Bestrahlung zu belegen, wurden Jurkat Zellen (Bcl-2 und *vector*) bestrahlt (0 und 5 Gy) und anschließend in An- und Abwesenheit der TRPM2-Inhibitoren ACA und Clotrimazol inkubiert (Hill et al. 2004; Chung et al. 2011). Im Anschluss wurde die Kinaseaktivität von CaMKII und cdc-2 mit Hilfe von *Immunoblots* bestimmt sowie Zellzyklus- und Zelltodrate mittels Durchflusszytometrie analysiert. Die Messwerte wurden jeweils 4 h beziehungsweise 24 h nach Bestrahlung erstellt. Die Auswertung ergab eine verringerte basale und strahlungsinduzierte Menge an phosphoryliertem CaMKII in den ACA behandelten (Klumpp *et al*., 2016a; Abb. 6A). Weiterhin verhinderte ACA die strahlungsinduzierte Inaktivierung von cdc-2 in beiden untersuchten Zelltypen (Klumpp *et al*., 2016a; Abb. 6A). Daraus lässt sich folgern, dass der ACA-sensitive Ca^{2+}-Anstieg essentiell für den Zellzyklus Arrest in der G_2/M-Phase ist (Klumpp *et al*., 2016a; Abb. 6B-E). Die Zellzahl in G_2/M verringerte sich unter der Behandlung mit ACA und Clotrimazol, während die Anzahl der toten Zellen anstieg (Klumpp *et al*., 2016a; Abb. 6B-E). Dieser ACA- und Clotrimazol-vermittelte Zelltod war in bestrahlten Jurkat *vector* Zellen wesentlich stärker ausgeprägt als in Bcl-2 überexprimierenden Zellen (Klumpp *et al*., 2016a; Abb. 6B-E). Die Beteiligung von TRPM2 in diesem Zusammenhang wurde anhand eines TRPM2 *knock-downs* näher untersucht. Das reduzierte TRPM2-Proteinlevel, nach erfolgter Transfektion mit der TRPM2 siRNA, wurde hierbei im *Immunoblot* erfolgreich nachgewiesen. (Klumpp *et al*., 2016a; Abb. 6F). Daraufhin wurden die transfizierten Jurkat Zellen bestrahlt (0

und 5 Gy) und der Zellzyklus 24 h später analysiert. Der beobachtete Effekt war, ähnlich dem von ACA und Clotrimazol, eine verringerte G_2-Population und ein Anstieg der Zahl toter Zellen (Klumpp *et al*., 2016a; Abb. 6F).

Diskussion TRPM2

Der Kationenkanal TRPM2 spielt bei der Resistenzentwicklung von Krebszellen gegenüber einer Bestrahlung eine bedeutende Rolle. Vor allem, wie in dieser Arbeit gezeigt, im Zusammenspiel mit dem anti-apoptotischen Protein Bcl-2 führt TRPM2 durch Veränderungen des Ca^{2+}-Signalosoms zu strahlungsresistenteren T-Zell-Leukämiezellen, wodurch eine effektive Behandlung erheblich erschwert wird.

Aktivierung von TRPM2. Eine Art der Aktivierung von TRPM2 erfolgt durch ADP-Ribose. Hierbei handelt es sich um ein kleines Molekül, welches u.a. in den Mitochondrien produziert wird. Es kann als Zwischenprodukt der NAD-abhängigen Deacetylierung, aus Mono- und Poly-ADP-ribosylierten Proteinen oder aus NAD^+ freigesetzt werden (Dolle et al. 2013). In früheren Studien konnte bereits gezeigt werden, dass oxidativer sowie nitrosativer Stress die Freisetzung von ADP-Ribose aus den Mitochondrien begünstigt, wodurch die Kanalaktivität von TRPM2 zunimmt, der Ca^{2+}-Einstrom über die Membran ansteigt, was schlussendlich zu einer Depolarisierung der Plasmamembran führt (Perraud et al. 2005). Eine übermäßige Aktivität von TRPM2 steht allerdings im Verdacht, Signale zu erzeugen und zu verstärken, welche zum Zelltod führen können. Eine erhöhte $[Ca^{2+}]_i$ führt dabei zu einer Entkoppelung der Atmungskette, was eine Hyperpolarisierung von $\Delta\Psi_m$ und somit die Freisetzung von Superoxidanionen bedingt. Anschließend kommt es zu einem mitochondrialen Ca^{2+}-Überschuss und zum Zusammenbruch des $\Delta\Psi_m$ (Review siehe (Huber et al. 2013)).

Interaktion von TRPM2 und Bcl-2. In dieser Arbeit konnte gezeigt werden, dass bestrahlte T-Zell-Leukämiezellen den Kanal TRPM2 verwenden, um wichtige Ca^{2+}-Signale für das Überleben zu generieren. Der Vergleich von Jurkat *vector* und Jurkat Bcl-2 Zellen ließ erkennen, dass die strahlungsinduzierten Membranströme und der Ca^{2+}-Einstrom bei den Bcl-2 überexprimierenden Jurkat Zellen höher war als in den *vector* Kontrollzellen. Dies lässt den Schluss zu, dass es eine Verbindung zwischen Bcl-2 im ER sowie in der äußeren Mitochondrienmembran und TRPM2 in der Plasmamembran gibt. Die positive Korrelation zwischen den mRNA Level von Bcl-2 und TRPM2 in verschiedenen Lymphohematopoetischen Krebszelllinien stützt diese Vermutung (Klumpp *et al*., 2016a; Abb. 2A). In einigen Zellmodellen konnte zudem

beobachtet werden, dass Zellen, die durch die Überexpression von Bcl-2 einem erhöhten Austritt von Ca^{2+} aus den intrazellulären Speichern ausgesetzt waren, diesem entgegenwirkten, indem sie den Ca^{2+}-Einstrom über die Plasmamembran aktiv herunterregulierten (Review siehe (Dolle et al. 2013)). Dies kann auch eine mögliche Erklärung für die, im Vergleich zu den *vector* Zellen, unter basalen Bedingungen beobachtete geringere Protein-Abundanz von TRPM2 in Bcl-2 überexprimierenden Jurkat Zellen sein (Klumpp *et al*., 2016a; Abb. 2B). Ein basaler, ACA-sensitiver Ca^{2+}-Einstrom konnte in den hier gezeigten Experimenten nur in Bcl-2 überexprimierenden Jurkat Zellen beobachtet werden. Dies liegt möglicherweise an einer Inaktivität von TRPM2, wie sie bei Kontrollzellen vorkommt, welche sich im Ruhezustand befinden (Klumpp *et al*., 2016a; Abb. 4E). Verglichen mit den Jurkat *vector* Zellen ist der in Bcl-2 überexprimierenden Zellen andauernde, erhöhte Ca^{2+}-Einstrom mit einer Verschiebung des $[Ca^{2+}]_i$-Setpoints hin zu einem höheren Normalwert zu erklären (Klumpp *et al*., 2016a; Abb. 4D-E). Fura-2 und fluo-3 Ca^{2+}-Messungen bestätigen die erhöhte $[Ca^{2+}]_i$ sowohl in konstitutiv als auch in induzierbaren Bcl-2 überexprimierenden Jurkat Zellen (Klumpp *et al*., 2016a; Suppl. Abb. A). Es ist bekannt, dass eine erhöhte $[Ca^{2+}]_i$ nachweislich die ADP-Ribose-vermittelte Aktivität von TRPM2 steigert (McHugh et al. 2003). Aus diesem Grund können die, nur in Jurkat Bcl-2 Zellen beobachteten basalen, ACA-sensitiven Ströme auf dieses erhöhte basale Ca^{2+}-Level zurückzuführen sein.

Bcl-2 und ROS. Bemerkenswerterweise fällt die mitochondriale ROS Produktion trotz des erhöhten $[Ca^{2+}]_i$ in Jurkat Bcl-2 Zellen, verglichen mit den Jurkat *vector* Zellen geringer aus (Klumpp *et al*., 2016a; Abb. 3C). Erklären lässt sich dies durch eine Bcl-2-vermittelte Hemmung der mitochondrialen Superoxid-Produktion. So stimuliert Bax, ein pro-apoptotisches Mitglied der Bcl-2 Familie und Antagonist des anti-apoptotischen Proteins Bcl-2 in neuronalen Zellen, die Produktion von ROS und bewirkt somit den gegenteiligen Effekt (Kirkland et al. 2010).

Strahlungsinduzierte Kanalaktivierung. Ein verändertes Ca^{2+}-Signalosom in unterschiedlichen Tumorentitäten ist das Ergebnis vieler Studien. Beispielsweise geht die maligne Progression in Prostatatumoren mit einer TRPM8-vermittelten Speicherentleerung und der Herunterregulierung des Speicher-abhängigen Ca^{2+}-Einstromes einher. Im Gegenzug werden andere TRP-Kanäle wie zum Beispiel

TRPV6 hochreguliert und in die Plasmamembran rekrutiert. Zusammen mit IK (intermediate conductance) K^+-Kanälen generieren sie Wachstumsfaktor-unabhängige Ca^{2+}-Signale, die das Überleben fortgeschrittener Prostatatumoren sichern (Review siehe (Huber 2013)). In dieser Arbeit konnte eindeutig belegt werden, dass Bestrahlung einen aktivierenden Effekt auf TRPM2 hat. So stimulierte Bestrahlung ACA-sensitive Ströme in *Patch-Clamp*-Messungen und führte zu einer Erhöhung des ACA-sensitiven Ca^{2+}-Einstroms in den untersuchten Jurkat Zellen. Eine strahlungsinduzierte Modifikation der Ionenkanal-Aktivität konnte bereits in Studien zu verschiedenen Tumoren belegt werden. Diese Modifikationen werden in Verbindung mit Stress-Antwort (Steinle et al. 2011), dem Glucosegehalt (Huber et al. 2012; Dittmann et al. 2013), der Zellzykluskontrolle (Heise et al. 2010; Palme et al. 2013) oder Radioresistenz (Stegen et al. 2015) gebracht.

TRPM2 als Radioresistenzfaktor. Die p53-mutierten Jurkat Zellen (Cheng and Haas 1990) akkumulierten aufgrund von strahlungsinduzierten DNA-Schäden in einem G_2/M-Phase Arrest (Klumpp *et al*., 2016a; Abb. 5D), welcher mit großer Wahrscheinlichkeit durch den strahlungsinduzierten erhöhten Ca^{2+}-Einstrom mit-hervorgerufen wurde. Diese Annahme wird dadurch bestätigt, dass zwei unspezifische TRPM2-Inhibitoren sowie der *knock-down* von TRPM2 mittels siRNA die Zahl der arretierten Zellen in der G_2-Phase verringerte und die der toter Zellen erhöhte (Klumpp *et al*., 2016a; Abb. 6). Möglicherweise wird durch die pharmakologische Inhibition sowie durch den TRPM2 *knock-down* der G_2-Kontrollpunkt des Zellzyklus übergangen, so dass die Zellen mit DNA-Schäden in die Mitose eingeschleust werden, was zu der sogenannten *mitotic catastrophe* und schlussendlich zum Zelltod führt. Bestätigt wird dies durch die Beobachtung, dass Bestrahlung die $[Ca^{2+}]_i$-abhängige Phosphorylierung von CaMKII und derer Zielproteine cdc25b und cdc-2 in einer ACA-sensitiven Weise förderte (Klumpp *et al*., 2016a; Abb. 5C und 6A). Durch die Phosphorylierungs-abhängige Inaktivierung der Phosphatase cdc25b akkumuliert die ebenfalls durch Phosphorylierung inaktiv-gehaltene Form von cdc-2, welche Teil des MPF (*mitosis promoting factor*) ist (Palme et al. 2013). Zusammenfassend lässt sich sagen, dass durch Steigerung der Aktivität von TRPM2 Ca^{2+}-Signale generiert werden, die in der Lage sind, eine Autophosphorylierung und somit eine Aktivierung von CaMKII zu induzieren.

Interaktionen von TRPM2 und K^+-Kanälen. Wie auch in den hier untersuchten T-Zell-Leukämiezellen konnte in einer früheren Arbeit mit myeloischen Leukämiezellen belegt werden, dass durch ein Zusammenspiel von TRP- und K^+-Kanälen in der Membran Ca^{2+}-Signale erzeugt werden, welche in einem G_2/M-Arrest gipfeln, ähnlich dem in dieser Arbeit untersuchten Mechanismus über CaMKII, cdc25b und cdc-2 (Heise et al. 2010; Palme et al. 2013). Befinden sich aktive K^+-Kanäle in direkter Nachbarschaft zu Ca^{2+}-Kanälen führt dies durch den zellulären Ausstrom von K^+-Ionen zu einem stark einwärtsgerichteten elektrochemischen Gradienten für Ca^{2+}, was für stabile Ca^{2+}-Signale unverzichtbar ist. Ebenso wie bei K562 Leukämiezellen stimuliert Bestrahlung die Aktivität von IK K^+-Kanälen in der Plasmamembran von Jurkat Zellen (Klumpp *et al*., 2016a; Suppl. Abb. B). Diese gewonnenen Erkenntnisse lassen zwei verschiedene Schlüsse zu: Zum einen ähneln sich die strahlungsinduzierten Signalwege in myeloischer und lymphatischer Leukämie und zum Anderen können die während der DNA-Reparatur generierten Ca^{2+}-Signale durch verschiedene Kombinationen aus sich in der Plasmamembran befindlichen TRP- und K^+-Kanälen erzeugt werden.

Zusammenfassung. Im Ca^{2+}-Signalosom humaner T-Zell-Leukämiezellen spielt TRPM2 eine bedeutende Rolle. Er wird während der DNA-Schadensantwort aktiviert und reguliert in bestrahlten Jurkat Zellen den G_2/M-Arrest. Durch die Aktivierung der CaMKII und der daraus resultierenden Inhibition von cdc25b und cdc2 verbleiben die Zellen in G_2 und sind in der Lage DNA-Schäden zu reparieren. Das antiapoptotische Protein Bcl-2 im ER und der äußeren Mitochondrienmembran wiederum verstärkt die Aktivität von TRPM2 indem es höhere $[Ca^{2+}]_i$ induziert und gleichzeitig die Produktion reaktiver Sauerstoffspezies verhindert. Durch diesen Umstand sind Bcl-2 überexprimierende Jurkat Zellen dazu in der Lage, TRPM2-generierte Ca^{2+}-Signale zu nutzen, ohne einen gefährlichen *Ca^{2+}-Overload* und der damit verbundenen ROS-Produktion zu riskieren. Zusammen führen die stabilisierende Funktion von Bcl-2 auf die Mitochondrien und das stressbedingte, TRPM2-vermittelte Ca^{2+}-Signaling zur Radioresistenz von T-Zell-Leukämiezellen.

Ergebnisse TRPM8

TRPM8-vermitteltes Ca^{2+}-Signaling verstärkt die Migration und erhöht die Radioresistenz von Glioblastomzellen

Der Ionenkanal TRPM8 wird unter Standardbedingungen ausschließlich in sensorischen Neuronen exprimiert, wo er bei dem Empfinden von Kälte eine wichtige Rolle spielt. In benignem Gewebe ist das Vorkommen dieses Kationenkanals auf die Prostata, die Lunge und die Blase beschränkt. Es konnte jedoch auch gezeigt werden, dass TRPM8 neben diesen Organen in vielen Tumorentitäten überexprimiert ist. So zum Beispiel im Glioblastom, wo er die Krankheitsprogression und das Überleben der Patienten negativ beeinflusst (Alptekin et al. 2015). Zu Beginn dieser Arbeit wurde mit Hilfe des Onlineportals „*The Cancer Genome Atlas“* (TCGA) der Zusammenhang der TRPM8 mRNA Abundanz mit dem krankheitsfreien Überleben und dem Gesamtüberleben von Patienten mit *low-grade* Gliomen beziehungsweise mit Glioblastomen verglichen. Weiter wurde auch die mRNA Abundanz von TRPM8 in *low-grade* Gliomen und Glioblastomen mit der mRNA Abundanz des Ca^{2+}-aktivierten Kaliumkanals IK und dem Chemokinrezeptor CXCR4 verglichen, welche nachweislich an der Malignizität von Gliomen und Glioblastomen beteiligt sind (Chatterjee et al. 2014; Stegen et al. 2015). Es konnte bestätigt werden, dass eine höhere Expression von TRPM8 in *low-grade* Gliomen mit einem geringeren Gesamtüberleben und einer verkürzten krankheitsfreien Zeit der Patienten einhergeht (Klumpp *et al*., 2016b; Abb. 1A und B). Im Gegensatz dazu zeigte sich in Glioblastomen, welche durchschnittlich eine höhere TRPM8 Expression aufwiesen als *low-grade* Gliome (Klumpp *et al*., 2016b; Abb. 1C), kein Unterschied im Überleben in Abhängigkeit von der mRNA Abundanz (Daten nicht gezeigt). Die Expression von TRPM8 scheint außerdem signifikant mit jener der Malignitätsmarker CXCR4 und IK zu korrelieren. Dieser Zusammenhang war besonders deutlich bei Patienten, welche mit Bestrahlung und Temozolomid therapiert wurden (Stupp et al. 2009) (Klumpp *et al*., 2016b; Abb. 1D).

In den ersten Experimenten dieser Arbeit wurde die mRNA Abundanz von TRPM8 in unterschiedlichen Glioblastomzelllinien mittels *real-time RT-PCR* untersucht. Neben TRPV1 und TRPV2 (Klumpp *et al*., 2016b; Abb. 1E) konnte in den Zelllinien auch TRPM8 nachgewiesen werden, wobei die Abundanz an mRNA in den verschiedenen

Linien unterschiedlich ausfiel (Klumpp *et al*., 2016b; Abb. 1F). Für die weiteren Experimente wurden ausschließlich die Zelllinien mit hoher (U251, U-87MG), beziehungsweise niedriger (T98G) TRPM8 mRNA Abundanz genutzt. Anschließend wurde die Funktionalität der TRPM8-Kanäle mit Hilfe von *On-Cell-Patch-Clamp*-Messungen untersucht. Glioblastomzellen wurden hierfür mit dem pharmakologischen TRPM8-Agonist Icilin behandelt und die Aktivierung des Ca^{2+}-aktivierten Kaliumkanals BK untersucht, welcher als Surrogatmarker für den TRPM8-vermittelten Ca^{2+}-Einstrom in die Zelle diente (Klumpp *et al*., 2016b; Abb. 2 und 3). Die bereits dokumentierte Eigenschaft von TRPM8, eine Rolle bei der Migration von Glioblastomzellen zu spielen (Wondergem et al. 2008; Wondergem and Bartley 2009), konnte in Wundheilungs- (Klumpp *et al*., 2016b; Abb. 5A-D) und Transfiltermigrations-Assays (Klumpp *et al*., 2016b; Abb. 5 E-H) bestätigt werden. Zusammengefasst zeigen diese Daten eine funktionelle Expression von TRPM8 in den untersuchten humanen Glioblastomzelllinien und belegen eine essentielle Rolle von TRPM8 bei der Zellmigration.

Um einen möglichen Einfluss von TRPM8 bei der Radioresistenz des Glioblastoms zu untersuchen, wurden die Zelllinien T98G und U251 fraktioniert bestrahlt. Appliziert wurden Photonen-Einzeldosen zu je 2 Gy, was der gängigen Therapie von Patienten mit einem Glioblastom entspricht. Anschließend wurden strahlungsinduzierte Veränderungen in Expression und Funktion von TRPM8 mit Hilfe von *real-time RT-PCR* und Fura-2 Ca^{2+}-Messungen untersucht. Es konnte gezeigt werden, dass eine fraktionierte Bestrahlung (5 x 2 Gy) die mRNA Abundanz von TRPM8 erhöht (Klumpp *et al*., 2016b; Abb. 6A-D). Des Weiteren konnte bereits 2 h nach Applikation einer Einzeldosis von 2 Gy ein Menthol-stimulierter Anstieg des Ca^{2+}-Einstroms in T98G Zellen detektiert werden (Klumpp *et al*., 2016b; Abb. 6E und F). Dies zeigt, dass Bestrahlung sowohl die Expression als auch die Funktion von TRPM8 beeinflusst.

Um auszuschließen, dass die strahlungsinduzierte Aktivierung von TRPM8 kein Epiphänomen, sondern elementar am Überleben bestrahlter Glioblastomzellen beteiligt ist, wurde TRPM8 mittels siRNA in U251 und T98G Zellen herunterreguliert (Klumpp *et al*., 2016b; Abb. 4). In einem parallel durchgeführten Experiment ging die Herunterregulierung des mRNA-Bindeproteins Musashi (MSI1) mit einem Anstieg der TRPM8 mRNA Abundanz einher. In diesem speziellen Fall wurde der *knock-down* von MSI1 als Hilfsmittel verwendet, um eine Überexpression von TRPM8 zu

erzeugen (Klumpp *et al*., 2016b; Abb. 4). Anschließend wurden sowohl die Kontrollzellen (ntRNA), die TRPM8-herunterregulierten Zellen (U251, T98G) als auch die TRPM8-überexprimierenden Zellen (U251) auf ihr klonogenes Überleben untersucht. Zu diesem Zweck wurden die Zellen bestrahlt (0-6 Gy) und nach 24 h ein Koloniebildungstest durchgeführt. Es zeigte sich, dass sich ein *knock-down* von TRPM8 negativ auf das Überleben beider Zelllinien auswirkte (Klumpp *et al*., 2016b; Abb. 7A und B). Genauer verminderte der *knock-down* von TRPM8 den Anteil der überlebenden Zellen nach einer Bestrahlung mit 2 Gy bis zu 30% (U251) (Klumpp *et al*., 2016b; Abb. 7C) bzw. 10% (T98G) (Klumpp *et al*., 2016b; Abb. 7D). Gleichzeitig verschlechterte sich die *plating efficiency* um 30% (U251) (Klumpp *et al*., 2016b; Abb. 7E) beziehungsweise um 60% (T98G) (Klumpp *et al*., 2016b; Abb. 7F). Im Gegenzug dazu erhöhte die Überexpression von TRPM8 (MSI1 *knock-down*) die Radioresistenz in U251 Zellen verglichen mit den Kontrollzellen (ntRNA) (Klumpp *et al*., 2016b; Abb. 7A). Diese Daten zeigen, dass TRPM8 eine entscheidende Rolle in der Klonogenität und Radioresistenz von Glioblastomzellen spielt.

Anknüpfend an diese Experimente wurde untersucht, inwieweit sich die TRPM8-Aktivität auf die Apoptose-Resistenz der Glioblastomzellen auswirkt. Hierfür wurde die Caspasenaktivität 24 h nach Bestrahlung (0 und 4 Gy) mit Hilfe eines speziellen Farbstoffes untersucht. Ein siRNA-vermittelter TRPM8 *knock-down* erhöhte in beiden Zelllinien die Zellzahl mit einer Caspaseaktivität um den Faktor 3 (Klumpp *et al*., 2016b; Abb. 8B und C), was auf eine essentielle Funktion von TRPM8 schließen lässt. Interessanterweise war der kombinierte Effekt von Bestrahlung und TRPM8 *knock-down* auf die Aktivität der Caspasen lediglich additiv (T98G) (Klumpp *et al*., 2016b; Abb. 8B), wenn überhaupt vorhanden (U251) (Klumpp *et al*., 2016b; Abb. 8C). Dies lässt den Schluss zu, dass es einen anderen Mechanismus geben muss, welcher zu der beobachteten, TRPM8-vermittelten Radioresistenz führt (Klumpp *et al*., 2016b; Abb. 7). Im Folgenden wurde daher der Effekt eines TRPM8 *knock-downs* auf den Zellzyklus von T98G und U251 Glioblastomzellen 48 h nach Bestrahlung untersucht. Hierzu wurden die Zellen permeabilisiert, die DNA mit dem Fluoreszenzfarbstoff Propidiumiodid angefärbt und anschließend mittels Durchflusszytometrie analysiert (Nicoletti Protokoll, Klumpp *et al*., 2016b; Abb. 9A). In beiden Zelllinien erhöhte Bestrahlung die Zellpopulation in der G_2- und S-Phase und verringerte die Population in G_1 (Vergleich Balken 1 und 2 der ersten drei Diagramme, Klumpp *et al*., 2016b; Abb. 9B und C). Diese Daten deuten daher auf

einen durch Bestrahlung induzierten S- und G_2/M-Arrest hin, der in beiden Zelllinien beobachtet werden konnte.

Obwohl eine Signifikanz nicht immer erreicht werden konnte, zeigten sich nach einem TRPM8 *knock-down* in beiden Zelllinien vergleichbare Effekte auf den Zellzyklus. So führte die Herunterregulation von TRPM8 sowohl zu einem strahlungsinduzierten Arrest der Zellen in der G_2-Phase als auch zu einer Verminderung der Zellpopulation, welche sich in der G_1-Phase befindet. Gleichzeitig schwächte (U251) beziehungsweise verhinderte (T98G) der *knock-down* die durch Bestrahlung verursachte Akkumulation in der S-Phase (Klumpp *et al*., 2016b; Abb. 9B und C, ersten drei Diagramme) und erhöhte die hyperG Population in bestrahlten Zellen ausschließlich (U251) beziehungsweise in verstärktem Maße (T98G) (Klumpp *et al*., 2016b; Abb. 9B und C, letztes Diagramm). Da die hyperG Population jene Zellen repräsentiert, die einen abnorm erhöhten DNA-Gehalt besitzen, lässt dies auf eine Störung in der Mitose oder Zytokinese schließen, welche durch einen TRPM8 *knock-down* hervorgerufen wird. Dieses Fehlverhalten in der Zellteilung deckt sich mit der Beobachtung, dass nach einem TRPM8 *knock-down* die Zellen in der G_2-Phase akkumulierten und sich demzufolge die G_1-Population verringerte. Um den direkten Einfluss von TRPM8 auf den Wiedereintritt in die Mitose und den Zellyklus zu untersuchen, wurden T98G und U251 Glioblastomzellen bestrahlt (0 und 4 Gy) und für 48 h inkubiert. Anschließend wurde 5-Ethynyl-2`-Deoxyuridin (EdU) hinzugegeben und für weitere 8 h inkubiert. Die Auswertung erfolgte anschließend mittels Durchflusszytometrie (Klumpp *et al*., 2016b; Abb. 10A).

In beiden Zelllinien verursachte Bestrahlung einen Anstieg EdU-negativer Zellen in der S- und G_2-Phase (Klumpp *et al*., 2016b; Abb. 10B und C, vergleiche Balken 1 und 2) sowie einen Rückgang in der G_1-Phase (Klumpp *et al*., 2016b; Abb. 10B und C, vergleiche Diagramme 1-3). Auf Zellen in der S- und G_2-Phase, welche EdU in ihre DNA eingebaut hatten, nahm die Bestrahlung keinen Einfluss (Klumpp *et al*., 2016b; Abb. 10B und C, Vergleich Diagramme 4-5). Diese Beobachtung lässt den Schluss zu, dass der Übergang von der G_1- zur S-Phase, so wie das Fortführen der S-Phase (DNA-Replikation) bereits 48-56 h nach Bestrahlung mit 4 Gy auf dem Level von unbestrahlten Zellen war. Die Herunterregulation von TRPM8 führte bei beiden Zelllinien sowohl zu einem weiteren Anstieg EdU-negativer Zellen in der S- und G_2-Phase wie auch zu einem Rückgang der EdU-negativen Zellen in der G_1-Phase. Dies war in bestrahlten und unbestrahlten Zellen gleichermaßen der Fall (Klumpp *et al*.,

2016b; Abb. 10B und C, vergleiche Balken 1 mit 3 und 2 mit 4 der Diagramme 1-3). Zusammen deutet dies auf eine entscheidende Rolle von TRPM8 bei der Mitose hin. Mehr noch, der TRPM8 *knock-down*-vermittelte Anstieg EdU-negativer Zellen in der S-Phase legt nahe, dass TRPM8 neben der Mitose ebenfalls eine Funktion in der S-Phase zu haben scheint.

Die Verringerung der Anzahl an EdU-positiven Zellen in der S- und G_2-Population nach einem TRPM8 *knock-down* stimmt überein mit dem gleichzeitigen Anstieg EdU-negativer Zellen unter diesen Bedingungen. (Klumpp *et al*., 2016b; Abb. 10B und C, 4.-5.Diagramm). Ein Vergleich der Populationen EdU-positiver mit EdU-negativer Zellen zeigt, dass Bestrahlung alleine keinen Effekt auf den Zellzyklus hat (Klumpp *et al*., 2016b; Abb. 10D und E, vergleiche 1. und 2. Balken), was ebenfalls auf eine normalisierte DNA-Replikation, 48-56 h nach Bestrahlung schließen lässt (siehe oben). Nach einem *knock-down* von TRPM8 jedoch verändert sich dieses Verhältnis EdU-positiver zu EdU-negativer Zellen (Klumpp *et al*., 2016b; Abb. 10D und E, vergleiche 1. und 3. Balken). In U251 Zellen reduzierte eine kombinierte Behandlung mit TRPM8 *knock-down* und Bestrahlung dieses Verhältnis noch weiter (Klumpp *et al*., 2016b; Abb. 10D, vergleich 3. und 4. Balken). In T98G Zellen war dies nicht der Fall (Klumpp *et al*., 2016b; Abb. 10E, vergleiche 3. und 4. Balken). Zusammengefasst zeigen diese Daten, dass TRPM8 eine signifikante Funktion im Zellzyklus unbestrahlter Glioblastomzellen einnimmt. Weiter konnte in U251 Zellen gezeigt werden, dass ein TRPM8 *knock-down* die hyperG Population, speziell in bestrahlten Zellen, erhöhte (Klumpp *et al*., 2016b; Abb. 9B, 4. Diagramm). Zusammen mit den Ergebnissen der EdU-Messungen lässt sich ebenfalls eine Rolle von TRPM8 in der Zellzykluskontrolle von bestrahlten Glioblastomzellen belegen (Klumpp *et al*., 2016b; Abb. 10D).

Diskussion TRPM8

Es ist bekannt, dass TRPM8-Kanäle für die Generierung von Ca^{2+}-Signalen in Glioblastomzellen verantwortlich und maßgeblich an der Zellmigration von Tumorzellen beteiligt sind. Neue Erkenntnisse aus dieser Arbeit zeigen nun, dass eine fraktionierte Bestrahlung, wie sie in der Klinik bei der Behandlung von Glioblastompatienten angewandt wird, zu einer Hochregulation von TRPM8 führt, was wiederum eine erhöhte Radioresistenz zur Folge hat.

Bestrahlungsinduziertes Ca^{2+}-Signaling. Ähnlich wie in Glioblastomzellen konnte bereits in chronisch myeloischen sowie in T-Zell Leukämiezellen gezeigt werden, dass Bestrahlung Einfluss auf die durch TRP-Kanäle generierten Ca^{2+}-Signale nimmt (Heise et al. 2010; Klumpp et al. 2016a). Diese TRP-Kanäle besitzen nachweislich eine regulatorische Funktion im Zellzyklus und beeinflussen im Zusammenspiel mit spannungsaktivierten $K_v3.4$ (Palme et al. 2013) sowie Ca^{2+}-aktivierten IK K^+ Kanälen (Klumpp et al. 2016b) das zelluläre Überleben. Durch Re- beziehungsweise Hyperpolarisierung der Plasmamembran wirken diese spannungs- und Ca^{2+}-aktivierten K^+-Kanäle einer, durch Eintritt von Ca^{2+} verursachten, Depolarisation der Zellmembran entgegen. Befinden sich diese K^+-Kanäle in direkter Nachbarschaft zu Ca^{2+}-Kanälen, halten sie einen starken einwärts gerichteten elektrochemischen Ca^{2+} Gradienten aufrecht und steuern die Aktivität von spannungsabhängigen und spannungsaktivierten Ca^{2+}-Kanälen. Somit spielen K^+-Kanäle eine bedeutende Rolle im Ca^{2+}-Signalosom von Tumorzellen (Review siehe (Huber 2013)).

TRPM8, IK- und BK-Kanal Interaktionen. Wie bereits mehrfach dokumentiert, führt die Bestrahlung von Glioblastomzellen zu einer Aktivierung von BK (Steinle et al. 2011) und IK Ca^{2+}-aktivierten K^+-Kanälen (Stegen et al. 2015), was wiederum eine Signalkaskade, bestehend aus Ca^{2+} und anderen biochemischen Signalen, erzeugt. Es konnte gezeigt werden, dass die strahlungsinduzierte Aktivierung von BK für die Aktivierung von *downstream* Effektoren wie der Ca^{2+}/Calmodulin-abhängigen Protein-Kinase II (CaMKII) essentiell ist und eine wichtige Rolle bei der Migration von Glioblastomzellen spielt (Steinle et al. 2011). Gleichzeitig sind die durch Bestrahlung aktivierten IK K^+-Kanal-Signale nachweislich an der Zellzykluskontrolle, der Reparatur von DNA-Schäden und dem klonogenen Überleben beteiligt (Stegen et al.

2015). Der Kationenkanal TRPM8 scheint sowohl Einfluss auf die Zellmigration, als auch auf das Zellüberleben zu haben. Es ist daher anzunehmen, dass in Glioblastomzellen der TRPM8-Kanal in einem sehr engen räumlichen Verhältnis zu den beiden K^+-Kanälen steht und mit diesen interagiert. Die Kationenströme des stark auswärts gleichrichtenden Kanals TRPM8 (Review siehe (Yudin and Rohacs 2012)) nehmen mit steigender Hyperpolarisation der Plasmamembran immer weiter ab. Ein möglicher Ablauf wäre somit folgender: Die Aktivität von IK und BK führt zu einer Hyperpolarisation der Membran, welche wiederum den TRPM8-vermittelten Ca^{2+}-Einstrom schwächt. Dies hat zur Folge, dass IK und BK aufgrund des fehlenden Ca^{2+}-Signals inaktiviert werden, die Membran repolarisiert und durch diese Depolarisierung TRPM8 erneut aktiviert wird. Diese wechselseitigen Aktivierungen und Inaktivierungen generieren Ca^{2+}-Oszillationen, die im Inneren der Zelle von speziellen Ca^{2+}-Effektoren, wie zum Beispiel CaMKII Isoformen erkannt werden (Review siehe (Huber 2013)) und somit die Migration (Cuddapah and Sontheimer 2010; Steinle et al. 2011; Cuddapah et al. 2013) sowie die Zellteilung (Cuddapah et al. 2012) von Glioblastomzellen regulieren.

Aktivierung von TRPM8 in Glioblastomzellen. Im Gegensatz zu seiner physiologischen Funktion in sensorischen Neuronen ist TRPM8 im Gehirn unter Normalbedingungen keinen Temperaturen unter 20°C ausgesetzt, welche zu einer Aktivierung führen könnten. Zudem wurde die Osmolariät in den Experimenten dieser Arbeit (z.B. Migration, Koloniebildungstest) stets stabil gehalten, weshalb auch die bereits dokumentierte Funktion von TRPM8 als Sensor für Osmolarität (Quallo et al. 2015) keine Erklärung für die Aktivität im Glioblastom darstellt. Belegt ist, dass die Kanalaktivität von TRPM8 durch G-Protein gekoppelte Rezeptoren (Bavencoffe et al. 2010), Phosphatidylinositolen (Yudin and Rohacs 2012), Serin/Threonin- (Mandadi et al. 2011), Tyrosin-Kinasen/-Phosphatasen (Morgan et al. 2014) sowie UBA1-abhängige Ubiquitinilierung (Asuthkar et al. 2015) moduliert wird. Des Weiteren steuern Protein-Protein-Interaktionen mit dem Zwei-Transmembrandomänen Protein Pirt (Tang et al. 2015) und TRP-Kanal-assoziierten Faktoren (TCAFs) (Gkika et al. 2015) die räumliche Verteilung und die Aktivität von TRPM8 in der Zelle. Ein weiterer Antagonist von TRPM8 scheint Testosteron zu sein. Es konnte gezeigt werden, dass bereits Konzentrationen im picomolaren Bereich die Öffnung von TRPM8-Kanälen in planaren Lipiddoppelschichten stimulierten (Asuthkar et al. 2015).

Zusammenfassend lässt sich sagen, dass die Regulation von TRPM8 höchst komplex ist und die gesteigerte Aktivität im Glioblastom möglicherweise mit einer Sollwertverschiebung der Aktivierungstemperatur zur normalen Körpertemperatur zu erklären ist. Der genaue molekulare Mechanismus bleibt bislang jedoch noch unverstanden.

Erhöhte Expression von TRPM8 in Glioblastomzellen. Wie bereits dokumentiert, handelt es sich bei TRPM8 unter anderem um ein Zielgen des Androgenrezeptors sowie des Tumorsupressorproteins p53 (Bidaux et al. 2005; Asuthkar et al. 2015). Die erhöhte Expression des Androgenrezeptors im Glioblastom (Yu et al. 2015) kann somit auch an der Überexpression von TRPM8 beteiligt sein. In U251 Glioblastomzellen ging eine Herunterregulation des Genes musashi-1 (MSI1) mit einer Hochregulation von TRPM8 einher, was in den Experimenten dieser Arbeit dazu genutzt wurde, eine Überexpression von TRPM8 zu simulieren (Klumpp *et al*., 2016b; Abb. 4). Dies kann wiederum auf eine negative Regulation des mRNA Bindeproteins MSI1 auf TRPM8 hindeuten. Nach eigenen Recherchen im *Cancer Genome Atlas* auf mögliche Korrelationen zwischen den mRNA Abundanzen von MSI1 und TRPM8 in Glioblastompatienten, konnte diese Hypothese nicht belegt werden (Daten nicht gezeigt). Das Phänomen scheint somit auf die Zelllinie U251 beschränkt zu sein. Durch fraktionierte Bestrahlung konnte in dieser Arbeit ebenfalls eine Steigerung der TRPM8-Expression induziert werden, was in den Glioblastomzelllinien T98G und U251 signifikant und in U-87MG schwach, aber erkennbar ausgeprägt war (Klumpp *et al*., 2016b; Abb. 6A-D). Dieser Effekt resultiert möglicherweise aus der durch Bestrahlung erfolgenden Akkumulation/Selektion TRPM8-überexprimierender und somit resistenterer Zellen. Eine weitere Erklärung wäre eine Adaptation an die Bestrahlung, was auf eine Stabilisierung von p53 schließen lässt. Diese Vermutung konnte allerdings nicht belegt werden, da U251 Glioblastomzellen, welche p53-mutiert sind, eine ähnliche TRPM8-Expression wie die heterogenen p53-Wildtyp/-mutierten T98G Zellen und sogar eine gesteigerte Expression gegenüber den p53-Wiltyp U-87MG Zellen zeigten. Eine p53-vermittelte Regulierung von TRPM8 scheint somit nicht ausschlaggebend für die Resistenz zu sein.

Mögliche Funktion von TRPM8 in der malignen Progression. In den hier durchgeführten Koloniebildungsassays konnte gezeigt werden, dass ein *knock-down* von TRPM8 eine Radiosensibilisierung von T98G und U251 Glioblastomzellen zur Folge hat, weswegen TRPM8 als möglicher Resistenzfaktor betrachtet werden kann. Zusätzlich war TRPM8 auch essentiell für die Migration von Glioblastomzellen. Da die Fähigkeit von Glioblastomzellen, infiltrativ in das Gehirnparenchym einzuwandern, ein bedeutender Grund für die Schwere der Erkrankung darstellt, kommt TRPM8 ebenfalls als Malignitätsfaktor in Betracht. Dies lässt sich auch durch die schlechte Prognose von *low-grade* Gliompatienten belegen, welche im Gegensatz zu anderen *low-grade* Patienten eine höhere TRPM8-Expression aufwiesen (Klumpp *et al*., 2016b; Abb. 1A-B). Obwohl in diesem Falle weder eine Subgruppenanalyse stattfand, noch eine zweite Patientengruppe hinzugezogen wurde, lässt dieses Ergebnis darauf schließen, in Zukunft TRPM8 als prognostischen Marker in der Diagnose hinzuzuziehen. Diese Theorie wird gestützt durch die Beobachtung, dass *low-grade* Gliompatienten mit IDH1-Wildtyp (Isocitratdehydrogenase) eine signifikant höhere TRPM8-Expression zeigten als Patienten mit einer Mutation in IDH1 (ähnlich der von Glioblastompatienten). Die Prognose für das Langzeitüberleben von *low-grade* Gliompatienten mit mutiertem IDH1 ist dabei wesentlich besser im Vergleich zu IDH1-Wildtyp Patienten (Wick et al. 2009).

Verbindung von TRPM8 mit dem Chemokinrezeptor CXCR4 und dem IK K+-Kanal. Gewebeproben von Glioblastompatienten zeigten eine positive Korrelation von TRPM8 mRNA mit der des CXCR4 Chemokinrezeptors sowie des IK K^+-Kanals (Klumpp *et al*., 2016b; Abb. 1D). Frühere Arbeiten belegen, dass IK sowohl zur Radioresistenz von Glioblastomen beiträgt (Stegen et al. 2015) als auch bei der Infiltration des Gehirns benötigt wird (Catacuzzeno et al. 2012; Cuddapah et al. 2013; D'Alessandro et al. 2013). CXCR4 wiederum wird als Biomarker für die Radioresistenz von Krebsstammzellen beschrieben und das Vorkommen dieses Rezeptors geht mit einer schlechten Prognose des Krankheitsverlaufes einher (Review siehe (Chatterjee et al. 2014; Trautmann et al. 2014)). Dies wiederum lässt die Vermutung zu, dass die Expression von TRPM8 im Zusammenhang mit einem hoch infiltrativen und radioresistenten Glioblastom Phänotyp steht. Im Gegensatz zu dieser Annahme zeigt eine kürzlich veröffentliche Studie, dass bei 33

Glioblastompatienten mit erhöhter TRPM8-Expression ein längeres Überleben dokumentiert wurde als bei Vergleichspatienten (Alptekin et al. 2015). Die in dieser Arbeit, mit Hilfe des *Cancer Genom Atlas,* erhobenen Daten, in welcher mRNAs von mehr als 500 Glioblastompatienten verglichen wurden, bestätigen diese Ergebnisse nicht (Daten nicht gezeigt).

Zusammenfassung. Die hier vorliegende *in vitro* Studie belegt eine mögliche funktionelle Signifikanz des nichtselektiven Kationenkanals TRPM8 für die Migration und die Radioresistenz von Glioblastomzellen. TRPM8 als alleiniges Target beziehungsweise in Kombination mit fraktionierter Bestrahlung eröffnet nun ein weiteres Fenster in der zukünftigen Behandlung von Glioblastompatienten. Aktuell kommen immer neuere und spezifischere pharmakologische Inhibitoren gegen TRPM8 auf den Markt (Ohmi et al. 2014; Lehto et al. 2015). Zudem werden Antikörper entwickelt, welche an extrazelluläre Domänen von TRPM8 binden und den Kanal somit blockieren (Miller et al. 2014). Diese Erkenntnisse und Errungenschaften machen eine Therapie mit TRPM8 als Target somit theoretisch möglich. Ob und inwiefern eine Therapie mit TRPM8 in Kombination oder als alleiniges Ziel Nebenwirkungen beinhaltet und ob eine Behandlung tatsächlich das Überleben von Glioblastompatienten verlängern kann, muss in kommenden, vorklinischen Studien am orthotopen Mausmodell untersucht werden.

Literaturverzeichnis

Adachi, T., H. Tanaka, S. Nonomura, H. Hara, S. Kondo and M. Hori (2014). "Plasma-Activated Medium Induces A549 Cell Injury Via a Spiral Apoptotic Cascade Involving the Mitochondrial-Nuclear Network." Free Radic Biol Med 79C: 28-44.

Alptekin, M., S. Eroglu, E. Tutar, S. Sencan, M. A. Geyik, M. Ulasli, A. T. Demiryurek and C. Camci (2015). "Gene Expressions of Trp Channels in Glioblastoma Multiforme and Relation with Survival." Tumour Biol.

Andersson, D. A., M. Nash and S. Bevan (2007). "Modulation of the Cold-Activated Channel Trpm8 by Lysophospholipids and Polyunsaturated Fatty Acids." J Neurosci 27(12): 3347-3355.

Asuthkar, S., L. Demirkhanyan, X. Sun, P. A. Elustondo, V. Krishnan, P. Baskaran, K. K. Velpula, B. Thyagarajan, E. V. Pavlov and E. Zakharian (2015). "The Trpm8 Protein Is a Testosterone Receptor: Ii. Functional Evidence for an Ionotropic Effect of Testosterone on Trpm8." J Biol Chem 290(5): 2670-2688.

Asuthkar, S., K. K. Velpula, P. A. Elustondo, L. Demirkhanyan and E. Zakharian (2015). "Trpm8 Channel as a Novel Molecular Target in Androgen-Regulated Prostate Cancer Cells." Oncotarget.

Bautista, D. M., J. Siemens, J. M. Glazer, P. R. Tsuruda, A. I. Basbaum, C. L. Stucky, S. E. Jordt and D. Julius (2007). "The Menthol Receptor Trpm8 Is the Principal Detector of Environmental Cold." Nature 448(7150): 204-208.

Bavencoffe, A., D. Gkika, A. Kondratskyi, B. Beck, A. S. Borowiec, G. Bidaux, J. Busserolles, A. Eschalier, Y. Shuba, R. Skryma and N. Prevarskaya (2010). "The Transient Receptor Potential Channel Trpm8 Is Inhibited Via the Alpha 2a Adrenoreceptor Signaling Pathway." J Biol Chem 285(13): 9410-9419.

Bavencoffe, A., A. Kondratskyi, D. Gkika, B. Mauroy, Y. Shuba, N. Prevarskaya and R. Skryma (2011). "Complex Regulation of the Trpm8 Cold Receptor Channel: Role of Arachidonic Acid Release Following M3 Muscarinic Receptor Stimulation." J Biol Chem 286(11): 9849-9855.

Berridge, M. J., M. D. Bootman and H. L. Roderick (2003). "Calcium Signalling: Dynamics, Homeostasis and Remodelling." Nat Rev Mol Cell Biol 4(7): 517-529.

Berridge, M. J., P. Lipp and M. D. Bootman (2000). "The Versatility and Universality of Calcium Signalling." Nat Rev Mol Cell Biol 1(1): 11-21.

Bidaux, G., B. Beck, A. Zholos, D. Gordienko, L. Lemonnier, M. Flourakis, M. Roudbaraki, A. S. Borowiec, J. Fernandez, P. Delcourt, G. Lepage, Y. Shuba, R. Skryma and N. Prevarskaya (2012). "Regulation of Activity of Transient Receptor Potential Melastatin 8 (Trpm8) Channel by Its Short Isoforms." J Biol Chem 287(5): 2948-2962.

Bidaux, G., M. Flourakis, S. Thebault, A. Zholos, B. Beck, D. Gkika, M. Roudbaraki, J. L. Bonnal, B. Mauroy, Y. Shuba, R. Skryma and N. Prevarskaya (2007). "Prostate Cell Differentiation Status Determines Transient Receptor Potential Melastatin Member 8 Channel Subcellular Localization and Function." J Clin Invest 117(6): 1647-1657.

Bidaux, G., M. Roudbaraki, C. Merle, A. Crepin, P. Delcourt, C. Slomianny, S. Thebault, J. L. Bonnal, M. Benahmed, F. Cabon, B. Mauroy and N. Prevarskaya (2005). "Evidence for Specific Trpm8 Expression in Human Prostate Secretory Epithelial Cells: Functional Androgen Receptor Requirement." Endocr Relat Cancer 12(2): 367-382.

Blaustein, M. P. and W. J. Lederer (1999). "Sodium/Calcium Exchange: Its Physiological Implications." Physiol Rev 79(3): 763-854.
Catacuzzeno, L., B. Fioretti and F. Franciolini (2012). "Expression and Role of the Intermediate-Conductance Calcium-Activated Potassium Channel Kca3.1 in Glioblastoma." J Signal Transduct 2012: 421564.
Chatterjee, S., B. Behnam Azad and S. Nimmagadda (2014). "The Intricate Role of Cxcr4 in Cancer." Adv Cancer Res 124: 31-82.
Cheng, J. and M. Haas (1990). "Frequent Mutations in the P53 Tumor Suppressor Gene in Human Leukemia T-Cell Lines." Mol Cell Biol 10(10): 5502-5509.
Chodon, D., A. Guilbert, I. Dhennin-Duthille, M. Gautier, M. S. Telliez, H. Sevestre and H. Ouadid-Ahidouch (2010). "Estrogen Regulation of Trpm8 Expression in Breast Cancer Cells." BMC Cancer 10: 212.
Chung, K. K., P. S. Freestone and J. Lipski (2011). "Expression and Functional Properties of Trpm2 Channels in Dopaminergic Neurons of the Substantia Nigra of the Rat." J Neurophysiol 106(6): 2865-2875.
Clapham, D. E. (2003). "Trp Channels as Cellular Sensors." Nature 426(6966): 517-524.
Clapham, D. E., D. Julius, C. Montell and G. Schultz (2005). "International Union of Pharmacology. Xlix. Nomenclature and Structure-Function Relationships of Transient Receptor Potential Channels." Pharmacol Rev 57(4): 427-450.
Clark, K., J. Middelbeek, N. A. Morrice, C. G. Figdor, E. Lasonder and F. N. van Leeuwen (2008). "Massive Autophosphorylation of the Ser/Thr-Rich Domain Controls Protein Kinase Activity of Trpm6 and Trpm7." PLoS One 3(3): e1876.
Craven, K. B. and W. N. Zagotta (2006). "Cng and Hcn Channels: Two Peas, One Pod." Annu Rev Physiol 68: 375-401.
Cuddapah, V. A., C. W. Habela, S. Watkins, L. S. Moore, T. T. Barclay and H. Sontheimer (2012). "Kinase Activation of Clc-3 Accelerates Cytoplasmic Condensation During Mitotic Cell Rounding." Am J Physiol Cell Physiol 302(3): C527-538.
Cuddapah, V. A. and H. Sontheimer (2010). "Molecular Interaction and Functional Regulation of Clc-3 by Ca2+/Calmodulin-Dependent Protein Kinase Ii (Camkii) in Human Malignant Glioma." J Biol Chem 285(15): 11188-11196.
Cuddapah, V. A., K. L. Turner, S. Seifert and H. Sontheimer (2013). "Bradykinin-Induced Chemotaxis of Human Gliomas Requires the Activation of Kca3.1 and Clc-3." J Neurosci 33(4): 1427-1440.
D'Alessandro, G., M. Catalano, M. Sciaccaluga, G. Chece, R. Cipriani, M. Rosito, A. Grimaldi, C. Lauro, G. Cantore, A. Santoro, B. Fioretti, F. Franciolini, H. Wulff and C. Limatola (2013). "Kca3.1 Channels Are Involved in the Infiltrative Behavior of Glioblastoma in Vivo." Cell Death Dis 4: e773.
Dhennin-Duthille, I., M. Gautier, M. Faouzi, A. Guilbert, M. Brevet, D. Vaudry, A. Ahidouch, H. Sevestre and H. Ouadid-Ahidouch (2011). "High Expression of Transient Receptor Potential Channels in Human Breast Cancer Epithelial Cells and Tissues: Correlation with Pathological Parameters." Cell Physiol Biochem 28(5): 813-822.
Dittmann, K., C. Mayer, H. P. Rodemann and S. M. Huber (2013). "Egfr Cooperates with Glucose Transporter Sglt1 to Enable Chromatin Remodeling in Response to Ionizing Radiation." Radiother Oncol 107(2): 247-251.
Dolle, C., J. G. Rack and M. Ziegler (2013). "Nad and Adp-Ribose Metabolism in Mitochondria." FEBS J 280(15): 3530-3541.
Duncan, L. M., J. Deeds, J. Hunter, J. Shao, L. M. Holmgren, E. A. Woolf, R. I. Tepper and A. W. Shyjan (1998). "Down-Regulation of the Novel Gene

Melastatin Correlates with Potential for Melanoma Metastasis." Cancer Res 58(7): 1515-1520.

Eisfeld, J. and A. Luckhoff (2007). "Trpm2." Handb Exp Pharmacol(179): 237-252.

Fonfria, E., I. C. Marshall, C. D. Benham, I. Boyfield, J. D. Brown, K. Hill, J. P. Hughes, S. D. Skaper and S. McNulty (2004). "Trpm2 Channel Opening in Response to Oxidative Stress Is Dependent on Activation of Poly(Adp-Ribose) Polymerase." Br J Pharmacol 143(1): 186-192.

Gaudet, R. (2008). "Trp Channels Entering the Structural Era." J Physiol 586(Pt 15): 3565-3575.

Gaudet, R. (2009). "Divide and Conquer: High Resolution Structural Information on Trp Channel Fragments." J Gen Physiol 133(3): 231-237.

Gees, M., B. Colsoul and B. Nilius (2010). "The Role of Transient Receptor Potential Cation Channels in Ca2+ Signaling." Cold Spring Harb Perspect Biol 2(10): a003962.

Gkika, D., L. Lemonnier, G. Shapovalov, D. Gordienko, C. Poux, M. Bernardini, A. Bokhobza, G. Bidaux, C. Degerny, K. Verreman, B. Guarmit, M. Benahmed, Y. de Launoit, R. J. Bindels, A. Fiorio Pla and N. Prevarskaya (2015). "Trp Channel-Associated Factors Are a Novel Protein Family That Regulates Trpm8 Trafficking and Activity." J Cell Biol 208(1): 89-107.

Halliwell, B. (2006). "Oxidative Stress and Neurodegeneration: Where Are We Now?" J Neurochem 97(6): 1634-1658.

Hara, Y., M. Wakamori, M. Ishii, E. Maeno, M. Nishida, T. Yoshida, H. Yamada, S. Shimizu, E. Mori, J. Kudoh, N. Shimizu, H. Kurose, Y. Okada, K. Imoto and Y. Mori (2002). "Ltrpc2 Ca2+-Permeable Channel Activated by Changes in Redox Status Confers Susceptibility to Cell Death." Mol Cell 9(1): 163-173.

Harteneck, C. (2005). "Function and Pharmacology of Trpm Cation Channels." Naunyn Schmiedebergs Arch Pharmacol 371(4): 307-314.

Harteneck, C., T. D. Plant and G. Schultz (2000). "From Worm to Man: Three Subfamilies of Trp Channels." Trends Neurosci 23(4): 159-166.

Heiner, I., J. Eisfeld and A. Luckhoff (2003). "Role and Regulation of Trp Channels in Neutrophil Granulocytes." Cell Calcium 33(5-6): 533-540.

Heise, N., D. Palme, M. Misovic, S. Koka, J. Rudner, F. Lang, H. R. Salih, S. M. Huber and G. Henke (2010). "Non-Selective Cation Channel-Mediated Ca2+-Entry and Activation of Ca2+/Calmodulin-Dependent Kinase Ii Contribute to G2/M Cell Cycle Arrest and Survival of Irradiated Leukemia Cells." Cell Physiol Biochem (in press).

Hill, K., S. McNulty and A. D. Randall (2004). "Inhibition of Trpm2 Channels by the Antifungal Agents Clotrimazole and Econazole." Naunyn Schmiedebergs Arch Pharmacol 370(4): 227-237.

Huber, S. M. (2013). "Oncochannels." Cell Calcium 53(4): 241-255.

Huber, S. M., L. Butz, B. Stegen, D. Klumpp, N. Braun, P. Ruth and F. Eckert (2013). "Ionizing Radiation, Ion Transports, and Radioresistance of Cancer Cells." Front Physiol 4: 212.

Huber, S. M., M. Misovic, C. Mayer, H. P. Rodemann and K. Dittmann (2012). "Egfr-Mediated Stimulation of Sodium/Glucose Cotransport Promotes Survival of Irradiated Human A549 Lung Adenocarcinoma Cells." Radiother Oncol 103(3): 373-379.

Hunter, J. J., J. Shao, J. S. Smutko, B. J. Dussault, D. L. Nagle, E. A. Woolf, L. M. Holmgren, K. J. Moore and A. W. Shyjan (1998). "Chromosomal Localization and Genomic Characterization of the Mouse Melastatin Gene (Mlsn1)." Genomics 54(1): 116-123.

Hussain, A. and G. Inesi (1999). "Involvement of Sarco/Endoplasmic Reticulum Ca(2+) Atpases in Cell Function and the Cellular Consequences of Their Inhibition." J Membr Biol 172(2): 91-99.

Inamura, K., Y. Sano, S. Mochizuki, H. Yokoi, A. Miyake, K. Nozawa, C. Kitada, H. Matsushime and K. Furuichi (2003). "Response to Adp-Ribose by Activation of Trpm2 in the Cri-G1 Insulinoma Cell Line." J Membr Biol 191(3): 201-207.

Ishii, M., A. Oyama, T. Hagiwara, A. Miyazaki, Y. Mori, Y. Kiuchi and S. Shimizu (2007). "Facilitation of H2o2-Induced A172 Human Glioblastoma Cell Death by Insertion of Oxidative Stress-Sensitive Trpm2 Channels." Anticancer Res 27(6B): 3987-3992.

Kirkland, R. A., G. M. Saavedra, B. S. Cummings and J. L. Franklin (2010). "Bax Regulates Production of Superoxide in Both Apoptotic and Nonapoptotic Neurons: Role of Caspases." J Neurosci 30(48): 16114-16127.

Klumpp, D., M. Misovic, K. Szteyn, E. Shumilina, J. Rudner and S. M. Huber (2016a). "Targeting Trpm2 Channels Impairs Radiation-Induced Cell Cycle Arrest and Fosters Cell Death of T Cell Leukemia Cells in a Bcl-2-Dependent Manner." Oxidative Medicine and Cellular Longevity (in press).

Kraft, R., C. Grimm, H. Frenzel and C. Harteneck (2006). "Inhibition of Trpm2 Cation Channels by N-(P-Amylcinnamoyl)Anthranilic Acid." Br J Pharmacol 148(3): 264-273.

Lehto, S. G., A. D. Weyer, M. Zhang, B. D. Youngblood, J. Wang, W. Wang, P. C. Kerstein, C. Davis, K. D. Wild, C. L. Stucky and N. R. Gavva (2015). "Amg2850, a Potent and Selective Trpm8 Antagonist, Is Not Effective in Rat Models of Inflammatory Mechanical Hypersensitivity and Neuropathic Tactile Allodynia." Naunyn Schmiedebergs Arch Pharmacol 388(4): 465-476.

Li, Q., X. Wang, Z. Yang, B. Wang and S. Li (2009). "Menthol Induces Cell Death Via the Trpm8 Channel in the Human Bladder Cancer Cell Line T24." Oncology 77(6): 335-341.

Liu, X., Y. Chang, P. H. Reinhart, H. Sontheimer and Y. Chang (2002). "Cloning and Characterization of Glioma Bk, a Novel Bk Channel Isoform Highly Expressed in Human Glioma Cells." J Neurosci 22(5): 1840-1849.

Mandadi, S., P. J. Armati and B. D. Roufogalis (2011). "Protein Kinase C Modulation of Thermo-Sensitive Transient Receptor Potential Channels: Implications for Pain Signaling." J Nat Sci Biol Med 2(1): 13-25.

McHugh, D., R. Flemming, S. Z. Xu, A. L. Perraud and D. J. Beech (2003). "Critical Intracellular Ca2+ Dependence of Transient Receptor Potential Melastatin 2 (Trpm2) Cation Channel Activation." J Biol Chem 278(13): 11002-11006.

Mergler, S., M. Z. Strowski, S. Kaiser, T. Plath, Y. Giesecke, M. Neumann, H. Hosokawa, S. Kobayashi, J. Langrehr, P. Neuhaus, U. Plockinger, B. Wiedenmann and C. Grotzinger (2007). "Transient Receptor Potential Channel Trpm8 Agonists Stimulate Calcium Influx and Neurotensin Secretion in Neuroendocrine Tumor Cells." Neuroendocrinology 85(2): 81-92.

Miller, S., S. Rao, W. Wang, H. Liu, J. Wang and N. R. Gavva (2014). "Antibodies to the Extracellular Pore Loop of Trpm8 Act as Antagonists of Channel Activation." PLoS One 9(9): e107151.

Monaco, G., T. Vervliet, H. Akl and G. Bultynck (2013). "The Selective Bh4-Domain Biology of Bcl-2-Family Members: Ip3rs and Beyond." Cell Mol Life Sci 70(7): 1171-1183.

Montell, C. (2005). "The Trp Superfamily of Cation Channels." Sci STKE 2005(272): re3.

Morgan, K., L. R. Sadofsky, C. Crow and A. H. Morice (2014). "Human Trpm8 and Trpa1 Pain Channels, Including a Gene Variant with Increased Sensitivity to Agonists (Trpa1 R797t), Exhibit Differential Regulation by Src-Tyrosine Kinase Inhibitor." Biosci Rep 34(4).

Nagamine, K., J. Kudoh, S. Minoshima, K. Kawasaki, S. Asakawa, F. Ito and N. Shimizu (1998). "Molecular Cloning of a Novel Putative Ca2+ Channel Protein (Trpc7) Highly Expressed in Brain." Genomics 54(1): 124-131.

Naziroglu, M. (2007). "New Molecular Mechanisms on the Activation of Trpm2 Channels by Oxidative Stress and Adp-Ribose." Neurochem Res 32(11): 1990-2001.

Naziroglu, M. and A. Luckhoff (2008). "A Calcium Influx Pathway Regulated Separately by Oxidative Stress and Adp-Ribose in Trpm2 Channels: Single Channel Events." Neurochem Res 33(7): 1256-1262.

Naziroglu, M. and A. Luckhoff (2008). "Effects of Antioxidants on Calcium Influx through Trpm2 Channels in Transfected Cells Activated by Hydrogen Peroxide." J Neurol Sci 270(1-2): 152-158.

Naziroglu, M., A. Luckhoff and E. Jungling (2007). "Antagonist Effect of Flufenamic Acid on Trpm2 Cation Channels Activated by Hydrogen Peroxide." Cell Biochem Funct 25(4): 383-387.

Nilius, B. and G. Owsianik (2011). "The Transient Receptor Potential Family of Ion Channels." Genome Biol 12(3): 218.

Nilius, B., G. Owsianik, T. Voets and J. A. Peters (2007). "Transient Receptor Potential Cation Channels in Disease." Physiol Rev 87(1): 165-217.

Nilius, B. and A. Szallasi (2014). "Transient Receptor Potential Channels as Drug Targets: From the Science of Basic Research to the Art of Medicine." Pharmacol Rev 66(3): 676-814.

Nilius, B. and T. Voets (2004). "Diversity of Trp Channel Activation." Novartis Found Symp 258: 140-149; discussion 149-159, 263-146.

Oakes, S. A., J. T. Opferman, T. Pozzan, S. J. Korsmeyer and L. Scorrano (2003). "Regulation of Endoplasmic Reticulum Ca2+ Dynamics by Proapoptotic Bcl-2 Family Members." Biochem Pharmacol 66(8): 1335-1340.

Ohmi, M., Y. Shishido, T. Inoue, K. Ando, A. Fujiuchi, A. Yamada, S. Watanabe and K. Kawamura (2014). "Identification of a Novel 2-Pyridyl-Benzensulfonamide Derivative, Rq-00203078, as a Selective and Orally Active Trpm8 Antagonist." Bioorg Med Chem Lett 24(23): 5364-5368.

Okamoto, Y., T. Ohkubo, T. Ikebe and J. Yamazaki (2012). "Blockade of Trpm8 Activity Reduces the Invasion Potential of Oral Squamous Carcinoma Cell Lines." Int J Oncol 40(5): 1431-1440.

Orfanelli, U., A. K. Wenke, C. Doglioni, V. Russo, A. K. Bosserhoff and G. Lavorgna (2008). "Identification of Novel Sense and Antisense Transcription at the Trpm2 Locus in Cancer." Cell Res 18(11): 1128-1140.

Palme, D., M. Misovic, E. Schmid, D. Klumpp, H. R. Salih, J. Rudner and S. M. Huber (2013). "Kv3.4 Potassium Channel-Mediated Electrosignaling Controls Cell Cycle and Survival of Irradiated Leukemia Cells." Pflugers Arch 465(8): 1209-1221.

Parkash, J. and K. Asotra (2010). "Calcium Wave Signaling in Cancer Cells." Life Sci 87(19-22): 587-595.

Perraud, A. L., A. Fleig, C. A. Dunn, L. A. Bagley, P. Launay, C. Schmitz, A. J. Stokes, Q. Zhu, M. J. Bessman, R. Penner, J. P. Kinet and A. M. Scharenberg (2001). "Adp-Ribose Gating of the Calcium-Permeable Ltrpc2 Channel Revealed by Nudix Motif Homology." Nature 411(6837): 595-599.

Perraud, A. L., C. L. Takanishi, B. Shen, S. Kang, M. K. Smith, C. Schmitz, H. M. Knowles, D. Ferraris, W. Li, J. Zhang, B. L. Stoddard and A. M. Scharenberg (2005). "Accumulation of Free Adp-Ribose from Mitochondria Mediates Oxidative Stress-Induced Gating of Trpm2 Cation Channels." J Biol Chem 280(7): 6138-6148.

Pinton, P. and R. Rizzuto (2006). "Bcl-2 and Ca2+ Homeostasis in the Endoplasmic Reticulum." Cell Death Differ 13(8): 1409-1418.

Prevarskaya, N., R. Skryma and Y. Shuba (2010). "Ion Channels and the Hallmarks of Cancer." Trends Mol Med 16(3): 107-121.

Quallo, T., N. Vastani, E. Horridge, C. Gentry, A. Parra, S. Moss, F. Viana, C. Belmonte, D. A. Andersson and S. Bevan (2015). "Trpm8 Is a Neuronal Osmosensor That Regulates Eye Blinking in Mice." Nat Commun 6: 7150.

Ransom, C. B., X. Liu and H. Sontheimer (2002). "Bk Channels in Human Glioma Cells Have Enhanced Calcium Sensitivity." Glia 38(4): 281-291.

Ransom, C. B. and H. Sontheimer (2001). "Bk Channels in Human Glioma Cells." J Neurophysiol 85(2): 790-803.

Rohacs, T. and B. Nilius (2007). "Regulation of Transient Receptor Potential (Trp) Channels by Phosphoinositides." Pflugers Arch 455(1): 157-168.

Rudner, J., V. Jendrossek and C. Belka (2002). "New Insights in the Role of Bcl-2 Bcl-2 and the Endoplasmic Reticulum." Apoptosis 7(5): 441-447.

Stegen, B., L. Butz, L. Klumpp, D. Zips, K. Dittmann, P. Ruth and S. M. Huber (2015). "Ca2+-Activated Ik K+ Channel Blockade Radiosensitizes Glioblastoma Cells." Mol Cancer Res.

Steinhardt, R. A. and J. Alderton (1988). "Intracellular Free Calcium Rise Triggers Nuclear Envelope Breakdown in the Sea Urchin Embryo." Nature 332(6162): 364-366.

Steinle, M., D. Palme, M. Misovic, J. Rudner, K. Dittmann, R. Lukowski, P. Ruth and S. M. Huber (2011). "Ionizing Radiation Induces Migration of Glioblastoma Cells by Activating Bk K(+) Channels." Radiother Oncol 101(1): 122-126.

Stewart, T. A., K. T. Yapa and G. R. Monteith (2014). "Altered Calcium Signaling in Cancer Cells." Biochim Biophys Acta.

Stupp, R., M. E. Hegi, W. P. Mason, M. J. van den Bent, M. J. Taphoorn, R. C. Janzer, S. K. Ludwin, A. Allgeier, B. Fisher, K. Belanger, P. Hau, A. A. Brandes, J. Gijtenbeek, C. Marosi, C. J. Vecht, K. Mokhtari, P. Wesseling, S. Villa, E. Eisenhauer, T. Gorlia, M. Weller, D. Lacombe, J. G. Cairncross, R. O. Mirimanoff, R. European Organisation for, T. Treatment of Cancer Brain, G. Radiation Oncology and G. National Cancer Institute of Canada Clinical Trials (2009). "Effects of Radiotherapy with Concomitant and Adjuvant Temozolomide Versus Radiotherapy Alone on Survival in Glioblastoma in a Randomised Phase Iii Study: 5-Year Analysis of the Eortc-Ncic Trial." Lancet Oncol 10(5): 459-466.

Tang, M., G. Y. Wu, X. Z. Dong and Z. X. Tang (2015). "Phosphoinositide Interacting Regulator of Trp (Pirt) Enhances Trpm8 Channel Activity in Vitro Via Increasing Channel Conductance." Acta Pharmacol Sin.

Taylor, J. T., X. B. Zeng, J. E. Pottle, K. Lee, A. R. Wang, S. G. Yi, J. A. Scruggs, S. S. Sikka and M. Li (2008). "Calcium Signaling and T-Type Calcium Channels in Cancer Cell Cycling." World J Gastroenterol 14(32): 4984-4991.

Tominaga, M. and M. J. Caterina (2004). "Thermosensation and Pain." J Neurobiol 61(1): 3-12.

Trautmann, F., M. Cojoc, I. Kurth, N. Melin, L. C. Bouchez, A. Dubrovska and C. Peitzsch (2014). "Cxcr4 as Biomarker for Radioresistant Cancer Stem Cells." Int J Radiat Biol 90(8): 687-699.

Tsavaler, L., M. H. Shapero, S. Morkowski and R. Laus (2001). "Trp-P8, a Novel Prostate-Specific Gene, Is up-Regulated in Prostate Cancer and Other Malignancies and Shares High Homology with Transient Receptor Potential Calcium Channel Proteins." Cancer Res 61(9): 3760-3769.

Vanden Abeele, F., A. Zholos, G. Bidaux, Y. Shuba, S. Thebault, B. Beck, M. Flourakis, Y. Panchin, R. Skryma and N. Prevarskaya (2006). "Ca2+-Independent Phospholipase A2-Dependent Gating of Trpm8 by Lysophospholipids." J Biol Chem 281(52): 40174-40182.

Vay, L., C. Gu and P. A. McNaughton (2012). "The Thermo-Trp Ion Channel Family: Properties and Therapeutic Implications." Br J Pharmacol 165(4): 787-801.

Vennekens, R., G. Owsianik and B. Nilius (2008). "Vanilloid Transient Receptor Potential Cation Channels: An Overview." Curr Pharm Des 14(1): 18-31.

Volpe, P., B. H. Alderson-Lang, L. Madeddu, E. Damiani, J. H. Collins and A. Margreth (1990). "Calsequestrin, a Component of the Inositol 1,4,5-Trisphosphate-Sensitive Ca2+ Store of Chicken Cerebellum." Neuron 5(5): 713-721.

Watanabe, H., M. Murakami, T. Ohba, Y. Takahashi and H. Ito (2008). "Trp Channel and Cardiovascular Disease." Pharmacol Ther 118(3): 337-351.

Wick, W., C. Hartmann, C. Engel, M. Stoffels, J. Felsberg, F. Stockhammer, M. C. Sabel, S. Koeppen, R. Ketter, R. Meyermann, M. Rapp, C. Meisner, R. D. Kortmann, T. Pietsch, O. D. Wiestler, U. Ernemann, M. Bamberg, G. Reifenberger, A. von Deimling and M. Weller (2009). "Noa-04 Randomized Phase Iii Trial of Sequential Radiochemotherapy of Anaplastic Glioma with Procarbazine, Lomustine, and Vincristine or Temozolomide." J Clin Oncol 27(35): 5874-5880.

Wondergem, R. and J. W. Bartley (2009). "Menthol Increases Human Glioblastoma Intracellular Ca2+, Bk Channel Activity and Cell Migration." J Biomed Sci 16: 90.

Wondergem, R., T. W. Ecay, F. Mahieu, G. Owsianik and B. Nilius (2008). "Hgf/Sf and Menthol Increase Human Glioblastoma Cell Calcium and Migration." Biochem Biophys Res Commun 372(1): 210-215.

Wu, L. J., T. B. Sweet and D. E. Clapham (2010). "International Union of Basic and Clinical Pharmacology. Lxxvi. Current Progress in the Mammalian Trp Ion Channel Family." Pharmacol Rev 62(3): 381-404.

Yamamura, H., S. Ugawa, T. Ueda, A. Morita and S. Shimada (2008). "Trpm8 Activation Suppresses Cellular Viability in Human Melanoma." Am J Physiol Cell Physiol 295(2): C296-301.

Yee, N. S., A. S. Chan, J. D. Yee and R. K. Yee (2012). "Trpm7 and Trpm8 Ion Channels in Pancreatic Adenocarcinoma: Potential Roles as Cancer Biomarkers and Targets." Scientifica (Cairo) 2012: 415158.

Yee, N. S., W. Zhou and M. Lee (2010). "Transient Receptor Potential Channel Trpm8 Is over-Expressed and Required for Cellular Proliferation in Pancreatic Adenocarcinoma." Cancer Lett 297(1): 49-55.

Yu, X., Y. Jiang, W. Wei, P. Cong, Y. Ding, L. Xiang and K. Wu (2015). "Androgen Receptor Signaling Regulates Growth of Glioblastoma Multiforme in Men." Tumour Biol 36(2): 967-972.

Yudin, Y. and T. Rohacs (2012). "Regulation of Trpm8 Channel Activity." Mol Cell Endocrinol 353(1-2): 68-74.

Zeng, X., S. C. Sikka, L. Huang, C. Sun, C. Xu, D. Jia, A. B. Abdel-Mageed, J. E. Pottle, J. T. Taylor and M. Li (2010). "Novel Role for the Transient Receptor Potential Channel Trpm2 in Prostate Cancer Cell Proliferation." Prostate Cancer Prostatic Dis 13(2): 195-201.

Zhang, L. and G. J. Barritt (2004). "Evidence That Trpm8 Is an Androgen-Dependent Ca2+ Channel Required for the Survival of Prostate Cancer Cells." Cancer Res 64(22): 8365-8373.

Zhang, W., X. Chu, Q. Tong, J. Y. Cheung, K. Conrad, K. Masker and B. A. Miller (2003). "A Novel Trpm2 Isoform Inhibits Calcium Influx and Susceptibility to Cell Death." J Biol Chem 278(18): 16222-16229.

Zhang, W., I. Hirschler-Laszkiewicz, Q. Tong, K. Conrad, S. C. Sun, L. Penn, D. L. Barber, R. Stahl, D. J. Carey, J. Y. Cheung and B. A. Miller (2006). "Trpm2 Is an Ion Channel That Modulates Hematopoietic Cell Death through Activation of Caspases and Parp Cleavage." Am J Physiol Cell Physiol 290(4): C1146-1159.

Anhang – Publikationen

Akzeptierte Publikationen

Klumpp, D., M. Misovic, K. Szteyn, E. Shumilina, J. Rudner and S. M. Huber (2016). "Targeting Trpm2 Channels Impairs Radiation-Induced Cell Cycle Arrest and Fosters Cell Death of T Cell Leukemia Cells in a Bcl-2-Dependent Manner." Oxidative Medicine and Cellular Longevity (in press).

Braun, N., D. Klumpp, J. Hennenlotter, J. Bedke, C. Duranton, M. Bleif, SM. Huber (2015). "UCP-3 uncoupling protein confers hypoxia resistance to renal epithelial cells and is upregulated in renal cell carcinoma." Sci. Rep. 5: 13450.

Huber, SM., L. Butz, B. Stegen, L. Klumpp, D. Klumpp, F. Eckert (2014). "Role of ion channels in ionizing radiation-induced cell death." Biochim Biophys Acta. 1848: 2657-64

Huber, S. M., L. Butz, B. Stegen, D. Klumpp, N. Braun, P. Ruth and F. Eckert (2013). "Ionizing Radiation, Ion Transports, and Radioresistance of Cancer Cells." Front Physiol 4: 212.

Palme, D., M. Misovic, E. Schmid, D. Klumpp, H. R. Salih, J. Rudner and S. M. Huber (2013). "Kv3.4 Potassium Channel-Mediated Electrosignaling Controls Cell Cycle and Survival of Irradiated Leukemia Cells." Pflugers Arch 465(8): 1209-1221.

Eingereichte Manuskripte

Stegen, B., L. Klumpp, M. Misovic, L. Edalat, M. Eckert, D. Klumpp, P. Ruth, SM. Huber (2016) K^+ channels signaling in irradiated tumor cells (submitted)

Klumpp, D., SC. Frank, L. Klumpp, M. Eckert, L. Edalat, M. Bastmeyer, P. Ruth, SM. Huber. "TRPM8-mediated Ca^{2+}-signaling confers radioresistance and promotes migration of glioblastoma cells." Radiotherapy and Oncology (submitted)

Danksagung

Zuerst möchte ich mich bei Prof. Dr. Stephan Huber bedanken. Nicht nur für das interessante Thema welches er mir zur Verfügung gestellt hat sondern auch dafür in der AG Huber arbeiten zu dürfen. Die Atmosphäre, die Unterstützung und die Möglichkeit bei Problemen, auch ohne Termin, zu ihm zu kommen, trugen maßgeblich zum Erfolg dieser Doktorarbeit bei.

Mein zweiter Dank gebührt Prof. Dr. Peter Ruth, der sich dazu bereit erklärt hat, mein Doktorvater sowie Zweitgutachter zu sein.

Bedanken möchte ich mich auch bei den Professoren … und …, die sich als Prüfer für die Promotionsprüfung zur Verfügung gestellt haben.

Ein großer Dank geht auch an die gesamte AG Huber für die Unterstützung und Hilfsbereitschaft die mir zu Teil wurde. Allen voran den beiden technischen Assistentinnen Heidrun Faltin und Ilka Müller, den guten Seelen des Labors. Meinen Mitstreitern Benjamin, Lukas, Ivan und Erik danke ich für die Hilfe und die Zeit die wir gemeinsam verbrachten. Es war mir eine Freude.

Ein weiteres Dankeschön an Steffi, Kadda und Lukas für das fleißige Korrekturlesen.

Meinen Freunden und Familie danke ich ebenfalls für die Unterstützung - egal in welcher Hinsicht. Ohne euch wäre ich nicht das was ich bin.

Zu guter Letzt ein besonderes Dankeschön an meine Freundin Steffi. Oft hat sie mich motiviert, wenn wieder einmal nichts so funktioniert hat wie es sollte. Zusammen mit dir konnte ich dieses Kapitel erfolgreich abschließen und freue mich auf die vielen die noch kommen werden. Vielen Dank für alles.

Hindawi Publishing Corporation
Oxidative Medicine and Cellular Longevity
Volume 2016, Article ID 8026702, 14 pages
http://dx.doi.org/10.1155/2016/8026702

Research Article

Targeting TRPM2 Channels Impairs Radiation-Induced Cell Cycle Arrest and Fosters Cell Death of T Cell Leukemia Cells in a Bcl-2-Dependent Manner

Dominik Klumpp,[1] Milan Misovic,[1] Kalina Szteyn,[2,3] Ekaterina Shumilina,[2] Justine Rudner,[4] and Stephan M. Huber[1]

[1]*Department of Radiation Oncology, University of Tübingen, 72076 Tübingen, Germany*
[2]*Department of Physiology, University of Tübingen, 72076 Tübingen, Germany*
[3]*Department of Oral & Maxillofacial Surgery, The University of Texas Health Science Center, San Antonio, TX 78229, USA*
[4]*Institute for Cell Biology (Cancer Research), University Hospital Essen, University of Duisburg-Essen, 45122 Essen, Germany*

Correspondence should be addressed to Stephan M. Huber; stephan.huber@uni-tuebingen.de

Received 22 June 2015; Accepted 15 October 2015

Academic Editor: Lokesh Deb

Messenger RNA data of lymphohematopoietic cancer lines suggest a correlation between expression of the cation channel TRPM2 and the antiapoptotic protein Bcl-2. The latter is overexpressed in various tumor entities and mediates therapy resistance. Here, we analyzed the crosstalk between Bcl-2 and TRPM2 channels in T cell leukemia cells during oxidative stress as conferred by ionizing radiation (IR). To this end, the effects of TRPM2 inhibition or knock-down on plasma membrane currents, Ca^{2+} signaling, mitochondrial superoxide anion formation, and cell cycle progression were compared between irradiated (0–10 Gy) Bcl-2-overexpressing and empty vector-transfected Jurkat cells. As a result, IR stimulated a TRPM2-mediated Ca^{2+}-entry, which was higher in Bcl-2-overexpressing than in control cells and which contributed to IR-induced G_2/M cell cycle arrest. TRPM2 inhibition induced a release from G_2/M arrest resulting in cell death. Collectively, this data suggests a pivotal function of TRPM2 in the DNA damage response of T cell leukemia cells. Apoptosis-resistant Bcl-2-overexpressing cells even can afford higher TRPM2 activity without risking a hazardous Ca^{2+}-overload-induced mitochondrial superoxide anion formation.

1. Introduction

Transient Receptor Potential (TRP) Cation Channels. The TRP superfamily comprises a diverse range of Ca^{2+}-permeable cation channels [1]. TRP channels contribute to changes in cytosolic free Ca^{2+} ($_{free}[Ca^{2+}]_i$) by directly acting as Ca^{2+} entry channels in the plasma membrane or by changing membrane potentials, modulating the activity and/or driving forces for the Ca^{2+} entry channels [2]. The melastatin subfamily (TRPM) has been subdivided into three subgroups on the basis of sequence homology (TRPM1/TRPM3, TRPM4/TRPM5, and TRPM6/7) with TRPM8 and TRPM2 being distinct proteins [3]. The Ca^{2+}-permeable TRPM2 channels, formerly known as TRPC2 and LTRPC2, were first identified in 1998 [4]. Reactive oxygen species (ROS) have been demonstrated to induce TRPM2 currents and increase $_{free}[Ca^{2+}]_i$ in various cell types transfected with TRPM2 [5], as well as in pancreatic β-cells [6], neutrophil granulocytes [7], and U937 monocytes [8].

TRPM2 and Cell Death. By increasing $_{free}[Ca^{2+}]_i$, TRPM2 may increase the susceptibility to cell death suggesting that TRPM2 channels function as "death channels." As a matter of fact, heterologous expression of TRPM2 in human embryonic kidney cells [9] or A172 human glioblastoma cells [10] facilitates oxidative stress-induced cell death. Moreover, expression of TRPM2 has been demonstrated in several tumor entities such as insulinoma [6], hepatocellular carcinoma [6],

prostate cancer [11], lymphoma [12], leukemia [13], and lung cancer cell lines [14] in which TRPM2 reportedly may foster cell death [15].

Ca^{2+}-Signaling by TRPM2, Bcl-2, and Mitochondria. ROS-induced TRPM2 channel activation most probably occurs indirectly via formation of adenosine diphosphate ribose (ADPR) which activates the channel by binding to a special domain located at the C-terminus of the channel [16]. ADP-ribose polymers are formed during DNA damage response by poly(ADP-ribose) polymerases (PARPs). Upon DNA repair ADPR is released from the ADPR polymers by glycohydrolases [17, 18]. Another main source of ADPR is the mitochondria [19].

Mitochondrial Ca^{2+} absorbance exerts Ca^{2+} buffering function (for review see [20]). The mitochondrial respiratory chain and the mitochondrial permeability transition pore (PTP) are regulated by Ca^{2+}. Moderate mitochondrial Ca^{2+} increase may disinhibit the respiratory chain leading to $\Delta\Psi_m$ hyperpolarisation [21] which in turn is accompanied by increasing superoxide anion formation [22]. Mitochondrial Ca^{2+} overload, in contrast, opens the PTP leading to $\Delta\Psi_m$ dissipation, cytochrome C release, and apoptotic cell death [20].

The antiapoptotic protein Bcl-2 is a key player in cellular Ca^{2+} homeostasis. In some cell models, overexpression of Bcl-2 reportedly may increase the Ca^{2+} leakage through IP_3 receptor subtypes in the ER membrane and decrease the ER Ca^{2+} filling. More recent studies, in contrast, suggest an inhibition of IP_3-receptor-mediated Ca^{2+} release by Bcl-2. Like Bcl-2-caused Ca^{2+} store depletion, Bcl-2-mediated IP_3-receptor inhibition is thought to prevent proapoptotic bulk Ca^{2+} release from the ER (for review see [23–26]).

Direct and Indirect Oxidative Stress Conferred by Ionizing Radiation. Most energy of ionizing radiation (IR) is absorbed by cell water leading to formation of hydroxyl radicals (for review see [27]). Oxidative stress- and DNA repair-associated release of ADP-ribose is supposed to increase the plasma membrane Ca^{2+} permeability by activating TRPM2 channels. Subsequent changes in ${}_{\text{free}}[Ca^{2+}]_i$ and mitochondrial function are under the control of Bcl-2. Together, this hints to a crosstalk between Ca^{2+} and ROS signaling involving TRPM2 Ca^{2+}-permeable channels in the plasma membrane, the Ca^{2+}-regulated $\Delta\Psi_m$ across the inner mitochondrial membrane, and the antiapoptotic protein Bcl-2 in the ER and outer mitochondrial membrane of irradiated cells.

Aim of the Study. The present study aimed to define this crosstalk in human T cell leukemia cells subjected to ionizing radiation. To this end, Jurkat cells stably transfected with Bcl-2 or the empty control vector were irradiated with 0, 5, or 10 Gy by 6 MV photons. Ion channel activity, Ca^{2+} signaling, mitochondrial superoxide anion formation, cell cycle control, and cell death were assessed by patch-clamp whole-cell recording, fura-2 Ca^{2+} imaging, immunoblotting, and flow cytometry in irradiated and nonirradiated cells, respectively. In addition, mRNA data of hematopoietic and lymphoid tissue cancer cell lines of the Novartis and Broad Institute Cancer Cell Line Encyclopedia were queried for TRPM2 and Bcl-2 mRNA abundance.

2. Material and Methods

2.1. Cell Culture. Jurkat E6.1 T cell leukemia cells were from ATCC (Bethesda, Maryland, USA). Jurkat cells stably expressing Bcl-2 (Jurkat-Bcl-2) or a control vector (Jurkat-vector) were prepared as described before [28, 29]. Inducible Bcl-2 transfectants were generated as described [30]. To suppress Bcl-2 expression in Tet-off Jurkat cells, Bcl-2 transfectants were treated with 1 μg/mL doxycycline (Clontech, Heidelberg, Germany) for 48 h. As control cells, the maternal Jurkat Tet-off cells were used. Cells were grown in RPMI 1640 medium supplemented with 10% fetal calf serum (Gibco Life Technologies, Eggenstein, Germany) and maintained in a humidified incubator at 37°C and 5% CO_2.

2.2. Transfection with siRNA. Transfection with siRNA was performed as described [31]. In brief, cells were cultured at a low density to ensure log phase growth. For transfection, 2×10^6 cells were resuspended in 200 μL RPMI 1640 without phenol red. Shortly before transfection, TRPM2 or nontargeting siRNA was added at a concentration of 1 μM. TRPM2 ON-TARGET SMARTpool and the siCONTROL NON-TARGETING pool siRNA were purchased from Dharmacon (Chicago, IL, USA). Cells were electroporated in a 4 mm cuvette in an EPI2500 electroporator (Fischer, Heidelberg, Germany) at 370 V for 10 ms. Immediately after transfection, cells were resuspended in 6 mL prewarmed medium and continued to be cultured as described above. Transfection efficiency as well as viability was determined by transfecting the cells with 400 nM green fluorescence siRNA (siGLO from Dharmacon, Chicago, IL, USA) followed by propidium iodide exclusion dye and flow cytometric analysis.

2.3. Patch-Clamp Recording. Maternal, Bcl-2-overexpressing, and control vector-transfected Jurkat cells were irradiated (IR) with 0, 5, or 10 Gy 6 MV photons by the use of linear accelerator (LINAC SL25 Philips) at a dose rate of 4 Gy/min at room temperature. Whole-cell currents were evoked by 9–11 voltage pulses (700 ms each) to voltages between −100 (−80) mV and +100 (+80) mV delivered in 20 mV increments. Mean steady state current values were analyzed 2–49 h after IR. The liquid junction potentials between the pipette and the bath solutions were estimated according to [32], and data were corrected for the estimated liquid junction potentials. Applied voltages refer to the cytoplasmic face of the membrane with respect to the extracellular space. Inward currents, defined as flow of positive charge from the extracellular to the cytoplasmic membrane face, are negative currents and depicted as downward deflections of the original current traces.

Cells were superfused at 37°C temperature with NaCl ringer solution (in mM: 125 NaCl, 32 N-2-hydroxyethylpiperazine-N-2-ethanesulfonic acid (HEPES), 5 KCl, 5 D-glucose, 1 $MgCl_2$, and 1 $CaCl_2$, titrated with NaOH to pH 7.4). Upon GΩ-seal formation and entry into the whole-cell recording

mode, cells were recorded with NaCl bath solution (in mM: 140 NaCl, 10 HEPES titrated with NaOH to pH 7.4), KCl bath solution (in mM: 140 KCl, 10 HEPES titrated with KOH to pH 7.4), $CaCl_2$ bath solution (in mM: 100 $CaCl_2$, 10 HEPES, titrated with $Ca(OH)_2$ to pH 7.4), or N-methyl-D-glucamine-Cl (NMDG-Cl) bath solution (in mM: 180 mM N-methyl-D-glucamine titrated with HCl to pH 7.4). The K-D-gluconate/KCl pipette solution contained (in mM) 60 K-D-gluconate, 80 KCl, 5 HEPES, 1 $MgCl_2$, 1 K_2-EGTA, and 1 K_2-ATP, titrated with KOH to pH 7.4. To activate TRPM2 channels, ADP-ribose (1 μM, Sigma, Taufkirchen, Germany) was added to the pipette solution. To inhibit TRPM2 and IK channels *N*-(*p*-amylcinnamoyl)anthranilic acid (ACA, 0 or 20 μM) and TRAM-34 (0 or 10 μM, both from Sigma, both prepared from a 10 mM stock solution in DMSO) were added to the bath solution, respectively.

2.4. Querying the Cancer Genome Atlas (TGCA) Data Sets. Via the cBIOportal Web resource [33, 34], 178 hematopoietic and lymphoid tissue cancer cell lines of the Novartis and Broad Institute Cancer Cell Line Encyclopedia [35] were queried for TRPM2 and Bcl-2 mRNA abundance.

2.5. Western Blotting. Irradiated Jurkat cells (0, 5, or 10 Gy, 2–4 h after IR) were lysed in a buffer (containing in mM 50 HEPES, pH 7.5, 150 NaCl, 1 EDTA, 10 sodium pyrophosphate, 10 NaF, 2 Na_3VO_4, 1 phenylmethylsulfonyl fluoride (PMSF) additionally containing 1% triton X-100, 5 μg/mL aprotinin, 5 μg/mL leupeptin, and 3 μg/mL pepstatin) and separated by SDS-PAGE under reducing condition. In some experiments, cells were preincubated (0.25 h), irradiated (5 Gy), and postincubated (4 h) in the presence of the TRPM2 channel inhibitor ACA (20 μM). Segregated proteins were electrotransferred onto PVDF membranes (Roth, Karlsruhe, Germany). Blots were blocked in TBS buffer containing 0.05% Tween 20 and 5% nonfat dry milk for 1 h at room temperature. The membrane was incubated overnight at 4°C with the following primary antibodies: rabbit anti-phospho-CaMKII (Thr286) antibody (Cell Signaling #3361, New England Biolabs, Frankfurt, Germany, 1 : 1000), rabbit anti-CaMKII (pan) antibody (Cell Signaling #3362, 1 : 1000), rabbit anti-phospho-cdc25b (Ser187) antibody (Epitomics #T1162, Biomol Hamburg, Germany, 1 : 1000), rabbit anti-cdc25b antibody (Cell Signaling #9525, 1 : 1000), rabbit-anti TRPM2 (Bethyl Laboratories Inc., #A300-414A-2, Montgomery, TX, USA, 1 : 300), or mouse anti-Bcl-2 antibody (Santa Cruz Biotechnology, sc-509, Heidelberg, Germany, 1 : 1000). Equal gel loading was verified by an antibody against β-actin (mouse anti-β-actin antibody, clone AC-74, Sigma #A2228 1 : 20,000). Antibody binding was detected with a horseradish peroxidase-linked goat anti-rabbit or horse anti-mouse IgG antibody (Cell Signaling #7074 and #7076, resp.; 1 : 1000–1 : 2000 dilution in TBS-Tween/5% milk) incubated for 1 h at room temperature and enhanced chemoluminescence (ECL Western blotting analysis system, GE Healthcare/Amersham-Biosciences, Freiburg, Germany) was detected by film autography.

2.6. Fura-2 Ca^{2+} Imaging. Fluorescence measurements were performed using an inverted phase-contrast microscope (Axiovert 100; Zeiss, Oberkochen, Germany). Fluorescence was evoked by a filter wheel (Visitron Systems, Puchheim, Germany) mediated alternative excitation at 340/26 or 387/11 nm (AHF, Analysentechnik, Tübingen, Germany). Excitation and emission light was deflected by a dichroic mirror (409/LP nm beamsplitter, AHF) into the objective (Fluar x40/1.30 oil; Zeiss) and transmitted to the camera (Visitron Systems), respectively. Emitted fluorescence intensity was recorded at 587/35 nm (AHF). Excitation was controlled and data acquired by Metafluor computer software (Universal Imaging, Downingtown, PA, USA). The 340/380 nm fluorescence ratio was used as a measure of cytosolic free Ca^{2+} concentration ($_{free}[Ca^{2+}]_i$). The cells were irradiated (0 or 5 Gy) and loaded with fura-2/AM (2 μM for 30 min at 37°C; Molecular Probes, Goettingen, Germany) in supplemented RPMI medium. $_{free}[Ca^{2+}]_i$ was determined 1.5–5 h after IR at 37°C during superfusion with NaCl ringer (see above), upon Ca^{2+} depletion with Ca^{2+}-free NaCl ringer solution (in mM: 125 NaCl, 32 HEPES, 5 KCl, 5 D-glucose, 1 $MgCl_2$, and 0.5 EGTA, titrated with NaOH to pH 7.4), and during Ca^{2+} readdition in NaCl ringer solution additionally containing ACA (0 or 20 μM).

2.7. Flow Cytometry. To test for mitochondrial production of superoxide anion, Jurkat cells were irradiated (0 or 10 Gy), further cultured for 6 h, harvested, washed, and incubated for 10 min at 37°C in NaCl ringer solution (see above) containing 5 μM of the superoxide anion-sensitive dye MitoSOX (Invitrogen) and 0 or 20 μM ACA, and superoxide anion-sensitive fluorescence was recorded by flow cytometry in fluorescence channel Fl-2 (logarithmic scale, 488 nm excitation and 564–606 nm emission wavelengths). To confirm equal fluorescence dye loading, samples were oxidized (10 mM *tert*-butylhydroperoxide) for 12 min and recorded (data not shown).

To monitor mitochondrial function, Jurkat cells were irradiated (0 or 10 Gy) and further cultured for 6 h. Thereafter, cells were harvested, washed, and incubated for 30 min at 37°C in NaCl ringer solution (see above) containing 25 nM of the inner mitochondrial membrane potential ($\Delta\Psi_m$) specific dye tetramethylrhodamine ethyl ester perchlorate (TMRE, Invitrogen) and $\Delta\Psi_m$ was analyzed by flow cytometry in fluorescence channel FL-2 (logarithmic scale).

For cell cycle analysis, Jurkat cells were preincubated (0.25 h), irradiated (0, 5 or 10 Gy), and incubated for further 24 h in supplemented RPMI 1640 medium additionally containing either ACA or clotrimazole (Sigma, 0 or 20 μM, each). Cells were permeabilized and stained (0.5 h at room temperature) with unsteril (i.e., not RNase-free) propidium iodide (PI) solution (containing 0.1% Na-citrate, 0.1% triton X-100, 10 μg/mL PI in phosphate-buffered saline, PBS), and the DNA amount was analyzed by flow cytometry (FACS Calibur, Becton Dickinson, Heidelberg, Germany, 488 nm excitation wavelength) in fluorescence channel FL-3 (linear scale, >670 nm emission wavelength). In parallel, cells with degraded DNA were defined by the $subG_1$ population of the

PI histogram recorded in fluorescence channel FL-2 (logarithmic scale).

For determination of $_{free}[Ca^{2+}]_i$ cells were loaded in NaCl ringer solution (see above) for 0.5 h with fluo-3-AM (2 μM in NaCl ringer, Calbiochem; Bad Soden, Germany) and recorded in fluorescence channels FL-1 (logarithmic scale, 515–545 nm emission wavelengths). As loading control for fluo-3, cells were incubated with the Ca^{2+} ionophore ionomycin (1 μM for 10 min) prior to analysis by flow cytometry. Data were analyzed with the FCS Express 3 software (De Novo Software, Los Angeles, CA, USA).

2.8. Statistics. Data are expressed as means ± SE and statistical analysis was made by normal or Welch-corrected two-tailed t-test or ANOVA where appropriate using InStat software (GraphPad Software Inc., San Diego, CA, USA).

3. Results and Discussion

3.1. Modulation of on Channel Activity by Ionizing Radiation. To assess the effect of ionizing radiation (IR) of ion channel activity, Jurkat cells were irradiated with 10 Gy and whole-cell currents were recorded at different time periods after IR. As shown in Figures 1(a) and 1(b), IR induced an increase in whole-cell currents 2–6 h after IR. Substitution of Na^+ in the bathing solution by Ca^{2+} or the impermeable Na^+ substitute $NMDG^+$ indicated both cation-selectivity and Ca^{2+} permeability of the IR-induced currents (Figures 1(c)–1(e)).

Next, the functional expression of TRPM2 channels and its dependence on Bcl-2 was determined in Jurkat cells. Such dependence was suggested by a positive correlation of the TRPM2 and Bcl-2 mRNA abundances in 178 hematopoietic and lymphoid tissue cancer cell lines of the Novartis and Broad Institute Cancer Cell Line Encyclopedia (Figure 2(a)). In the Jurkat cell model, in contrast, TRPM2 protein abundance seemed to be lower in Bcl-2-overexpressing (Jurkat-Bcl-2) cells as in the control vector-transfected (Jurkat-vector) cells as suggested by immunoblotting (Figure 2(b)). IR did not modify total TRPM2 protein content of the cells (Figure 2(b)).

To activate TRPM2 in Jurkat cells, whole-cell currents were recorded with the TRPM2 agonist ADP-ribose in the pipette and compared in unpaired experiments with those recorded under control conditions. Intracellular ADP-ribose stimulated a whole-cell current fraction which was sensitive to the unspecific TRPM2 inhibitor ACA [36] (Figures 2(c) and 2(d)). Importantly, ADP-ribose-stimulated currents exhibited unitary current transitions with a unitary conductance of some 50 pS as reported for heterologously expressed TRPM2 channels [37] (Figure 2(e)). Together, these data indicated functional expression of TRPM2 in Jurkat cells.

3.2. Mitochondrial Superoxide Anion Formation: Effect of Ionizing Radiation, Bcl-2 Overexpression, and TRPM2 Inhibition. To assess IR-stimulated formation of superoxide anion by mitochondria and to estimate a potential role of TRPM2 channels herein, Jurkat-Bcl-2 and Jurkat-vector cells were irradiated (0 or 10 Gy), postcultured for 6 h, and incubated for 10 min with the superoxide anion-sensitive fluorescence dye MitoSOX. The dye incubation was performed in the absence or presence of the TRPM2 inhibitor ACA. As shown in Figure 3(a), upper panel, and Figure 3(b), three distinct cell populations with low, intermediate, or high MitoSOX fluorescence were apparent. The latter two showed lower cell sizes as compared to the low-fluorescent population, suggestive of superoxide anion formation-associated cell shrinkage. Staining of the cells in parallel experiments with the inner mitochondrial membrane potential ($\Delta\Psi_m$) specific dye TMRE indicated dissipation of $\Delta\Psi_m$ in most of the shrunken cells (Figure 3(a), lower panel) suggesting that the vast majority of cells with intermediate and high MitoSOX fluorescence underwent apoptotic cell death.

The low-fluorescent, nonshrunken cell population was larger and exhibited significant lower superoxide anion formation in Jurkat-Bcl-2 cells as compared to this population in Jurkat-vector cells (open bars in Figures 3(c) and 3(d), left). In the low-fluorescent populations, irradiation significantly increased the superoxide formation only in Jurkat-Bcl-2 cells to levels which still remained below those of control or irradiated Jurkat-vector cells (compare open and closed bars in Figure 3(c)). Importantly, ACA slightly but significantly ($p \leq 0.05$, ANOVA) decreased superoxide anion formation in unirradiated (from 20.9 ± 0.21 to 18.2 ± 0.22 relative units, $n = 4$) and irradiated (from 23.8 ± 0.26 to 21.6 ± 0.79 rel. units, $n = 4$) low-fluorescent Jurkat-Bcl-2 cells while having no inhibiting effect on superoxide anion formation in low-fluorescent Jurkat-vector cells (data not shown). IR effects on the intermediate- or high-fluorescent populations of both cell clones, in contrast, were not apparent (Figure 3(a)). ACA markedly decreased the superoxide formation of the intermediate- or high-fluorescent populations in all control or irradiated cells (compare Figures 3(a) and 3(b)) resulting in the disappearance of the high-fluorescent cells (Figure 3(e)).

Combined, these data demonstrate lower mitochondrial superoxide anion formation in Jurkat-Bcl-2 cells as compared to Jurkat-vector cells. Only in the former cells, IR induced an increase in superoxide anion formation. In addition, superoxide anion formation was lowered by the TRPM2 inhibitor ACA in cells of both clones independent of IR stress. This might suggest a contribution of TRPM2-mediated Ca^{2+} uptake to mitochondrial ROS formation.

3.3. Ionizing Radiation-Stimulated Ca^{2+} Uptake: Regulation by Bcl-2 and Involvement of TRPM2 Channels. To determine IR-induced changes in TRPM2 activity, irradiated (0 or 5 Gy) Jurkat-Bcl-2 and Jurkat-vector cells were whole-cell recorded in the absence and presence of ACA (Figures 4(a)–4(c)). The ACA-sensitive current fraction of nonirradiated cells was higher in Jurkat-vector than in Jurkat-Bcl-2 cells (compare 1st with 3rd and 5th with 7th bar in Figure 4(c), resp.) which might reflect the observed differences in TRPM2 protein abundance and which is in accordance with the observed differences in mitochondrial ROS formation. IR (5 Gy) stimulated an increase in the ACA-sensitive currents predominately in Jurkat-Bcl-2 cells (Figure 4(c)) which again might be mirrored by the observed IR sensitivity of mitochondrial ROS formation exclusively in Jurkat-Bcl-2 cells.

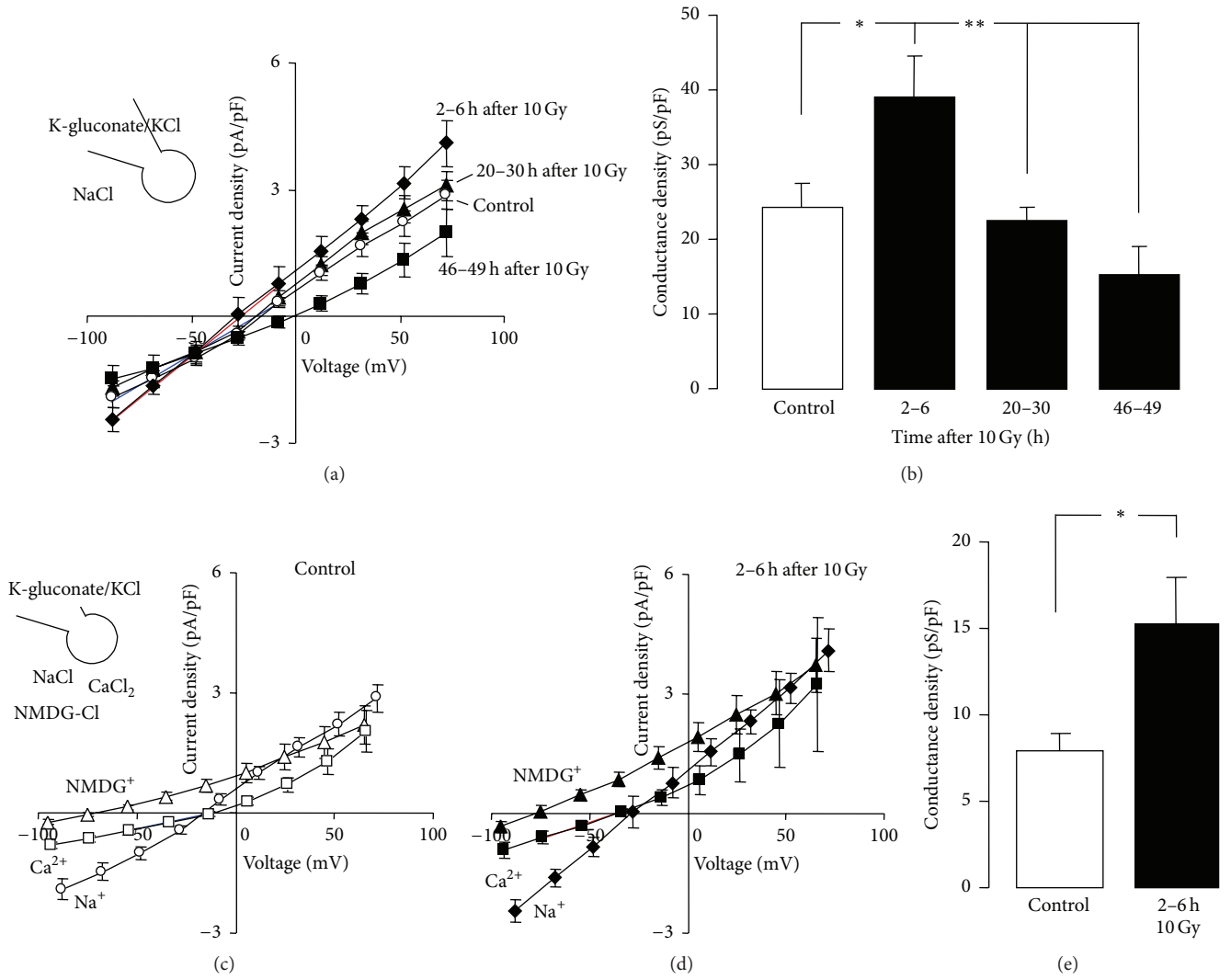

FIGURE 1: Ionizing radiation (IR) increases the cation and the Ca^{2+} conductance of the plasma membrane in human Jurkat T cell leukemia cells. (a, b) Current density-voltage relationships (*I*/*V* curves, a) and conductance densities (b) of Jurkat cells at different time periods (as indicated) after IR with 0 Gy (control, open circles and bar) or 10 Gy (closed symbols and bars). Currents were recorded in whole-cell voltage-clamp mode with K-gluconate/KCl pipette and NaCl bath solution and elicited by 9 voltage square pulses to voltages between −80 mV and +80 mV (20 mV increments). Conductance densities were calculated for the inward currents as shown by the blue and red line in (a) for control cells and irradiated cells (2–6 h after IR), respectively. (c, d) *I*/*V* curves of control (c) and irradiated Jurkat cells (2–6 h after 10 Gy, d) recorded as in (a) with NaCl bath solutions (circles) or after replacement of Na^+ with Ca^{2+} (squares) or the impermeable cation N-methyl-D-glucamine (NMDG, triangles). (e) Ca^{2+} conductance density of control cells (open bar) and irradiated Jurkat cells (2–6 h after 10 Gy, closed bar). The blue and red line in (c) and (d), respectively, show the voltage range used for calculation of the Ca^{2+} conductance densities. Data are means ± SE, $n = 5$ for the 46–49 h values in (a) and $n = 8$–15 for all other data. ∗ and ∗∗ indicate $p \leq 0.05$ and 0.01 as tested by ANOVA (b) and Welch-corrected *t*-test (e), respectively.

In accordance with an IR-induced increase in TRPM2 activity, IR stimulated an ACA-sensitive Ca^{2+} uptake as measured by fura-2 Ca^{2+} imaging using an extracellular Ca^{2+} depletion/repletion protocol (Figure 4(d)). In contrast to the ACA-sensitive basal whole cell currents (Figure 4(b)), basal (ACA-sensitive) Ca^{2+} uptake was higher in Jurkat-Bcl-2 than in Jurkat-vector cells (compare 1st with 5th bar in Figure 4(e)). Similarly to the whole-cell currents, IR (5 Gy) stimulated a larger Ca^{2+} uptake in Jurkat-Bcl-2 as compared to Jurkat-vector cells (compare 2nd with 6th bar in Figure 4(e)). In the presence of ACA, Ca^{2+} uptake did not differ between control and irradiated Jurkat-vector and Jurkat-Bcl-2 cells (3rd, 4th, 7th, and 8th bar in Figure 4(e)). Together, these observations indicated an IR-stimulated Bcl-2-regulated Ca^{2+} uptake in Jurkat cells which probably involves TRPM2 channels.

3.4. Role of TRPM2 Channels in Ionizing Radiation-Stimulated Activation of Ca^{2+} Effector Proteins Involved in Cell Cycle Arrest. This IR-stimulated Ca^{2+} uptake might be hazardous for the cells leading to Ca^{2+} overflow and subsequent cell death. In fact, 24 h after IR with 10 Gy, some 25% of the Jurkat cells

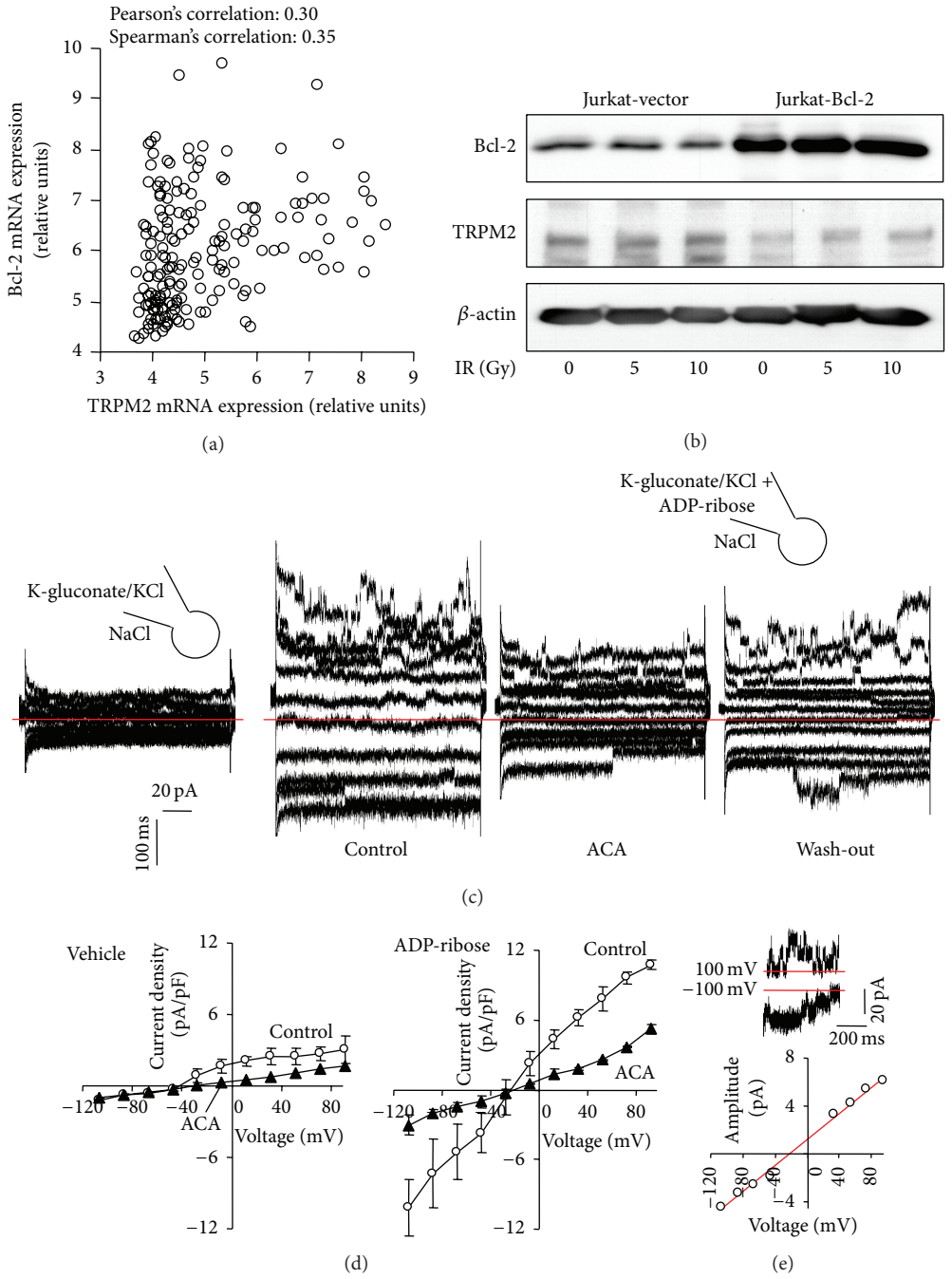

Figure 2: T cell leukemia cells functionally express TRPM2 Ca^{2+}-permeable cation channels and TRPM2 expression correlates with that of the antiapoptotic protein Bcl-2. (a) Dot blot showing the relative mRNA abundances of TRPM2 and Bcl-2 in 178 hematopoietic and lymphoid tissue cancer cell lines. Data are from the Novartis and Broad Institute Cancer Cell Line Encyclopedia. (b) Immunoblots from whole lysates of irradiated (0, 5, or 10 Gy, 4 h after IR) stably transfected control (Jurkat-vector) and Bcl-2-overexpressing (Jurkat-Bcl-2) cells probed against Bcl-2, TRPM-2, and β-actin. (c) Current tracings recorded as in Figure 1(a) in Jurkat-Bcl-2 cells with vehicle alone (1st tracings) or in an unpaired experiment with the TRPM-2 activator ADP-ribose (1 μM) in the pipette (2nd–4th tracings). The recordings with ADP-ribose were performed before (2nd tracings, control), during (3rd tracings, ACA), and after (4th tracings, wash-out) bath application of the TRPM-2 inhibitor N-(p-amylcinnamoyl)-anthranilic acid (ACA, 20 μM, zero currents are shown by red lines). (d) I/V curves of the mean whole cell currents (± SE, $n = 3$) of Jurkat-Bcl-2 cells recorded the absence (left) or presence of the TRPM2-activator ADP-ribose (right) in the pipette before (open circles) and after bath superfusion with the TRPM2 inhibitor ACA (closed triangles). (e) Single channel characteristics of the ADP-ribose-stimulated channel. Unitary current transitions were apparent in whole-cell currents tracings as depicted here for −100 mV and +100 mV clamp-voltage in the upper panel. The lower panel shows the relationship between unitary current transitions and voltage indicating a unitary conductance of about 50 pS.

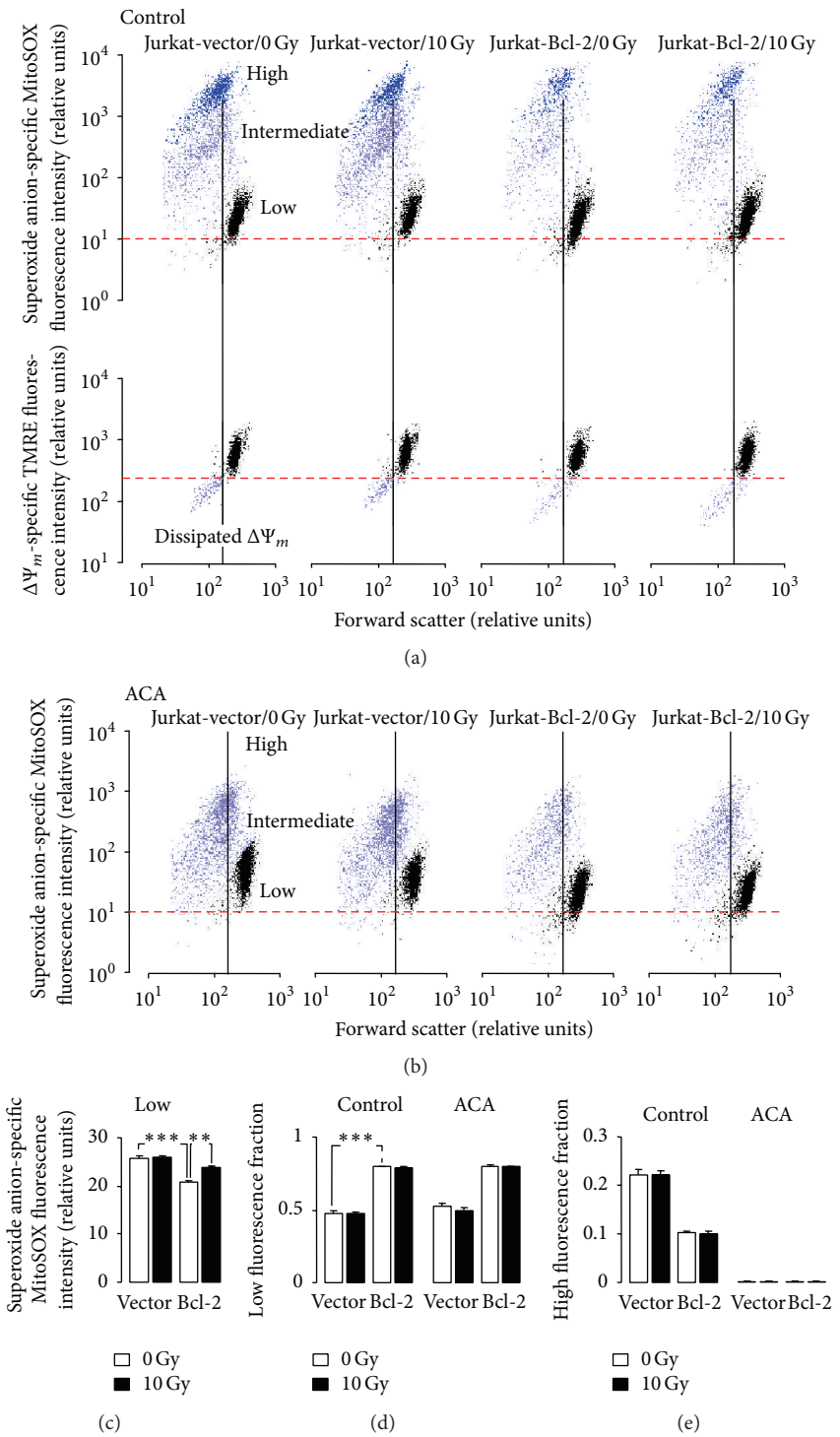

FIGURE 3: IR increases mitochondrial superoxide anion formation in Bcl-2-overexpressing cells. (a, b) Dot plots showing forward scatter and the superoxide anion-selective MitoSOX fluorescence (a, upper panel, and b) as well as the inner mitochondrial membrane potential $\Delta\Psi_m$-specific TMRE fluorescence (a, lower panel) of Jurkat-vector- (1st and 2nd panels) and Jurkat-Bcl-2 cells (3rd and 4th panels) 6 h after irradiation with 0 Gy (1st and 3rd panels) or 10 Gy (2nd and 4th panels). Incubation (10 min at 37°C) with the superoxide anion-sensitive fluorescence dye was carried out in the absence (a) or presence (b) of the TRPM2 inhibitor ACA (20 μM). Three distinct cell populations with low (black), intermediate (lilac), or high (blue) superoxide anion formation were apparent. The majority of intermediate and high superoxide anion-forming cells exhibited a low forward scatter which was associated with dissipation of $\Delta\Psi_m$ (a, lower panel). (c) Mean (± SE, $n = 4$) MitoSOX fluorescence intensity in the low-fluorescent populations of 0 Gy- (open bars) or 10 Gy-irradiated (closed bars, 6 h after irradiation) Jurkat-vector- (left) and Jurkat-Bcl-2 cells (right). (d, e) Mean (± SE, $n = 4$) fraction of MitoSOX low-fluorescent (d) and high-fluorescent Jurkat-vector- (1st, 2nd, 5th, and 6th bars) and Jurkat-Bcl-2 cells (3rd, 4th, 7th, and 8th bars) 6 h after irradiation with 0 Gy (open bars) or 10 Gy (closed bars). The incubation with the fluorescence dye was carried out in the absence (1st–4th bars) or presence (5th–8th bars) of ACA (20 μM). ∗∗ and ∗ ∗ ∗ indicate $p \leq 0.01$ and $p \leq 0.001$, respectively, ANOVA.

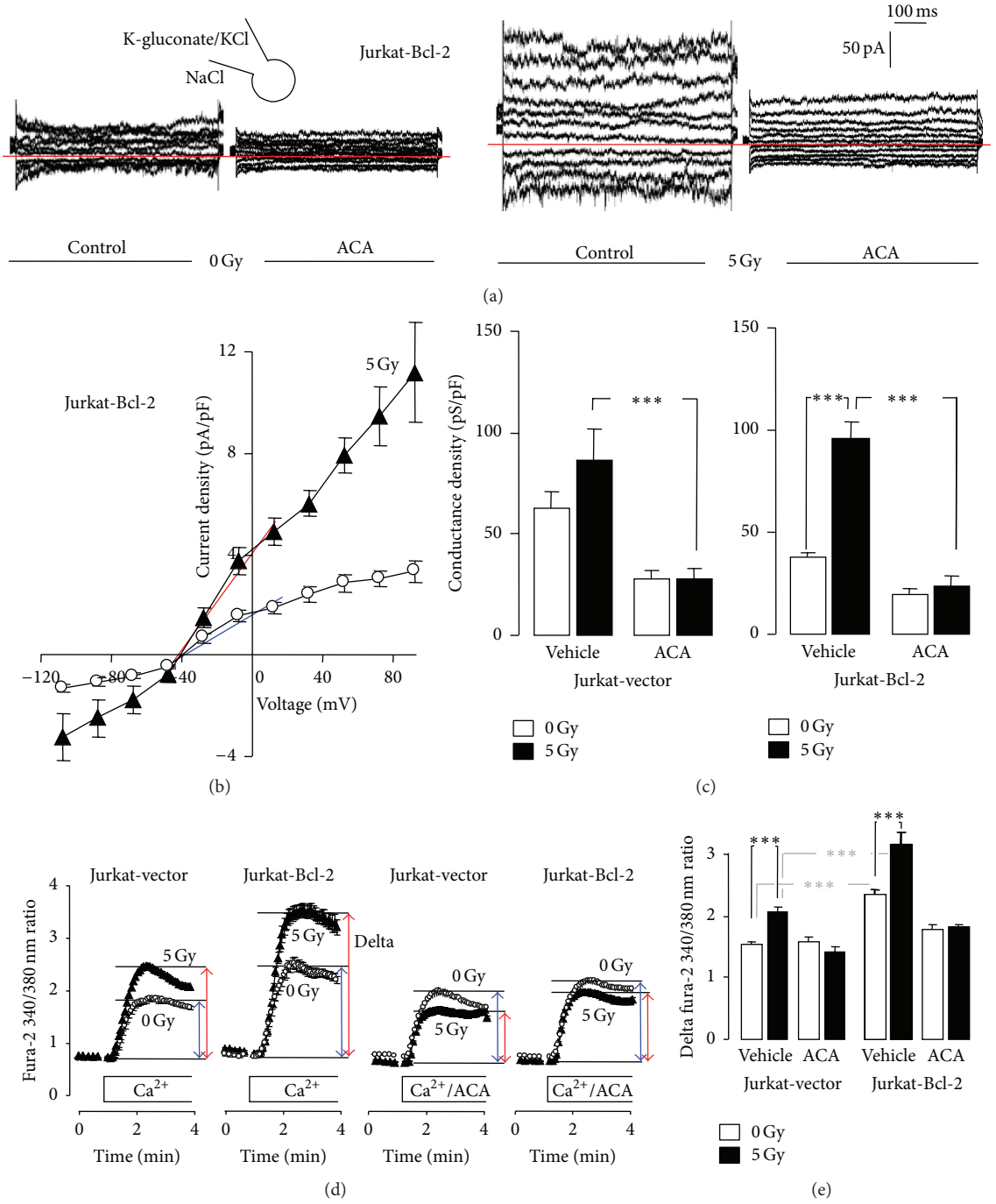

FIGURE 4: IR stimulates Ca^{2+} entry through TRPM2 channels especially in Bcl-2-overexpressing Jurkat cells. (a) Whole-cell current tracings recorded in Jurkat-Bcl-2 cells irradiated with 0 Gy (1st and 2nd tracings) or 5 Gy (3rd and 4th tracings, 2 h after IR). Records were obtained in unpaired experiments as described in Figure 1(a) before (1st and 3rd tracings) and during bath application of the TRPM2 inhibitor ACA (20 μM, 2nd and 4th tracings). (b) Relationship of the mean (± SE, n = 7–10) current density and the voltage recorded as in (a) in Jurkat-Bcl-2 cells irradiated with 0 Gy (open circles) or 5 Gy (closed triangles). (c) Mean (± SE, n = 6–12) conductance density of control (0 Gy, open bars) and irradiated (5 Gy, 2–5 h after IR) Jurkat-vector (left) and Jurkat-Bcl-2 cells (right) recorded as in (a) in the absence or presence of ACA. Conductance densities were calculated for the outward currents as shown by the blue and red line in (b) for control and irradiated cells, respectively. (d, e) Mean (± SE, n = 197–336) fura-2 340/380 nm ratio (d) and delta fura-2 ratio (e) as measures of cytosolic free Ca^{2+} concentration and Ca^{2+} entry in Ca^{2+}-depleted cells, respectively. Ca^{2+}-specific fura-2 fluorescence was recorded by imaging in control (0 Gy, open circles and bars) and irradiated (5 Gy, closed triangles and bars, 1.5–5 h after IR) Jurkat-vector and Jurkat-Bcl-2 cells using extracellular Ca^{2+} removal/readdition protocol. Ca^{2+} readdition was performed in the absence (vehicle) or presence of ACA (20 μM). $***$ indicates $p \leq 0.001$, ANOVA.

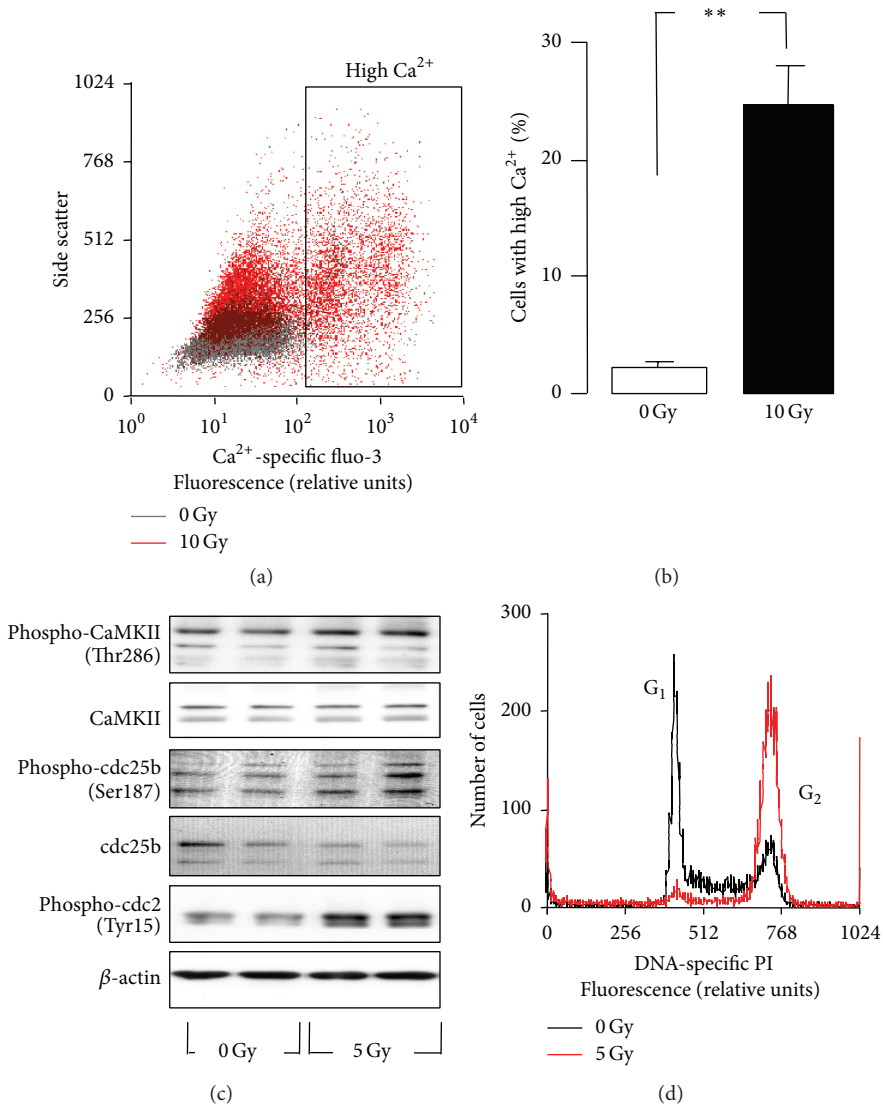

FIGURE 5: IR induces Ca^{2+} signaling and a G_2/M cell cycle arrest in Jurkat cells. (a) Dot plot recorded by flow cytometry showing the Ca^{2+}-specific fluo-3 fluorescence intensity in dependence on side scatter of Jurkat cells 24 h after IR with 0 Gy (grey) or 10 Gy (red). (b) Mean (± SE, $n = 4$) percentage of control and irradiated Jurkat cells with high cytosolic free Ca^{2+} concentrations (determined by fluo-3 fluorescence in flow cytometry as described in (a), ** indicates $p \leq 0.01$, Welch-corrected t-test). (c) Immunoblots from whole lysates of irradiated (0 or 5 Gy, 4 h after IR) Jurkat cells probed against phosphorylated and total Ca^{2+}/CaM-dependent kinase II (CaMKII) isoforms, against the phosphorylated and total phosphatase cdc25b, the phosphorylated cell division cycle protein 2 (cdc2), and β-actin for loading control. (d) Flow cytometry histogram depicting the fluorescence intensity of the DNA-specific dye propidium iodide (PI) in Jurkat cells 24 h after IR with 0 (black) or 5 Gy (red).

exhibited a highly increased $_{free}[Ca^{2+}]_i$ as deduced from fluo-3 flow cytometry (Figures 5(a) and 5(b)). Ca^{2+} uptake might also contribute to Ca^{2+} signaling that is required for DNA damage response of the irradiated T cell leukemia cells. IR (5 Gy) stimulated autophosphorylation and activation of Ca^{2+}/calmodulin-dependent protein kinase II (CaMKII) isoforms and phosphorylation-dependent inactivation of the CaMKII downstream target cdc25b as suggested by immunoblotting (Figure 5(c)). Inactivation of the phosphatase cdc25b was parallel by radiation-induced phosphorylation-dependent inactivation of the cdc25b substrate cdc2 (Figure 5(c)). This might hint to an involvement of Ca^{2+} effector proteins such as CaMKII in G_2/M arrest as observed in PI flow cytometry 24 h after IR (5 Gy, Figure 5(d)).

To confirm an involvement of TRPM2 and CaMKII in the stress response of Jurkat cells, Jurkat-Bcl-2 and Jurkat-vector cells were irradiated (0 or 5 Gy) and postincubated in the presence or absence of the TRPM2 inhibitors ACA or clotrimazole [38, 39] and kinase activities of the CaMKII isoforms and cdc2 and cell cycle distribution and cell death were analyzed by immunoblotting and PI flow cytometry, 4 h and 24 after IR, respectively. ACA decreased the basal and

radiation-induced abundance of phosphorylated CaMKII in Jurkat-Bcl-2 and Jurkat-vector cells (Figure 6(a), 1st and 2nd blot). Most importantly, ACA blocked the radiation-induced phosphorylation-dependent inactivation of cdc2 in both genotypes (Figure 6(a), 3rd blot) suggesting a functional significance of ACA-sensitive Ca^{2+} entry for G_2/M cell cycle arrest. Accordingly, ACA and clotrimazole decreased the number of irradiated cells arrested in G_2/M (Figures 6(b)–6(e)) and increased the number of dead cells. ACA- and clotrimazole-induced cell death was more pronounced in irradiated Jurkat-vector than in Jurkat-Bcl-2 cells (subG_1 population, Figures 6(b)–6(e)).

Finally, the function of TRPM2 in radiation-induced G_2/M arrest of Jurkat cells was directly tested by TRPM2 knock-down. Transfection of Jurkat-vector cells with TRPM2 siRNA resulted in downregulation of TRPM2 protein level as compared to nontargeting (nt) RNA-transfected cells (Figure 6(f), insert). Transfected Jurkat cells were irradiated (0 or 5 Gy) and G_2/M arrest and cell death analyzed 24 h thereafter. TRPM2 knock-down exerted small but significant effects on radiation-induced G_2/M arrest and cell death mimicking those of ACA and clotrimazole (Figure 6(f)).

3.5. Regulation of TRPM2-Mediated Ca^{2+} Influx by Mitochondria and Bcl-2. ADP-ribose is liberated in the mitochondria from, for example, NAD-dependent deacetylation intermediates, from mono- or polyADP-ribosylated proteins, or from NAD^+, and released into the cytosol [19]. Oxidative and nitrosative stress have been demonstrated to stimulate the mitochondrial release of ADP-ribose into the cytosol which in turn activates TRPM2 channels in the plasma membrane resulting in Ca^{2+} entry and depolarization of the membrane potential [16]. Since an elevated $_{free}[Ca^{2+}]_i$ may disinhibit the respiration change leading to $\Delta\Psi_m$ hyperpolarisation and superoxide anion formation and, eventually, to mitochondrial Ca^{2+} overload and $\Delta\Psi_m$ dissipation, TRPM2 activation has been proposed to amplify signals that trigger cell death (for review see [27]).

The present study demonstrates that irradiated human T cell leukemia cells may utilize the TRPM2 "death channel" for prosurvival Ca^{2+} signaling. Noteworthy, IR-induced TRPM2 currents and Ca^{2+} entry were larger in cells overexpressing Bcl-2 pointing to a crosstalk between Bcl-2 in the ER and outer mitochondrial membrane and TRPM2 in the plasma membrane. The correlation between TRPM2 and Bcl-2 mRNA abundances in a panel of lymphohematopoietic cancer cell lines (see Figure 2(a)) further suggests a functional interdependence between both proteins.

In some cell models, Bcl-2-overexpressing cells have been proposed to counteract the Bcl-2-mediated Ca^{2+} leakage from the stores by downregulating Ca^{2+} uptake through the plasma membrane (for review see [19]). In line with such compensatory mechanism might be the observation of the present study that Bcl-2-overexpressing Jurkat cells exhibited under basal conditions lower TRPM2 protein abundance, smaller ACA-sensitive currents in patch-clamp whole-cell recordings than the control vector-transfected cells (see Figure 2(b)).

In intact cells (i.e., in fura-2 Ca^{2+} imaging experiments, see Figure 4(e)), however, a basal ACA-sensitive Ca^{2+} uptake fraction was only apparent in Bcl-2-overexpressing cells suggestive of a TRPM2 inactivity in control cells under resting conditions. Compared to control cells, the more sustained Ca^{2+} uptake in Bcl-2-overexpressing cells (see Figures 4(d) and 4(e)) suggests that Bcl-2 overexpression might be associated with a set-point shift of the resting $_{free}[Ca^{2+}]_i$ towards higher levels. Fura-2 Ca^{2+} imaging and fluo-3 flow cytometry recordings of the present study indeed demonstrated a higher basal $_{free}[Ca^{2+}]_i$ in constitutively and inducibly Bcl-2-overexpressing Jurkat cells as compared to the respective control cells (see Supplementary Figure A, in Supplementary Material available online at http://dx.doi.org/10.1155/2016/8026702). Elevated $_{free}[Ca^{2+}]_i$ levels reportedly facilitate TRPM2 activation by ADP-ribose [40]. The observed basal ACA-sensitive Ca^{2+} uptake that occurred exclusively in Bcl-2-overexpressing cells might, therefore, be simply explained by a higher basal $_{free}[Ca^{2+}]_i$ in Bcl-2-overexpressing as compared to control cells.

Noteworthy, despite higher basal $_{free}[Ca^{2+}]_i$, Bcl-2-overexpressing cells exhibited lower basal mitochondrial ROS formation than control cells (see Figure 3(c)) suggestive of a Bcl-2-mediated protection of mitochondrial superoxide anion formation. As a matter of fact, a direct promoting function of mitochondrial superoxide anion formation has been attributed to the Bcl-2 opponent Bax in neuronal cells [41].

3.6. Rearrangements of the Ca^{2+} Signalosome in Tumor Cells: Functional Significance for Cell Cycle Control and Stress Response. In many tumor entities rearrangements of the Ca^{2+} signalosome have been reported. In prostate cancer, for instance, malignant progression is reportedly accompanied by TRPM8-mediated Ca^{2+} store depletion and downregulation of store-dependent Ca^{2+} entry across the plasma membrane. In exchange, TRP channels such as TRPV6 are upregulated in the plasma membrane of advanced prostate cancer cells which have been proposed to generate in concert with IK K^+ channels survival and growth factor-independent Ca^{2+} signaling (for review see [42]).

In the present study, IR stimulated the ACA-sensitive currents of Jurkat cells in patch-clamp recordings and the ACA-sensitive Ca^{2+} uptake in fura-2 imaging experiments suggesting an IR-induced increase in TRPM2 activity. IR-induced modifications of ion channel activity have been reported in different tumor entities where they contribute to stress evasion [43], glucose fueling [44, 45], cell cycle control [46, 47], or radioresistance [48].

The p53-mutated Jurkat cells [49] accumulate in G_2M cell cycle arrest upon IR-mediated DNA damage (see Figure 5(d)). The proposed IR-stimulated Ca^{2+} entry through TRPM2 channels most probably contributed to the G_2M cell cycle arrest. This was evident from the observation of the present study that two nonspecific TRPM2 inhibitors or TRPM2 knock-down decreased the number of cells accumulating in G_2 and increased the number of dead cells (see Figure 6). One might speculate that TRPM2 inhibition or

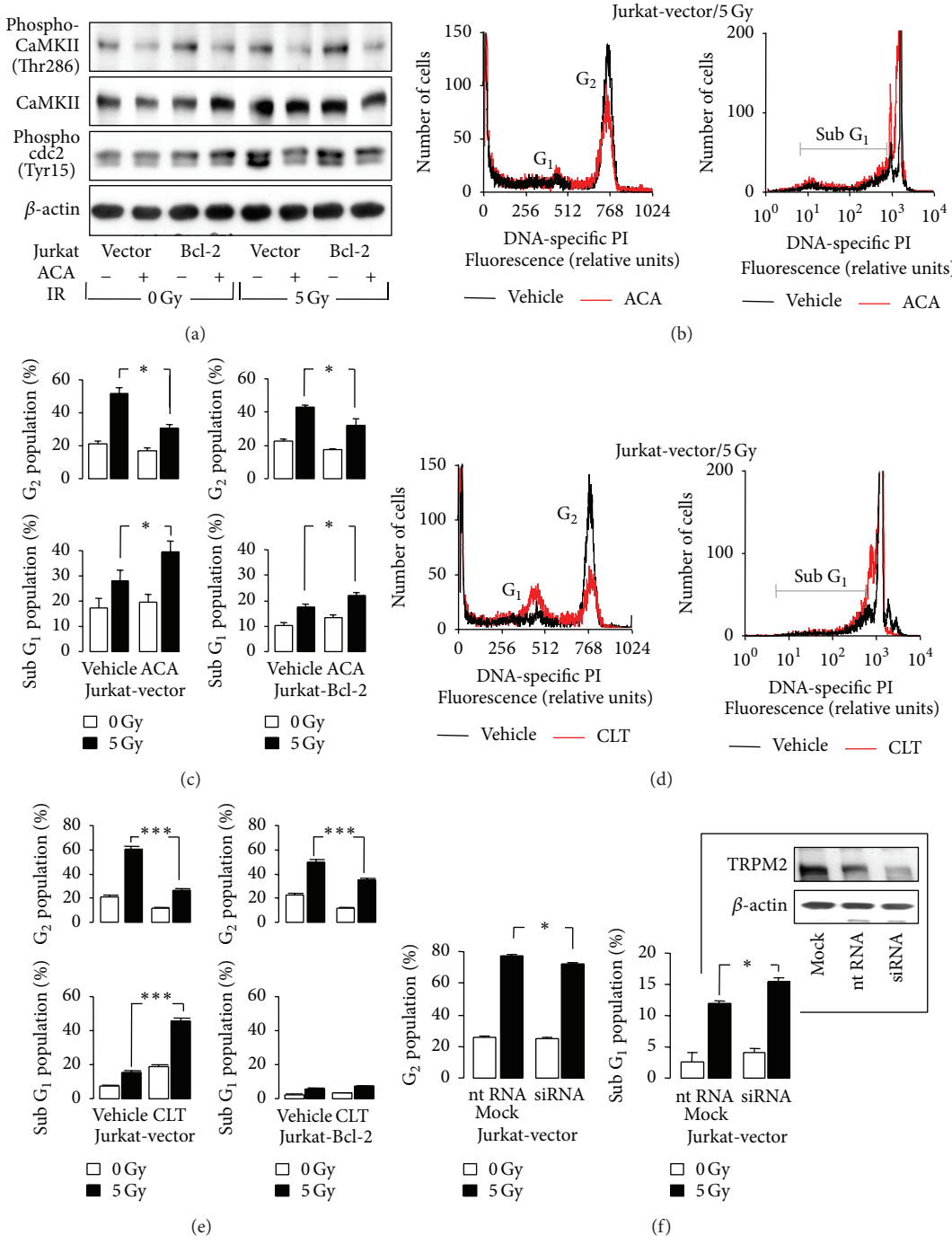

FIGURE 6: Ca^{2+}-signaling via ACA-sensitive Ca^{2+} entry contributes to IR-induced G_2/M cell cycle arrest and decreases IR-induced cell death of Jurkat cells. (a) Immunoblots from whole lysates of irradiated (0 or 5 Gy, 4 h after IR) Jurkat-vector and Jurkat-Bcl-2 cells probed against phospho-CaMKII and total CaMKII isoforms, against phospho-cdc2, and against β-actin. Cells were irradiated and postincubated in the presence of ACA (0 or 20 μM). (b, d) Histograms showing the DNA-specific PI fluorescence intensity of irradiated (5 Gy, 24 h after IR) Jurkat-vector cells pre- (0.25 h) and postincubated (24 h) with 0 μM (black) or 20 μM ACA (red) in (b) or 0 μM (black) or 20 μM clotrimazole (CLT, red) in (d). (c, e) Mean (± SE, n = 9–12) percentage of irradiated (0 Gy, open bars, or 5 Gy, closed bars) and ACA- in (d) or CLZ- in (e) (both 0 or 20 μM) cotreated Jurkat-vector and Jurkat-Bcl-2 cells arrested in G_2 phase of cell cycle (upper line) or belonging to the dead cells accumulating in the subG$_1$ population (lower line). (f) Knock-down of TRPM2 by RNA interference mimics the effect of ACA. Electroporation with TRPM2-specific siRNA decreases the TRPM2 protein abundance in Jurkat-vector cells to about a half of that of nontargeting RNA- (nt RNA-) transfected control cells as analyzed by TRPM2 and β-actin immunoblots, 48 h after electroporation (*insert*, mock: electroporation without RNA). Lower line: mean (± SE, n = 3–6) percentage of irradiated (0 Gy, open bars, or 5 Gy, closed bars, 24 h after IR) in G_2/M arrest (left) or in subG$_1$ population as analyzed by PI staining and flow cytometry as shown in (b, d). Cells were either mock-electroporated or transfected with nt RNA or TRPM2-specific siRNA. Mock and nt RNA data did not differ and were pooled. $*$ and $***$ indicate $p \leq 0.05$ and $p \leq 0.001$, ANOVA, respectively.

knock-down overrides G_2M cell cycle arrest and forces cells with unrepaired DNA damage into mitosis.

This scenario is strengthened by the observation that IR promoted the $_{free}[Ca^{2+}]_i$-dependent phosphorylation of CaMKIIs and their downstream targets cdc25b and cdc2 in an ACA-sensitive manner (see Figures 5(c) and 6(a)). CaMKIIs phosphorylate and thereby inactivate the phosphatase cdc25b which results in accumulation of the phosphorylated, inactive form of the mitosis promoting factor subunit cdc2 [47]. Combined, these observations suggest that IR-dependent TRPM2 activation contributes to Ca^{2+} signals that are able to induce autophosphorylation and thereby activation of CaMKIIs.

Likewise, irradiated human myeloid leukemia cells have been shown to generate Ca^{2+} signals by the concerted action of TRPV5/6 and Kv3.4 K^+ channels in the plasma membrane. These Ca^{2+} signals program G_2M cell cycle arrest similarly to proposed mechanism of the present study via CaMKIIs, cdc25b, and cdc2 [46, 47]. K^+ channel activity in close vicinity to Ca^{2+} entry pathways maintains a high inwardly directed driving force for Ca^{2+} and, thus, is indispensable for robust Ca^{2+} signals. In analogy to the leukemia cells [47], IR induced the coactivation of IK K^+ channels in the plasma membrane of Jurkat cells (see supplementary Figure B). This points to both a common signaling in irradiated myeloid and lymphoblastic leukemia cells and the possibility that functionally equivalent Ca^{2+} signals can be generated during DNA damage response by different sets of TRP and K^+ channels in the plasma membrane.

3.7. Conclusions. Plasma membrane TRPM2 channels have been attributed tumor suppressor function in several tumor entities. The Ca^{2+} signalosome of human T cell leukemia cells comprises TRPM2 channels that are activated during DNA damage response. In particular, irradiated Jurkat cells utilize TRPM2 to control the G_2/M cell cycle arrest probably via activation of the Ca^{2+} effector protein CaMKII and subsequent inhibition of cdc25b and cdc2. The antiapoptotic protein Bcl-2 in the ER or outer mitochondrial membrane even fosters TRPM2 activity presumably by inducing higher $_{free}[Ca^{2+}]_i$ levels and decreases at the same time mitochondrial ROS formation. By doing so, Bcl-2-overexpressing cells may harness TRPM2-generated Ca^{2+} signals without running into the risk of hazardous mitochondrial ROS formation. Thus, Bcl-2 function on mitochondrial integrity and stress-induced TRPM2-mediated Ca^{2+} signaling cooperate in resistance to radiation therapy in T cell leukemia cells.

Conflict of Interests

The authors declare that there is no conflict of interests regarding the publication of this paper.

Authors' Contribution

Dominik Klumpp cultured the cells and carried out patch-clamp, Ca^{2+} imaging, flow cytometry, TRPM2 knock-down, and immunoblotting. Milan Misovic performed patch-clamp recording and Ca^{2+} imaging. Kalina Szteyn did patch-clamp experiments. Ekaterina Shumilina analyzed the patch-clamp and imaging data, did the statistics, and compiled the figure parts with these methods. Justine Rudner designed and supervised the study, analyzed the flow cytometry and immunoblotting data, did the statistics, and wrote part of the paper draft. Stephan M. Huber co-conceived and co-supervised the study, compiled the remaining figure parts, and wrote the remaining paper draft. All authors read and approved the final paper. Justine Rudner and Stephan M. Huber contributed equally to this work and, thus, share senior authorship.

Acknowledgments

This work was supported by grants from the German Research Foundation DFG (RU 1641/1-1) donated to Justine Rudner and from the Wilhelm Sander Stiftung (2011.083.1) donated to Stephan M. Huber. Dominik Klumpp was supported by the DFG International Graduate School 1302 (TP T9 SH). The authors thank Heidrun Faltin and Ilka Müller for excellent technical assistance.

References

[1] D. E. Clapham, "TRP channels as cellular sensors," *Nature*, vol. 426, no. 6966, pp. 517–524, 2003.

[2] B. Nilius, G. Owsianik, T. Voets, and J. A. Peters, "Transient receptor potential cation channels in disease," *Physiological Reviews*, vol. 87, no. 1, pp. 165–217, 2007.

[3] M. Naziroğlu, "New molecular mechanisms on the activation of TRPM2 channels by oxidative stress and ADP-ribose," *Neurochemical Research*, vol. 32, no. 11, pp. 1990–2001, 2007.

[4] K. Nagamine, J. Kudoh, S. Minoshima et al., "Molecular cloning of a novel putative Ca^{2+} channel protein (TRPC7) highly expressed in brain," *Genomics*, vol. 54, no. 1, pp. 124–131, 1998.

[5] M. Nazıroğlu and A. Lückhoff, "A calcium influx pathway regulated separately by oxidative stress and ADP-ribose in TRPM2 channels: single channel events," *Neurochemical Research*, vol. 33, no. 7, pp. 1256–1262, 2008.

[6] K. Inamura, Y. Sano, S. Mochizuki et al., "Response to ADP-ribose by activation of TRPM2 in the CRI-G1 insulinoma cell line," *Journal of Membrane Biology*, vol. 191, no. 3, pp. 201–207, 2003.

[7] I. Heiner, J. Eisfeld, and A. Lückhoff, "Role and regulation of TRP channels in neutrophil granulocytes," *Cell Calcium*, vol. 33, no. 5-6, pp. 533–540, 2003.

[8] A.-L. Perraud, A. Fleig, C. A. Dunn et al., "ADP-ribose gating of the calcium-permeable LTRPC2 channel revealed by Nudix motif homology," *Nature*, vol. 411, no. 6837, pp. 595–599, 2001.

[9] Y. Hara, M. Wakamori, M. Ishii et al., "LTRPC2 Ca^{2+}-permeable channel activated by changes in redox status confers susceptibility to cell death," *Molecular Cell*, vol. 9, no. 1, pp. 163–173, 2002.

[10] M. Ishii, A. Oyama, T. Hagiwara et al., "Facilitation of H_2O_2-induced A172 human glioblastoma cell death by insertion of oxidative stress-sensitive TRPM2 channels," *Anticancer Research*, vol. 27, no. 6, pp. 3987–3992, 2007.

[11] X. Zeng, S. C. Sikka, L. Huang et al., "Novel role for the transient receptor potential channel TRPM2 in prostate cancer cell proliferation," *Prostate Cancer and Prostatic Diseases*, vol. 13, no. 2, pp. 195–201, 2010.

[12] W. Zhang, I. Hirschler-Laszkiewicz, Q. Tong et al., "TRPM2 is an ion channel that modulates hematopoietic cell death through activation of caspases and PARP cleavage," *American Journal of Physiology—Cell Physiology*, vol. 290, no. 4, pp. C1146–C1159, 2006.

[13] W. Zhang, X. Chu, Q. Tong et al., "A novel TRPM2 isoform inhibits calcium influx and susceptibility to cell death," *Journal of Biological Chemistry*, vol. 278, no. 18, pp. 16222–16229, 2003.

[14] U. Orfanelli, A.-K. Wenke, C. Doglioni, V. Russo, A. K. Bosserhoff, and G. Lavorgna, "Identification of novel sense and antisense transcription at the TRPM2 locus in cancer," *Cell Research*, vol. 18, no. 11, pp. 1128–1140, 2008.

[15] T. Adachi, H. Tanaka, S. Nonomura, H. Hara, S.-I. Kondo, and M. Hori, "Plasma-activated medium induces A549 cell injury via a spiral apoptotic cascade involving the mitochondrial-nuclear network," *Free Radical Biology and Medicine*, vol. 79, pp. 28–44, 2015.

[16] A.-L. Perraud, C. L. Takanishi, B. Shen et al., "Accumulation of free ADP-ribose from mitochondria mediates oxidative stress-induced gating of TRPM2 cation channels," *The Journal of Biological Chemistry*, vol. 280, no. 7, pp. 6138–6148, 2005.

[17] E. Fonfria, I. C. B. Marshall, C. D. Benham et al., "TRPM2 channel opening in response to oxidative stress is dependent on activation of poly(ADP-ribose) polymerase," *British Journal of Pharmacology*, vol. 143, no. 1, pp. 186–192, 2004.

[18] J. Eisfeld and A. Lückhoff, "TRPM2," in *Transient Receptor Potential (TRP) Channels*, vol. 179 of *Handbook of Experimental Pharmacology*, pp. 237–252, Springer, Berlin, Germany, 2007.

[19] C. Dölle, J. G. M. Rack, and M. Ziegler, "NAD and ADP-ribose metabolism in mitochondria," *The FEBS Journal*, vol. 280, no. 15, pp. 3530–3541, 2013.

[20] M. Giacomello, I. Drago, P. Pizzo, and T. Pozzan, "Mitochondrial Ca^{2+} as a key regulator of cell life and death," *Cell Death and Differentiation*, vol. 14, no. 7, pp. 1267–1274, 2007.

[21] P. Pizzo, I. Drago, R. Filadi, and T. Pozzan, "Mitochondrial Ca^{2+} homeostasis: mechanism, role, and tissue specificities," *Pflügers Archiv—European Journal of Physiology*, vol. 464, no. 1, pp. 3–17, 2012.

[22] N. Braun, D. Klumpp, J. Hennenlotter et al., "UCP-3 uncoupling protein confers hypoxia resistance to renal epithelial cells and is upregulated in renal cell carcinoma," *Scientific Reports*, vol. 5, article 13450, 2015.

[23] J. Rudner, V. Jendrossek, and C. Belka, "New insights in the role of Bcl-2 Bcl-2 and the endoplasmic reticulum," *Apoptosis*, vol. 7, no. 5, pp. 441–447, 2002.

[24] S. A. Oakes, J. T. Opferman, T. Pozzan, S. J. Korsmeyer, and L. Scorrano, "Regulation of endoplasmic reticulum Ca^{2+} dynamics by proapoptotic BCL-2 family members," *Biochemical Pharmacology*, vol. 66, no. 8, pp. 1335–1340, 2003.

[25] P. Pinton and R. Rizzuto, "Bcl-2 and Ca^{2+} homeostasis in the endoplasmic reticulum," *Cell Death and Differentiation*, vol. 13, no. 8, pp. 1409–1418, 2006.

[26] G. Monaco, T. Vervliet, H. Akl, and G. Bultynck, "The selective BH4-domain biology of Bcl-2-family members: IP3Rs and beyond," *Cellular and Molecular Life Sciences*, vol. 70, no. 7, pp. 1171–1183, 2013.

[27] S. M. Huber, L. Butz, B. Stegen et al., "Ionizing radiation, ion transports, and radioresistance of cancer cells," *Frontiers in Physiology*, vol. 4, article 212, 2013.

[28] J. Rudner, A. Lepple-Wienhues, W. Budach et al., "Wild-type, mitochondrial and ER-restricted Bcl-2 inhibit DNA damage-induced apoptosis but do not affect death receptor-induced apoptosis," *Journal of Cell Science*, vol. 114, no. 23, pp. 4161–4172, 2001.

[29] J. Rudner, S. J. Elsaesser, A.-C. Müller, C. Belka, and V. Jendrossek, "Differential effects of anti-apoptotic Bcl-2 family members Mcl-1, Bcl-2, and Bcl-xL on celecoxib-induced apoptosis," *Biochemical Pharmacology*, vol. 79, no. 1, pp. 10–20, 2010.

[30] J. Rudner, V. Jendrossek, K. Lauber, P. T. Daniel, S. Wesselborg, and C. Belka, "Type I and type II reactions in TRAIL-induced apoptosis—results from dose-response studies," *Oncogene*, vol. 24, no. 1, pp. 130–140, 2005.

[31] J. Rudner, S. J. Elsaesser, V. Jendrossek, and S. M. Huber, "Anti-apoptotic Bcl-2 fails to form efficient complexes with pro-apoptotic Bak to protect from Celecoxib-induced apoptosis," *Biochemical Pharmacology*, vol. 81, no. 1, pp. 32–42, 2011.

[32] P. H. Barry and J. W. Lynch, "Liquid junction potentials and small cell effects in patch-clamp analysis," *The Journal of Membrane Biology*, vol. 121, no. 2, pp. 101–117, 1991.

[33] E. Cerami, J. Gao, U. Dogrusoz et al., "The cBio cancer genomics portal: an open platform for exploring multidimensional cancer genomics data," *Cancer Discovery*, vol. 2, no. 5, pp. 401–404, 2012.

[34] J. Gao, B. A. Aksoy, U. Dogrusoz et al., "Integrative analysis of complex cancer genomics and clinical profiles using the cBioPortal," *Science Signaling*, vol. 6, no. 269, p. pl1, 2013.

[35] J. Barretina, G. Caponigro, N. Stransky et al., "The Cancer Cell Line Encyclopedia enables predictive modelling of anticancer drug sensitivity," *Nature*, vol. 483, no. 7391, pp. 603–607, 2012.

[36] R. Kraft, C. Grimm, H. Frenzel, and C. Harteneck, "Inhibition of TRPM2 cation channels by N-(p-amylcinnamoyl)anthranilic acid," *British Journal of Pharmacology*, vol. 148, no. 3, pp. 264–273, 2006.

[37] K. R. Laub, K. Witschas, A. Blicher, S. B. Madsen, A. Lückhoff, and T. Heimburg, "Comparing ion conductance recordings of synthetic lipid bilayers with cell membranes containing TRP channels," *Biochimica et Biophysica Acta—Biomembranes*, vol. 1818, no. 5, pp. 1123–1134, 2012.

[38] K. Hill, S. McNulty, and A. D. Randall, "Inhibition of TRPM2 channels by the antifungal agents clotrimazole and econazole," *Naunyn-Schmiedeberg's Archives of Pharmacology*, vol. 370, no. 4, pp. 227–237, 2004.

[39] K. K. H. Chung, P. S. Freestone, and J. Lipski, "Expression and functional properties of TRPM2 channels in dopaminergic neurons of the substantia nigra of the rat," *Journal of Neurophysiology*, vol. 106, no. 6, pp. 2865–2875, 2011.

[40] F. J. P. Kühn, I. Heiner, and A. Lückhoff, "TRPM2: a calcium influx pathway regulated by oxidative stress and the novel second messenger ADP-ribose," *Pflugers Archiv European Journal of Physiology*, vol. 451, no. 1, pp. 212–219, 2005.

[41] R. A. Kirkland, G. M. Saavedra, B. S. Cummings, and J. L. Franklin, "Bax regulates production of superoxide in both apoptotic and nonapoptotic neurons: role of caspases," *Journal of Neuroscience*, vol. 30, no. 48, pp. 16114–16127, 2010.

[42] S. M. Huber, "Oncochannels," *Cell Calcium*, vol. 53, no. 4, pp. 241–255, 2013.

[43] M. Steinle, D. Palme, M. Misovic et al., "Ionizing radiation induces migration of glioblastoma cells by activating BK K^+ channels," *Radiotherapy and Oncology*, vol. 101, no. 1, pp. 122–126, 2011.

[44] K. Dittmann, C. Mayer, H. P. Rodemann, and S. M. Huber, "EGFR cooperates with glucose transporter SGLT1 to enable chromatin remodeling in response to ionizing radiation," *Radiotherapy and Oncology*, vol. 107, no. 2, pp. 247–251, 2013.

[45] S. M. Huber, M. Misovic, C. Mayer, H.-P. Rodemann, and K. Dittmann, "EGFR-mediated stimulation of sodium/glucose cotransport promotes survival of irradiated human A549 lung adenocarcinoma cells," *Radiotherapy and Oncology*, vol. 103, no. 3, pp. 373–379, 2012.

[46] N. Heise, D. Palme, M. Misovic et al., "Non-selective cation channel-mediated Ca^{2+}-entry and activation of Ca^{2+}/calmodulin-dependent kinase II contribute to G_2/M cell cycle arrest and survival of irradiated leukemia cells," *Cellular Physiology and Biochemistry*, vol. 26, no. 4-5, pp. 597–608, 2010.

[47] D. Palme, M. Misovic, E. Schmid et al., "Kv3.4 potassium channel-mediated electrosignaling controls cell cycle and survival of irradiated leukemia cells," *Pflugers Archiv European Journal of Physiology*, vol. 465, no. 8, pp. 1209–1221, 2013.

[48] B. Stegen, L. Butz, L. Klumpp et al., "Ca^{2+}-activated IK K^+ channel blockade radiosensitizes glioblastoma cells," *Molecular Cancer Research*, vol. 13, no. 9, pp. 1283–1295, 2015.

[49] J. Cheng and M. Haas, "Frequent mutations in the p53 tumor suppressor gene in human leukemia T-cell lines," *Molecular and Cellular Biology*, vol. 10, no. 10, pp. 5502–5509, 1990.

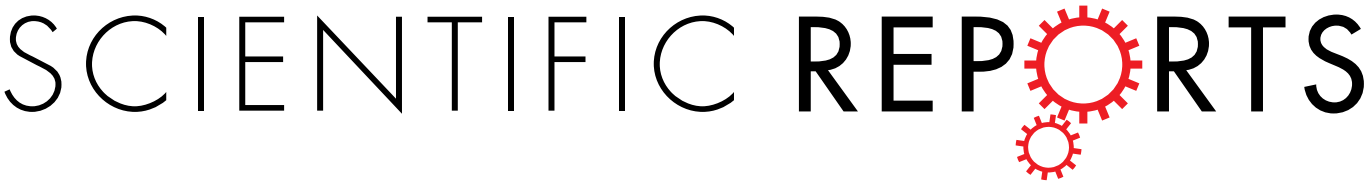

OPEN

UCP-3 uncoupling protein confers hypoxia resistance to renal epithelial cells and is upregulated in renal cell carcinoma

Received: 03 November 2014
Accepted: 01 July 2015
Published: 25 August 2015

Norbert Braun[1], Dominik Klumpp[1], Jörg Hennenlotter[2], Jens Bedke[2], Christophe Duranton[3], Martin Bleif[1,†] & Stephan M. Huber[1]

Tumor cells can adapt to a hostile environment with reduced oxygen supply. The present study aimed to identify mechanisms that confer hypoxia resistance. Partially hypoxia/reoxygenation (H/R)-resistant proximal tubular (PT) cells were selected by exposing PT cultures to repetitive cycles of H/R. Thereafter, H/R-induced changes in mRNA and protein expression, inner mitochondrial membrane potential ($\Delta\Psi_m$), formation of superoxide, and cell death were compared between H/R-adapted and control PT cultures. As a result, H/R-adapted PT cells exhibited lower H/R-induced hyperpolarization of $\Delta\Psi_m$ and produced less superoxide than the control cultures. Consequently, H/R triggered $\Delta\Psi_m$ break-down and DNA degradation in a lower percentage of H/R-adapted than control PT cells. Moreover, H/R induced upregulation of mitochondrial uncoupling protein-3 (UCP-3) in H/R-adapted PT but not in control cultures. In addition, ionizing radiation killed a lower percentage of H/R-adapted as compared to control cells suggestive of an H/R-radiation cross-resistance developed by the selection procedure. Knockdown of UCP-3 decreased H/R- and radioresitance of the H/R-adapted cells. Finally, UCP-3 protein abundance of PT-derived clear cell renal cell carcinoma and normal renal tissue was compared in human specimens indicating upregulation of UCP-3 during tumor development. Combined, our data suggest functional significance of UCP-3 for H/R resistance.

Intermittent or chronic hypoxia due to insufficient vascularization and tissue malperfusion is a common feature of human solid tumors. In anti-cancer therapy, tumor hypoxia is a severe risk factor since the causative malperfusion limits not only oxygen supply but also the perfusion of the tumor with chemotherapeutics. In addition, low oxygen pressure during radiation therapy decreases the number of ionizing radiation-induced DNA double strand breaks and thereby the therapy efficacy by a factor of up to 3. Moreover, adaptation of tumor cells to a malperfused hypoxic microenvironment often induces/selects tumor cells with higher malignancy, metastatic potential and intrinsic resistance to radiation or chemotherapy. For instance, upregulation of highly efficient Na^+-coupled glucose uptake by several tumor entities does not only ensure glucose supply by the malperfused glucose-depleted environment but also confer radioresistance[1–3].

Hypoxia and reoxygenation may result in oxidative insults as reported for ischemia/reperfusion injury of the heart. During reoxygenation of hypoxic tissue, oxidative stress may be triggered by Ca^{2+} overload of the mitochondria, concomitant hyperpolarization of the voltage ($\Delta\Psi_m$) across the inner mitochondrial membrane and superoxide formation as a consequence thereof (for review see Ref. 4). Tumor cells

[1]Department of Radiation Oncology, University of Tübingen Germany. [2]Department of Urology, University of Tübingen, Germany. [3]Department of Faculté de Médecine, Université de Nice-Sophia Antipolis, Nice, France. [†]Present address: Radiochirurgicum/Cyberknife Südwest & Department of Radiation Oncology, Göppingen, Germany. Correspondence and requests for materials should be addressed to S.M.H. (email: stephan.huber@uni-tuebingen.de)

surrounded by a microenvironment with varying oxygen pressure are, therefore, under continuous risk of mitochondria-derived oxidative insults.

The present study aimed to define mechanisms of hypoxia/reoxygenation (H/R) adaptation *in vitro* by comparing H/R-adapted with highly hypoxia-sensitive parental cells. For H/R adaptation, immortalized primary cultures of mouse proximal convoluted tubule (PT) which are highly dependent on oxidative respiration and, therefore, highly hypoxia-sensitive were subjected to repeated cycles of hypoxia and reoxygenation[5]. That way H/R-adapted PT cultures were then compared with the continuously normoxic-grown parental control cells in terms of H/R-induced impairment of mitochondrial function, formation of reactive oxygen species (ROS), cell death and gene expression. Our data suggest that up-regulation of the mitochondrial uncoupling protein-3 (UCP-3) contributes to H/R adaptation *in vitro*. Finally, to estimate whether this *in vitro* finding might be translated to the *in vivo* situation, the present study analyzed UCP-3 expression in PT-derived clear cell renal cell carcinoma demonstrating marked up-regulation of UCP-3 by the tumor cells.

Results

Selection of partial H/R-resistant proximal convoluted tubule (PT) cells. Four parallel cultures of PT cells were passaged (once per week) for 12 weeks. During this period of time, cells where subjected to weekly cycles of hypoxia (0.1% oxygen for 48 h) and reoxygenation (5 days). Each cycle started 2–3 d after passaging the cells. As a control, further four PT cultures were grown under continuous normoxia, and passaged twice weekly for 12 weeks (Fig. 1A). Thereafter, all cultures were passaged twice to increase the cell number, aliquoted and frozen. To test for an acquired H/R resistance, sub-confluent H/R-adapted and control cultures were grown for 48 h under normoxia or hypoxia (0.1% oxygen) followed by 0.5, 24 or 48 h of reoxygenation. Thereafter, the DNA of the cells was stained with propidium iodide (Nicoletti protocol). As shown in the histograms of Fig. 1B, H/R induced a G_2/M cell cycle arrest in both, control and H/R-adapted PT cells, suggestive of H/R-caused genotoxic stress. In addition, H/R resulted in cell death as defined by the sub G_1 population of the propidium iodide histogram. Cell death induction was dependent on reoxygenation time (Fig. 1B). Most importantly, cell death was significantly reduced in the H/R-adapted cells as compared to the control cultures (Fig. 1C) indicating acquisition of a partial H/R resistance during the selection time. Fig. 1D shows the selection cycle-dependent acquisition of the partial H/R resistance.

H/R-induced hyperpolarization of the inner mitochondrial membrane potential ($\Delta\Psi_m$). Reportedly, reoxygenation may be associated with hyperpolarization of $\Delta\Psi_m$. We, therefore, tested for the effect of hypoxia (48 h)/reoxygenation (24 h) on $\Delta\Psi_m$ in control and H/R-adapted PT-cultures by flow cytometry applying the voltage-sensitive fluorescence dye TMRE. H/R induced break-down of $\Delta\Psi_m$ (Fig. 2) in a significant cell fraction confirming H/R-induced cell death (Fig. 2A–C). In the surviving cells, on the other hand, H/R hyperpolarized $\Delta\Psi_m$ (Fig. 2B,D). Markedly, H/R-adapted PT cultures exhibited both, significantly less H/R-induced $\Delta\Psi_m$ break-down (Fig. 2C) and significantly less $\Delta\Psi_m$ hyperpolarization in the surviving cell population (Fig. 2D).

H/R-induced formation of reactive oxygen species (ROS). Mitochondrial superoxide formation increases with hyperpolarization of $\Delta\Psi_m$. Next, we analyzed cumulative superoxide formation of the control and selected cultures during normoxia and upon hypoxia (48 h)/reoxygenation (24 h) by flow cytometry using the redox-sensitive fluorescence dye MitoSOX. As shown in Fig. 3, H/R-induced superoxide formation was significantly lower in H/R-adapted than in control PT cultures.

Function of Uncoupling Protein-3 (UCP-3). To define candidate genes that might confer H/R resistance, mRNA abundances (quantitative RT-PCR microarrays) were compared between control and H/R-adapted PT cultures after normoxic culture conditions and upon hypoxia (48 h)/reoxygenation (24 h). Several gene transcripts involved in apoptosis and antioxidative defense seemingly differed in abundance between the control and H/R-adapted PT cultures (see Supplementary Material, Fig. I) suggesting that long-term H/R adaptation was accompanied by upregulation of oxidative defense, DNA-repair and the apoptosis inhibitor survivin on the one hand, and by an enhancement of the apoptotic cell death machinery on the other. In addition, H/R-adapted PT cultures upregulated uncoupling protein-3 (UCP-3) mRNA, in particular, upon acute H/R (Fig 4A). Western blotting experiments confirmed that H/R induced a significant upregulation of UCP-3 protein expression (~4-fold increase) in the H/R-adapted but not in the control cultures (Fig. 4B,C).

Since UCP-3 has been demonstrated to reduce mitochondrial ROS formation, to lower ischemia/reperfusion insults, and to become up-regulated by anaerobic muscle exercise (see discussion), upregulation of UCP-3 might directly contribute to the observed partial H/R resistance. Therefore, we knocked-down UCP-3 in control and H/R-adapted cultures by RNA interference (Fig 5A) and determined mitochondrial superoxide formation and the the sub G_1 fraction of propidium iodide-stained cells after normoxia or hypoxia (48 h)/reoxygenation (24 h). As shown in Fig. 5, a knock-down-mediated decrease by ~40% of UCP-3 protein abundance (Fig. 5A) significantly increased mitochondrial superoxide formation (Fig. 5B,C) in control and H/R-adapted PT cultures. Moreover UCP-3 knock-down lowered survival

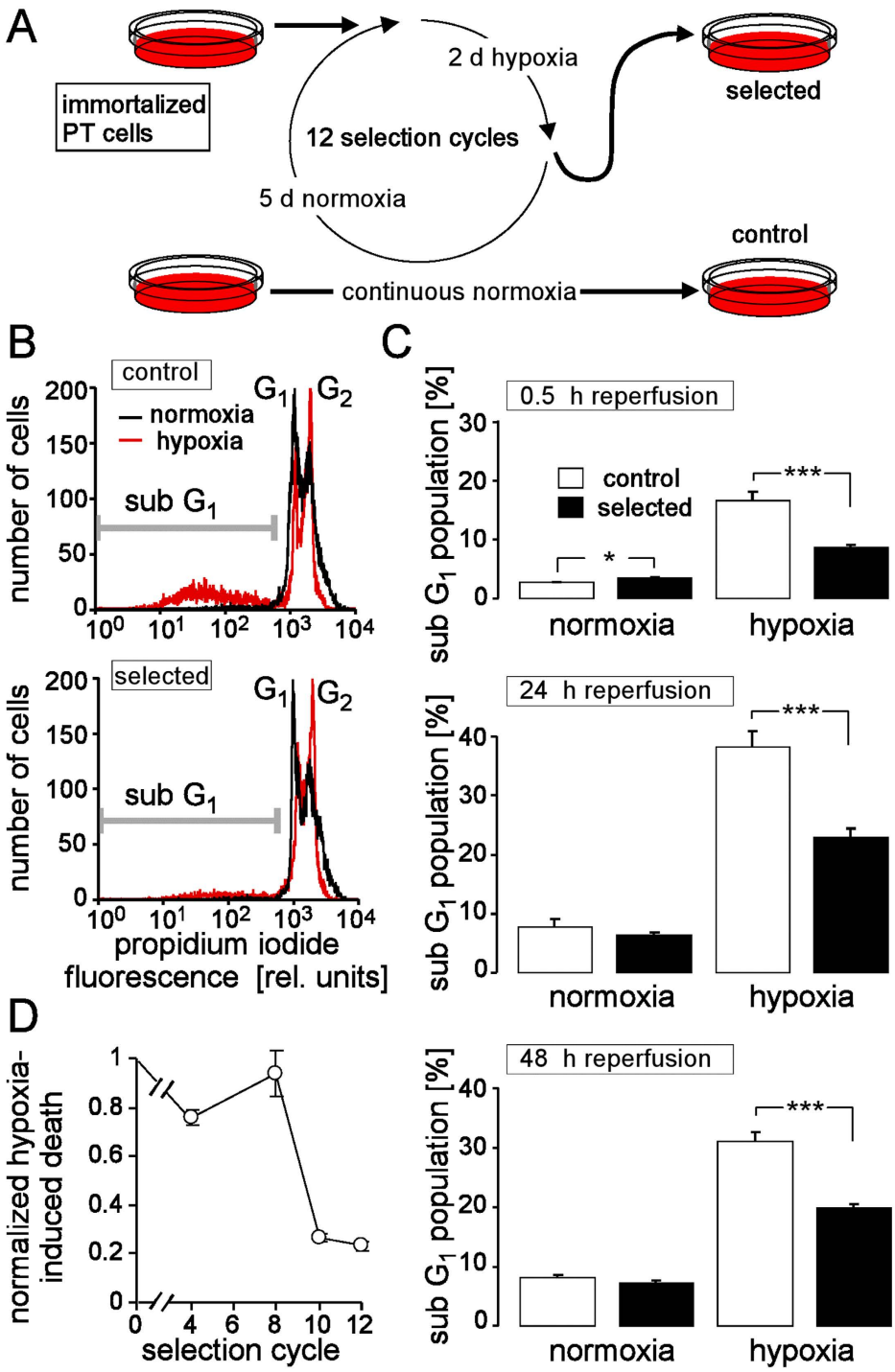

Figure 1. Repetitive exposure to hypoxia/reoxygenation (H/R) selected partial H/R-resistent proximal convoluted tubule (PT) cells. (**A**) Selection protocol. (**B**) Histograms showing the propidium iodide fluorescence intensity of permeabilized control and H/R-adapted PT cells. Cells were recorded by flow cytometry either under control conditions (72 h of normoxia, black line) or after 48 h of hypoxia (0.1% oxygen) followed by 24 h of reoxygenation (red line). The marker indicates the dead cells (sub G_1 population). (**C**) Mean percentage (±SE, n = 24 from 4 cultures each measured in hexaduplicate) of dead cells (sub G_1 population) in control (open bars) and H/R-adapted cultures (closed bars) grown under normoxia (left) or under hypoxia (48 h of 0.1% oxygen) followed by 0.5 h (top), 24 h (middle) and 48 h (bottom) of reoxygenation. * and *** indicate $p \leq 0.05$ and $p \leq 0.001$, respectively (ANOVA). (**D**) Time course of resistance acquisition. Shown is the selection-cycle-dependent H/R-induced cell death of the H/R-adapted cultures normalized to that of the particular control cultures (means ± SE, n = 4).

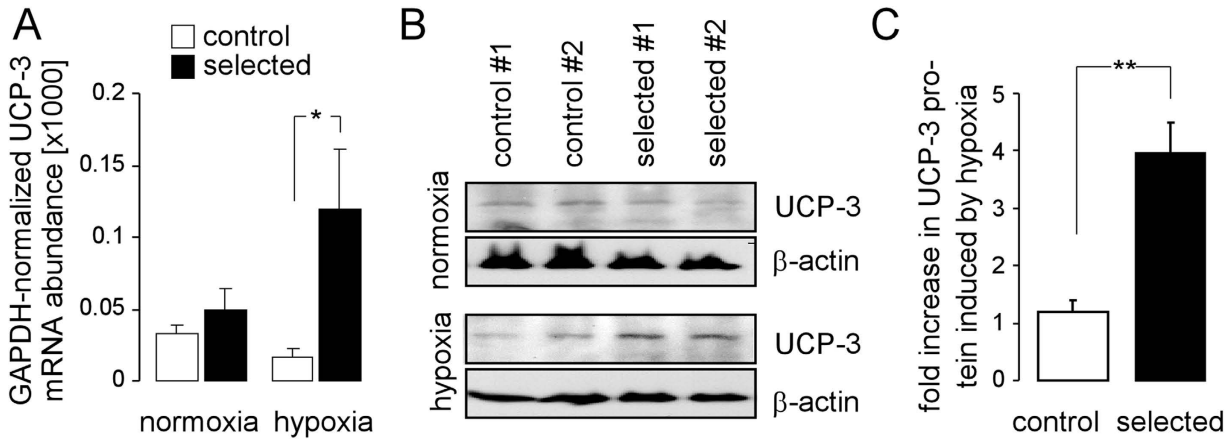

Figure 2. H/R induces an up-regulation of the mitochondrial uncoupling protein-3 (UCP-3) in H/R-adapted but not in control PT cultures. (**A**) Mean (±SE, n = 3) GAPDH-normalized UCP-3 mRNA abundance of control (open bars) and H/R-adapted PT cultures (closed bars) under normoxia (left) or after hypoxia (48 h)/reoxygenation (24 h) as determined by quantitative RT-PCR. (**B**) Immunoblot of PAGE-separated proteins from control (1st and 2nd lane) H/R-adapted PT cultures (3rd and 4th lane) probed against UCP-3 and β-actin. Cell lysates were prepared from normoxic (upper blot) and cultures which underwent H/R stress (lower blot). (**C**). Densitometrically semi-quantified increase in UCP-3 protein of control (open bar) and H/R-adapted PT-cultures induced by hypoxia(48 h)/reoxygenation (24 h; means ± SE, n = 3 cultures each; * indicates $p \leq 0.05$, two-tailed Welch-corrected t-test).

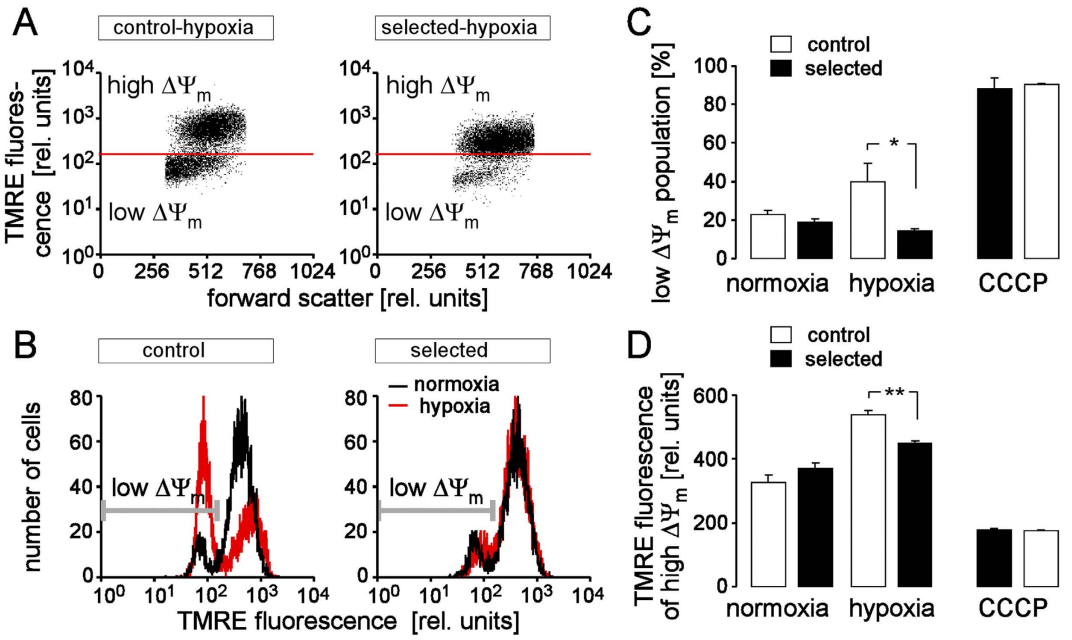

Figure 3. H/R-adapted cultures exhibit after H/R stress less hyperpolarization of the inner mitochondrial membrane potential ($\Delta\Psi_m$) than control cultures. (**A,B**) Dot plots (**A**) and histograms (**B**) showing forward scatter and tetramethylrhodamine-ethyl-ester-perchlorate (TMRE) fluorescence as a measure of cell size and $\Delta\Psi_m$, respectively. Depicted are a control (left) and a H/R-adapted PT culture (right) recorded by flow cytometry under normoxic conditions (black lines in (**B**)) and after H/R stress (48 h hypoxia/24 h reoxygenation; (**A**) and red histograms in (**B**)). Cell populations with dissipated $\Delta\Psi_m$ (low $\Delta\Psi_m$) are indicated by gate and marker in A and B, respectively. (**C,D**) Mean percentage of control (open bars) and H/R-adapted cells (closed bars) with broken-down $\Delta\Psi$m (**C**) and (**D**) mean TMRE fluorescence intensity of the cell population with high $\Delta\Psi_m$ (±SE, n = 9 from 3 cultures each determined in triplicate) recorded as in (**B**) under normoxic conditions (left), after H/R stress (48 h hypoxia/24 h reoxygenation, middle), or after pharmacological break-down of $\Delta\Psi_m$ by the proton ionophore carbonyl cyanide-3-chlorophenylhydrazone (CCCP, 1 μM). * and ** indicate $p \leq 0.05$ and $p \leq 0.01$, respectively (ANOVA).

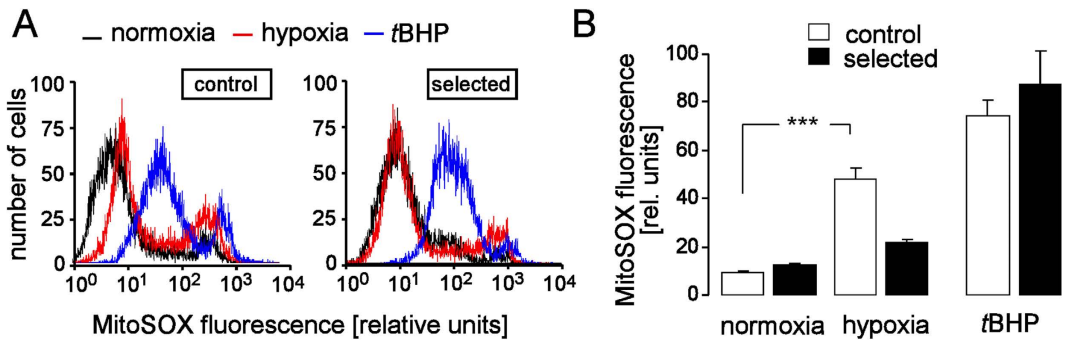

Figure 4. H/R produces less reactive oxygen species (ROS) in H/R-adapted than in control cultures. (**A**) Histograms showing the MitoSOX fluorescence as a measure of mitochondrial superoxide production. PT cells were recorded by flow cytometry from a control (top) and a H/R-adapted culture under normoxic conditions (black lines), after H/R stress (48 h hypoxia/24 h reoxygenation, red lines) or after oxidation with *tert*butylhydroperoxide (*t*BHP, 1 mM). (**B**) Mean MitoSOX fluorescence intensities recorded as in (**A**) under normoxic conditions (left), after H/R stress (48 h hypoxia/24 h reoxygenation, middle, data are means ± SE, n = 10–12 from 4 cultures each determined in duplicate or triplicate), or after oxidation with *t*BHP (means ± SE, n = 4 from 4 cultures recorded under normoxia) *** indicates $p \leq 0.001$ (ANOVA).

after H/R of the H/R-adapted but not of the control PT cultures (Fig. 5D,E). This suggests that UCP-3 upregulation contributes to the H/R adaptation.

UCP expression in renal cell carcinoma. To test whether UCP-3 might fulfill similar function *in vivo*, UCP-3 protein abundance was determined by immunoblotting in frozen specimens from human renal cell carcinoma (RCC) and normal renal tissue. Twentyseven tumor specimens (18 clear cell RCCs, ccRCS, 6 papillary RCCs, pRCCs, and 3 mixed clear cell/papillary RCCs, median histological grading G = 2) as well as 15 non-cancerous renal specimens were selected form 21 patients that underwent (partial) nephrectomy. The patients (11 men, 10 women, mean age = 67 ± 2 years) developed large tumors ranging from 3 cm to 21 cm in diameter (mean diameter = 8 ± 1 cm). These tumors had large necrotic areas pointing to insufficient vascularization (Fig. 6A). The majority of tumor specimens showed various levels of UCP-3 protein abundance (Fig. 6B) that was on average significantly higher than in the non-cancerous renal samples (Fig. 6C) indicating upregulation of UCP-3 during tumor development. Although some tumor specimens close to necrotic tumor areas (i.e., from presumed hypoxic regions, T_N in Fig. 6B) showed extremely high UCP-3 protein abundance while peripheral tumor (T_P in Fig. 6B) exhibited very low expression, the average UCP-3 abundance of T_N specimens was not significantly different from that of the tumor samples of non-defined origin (data not shown). No difference in UCP-3 protein abundance was found between ccRCCs (Fig. 6C, red triangles) and pRCCs (Fig. 6C, blue triangles). In addition, univariate testing of the data suggested that UCP-3 abundance was not associated with patients' age, gender, tumor size, occurrence of lymph node or distant metastasis, or histological tumor grading (data not shown).

To test whether RCCs similarly to UCP-3 upregulate other mitochondrial uncoupling proteins, UCP-1 and UCP-2 protein abundance was determined by immunoblotting in the RCC resection material (Suppl Fig. IIA). The results suggested downregulation of UCP-1 by all and upregulation of UCP-2 by some of the tested RCCs. In addition, the ccRCC database of The Cancer Genome Atlas (TCGA) was queried for UCP-1, -2, and 3 mRNA expression of the tumor and survival of the ccRCC patients (Suppl. Fig. IIB, C). The TCGA data suggest co-occurrence of high abundant UCP-2 and UCP3 mRNA in the ccRCC specimens (data not shown) as well as shorter survival of ccRCC patients with high UCP-2 or UCP-3 mRNA abundance in the tumors as compared to the patients with "middle-rate" UCP expressions (Suppl. Fig. IIB, C). High abundance of UCP-1 mRNA, by contrast, was not associated with altered survival of the ccRCC patients. Since subgroup analysis concerning tumor staging, treatment regimes, etc. could not be performed, the conclusions drawn from the TCGA data is constrained. Nevertheless, the observed associations might point to a prognostic value of the UCP-3 or UCP-2 expression by the ccRCC. In addition, the data might hint to a functional redundancy of UCP-2 and UCP-3.

H/R-adapted cultures exhibit higher resistance against ionizing radiation. Finally, we tested the possibility whether adaptation to H/R is accompanied by increased resistance against anti-cancer therapies such as radiation therapy. To this end, control and H/R-adapted cultures were irradiated under normoxia with a single dose of 0, 5, or 10 Gy, and $subG_1$ population was recorded by flow cytometry (DNA staining of propidium iodide-permeabilized cells applying the Nicoletti protocol) as a measure of cell death 24 h and 48 h thereafter. As shown in Fig. 7, irradiated (10 Gy) H/R-adapted cells died

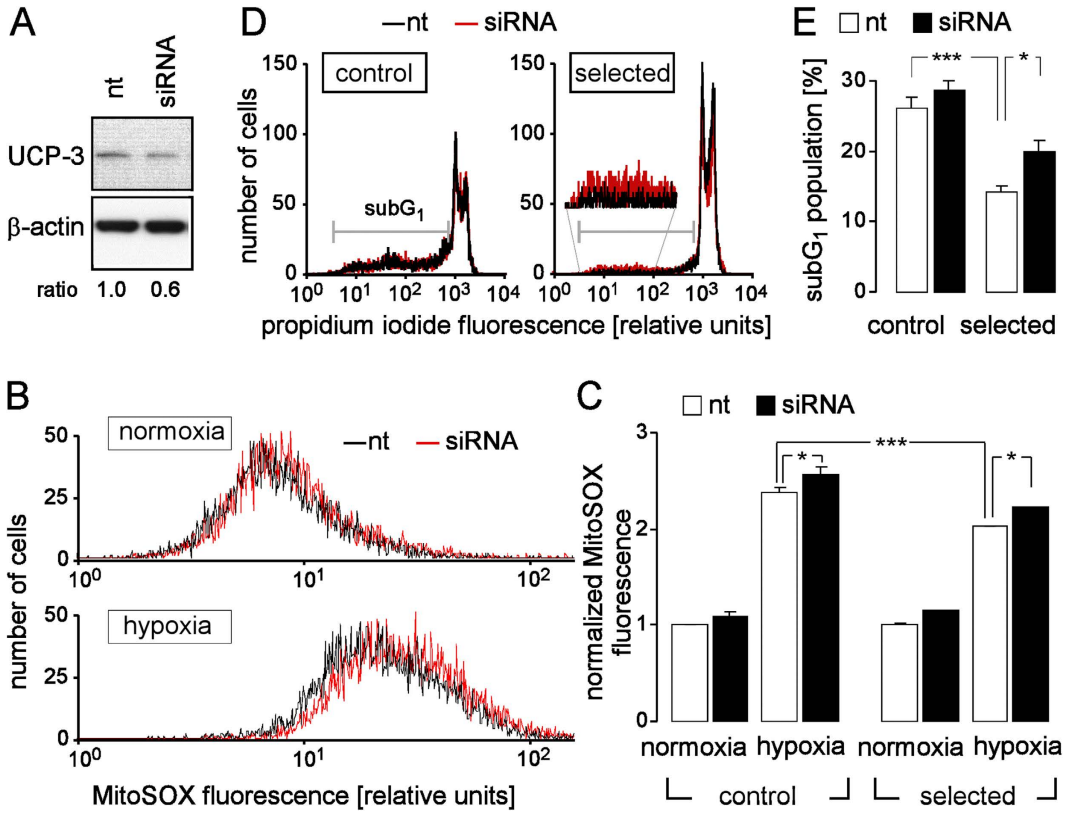

Figure 5. UCP-3 knock-down increases H/R-induced superoxide production and cell death. (**A**) Immunoblot showing the UCP-3 (upper gel) and—for loading control—the β-actin (lower gel) protein abundance in PT culture transfected with non-targeting (nt) RNA (left lane) or with UCP-3 siRNA (right lane). The ratio indicates the densitometrically semi-quantified β-actin-normalized relative UCP-3 protein abundance. (**B**) Histograms showing the MitoSOX fluorescence of nt- (black lines) and UCP-3 siRNA-transfected (red lines) PT cells after normoxia (top) or H/R stress (48 h hypoxia/24 h reoxygenation, bottom), recorded as in Fig. 4. (**C**) Mean normalized MitoSOX fluorescence intensities of nt- (open bars) and UCP-3 siRNA-transfected (closed bars) control and H/R-adapted PT cultures PT cells recorded in as in (**B**) under normoxic conditions or after H/R stress. Data are means ± SE, n = 6 from 2 cultures each determined in triplicate. (**D**) Histograms showing the propidium iodide fluorescence of permeabilized nt- (black line) and UCP-3 siRNA-transfected (red line) control (left) and H/R-adapted PT cultures (right) after hypoxia (48 h)/reoxygenation (24 h, recorded as in Fig. 1). (**E**) Mean percentage (±SE, n = 7–9 from 3 cultures each recorded in duplicate or triplicate) of dead cells (sub G_1 population) in nt- (open bars) or UCP-3 siRNA-transfected control and H/R-adapted PT cultures after H/R stress (48 h hypoxia/24 h reoxygenation. * and *** indicate $p \leq 0.05$ and $p \leq 0.001$, respectively (ANOVA).

significantly less than irradiated control cells as evident 48 h after irradiation. This might suggest that adaptation to H/R leads to partial cross-resistance against ionizing radiation possibly due to upregulation of DNA repair and oxidative defense (see Suppl. Fig. I). The latter might mitigate the radiation-caused cellular lesions.

To directly test for an involvement of UCP-3 in the acquired radioresitance of the H/R-adapted PT cultures, the effect of UCP-3 knockdown on radiogenic cell death was determined in control and H/R-adapted PT cultures. 48 h after irradiation (0 or 10 Gy) and 96 h after transfection with nt or UCP-3 siRNA, subG$_1$ population of propidium iodide-stained cells was determined by flow cytometry (Fig. 7C,D). While having no effect on control cultures, UCP-3 knockdown increased slightly but significantly the fraction of dead cells caused by radiation (Fig. 7D,E).

Discussion

UCP-3 uncoupling protein belongs to the mitochondrial anion transporter superfamily and is highly expressed in the mitochondrial inner membrane of brown adipose tissue, skeletal muscle and heart[6,7]. In the present study, selected, partially HR-resistant PT cultures differed from continuously normoxic grown control cultures by expression of genes involved in DNA repair, apoptosis and oxidative defense and by the ability to up-regulate mitochondrial UCP-3 uncoupling protein during H/R stress. Evidence for a functional significance of this UCP-3 upregulation for the partial H/R resistance in the selected

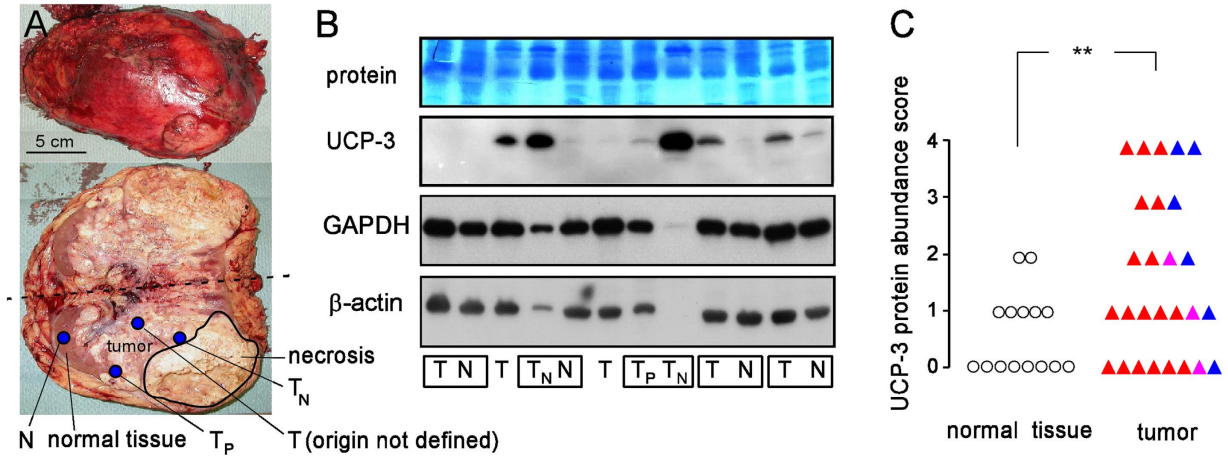

Figure 6. UCP-3 protein expression in human renal cell carcinoma and adjacent non-cancerous normal renal tissue. (**A**) Human nephrectomy specimen top view (upper panel) and opened cut halves (lower panel) with renal cell carcinoma (RCC). Areas of necrosis and residual normal tissue, as well as locations of the sample taking are indicated (N: normal renal tissue, T: tumor without defined origin. T_N: tumor close to necrotic area, T_P: tumor at the periphery). (**B**) Immunoblot of renal cell carcinoma and normal renal tissue (as shown in (**A**)) probed against UCP-3 (2nd panel), GAPDH (3rd panel) and β-actin (4th panel). The 1st panel depicts the corresponding protein stain (PageBlue). The low or even missing housekeeper bands of the 4th and 8th sample (from left) might be explained by strong overexpression of other proteins by theses two tumors. Since electrophoresis loading volume was adjusted to total protein concentration strong overexpression of some proteins dilutes the housekeeper proteins in these samples. Boxes indicate samples which originated from the same kidney. (**C**) Scoring of the UCP-3 protein abundance in non-cancerous renal tissue (open circles) and clear cell RCCs (closed red triangles), papillary RCCs (closed blue triangles) or mixed RCCs (closed violet triangles). ** indicates $p \leq 0.01$, Welch-corrected, two-tailed t-test.

cultures came from the observation that knockdown of UCP-3 by RNA interference significantly attenuated the H/R resistance in the selected cultures while having no effect in the control cultures.

An increasingly growing number of reports demonstrates that UCP-3 may lower mitochondrial ROS production by decreasing $\Delta\Psi_m$ as a "mild uncoupler". This mild uncoupling function of UCP-3 is in particular evident from the observation that UCP-3 knockout results in increased mitochondrial ROS formation and oxidative damage of isolated skeletal muscle mitochondria or permeabilized muscle cells[8–11]. Importantly, chemical uncoupling in UCP-3 knockout mitochondria partially mimics the function of UCP-3[11]. Moreover, UCP-3 knockout lowers fatty acid- or reactive aldehyde-stimulated increase in proton leak of the inner mitochondrial membrane[12,13]. Accordingly, overexpression of UCP-3 in myotubes decreases both $\Delta\Psi_m$[14–16] and mitochondrial ROS formation[15].

In addition to these *in vitro* data, animal studies utilizing UCP-3 knockout or UCP-3 overexpressing mice demonstrated that UCP-3 decreases mitochondrial ROS-formation in fasted mice[10] and protects from diet-induced obesity[17] and insulin resistance[18], two diseases associated with oxidative stress[15]. Moreover, downregulation of UCP-3 in rats that is associated with doxorubicin chemotherapy-induced heart failure improves efficiency of cardial ATP synthesis at an expense of increased mitochondrial ROS formation[19]. Finally, UCP-3 knockdown increased ischemia/reperfusion-induced mitochondrial ROS formation in the heart[20]. Again, chemical mitochondrial uncoupling partially compensated for UCP-3 function in the UCP-3 knock-out heart[20]. Combined these data provide overwhelming evidence that UCP-3 lowers stress-induced mitochondrial ROS formation by preventing excessive hyperpolarization of $\Delta\Psi_m$.

The UCP-3-generated transports that may short-circuit the inner mitochondrial membrane, however, are still ill-defined. It has been suggested that UCP-3 may export pyruvate[21] and fatty acids including lipid radicals[13,22] from the mitochondrial matrix along their electrochemical gradients. Besides lowering $\Delta\Psi_m$ and directly decreasing the concentration of lipid radicals in the matrix, pyruvate and fatty acids transports are thought to ensure an equilibrium between glycolysis and oxidative phosphorylation and to prevent Co-enzyme A shortage in the matrix and consecutive lipid-induced mitochondrial damage, respectively[23,24]. As matter of fact, UCP-3 upregulation increases the efficiency of fatty acid oxidation in exercising muscle[9]. Along those lines, in animal models and in human beings, fastening[25,26], high fat diet[27], or direct infusion of fatty acids[26] have been demonstrated to upregulate UCP-3 expression which is consistent with a specific function of UCP-3 in switching the metabolism from glucose to fatty acid respiration. A recent meta-analysis demonstrates an association between the -55C/T polymorphism in the UCP-3 gene and obesity further suggesting such a UCP-3 function[28].

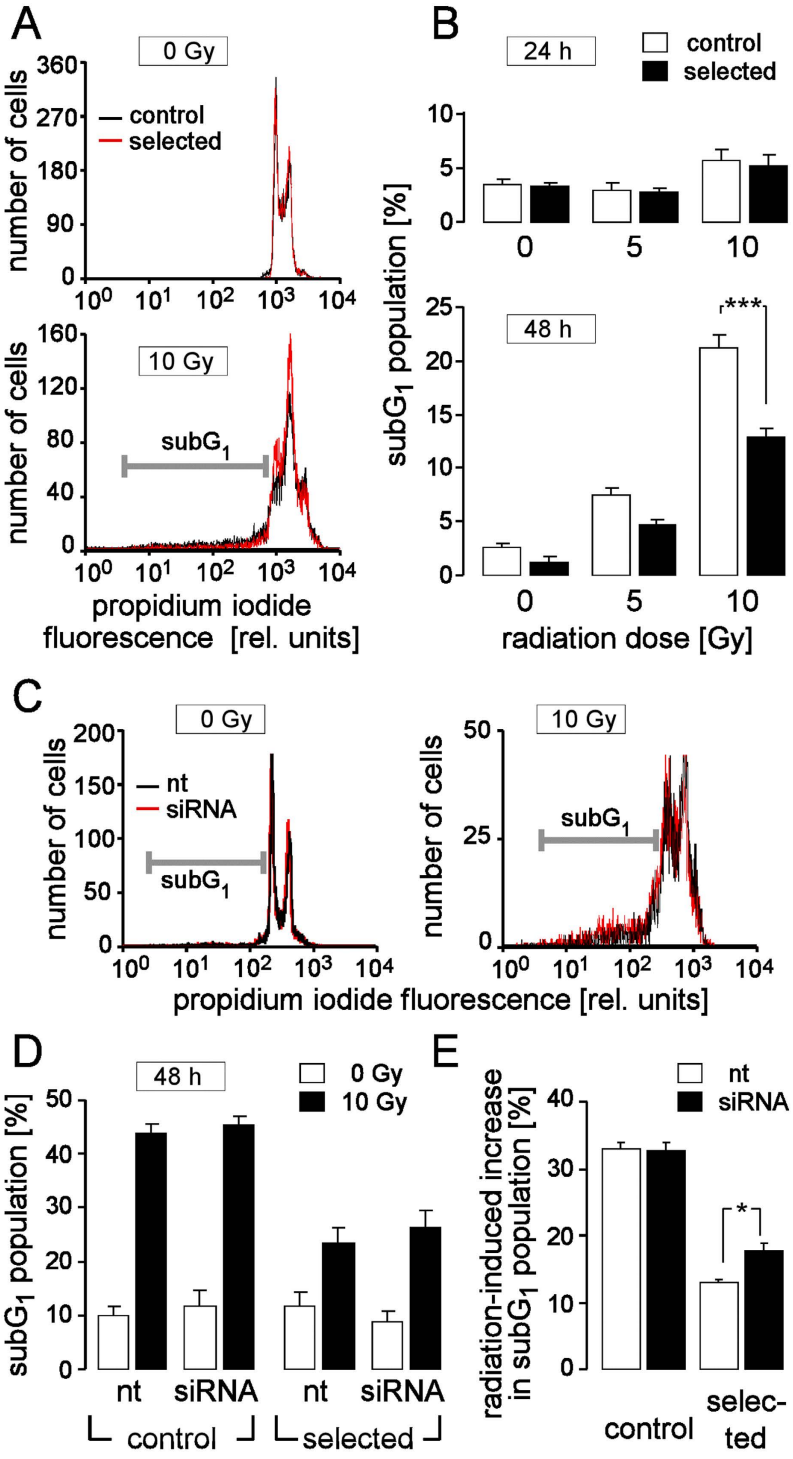

Figure 7. Cross resistance of H/R-adapted cultures against ionizing radiation. (**A**) Histograms showing the propidium iodide fluorescence of permeabilized control (black) and H/R-adapted (red) PT cells. Cells were recorded by flow cytometry 48 h after irradiation (under normoxic conditions) with 0 Gy (top) or 10 Gy (botom). The marker indicates the dead cells (sub G_1 population). Percentage of dead cells (sub G_1 population) in control (open bars) and H/R-adapted cultures (closed bars) 24 h (top) and 48 h (bottom) after irradiation (under normoxic conditions) with 0, 5, or 10 Gy. (**C**) Propidium iodide histograms of nt RNA- (black) and UCP-3 siRNA (red) transfected H/R-adapted PT cells 48 h after irradiation with 0 Gy (left) or 10 Gy (right). (**D**) Sub G_1 population control (left) and H/R-adapted PT cultures (right) 96 h after transfection with nt or UCP-3 siRNA (as indicated) and 48 h after irradiation with 0 Gy (open bars) and 10 Gy (closed bars). Data are means ± SE, n = 9 in (**B**) or n = 6 in (**D**,**E**) from 3 (**B**) or 2 (**D**,**E**) cultures each determined in triplicates. * and *** indicate $p \leq 0.05$ and $p \leq 0.001$ (ANOVA), respectively.

Further triggers of UCP-3 expression include (anaerobic) exercise of skeletal muscle[9,29] and ischemia/reperfusion of the heart[20,30]. Likewise, oxidative stress following inhibition of glutathione reductase have been demonstrated to upregulate UCP-3 expression in rat myocardium[31] where UCP-3 has been demonstrated to be indispensable for ischemic preconditioning[20]. Moreover, reversible glutathionylation during oxidative stress is reportedly required to activate/inhibit UCP-3[32]. Together, these reported data indicate a function of oxidative-stress induced up-regulation of UCP-3 in mitigating ischemic/hypoxia-reperfusion/reoxygenation injury of heart and skeletal muscle.

In the present study, UCP-3 upregulation was paralleled by an attenuated H/R-mediated $\Delta\Psi_m$ hyperpolarization and mitochondrial superoxide formation of the PT cultures hinting to a UCP-3 function similar to that proposed in ischemic heart or anaerobic muscle contraction. UCP-3 protein was also upregulated in the majority of specimens from human renal cell carcinoma (RCC) as compared to the protein abundance of co-resected normal kidney tissue. Since clear cell RCC originates from neoplastic transformation of proximal tubular cells it might be allowed to speculate that UCP-3 in RCC might also confer resistance to H/R. One might further speculate that UCP-3-mediated hypoxia tolerance and survival of the tumor cells in hypoxic areas indirectly confers resistance to chemo- and radiation therapy: the wash-in of chemotherapeutics is hampered by the malperfusion and the efficacy of ionizing radiation is lowered by the low oxygen pressure of hypoxic tumor areas. Along those lines, the TGCA query of the present study hint to the possibility that high UCP-3 expression by the RCC might be associated with poor prognosis.

Similar to the upregulation of UCP-3 by RCC in the present study, other UCPs such as UCP-1, UCP-2, UCP-4 or UCP-5 are reportedly upregulated in a number of aggressive human tumors (leukemia, breast-, colorectal-, ovarian-, bladder-, esophagus-, testicular-, kidney-, pancreatic-, lung-, and prostate cancer) where they are proposed to contribute to the malignant progression of tumors (for review see Ref. 4). Moreover, UCP-2 expression has been associated with paclitaxel resistance of p53 wildtype lung cancer, CPT-11 resistance of colon cancer, and gemcitabine resistance of pancreatic adenocarcinoma, non-small cell lung adenocarcinoma, or bladder carcinoma. Accordingly, experimental targeting of UCPs has been demonstrated to sensitize tumor cells to chemotherapy *in vitro*. (for review see Ref. 4).

In the present study, some RCC specimens exhibited elevated UCP-2 protein amounts as compared to normal renal tissue. UCP-1 protein, in sharp contrast, was downregulated in the RCCs. UCP-2 might exert a function in RCC similar to that proposed for UCP-3. This might be deduced from the TCGA database query of the present study which suggested that—likewise UCP-3—high RCC UCP-2 expression might be associated with bad prognosis.

In the present study, adaptation to H/R was accompanied by partial radioresistance. Knockdown of UCP-3 did, however, only slightly increase radiation-induced cell death of the H/R-adapted PT cultures. Upon UCP-3 knockdown the radiation-induced cell death of the control cultures was still much higher than in the selected cultures (see Fig. 7E) suggesting that radioresistance in the H/R-adapted PT cultures was substantially mediated by upregulation of DNA-repair and other oxidative defense mechanisms (see Suppl. Fig. I).

Ionizing radiation has been reported to upregulate UCP-2 expression in colon carcinoma cells[33] and in a radiosensitive subclone of B cell lymphoma[34], as well UCP-3 expression in rat retina[35]. Moreover, multi-resistant subclones of leukemia cells reportedly show higher UCP-2 protein expression, lower $\Delta\Psi_m$, lower radiation induced formation of reactive oxygen species and decreased DNA damage as compared to their parental sensitive cells[36]. Combined, these reported data hint to a possible function of UCPs in the development of radioresitance also in other tumor entities.

In conclusion, hypoxia/reoxygenation-tolerant PT cultures as well as renal cell carcinoma upregulate UCP-3 uncoupling protein in the inner mitochondrial membrane. UCP-3 upregulation attenuates at least in the *in vitro* PT model mitochondria-born oxidative stress during hypoxia/reoxygenation, and thus, confers partial hypoxia/reoxygenation resistance. Since tumor hypoxia promotes both, malignancy and therapy resistance, UCP-3 protein expression might be a prognostic and predictive marker in human neoplasms.

Methods

Selection of partially H/R-resistant proximal convoluted tubules (PT) cells. PT were microdissected from newborn mice as described elsewhere[37]. PT cells were immortalized by SV40 large T antigen transformation[38] as accomplished by transfection with SV3 neo, selected in geneticin-containing medium and cultured on collagenated surfaces in equal quantities of DMEM and Ham's F-12 (GIBCO) medium containing 29 mM $NaHCO_3$ (GIBCO), 5% serum, 2.5 mM glutamine, 2.5 mg/l insulin, 2.5 mg/l transferrin, 15 nM sodium selenite (ITSS Supplement, Roche Diagnostics), 25 nM dexamethasone (Sigma), 5 ng/l epidermal growth factor (Calbiochem) and G418-BC (60U/ml, Biochrom). Four parallel cultures of PT cells were passaged (once per week) for 12 weeks. In this period of time, cells where weekly subjected to hypoxia (0.1% oxygen for 48 h starting 2–3 d after passaging the cells as applied by the BD GasPak EZ Pouch System,Becton and Dickinson). For control, further four PT cultures were grown under continuous normoxia, passaged twice weekly for 12 weeks. Thereafter, all cultures were passaged twice to increase cell number, aliquoted and frozen.

H/R- and radiation-induced cell death. To test for an acquired hypoxia resistance, sub-confluent H/R-adapted and control cultures (from different selection cycles) were grown for 48 h under normoxia or hypoxia (0.1% oxygen) followed by 0.5, 24 or 48 h of reoxygenation. In further experiments, H/R-adapted and control cultures were irradiated with single doses of 0, 5, or 10 Gy photons by the use of a linear accelerator (LINAC SL25 Philips) at a dose rate of 4 Gy/min at room temperature under normoxia. Following irradiation, cells were post-incubated in supplemented medium for 24 h or 48 h. H/R-treated or irradiated cells were trypsinated and then permeabilized and stained (30 min at room temperature) with propidium iodide (PI) solution (containing 0.1% Na-citrate, 0.1% triton X-100, 10 μg/ml PI in phosphate-buffered saline, PBS), and the DNA amount was analyzed by flow cytometry (FACS Calibur, Becton Dickinson, Heidelberg, Germany, 488 nm excitation wavelength) in fluorescence channel FL-2 (logarithmic scale, 564–606 nm emission wavelength). Dead cells with degraded DNA were defined by the sub G_1 population of the PI histogram. Data were analyzed with the FCS Express 3 software (De Novo Software, Los Angeles, CA, USA).

Inner mitochondrial membrane potential ($\Delta\Psi_m$). To determine $\Delta\Psi_m$, hypoxia (48 h)/reoxygenation (24 h)-subjected as well as normoxic grown H/R-adapted and control PT cultures were trypsinated, washed and incubated for 30 min at room temperature in a NaCl solution (in mM: 125 NaCl, 5 D-glucose, 5 KCl, 1 $MgCl_2$, 1 $CaCl_2$, 32 N-2-hydroxyethylpiperazine-N-2-ethanesulfonic acid (HEPES) titrated with NaOH to pH 7.4) containing the $\Delta\Psi_m$ specific dye tetramethylrhodamine ethyl ester perchlorate (TMRE, 25 nM, Invitrogen). $\Delta\Psi_m$ was analyzed by flow cytometry in FL-2 in the absence or presence of the proton ionophore carbonyl cyanide-3-chlorophenylhydrazone (CCCP, 1 μM).

Formation of reactive oxygen species (ROS). To test for mitochondrial production of superoxide anion, control or H/R-adapted PT cells were pretreated (normoxia or hypoxia (48 h)/reoxygenation (24 h)), detached, incubated for 10 min at 37 °C in NaCl solution (see above) containing 5 μM of the superoxide anion-sensitive dye MitoSOX, Invitrogen), and ROS-specific fluorescence was recorded by flow cytometry in Fl-2. To test for fluorescence dye loading, control samples were oxidized (1 mM *tert*-butylhydroperoxide) for 30 min and recorded.

Quantitative RT-PCR. Messenger RNAs of H/R-adapted and control PT cultures (normoxic and after hypoxia (48 h)/reoxygenation (24 h)) were isolated (Qiagen RNA extraction kit, Hilden, Germany) and reversely transcribed in cDNA (RT^2 First Strand Kit, SABiosciences, Qiagen). mRNA fragments were amplified by the use of an "oxidative stress" and an "apoptosis" PCR array (RT Profiler PCR Array, SABiosciences, Qiagen, Hilden, Germany) and a Roche Light Cycler 480. C_t (threshold cycle) values of the PCR amplifications were normalized to that of the housekeeper genes. Mouse UCP-3 and GAPDH specific cDNAs were amplified by QuantiTect Primer Assays (#QT00115339 and QT01658692, respectively, Qiagen).

Transfection with siRNA. Adherent PT cells were grown in normal medium and transfected at 60% confluence with a transfection reagent (TransIT-TKO, Mirus Bio, Madison, WI, USA) according to the manufacturer's instructions. UCP-3 siRNA and non-targeting siRNA (ON-TARGETplus SMARTpool, ON-TARGET Non-targeting siRNA, ThermoScientific Dharmacon, Chicago, IL, USA) were used at a final concentration of 50 nM. Transfection efficiency and viability was determined by transfecting the cells with 400 nM green fluorescence siGLO siRNA (ThermoScientific Dharmacon) followed by propidium iodide exclusion dye and flow cytometric analysis (data not shown). Immediately after transfection, cells were cultured either under normal conditions or hypoxic (48 h)/reoxygenation (24 h). Downregulation of UCP-3 was controlled by immunoblotting.

Immunoblotting. Following normoxia or hypoxia (48 h)/reoxygenation (24 h) H/R-adapted and control PT cultures as well as frehly frozen specimens from dissected human renal cell carcinoma with adjacent normal renal tissue. Patients gave informed consent and the experiments were approved by the ethical committee of the Faculty of Medicine, University of Tübingen (Ethik-Kommission der Medizinischen Fakultät und am Universitätsklinikum Tübingen, Gartenstrasse 47, 72074 Tübingen, Germany) and carried out in accordance with the approved guidelines. Specimens were lysed in a buffer (containing in mM: 50 HEPES pH 7.5, 150 NaCl, 1 EDTA, 10 sodium pyrophosphate, 10 NaF, 2 Na_3VO_4, 1 phenylmethylsulfonylfluorid (PMSF) additionally containing 1% triton X-100, 5 μg/ml aprotinin, 5 μg/ml leupeptin, and 3 μg/ml pepstatin) and separated by SDS-PAGE under reducing condition. Segregated proteins were electro-transferred onto PVDF membranes (Roth, Karlsruhe, Germany). Blots were blocked in TBS buffer containing 0.05% Tween 20 and 5% non-fat dry milk for 1 h at room temperature. The membrane was incubated overnight at 4 °C with rabbit anti-UCP3 antibody (#ab3477, Abcam, Cambridge, UK). Equal gel loading was verified by an antibody against β-actin (mouse anti-β-actin antibody, clone AC-74, Sigma #A2228 1:20,000) or GAPDH (mouse anti-GAPDH, #ab8245 clone 6C5, Abcam, 1:20,000). Antibody binding was detected with a horseradish peroxidase-linked goat anti-rabbit or horse anti-mouse IgG antibody (Cell Signaling #7074 and #7076, New England Biolabs GmbH, Frankfurt am Main, Germany, 1:1000 and 1:2000 dilution in TBS-Tween/5% milk, respectively) incubated for 1 h at room temperature and enhanced chemoluminescence (ECL Western blotting analysis

system, GE Healthcare/Amersham-Biosciences, Freiburg, Germany). Where indicated protein levels were quantified by densitometry using ImageJ software (ImageJ 1.40 g NIH, USA). UCP-3 expression of the tumor samples were categorized using an arbitrary score from 0 (not expressed, see Fig. 6B, 1st lane) to 4 (highest expression, see Fig. 6B, 8th lane).

Statistics. Given data are means ± standard error (SE). Differences between experimental groups were assessed by (Welch-corrected) two-tailed student t-test or ANOVA where appropriate. P values of ≤ 0.05 were defined significant.

References

1. Huber, S. M., Misovic, M., Mayer, C., Rodemann, H. P. & Dittmann, K. EGFR-mediated stimulation of sodium/glucose cotransport promotes survival of irradiated human A549 lung adenocarcinoma cells. *Radiother Oncol* **103,** 373–379 (2012).
2. Dittmann, K., Mayer, C., Rodemann, H. P. & Huber, S. M. EGFR cooperates with glucose transporter SGLT1 to enable chromatin remodeling in response to ionizing radiation. *Radiother Oncol* **107,** 247–251 (2013).
3. Huber, S. M. Oncochannels. *Cell Calcium* **53,** 241–255 (2013).
4. Huber, S. M. *et al.* Ionizing radiation, ion transports, and radioresistance of cancer cells. *Front Physiol* **4,** 212 (2013).
5. Duranton, C. *et al.* CFTR is involved in the fine tuning of intracellular redox status: physiological implications in cystic fibrosis. *Am J Pathol* **181,** 1367–1377 (2012).
6. Boss, O. *et al.* Uncoupling protein-3: a new member of the mitochondrial carrier family with tissue-specific expression. *FEBS Lett* **408,** 39–42 (1997).
7. Vidal-Puig, A., Solanes, G., Grujic, D., Flier, J. S. & Lowell, B. B. UCP-3: an uncoupling protein homologue expressed preferentially and abundantly in skeletal muscle and brown adipose tissue. *Biochem Biophys Res Commun* **235,** 79–82 (1997).
8. Vidal-Puig, A. J. *et al.* Energy metabolism in uncoupling protein 3 gene knockout mice. *J Biol Chem* **275,** 16258–16266 (2000).
9. Anderson, E. J., Yamazaki, H. & Neufer, P. D. Induction of endogenous uncoupling protein 3 suppresses mitochondrial oxidant emission during fatty acid-supported respiration. *J Biol Chem* **282,** 31257–31266 (2007).
10. Seifert, E. L., Bezaire, V., Estey, C. & Harper, M. E. Essential role for uncoupling protein-3 in mitochondrial adaptation to fasting but not in fatty acid oxidation or fatty acid anion export. *J Biol Chem* **283,** 25124–25131 (2008).
11. Toime, L. J. & Brand, M. D. Uncoupling protein-3 lowers reactive oxygen species production in isolated mitochondria. *Free Radic Biol Med* **49,** 606–611 (2010).
12. Echtay, K. S. *et al.* Superoxide activates mitochondrial uncoupling proteins. *Nature* **415,** 96–99 (2002).
13. Lombardi, A. *et al.* UCP-3 translocates lipid hydroperoxide and mediates lipid hydroperoxide-dependent mitochondrial uncoupling. *J Biol Chem* **285,** 16599–16605 (2010).
14. Giacobino, J. P. Effects of dietary deprivation, obesity and exercise on UCP-3 mRNA levels. *Int J Obes Relat Metab Disord* **23 Suppl 6,** S60–63 (1999).
15. MacLellan, J. D. *et al.* Physiological increases in uncoupling protein 3 augment fatty acid oxidation and decrease reactive oxygen species production without uncoupling respiration in muscle cells. *Diabetes* **54,** 2343–2350 (2005).
16. Duval, C., Camara, Y., Hondares, E., Sibille, B. & Villarroya, F. Overexpression of mitochondrial uncoupling protein-3 does not decrease production of the reactive oxygen species, elevated by palmitate in skeletal muscle cells. *FEBS Lett* **581,** 955–961 (2007).
17. Costford, S. R., Chaudhry, S. N., Salkhordeh, M. & Harper, M. E. Effects of the presence, absence, and overexpression of uncoupling protein-3 on adiposity and fuel metabolism in congenic mice. *Am J Physiol Endocrinol Metab* **290,** E1304–1312 (2006).
18. Choi, C. S. *et al.* Overexpression of uncoupling protein 3 in skeletal muscle protects against fat-induced insulin resistance. *J Clin Invest* **117,** 1995–2003 (2007).
19. Bugger, H.*et al.* Uncoupling protein downregulation in doxorubicin-induced heart failure improves mitochondrial coupling but increases reactive oxygen species generation. *Cancer Chemother Pharmacol* **67,** 1381–1388 (2011).
20. Ozcan, C., Palmeri, M., Horvath, T. L., Russell, K. S. & Russell, R. R., 3rd. Role of uncoupling protein 3 in ischemia-reperfusion injury, arrhythmias, and preconditioning. *Am J Physiol Heart Circ Physiol* **304,** H1192–1200 (2013).
21. Criscuolo, F., Mozo, J., Hurtaud, C., Nubel, T. & Bouillaud, F. UCP2, UCP3, avUCP, what do they do when proton transport is not stimulated? Possible relevance to pyruvate and glutamine metabolism. *Biochim Biophys Acta* **1757,** 1284–1291 (2006).
22. Goglia, F. & Skulachev, V. P. A function for novel uncoupling proteins: antioxidant defense of mitochondrial matrix by translocating fatty acid peroxides from the inner to the outer membrane leaflet. *Faseb J* **17,** 1585–1591 (2003).
23. Himms-Hagen, J. & Harper, M. E. Physiological role of UCP3 may be export of fatty acids from mitochondria when fatty acid oxidation predominates: an hypothesis. *Exp Biol Med (Maywood)* **226,** 78–84 (2001).
24. Schrauwen, P. & Hesselink, M. K. The role of uncoupling protein 3 in fatty acid metabolism: protection against lipotoxicity? *Proc Nutr Soc* **63,** 287–292 (2004).
25. Millet, L. *et al.* Increased uncoupling protein-2 and -3 mRNA expression during fasting in obese and lean humans. *J Clin Invest* **100,** 2665–2670 (1997).
26. Weigle, D. S. *et al.* Elevated free fatty acids induce uncoupling protein 3 expression in muscle: a potential explanation for the effect of fasting. *Diabetes* **47,** 298–302 (1998).
27. Boudina, S. *et al.* UCP3 regulates cardiac efficiency and mitochondrial coupling in high fat-fed mice but not in leptin-deficient mice. *Diabetes* **61,** 3260–3269 (2012).
28. de Almeida Brondani, L. *et al.* Association of the UCP polymorphisms with susceptibility to obesity: case-control study and meta-analysis. *Mol Biol Rep* **41,** 5053–67 (2014).
29. Jiang, N. *et al.* Upregulation of uncoupling protein-3 in skeletal muscle during exercise: a potential antioxidant function. *Free Radic Biol Med* **46,** 138–145 (2009).
30. Safari, F. *et al.* Differential expression of cardiac uncoupling proteins 2 and 3 in response to myocardial ischemia-reperfusion in rats. *Life Sci* **98,** 68–74 (2014).
31. Kang, P. T., Chen, C. L., Ren, P., Guarini, G. & Chen, Y. R. BCNU-induced gR2 DEFECT mediates S-glutathionylation of Complex I and respiratory uncoupling in myocardium. *Biochem Pharmacol* **89,** 490–502 (2014).
32. Mailloux, R. J. & Harper, M. E. Uncoupling proteins and the control of mitochondrial reactive oxygen species production. *Free Radic Biol Med* **51,** 1106–1115 (2011).
33. Sreekumar, A. *et al.* Profiling of cancer cells using protein microarrays: discovery of novel radiation-regulated proteins. *Cancer Res* **61,** 7585–7593 (2001).
34. Voehringer, D. W. *et al.* Gene microarray identification of redox and mitochondrial elements that control resistance or sensitivity to apoptosis. *Proc Natl Acad Sci USA* **97,** 2680–2685 (2000).
35. Mao, X. W., Crapo, J. D. & Gridley, D. S. Mitochondrial oxidative stress-induced apoptosis and radioprotection in proton-irradiated rat retina. *Radiat Res* **178,** 118–125 (2012).

36. Harper, M. E. *et al.* Characterization of a novel metabolic strategy used by drug-resistant tumor cells. *Faseb J* **16,** 1550–1557 (2002).
37. Belfodil, R. *et al.* CFTR-dependent and -independent swelling-activated K+ currents in primary cultures of mouse nephron. *Am J Physiol Renal Physiol* **284,** F812–828 (2003).
38. l'Hoste, S. *et al.* CFTR mediates apoptotic volume decrease and cell death by controlling glutathione efflux and ROS production in cultured mice proximal tubules. *Am J Physiol Renal Physiol* **298,** F435–453 (2010).

Acknowledgements

This work was supported by grants from the Wilhelm-Sander-Stiftung awarded to SH (2011.083.1) and from the Deutsche Krebshilfe awarded to MB (D30.11089). We thank Ilka Müller and Heidrun Faltin for excellent technical assistance. D.K. was supported by the DFG International Graduate School 1302 (TP T9 SH).

Author Contributions

S.H., M.B. and N.B. designed the study, analyzed the data, did the statistics and wrote the manuscript. C.D., N.B. and D.K. selected and characterized the partially hypoxia-resistance PT cultures. J.H. and J.B. preserved normal renal tissue and renal cell carcinoma specimens from human nephrectomy material and analyzed the UCP-3 protein expression.

Additional Information

Supplementary information accompanies this paper at http://www.nature.com/srep

Competing financial interests: The authors declare no competing financial interests.

How to cite this article: Braun, N. *et al.* UCP-3 uncoupling protein confers hypoxia resistance to renal epithelial cells and is upregulated in renal cell carcinoma. *Sci. Rep.* **5**, 13450; doi: 10.1038/srep13450 (2015).

Biochimica et Biophysica Acta 1848 (2015) 2657–2664

Contents lists available at ScienceDirect

Biochimica et Biophysica Acta

journal homepage: www.elsevier.com/locate/bbamem

Review

Role of ion channels in ionizing radiation-induced cell death☆

Stephan M. Huber [a,*], Lena Butz [a,b], Benjamin Stegen [a], Lukas Klumpp [a], Dominik Klumpp [a], Franziska Eckert [a]

[a] Department of Radiation Oncology, University of Tübingen, Germany
[b] Department of Pharmacology, Toxicology and Clinical Pharmacy, Institute of Pharmacy, University of Tübingen, Germany

ARTICLE INFO

Article history:
Received 31 July 2014
Received in revised form 30 October 2014
Accepted 5 November 2014
Available online 15 November 2014

Keywords:
Ion transport
Radiation
Cancer
Cell death
Therapy resistance
Ca^{2+}-activated K^+ channels

ABSTRACT

Neoadjuvant, adjuvant or definitive fractionated radiation therapy are implemented in first line anti-cancer treatment regimens of many tumor entities. Ionizing radiation kills the tumor cells mainly by causing double strand breaks of their DNA through formation of intermediate radicals. Survival of the tumor cells depends on both, their capacity of oxidative defense and their efficacy of DNA repair. By damaging the targeted cells, ionizing radiation triggers a plethora of stress responses. Among those is the modulation of ion channels such as Ca^{2+}-activated K^+ channels or Ca^{2+}-permeable nonselective cation channels belonging to the super-family of transient receptor potential channels. Radiogenic activation of these channels may contribute to radiogenic cell death as well as to DNA repair, glucose fueling, radiogenic hypermigration or lowering of the oxidative stress burden. The present review article introduces these channels and summarizes our current knowledge on the mechanisms underlying radiogenic ion channel modulation. This article is part of a Special Issue entitled: Membrane channels and transporters in cancers.

Contents

1. Introduction

Ionizing radiation kills or inactivates cells mostly by damaging the nuclear DNA and cell survival critically depends on successful repair of the DNA damage [1]. Ionizing radiation may lead to necrotic as well as apoptotic cell death depending on cell type, dose and fractionation protocols [2]. The major death pathway in this scenario in normal tissue cells is apoptosis. However, cancer cells which often have developed strategies to evade apoptosis [3] may either undergo (regulated) necrosis or reenter the cell cycle with accumulated DNA damages. During the subsequent cell divisions those cells will not be able to segregate the chromosomes and end up as multinucleated giant cells in mitotic catastrophe. Mitotic catastrophe again leads either to apoptotic or necrotic cell death. Another possible mechanism of radiation-induced death in cells with disturbed apoptosis machinery is excess autophagy. While autophagy is a survival strategy [4] excess autophagy overdigests the cytoplasm and cell organelles forcing the cell into apoptosis or necrosis [5].

Meanwhile, the evidence is overwhelming that ion channels fulfill pivotal functions in cell death mechanisms such as apoptosis (for review see the article by Annarosa Arcangeli in this special issue on "Membrane channels and transporters in cancers") as well as in stress response and survival strategies. Notably, tumor cells have been demonstrated to express a set of ion channels which is different to that of the parental normal cells. These channels may fulfill specific oncogenic functions in neoplastic transformation, malignant progression or tissue

☆ This article is part of a Special Issue entitled: Membrane channels and transporters in cancers.

* Corresponding author at: Department of Radiation Oncology, University of Tübingen, Hoppe-Seyler-Str. 3, 72076 Tübingen, Germany. Tel.: +49 7071 29 82183.
E-mail address: stephan.huber@uni-tuebingen.de (S.M. Huber).

http://dx.doi.org/10.1016/j.bbamem.2014.11.004
0005-2736/

invasion and metastasis (for review see [1]). In addition, they may contribute to the cellular stress response for instance during fractionated radiation therapy and may confer radioresistance.

The present review intends to sum up data on ion channel function in the stress response to ionizing radiation. In particular, ion channels that may induce cell death in tumor cells and facilitate radiogenic cell killing are introduced. In addition, data on ion channels which, in contrast to the before mentioned, confer radioresistance are reviewed. Finally, ion channels of tumor cells that might contribute to acquired radioresistance, e.g. by promoting radiogenic hypermigration or transition into relatively radioresistant ***c***ancer ***s***tem (cell)-like ***c***ells (CSCs) are described. Prior to that, a brief introduction into radiotherapy and its radiobiological principles is given in the next paragraphs.

2. Radiotherapy

Radiation therapy together with surgery and systemic chemotherapy is the main pillar of anti-cancer treatment. About half of all cancer patients receive radiation therapy, half of all cures from cancer include radiotherapy [6]. Despite modern radiation techniques and advanced multimodal treatments, local failures and distant metastases often limit the prognosis of the patients, especially due to limited salvage treatments [7].

Ionizing radiation impairs the clonogenic survival of tumor cells mainly by causing double strand breaks in the DNA backbone. The number of double strand breaks increases linearly with the absorbed radiation dose. The intrinsic capacity to detoxify radicals formed during transfer of radiation energy to cellular molecules such as H_2O (giving rise to hydroxyl radicals, $^{\cdot}OH$) and the ability to efficiently repair DNA double strand breaks by non-homologous end joining or homologous recombination determines the radiosensitivity of a given tumor cell. Irradiated tumor cells which leave residual DNA double strand breaks un-repaired lose their clonogenicity meaning that these cells can not restore tumor mass (for review see [8]).

In addition to these intrinsic resistance factors, the microenvironment may lower the radiosensitivity of tumor cells. Hypoxic areas are frequent in solid tumors reaching a certain mass. Tumor hypoxia, however, decreases the efficacy of radiation therapy [9]. Ionizing radiation directly or indirectly generates radicals in the deoxyribose moiety of the DNA backbone. In a hypoxic atmosphere, cellular thiols can react with those DNA radicals resulting in chemical DNA repair. At higher oxygen partial pressure, in sharp contrast, radicals of the deoxyribose moiety are chemically transformed to strand break precursors [10]. By this mechanism, hypoxia increases radioresistance by a factor of two to three (oxygen enhancement ratio) [11].

Fractionated treatment regimens which improve recovery of the normal tissue after irradiation but not of the tumor have been established in radiotherapy [12]. In addition to limit normal tissue toxicity, killing of tumor mass by initial radiation fractions has been demonstrated to reoxygenate and thereby radiosensitize solid tumors during further fractionated radiotherapy. Beyond that, fractionated radiation regimens aim to redistribute tumor cells in a more vulnerable phase of the cell cycle in the time intervals between two fractions [13]. Accelerated repopulation of the tumor after irradiation is a frequently reported phenomenon. Possible mechanisms of accelerated repopulation include induction of CSCs: It has been proposed that radiation therapy induces CSCs to switch from an asymmetrical into a symmetrical mode of cell division; i.e., a CSC which is thought to normally divide into a daughter CSC and a lineage-committed progenitor cells is induced by the radiotherapy to divide symmetrically into two proliferative CSC daughter cells. This is thought to accelerate repopulation of the tumor after end of radiotherapy. Importantly, CSCs are thought be relatively radioresistant possibly due to i) high oxidative defense and, therefore, low radiation-induced insults, ii) activated DNA checkpoints resulting in fast DNA repair, and iii) an attenuated radiation-induced cell cycle redistribution [14].

Finally, fractionated radiation therapy, which applies fractions of sublethal radiation doses (usually 2 Gy per fraction), has been demonstrated in a variety of tumor entities *in vitro* and in animal models to stimulate hypermigration and hypermetastasis of tumor cells as well as infiltration of the tumor by CD11b-positive myeloid cells and subsequent vasculogenesis. It is tempting to speculate that radiogenic hypermigration boosts cellular interaction of tumor cells with non-tumor cells, e.g. endothelial cells. It has been proposed that CSCs lodge within perivascular niches where a complex regulatory network supports CSC survival [15]. As a matter of fact, CSCs but not non-CSCs gain radioresistance when transplanted orthotopically in mice [16] supporting the idea of a tumor microenvironment-dependent acquired radioresistance. Ion channels contribute to both, intrinsic and acquired radioresistance of tumor cells as discussed in the next paragraphs

3. Radiosensitizing ion channels

Member 2 of the melastatin family of transient receptor potential channel (TRPM2) is a Ca^{2+}-permeable nonselective cation channel. Heterologous expression of TRPM2 in human embryonic kidney cells [17] or A172 human glioblastoma cells [18] facilitates oxidative stress-induced cell death. Reactive oxygen species (ROS) have been demonstrated to trigger TRPM2 activation [19,20]. The principal activator, however, of TRPM2 is ADP-ribose (ADPR) that binds to a special domain located at the C-terminus of the channel [21,22]. Sources of ADPR are the mitochondria [23] or ADPR polymers. The latter are formed, e.g., during DNA repair by poly (ADP-ribose) polymerases (PARPs). ADPR is released from the ADPR polymers by glycohydrolases [21,24].

Expression of TRPM2 has been demonstrated in several tumor entities such as insulinoma [25], hepatocellular carcinoma [25], prostate cancer [26], lymphoma [27], leukemia [28] and lung cancer cell lines [29]. TRPM2 activity increases the susceptibility to cell death [30] probably by overloading cells with Ca^{2+} (Fig. 1A).

Remarkably, cancer cells may evade TRPM2-mediated cell death. In lung cancer cells, de-methylation of a GpC island within the TRPM2 gene gives rise to new promoters that regulate transcription of a non-functional truncated TRPM2 channel [29] and to a TRPM2 specific antisense RNA. This antisense RNA inhibits TRPM2 translation. Moreover, the truncated channel is non-functional and acts dominant negative, thus switching off the tumor-suppressing function of the full-length TRPM2 protein [29] (Fig. 1B).

The initially described member of the vanilloid family of TRP channels, the nociceptive and heat receptor TRPV1, is reportedly expressed in several tumor entities such as uveal melanoma [31], pancreatic [32] and prostatic neuroendocrine tumors [33], glioblastoma [34] and urothelial cancer of human bladder [35]. At least in the latter two tumor entities, TRPV1 exerts anti-oncogenic effects [35,36]. TRPV1 expression inversely correlates with glioma grading [34]. Remarkably, neural precursor cells have been demonstrated to induce ER stress-mediated cell death of glioblastoma cells by activating glioblastoma TRPV1 channels through secretion of endogenous vanilloids [37]. Along those lines is the observation that a TRPV1 antagonist promotes tumorigenesis in mouse skin [38].

Notably, targeting of TRPM2 and TRPV1 by RNA interference has been demonstrated to decrease gamma irradiation-induced formation of nuclear γH2AX foci and further DNA damage response in A549 lung adenocarcinoma cells [39]. Since γH2AX foci are used as a surrogate for DNA double strand breaks, one might speculate that TRPM2 or TRPV1 may amplify ionizing radiation-induced insults (Fig. 1). Another interpretation which has been favored by the author of the study [39] would be that activity of TRPM2 and TRPV1 is required for the formation of DNA repair complexes. In combination, the data hint to the possibility of radiosensitizing cancer cells by pharmacologically activating TRPM2 or TRPV1 channels. Whether this might become a promising new strategy of tumor radiosensitization has to await animal studies.

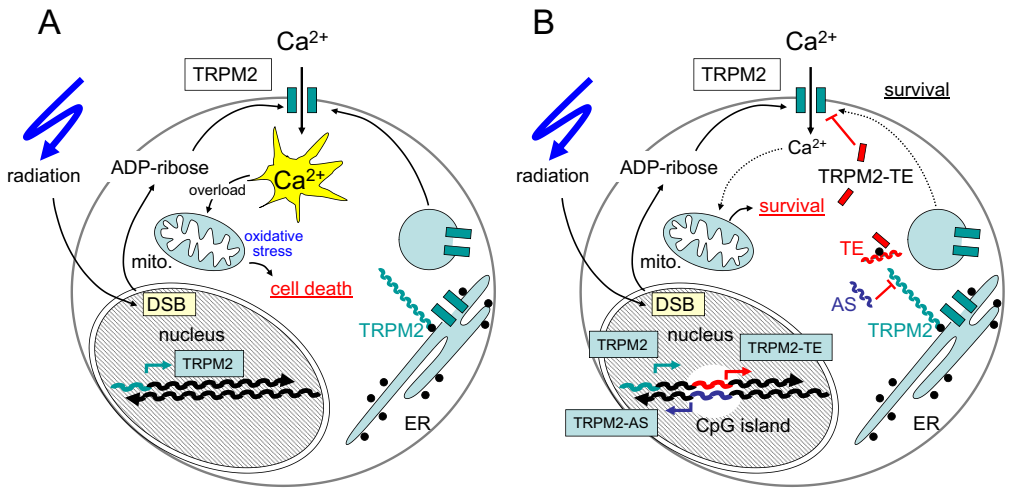

Fig. 1. Speculative mechanism of a putative TRPM2-mediated radiosensitization (A) and reported strategy [29] of lung cancer cells to avoid TRPM2-mediated susceptibility to cell death (B), for details see text. TRPM2-TE (TE): truncated TRPM2, TRPM2-AS (AS): TRPM2 antisense RNA, mito.: mitochondrion).

4. Ion channels conferring intrinsic radioresistance

DNA repair involves cell cycle arrest, chromatin relaxation and formation of repair complexes at the site of DNA damage. Moreover, radiation-induced formation of radicals requires activated radical detoxification pathways and increased oxidative defense to constrain the radiation-induced insults. All these processes of stress response lead to elevated ATP consumption which requires intensified energy supply. Recent *in vitro* observations suggest that these processes depend at least partially on radiation-induced ion channel activation.

Studies of our laboratory indicate that survival of irradiated human leukemia cells critically depends on Ca^{2+} signaling involving radiogenic activation of TRPV5/6-like nonselective cation and $K_v3.4$ voltage-gated K^+ channels [40,41]. The nonselective cation channels in concert with $K_v3.4$ generate radiogenic Ca^{2+} signals that contribute to G_2/M cell cycle arrest by CaMKII-mediated inhibition of the phosphatase cdc25B. Activity of the latter is required in these cells for release from radiation-induced G_2/M arrest via dephosphorylation and thereby activation of cdc2, a component of the mitosis promoting factor. Experimental interference with the radiogenic Ca^{2+} signals, e.g. by pharmacological inhibition or knock-down of $K_v3.4$ overrides cell cycle arrest resulting in increased apoptosis and decreased clonogenic survival of irradiated leukemia cells [40,41]. This radiosensitization by $K_v3.4$ targeting demonstrates the pivotal role of radiogenic $K_v3.4$ channel activation for cell cycle arrest and DNA repair.

Similar to leukemia cells, A549 lung adenocarcinoma cells reportedly respond to ionizing radiation with activation of K_v K^+ channels [42] and transient hyperpolarization of the plasma membrane. Later on, the membrane potential of the irradiated A549 cells strongly depolarizes. This depolarization is dependent on external glucose and inhibited by phlorizin, a sodium glucose cotransporter (SGLT) blocker. In parallel, irradiation induces phlorizin-sensitive ^{3}H-glucose uptake within few minutes after irradiation [43]. Combined, these data suggest that radiogenic activation of SGLT transporters and K_v K^+ channels cooperate in glucose fuelling of the irradiated A549 cells, the former by generating the glucose entry routes, the latter by increasing and maintaining the driving force for Na^+-coupled glucose entry. Glucose uptake by SGLTs is mainly driven by the inwardly directed electrochemical driving force for Na^+ which in turn is highly dependent on the K^+ channel-regulated membrane potential. SGLTs allow efficient glucose uptake even from a glucose-depleted microenvironment which is typical for malperfused solid tumors [44]. It is therefore not surprising that several tumor entities such as colorectal, pancreatic, lung, head and neck, prostate, kidney, cervical, breast, bladder and prostate cancer as well as chondrosarcomas and leukemia upregulate SGLTs [45–53].

SGLT has been shown to be in complex with the EGFR [50,53] and radiogenic SGLT activation depends on EGFR tyrosine kinase activity [43]. Importantly, radiogenic increase in glucose fuelling seems to be required for cell survival since the SGLT inhibitor phlorizin radiosensitizes A549 lung adenocarcinoma and FaDu head and neck squamous carcinoma cells [43].

Intracellular ATP concentration has been reported to drop in irradiated A549 cells indicative of an irradiation-caused energy crisis. Notably, recovery from radiation-induced ATP decline is EGFR/SGLT-dependent and associated with improved DNA-repair leading to increased clonogenic cell survival. This is evident from the fact that EGFR or SGLT blockade delays recovery of intracellular ATP concentration and histone modifications necessary for chromatin remodeling during DNA repair. *Vice versa*, inhibition of the histone H3 modification prevents chromatin remodeling as well as energy crisis [8]. Together, these data suggest that irradiation-associated interactions between SGLT1 and EGFR result in increased glucose uptake, which counteracts the energy crisis in tumor cells caused by chromatin remodeling required for DNA repair (Fig. 2) [8,43].

Besides plasma membrane ion channels, mitochondrial transport pathways have been shown to contribute to cellular stress response. Stress-induced upregulation of uncoupling proteins (UCPs) conveys hyperpolarization of the membrane potential across the inner mitochondrial membrane ($\Delta\Psi_m$,) and thereby formation of reactive oxygen species [54]. UCPs are reportedly upregulated in a number of aggressive human tumors (leukemia, breast, colorectal, ovarian, bladder, esophagus, testicular, kidney, pancreatic, lung, and prostate cancer) in which they are proposed to contribute to malignant progression (for review see [54]).

In addition to malignant progression, UCPs may alter the therapy sensitivity of tumor cells. UCP-2 expression has been associated with paclitaxel resistance of p53 wildtype lung cancer, CPT-11 resistance of colon cancer and gemcitabine resistance of pancreatic adenocarcinoma, lung adenocarcinoma, or bladder carcinoma. Accordingly, experimental targeting of UCPs has been demonstrated to sensitize tumor cells to chemotherapy *in vitro* (for review see [54]).

Notably, ionizing radiation induces up-regulation of UCP-2 expression in colon carcinoma cells [55] and in a radiosensitive subclone of B cell lymphoma [56], as well as UCP-3 expression in rat retina [57]. Radioprotection might result from lowering the radiation-induced burden of reactive oxygen species. As a matter of fact, multi-resistant subclones of leukemia cells reportedly show higher UCP-2 protein expression, lower $\Delta\Psi_m$, lower radiation induced formation of reactive oxygen species, and decreased DNA damage as compared to their parental sensitive cells [58].

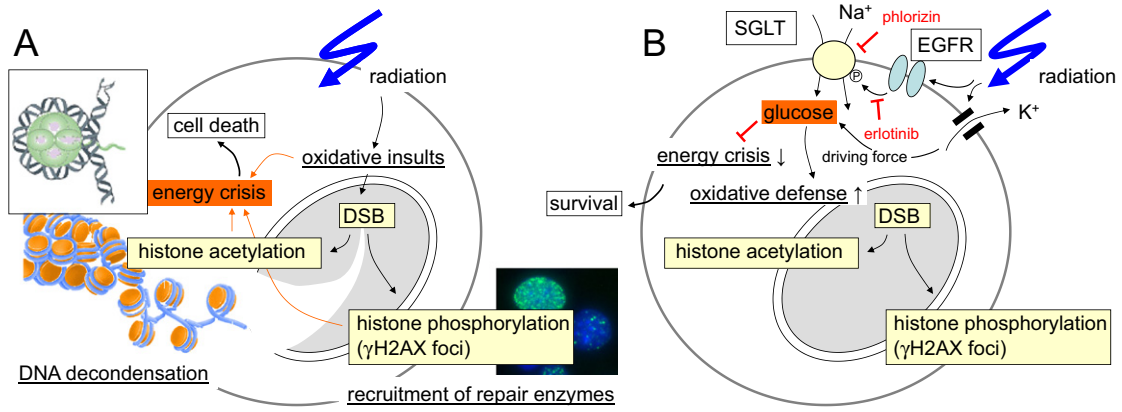

Fig. 2. Radiation-caused energy crisis (A) and functional significance of SGLT1-mediated glucose fueling for DNA repair and cell survival (B) of irradiated A549 lung adenocarcinoma cells (DSB: double strand breaks).

In summary, these data indicate that ion transports through channels may regulate processes that mediate intrinsic radioresistance. Only few laboratories worldwide including ours are working on the radiophysiology of tumor cells. The investigation of ion transports in irradiated cells therefore is at its very beginning and the few data available are mostly phenomenological in nature. The molecular mechanisms that underlie e.g. radiogenic channel activation are still ill-defined. Nevertheless, the data prove functional significance of ion transports and electrosignaling for the survival of irradiated tumor cells and might have translational implications for radiotherapy in the future.

5. Ion channels in acquired radioresistance

Microenvironmental stress such as hypoxia, interstitial nutrient depletion or low pH has been proposed to switch tumor cells from a "Grow" into a "Go" phenotype. By migration and tissue invasion "Go" tumor cells may evade the locally confined stress burden and resettle in distant and less hostile regions. Once resettled, tumor cells may readapt the "Grow" phenotype by reentering cell cycling and may establish tumor satellites in more or less close vicinity of the primary focus (for review see [54]).

In accordance with this hypothesis, sublethal ionizing irradiation as applied in single fractions of fractionated radiotherapy has been demonstrated *in vitro* and/or in rodent tumor models to induce migration, invasion and metastasis or spreading of cervix carcinoma [59], head and neck squamous cell carcinoma [60], lung adenocarinoma [61,62], colorectal carcinoma [62], breast cancer [62–64], meningioma [65], medulloblastoma [66] and glioblastoma. In particular, in glioblastoma the experimental evidence for such radiogenic hypermigration is meanwhile overwhelming [67–80]. Glioblastoma cells show a highly migrative phenotype that may "travel" large distances through the brain [81]. At least in theory, radiogenic hypermigration might, therefore, contribute to locoregional treatment failure by promoting emigration of tumor cells from the target volume during fractionated radiation therapy.

Migration and radiogenic hypermigration are well documented in glioma cells. They invade the surrounding brain parenchyma primarily by moving along axon bundles and the vasculature. During brain invasion along those tracks cells have to squeeze between very narrow interstitial spaces which requires effective local cell volume decrease and reincrease. Glioblastoma cells are capable of losing all unbound cell water [82]. The electrochemical driving force for this tremendous cell volume decrease is provided by an unusually high cytosolic Cl^- concentration (100 mM) [83,84] which is utilized as an osmolyte. During local regulatory volume decrease, extrusion of Cl^- and K^+ along their electrochemical gradients involves ClC-3 Cl^-- channels [85,86], Ca^{2+}-activated high conductance BK- [74,87,88] and intermediate

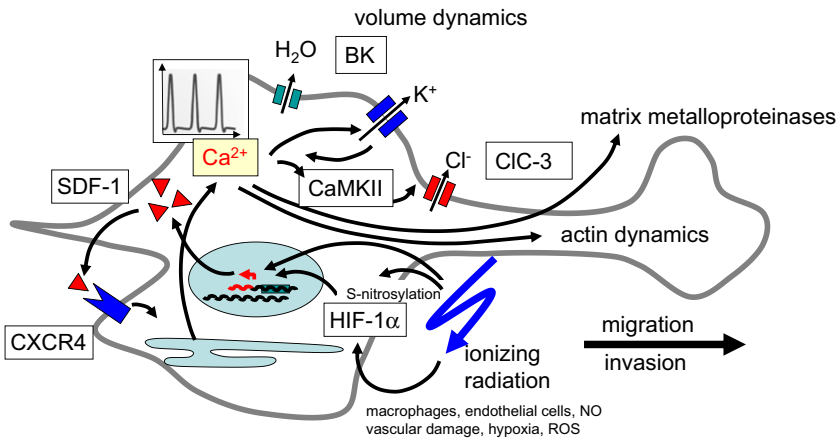

Fig. 3. Hypothetical signaling underlying radiogenic hypermigration of glioblastoma cells. SDF-1 is a HIF-1α target gene and hypoxia is a strong inductor of SDF-1 expression. IR-caused damage of the tumor vasculature and resultant tumor hypoxia has been proposed to induce SDF-1 expression [111]. Beyond that, ionizing radiation reportedly stimulates the generation of NO in tumor-associated macrophages leading to HIF-1α stabilization by S-nitrosylation [100]. Finally, radiation may directly stabilize HIF-1α as deduced from *in vitro* experiments (own unpublished results). SDF-1 induces Ca^{2+} signals through CXCR4 chemokine receptor that in turn contribute to the programming and mechanics of migration (for details see text) and possibly invasion, e.g., via calpain-dependent [112] activation of matrix metalloproteinases [113,114].

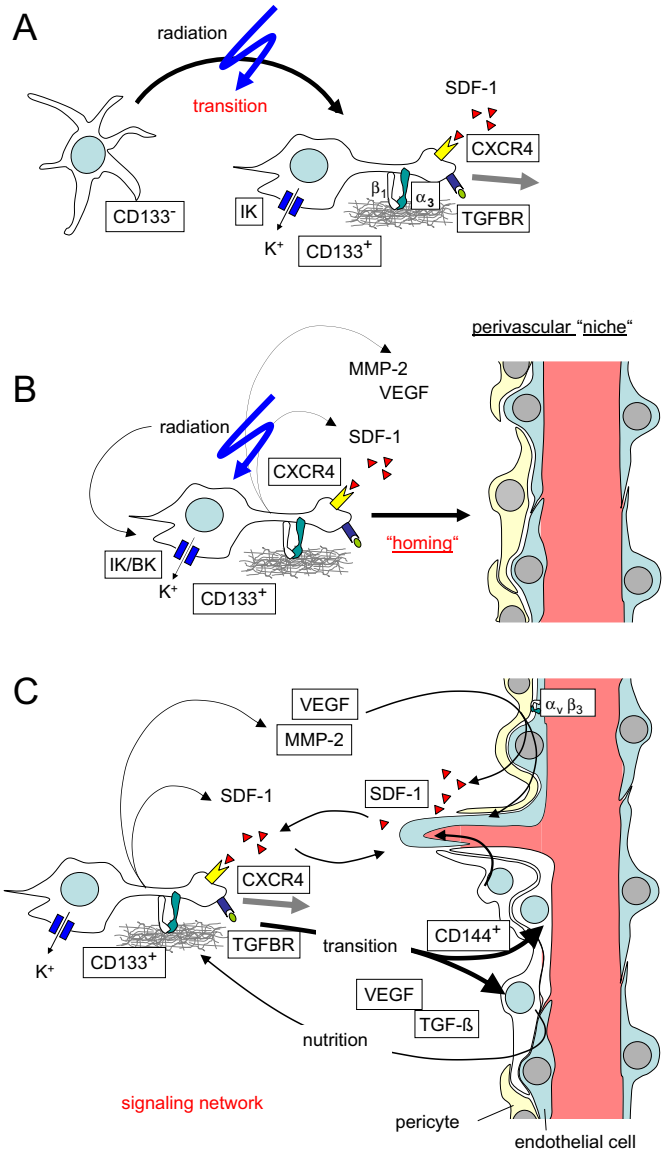

Fig. 4. Synopsis of the signaling network in glioblastoma conferring radioresistance and speculative role of ionizing radiation herein. A. Irradiation induces secretion of SDF-1 [80,95–97] and transition of $CD133^-$ "differentiated" glioblastoma cells to $CD133^+$ GSCs with up-regulated CXCR4 [106], β1/α3 integrins [108], TGFB2 receptor [115], TGF-β responsiveness [115], and IK Ca^{2+}-activated K^+ channel-dependent highly migratory and invasive phenotype [109] B. Irradiation promotes "homing" of GSCs to perivascular niches by stimulating cell migration. C. The reciprocal interaction between glioblastoma and endothelial cells strongly depends on matrix metalloproteinase-2 (MMP-2) expression by glioblastoma [114] and SDF-1 signaling of endothelial cells [110]. Importantly, irradiation induces upregulation of MMP-2 in glioblastoma cells (B) which is required for tissue invasion [67,71,72,79,114] and VEGF secretion (B) [71,75] which reportedly may promote angiogenesis [116]. In addition, transition of glioblastoma cells into endothelial cells [117] and pericytes [15] reconstruct the glioblastoma vasculature which supports both, vessel function and tumor growth.

conductance IK K^+ channels [86,89]. Inhibition of either of these channels attenuates glioblastoma cell migration or invasion [83,90–94] confirming their pivotal function in these processes.

Ionizing radiation has been demonstrated in our laboratory to activate BK K^+ channels in glioblastoma cells *in vitro* [74]. Radiogenic BK channel activity, in turn, is required for Ca^{2+}/calmodulin kinase II (CaMKII)- [74] and consecutive CaMKII-dependent ClC-3 channel activation (own unpublished observation and [85]). Inhibition of BK or CaMKII abolishes radiogenic hypermigration [74] indicating BK channel activation as key event of radiogenic hypermigration of glioblastoma cells. Radiogenic hypermigration is paralleled by radiogenic expression of the chemokine SDF-1 (stromal cell-derived factor-1, CXCL12) in different tumor entities including glioblastoma [80,95–97]. Glioblastoma cells reportedly express CXCR4 chemokine receptors and SDF-1 stimulates glioblastoma cell migration via CXCR4-mediated Ca^{2+} signaling [93]. CXCR4 receptors reportedly signal through phospholipase C and BK channels have been shown to be functionally coupled with IP_3 receptors in the ER [98] suggesting (and confirmed by own unpublished observations) that radiogenic SDF1/CXCR4 signaling is upstream of BK channel activation. SDF-1, in turn, is a target gene of the transcription factor HIF-1α which reportedly becomes stabilized, e.g. by S-nitrosylation, upon irradiation [95,99–101] (Fig. 3). Together, this gives a good example of radiogenic signaling which integrates biochemical signaling, electrosignaling (i.e., BK-dependent regulation of membrane potential) and Ca^{2+} signaling modules (more details are given in the legend to Fig. 3).

Ionizing radiation has been demonstrated to select stem (cell)-like glioblastoma cells (GSCs) or even induce transition of "differentiated" cancer cells to GSCs/CSCs in glioblastoma [102–104] and other tumor entities [14]. Notably, "stemness" is associated with SDF-1 secretion [105] and markedly increased CXCR4 chemokine expression [106]. Importantly, CXCR4 upregulation is required to maintain "stemness" of non-small cell lung cancer [107] and glioblastoma cells [105]. In accordance to CXCR4 upregulation, GSCs show a highly migratory/invasive phenotype [108,109]. Most importantly, this phenotype is highly dependent on the Ca^{2+}-activated IK K^+ channel [89,109]. Furthermore, IK channels have been demonstrated to be overexpressed in about one third of the glioma patients with IK protein expression correlating with poor patient survival [89].

Unexpectedly, a previous report demonstrated that *xeno*grafted $CD133^+$ stem-like subpopulations of glioblastoma exhibit a higher radioresistance than *xeno*grafted $CD133^-$ cells while radiosensitivity of both subpopulations does not differ *in vitro* [16]. This clearly indicates a function of the brain microenvironment for radioresistance. In particular, endothelial cells have been postulated to promote glioblastoma therapy resistance [110]. Part of the reported reciprocal interaction between glioblastoma cells and endothelial cells as well as of the complex signaling network in perivascular "niches" is schematically summarized in Fig. 4.

Albeit merely speculative, the idea that radiogenic hypermigration might promote "homing" of (CXCR4-highly-expressing stem-like) glioblastoma cells to perivascular niches is highly attractive. The subsequent reciprocal modifications of glioblastoma and endothelial cells might eventually induce radioresistance of glioblastoma cells. Together, these data suggest that radiogenic hypermigration might contribute to the apparently high radioresistance of glioblastoma cells either by promoting evasion from the radiation target volume or by stimulating the chemotaxis of glioblastoma cells to "radioprotective" perivascular niches.

6. Concluding remarks

The radiation physiology of cancer cells is yet a neglected research field. While the number of reports on ion channel function in neoplastic transformation, malignant progression or metastasis of cancer cells increases constantly only little is known about the role of ion channels in radiotherapy. The few data available strongly suggest that ionizing radiation-induced ion channel modifications are a common phenomenon. Importantly, these modifications impact on the stress response and survival of irradiated tumor cells. By modulating intracellular Ca^{2+} signals radiosensitive ion channels may directly crosstalk with the biochemical signaling of the DNA damage response. By driving local cell volume changes radiogenic ion channel modifications may promote cell migration and stress evasion of irradiated tumor cells. By stabilizing the membrane potential ionizing radiation-induced K^+ channel activity might facilitate Na^+-coupled glucose uptake providing the energy for DNA-repair. Finally, mitochondrial channels upregulated

by ionizing radiation might lower the oxidative insults associated with ionizing radiation. Given the aberrant and partly specific ion channel expression of tumor cells, a more profound understanding of the mechanisms underlying radiogenic ion channel modifications might be harnessed in the future to develop new strategies for the radiosensitization of tumors.

Acknowledgment

This work was supported by a grant from the Wilhelm-Sander-Stiftung awarded to SH (2011.083.1). BS and DK were supported by the DFG International Graduate School 1302 (TP T9 SH).

References

[1] S.M. Huber, Oncochannels, Cell Calcium 53 (2013) 241–255.
[2] M. Verheij, Clinical biomarkers and imaging for radiotherapy-induced cell death, Cancer Metastasis Rev. 27 (2008) 471–480.
[3] D. Hanahan, R.A. Weinberg, The hallmarks of cancer, Cell 100 (2000) 57–70.
[4] A. Apel, I. Herr, H. Schwarz, H.P. Rodemann, A. Mayer, Blocked autophagy sensitizes resistant carcinoma cells to radiation therapy, Cancer Res. 68 (2008) 1485–1494.
[5] S. Palumbo, S. Comincini, Autophagy and ionizing radiation in tumors: the "survive or not survive" dilemma, J. Cell. Physiol. 228 (2013) 1–8.
[6] German-Cancer-Aid, Information Booklet, http://www.krebshilfe.de/fileadmin/Inhalte/Downloads/PDFs/Blaue_Ratgeber/053_strahlen.pdf 2013.
[7] A.C. Muller, F. Eckert, V. Heinrich, M. Bamberg, S. Brucker, T. Hehr, Re-surgery and chest wall re-irradiation for recurrent breast cancer: a second curative approach, BMC Cancer 11 (2011) 197.
[8] K. Dittmann, C. Mayer, H.P. Rodemann, S.M. Huber, EGFR cooperates with glucose transporter SGLT1 to enable chromatin remodeling in response to ionizing radiation, Radiother. Oncol. (2013), http://dx.doi.org/10.1016/j.radonc.2013.03.016 (pii: S0167-8140(13)00145-X).
[9] H. Harada, How can we overcome tumor hypoxia in radiation therapy? J. Radiat. Res. 52 (2011) 545–556.
[10] P.M. Cullis, G.D.D. Jones, J. Lea, M.C.R. Symons, M. Sweeney, The effects of ionizing radiation on deoxyribonucleic acid. Part 5. The role of thiols in chemical repair, J. Chem. Soc. Perkin Trans. 2 (1987) 1907–1914.
[11] M. Langenbacher, R.J. Abdel-Jalil, W. Voelter, M. Weinmann, S.M. Huber, *In vitro* hypoxic cytotoxicity and hypoxic radiosensitization. Efficacy of the novel 2-nitroimidazole N, N, N-tris[2-(2-nitro-1H-imidazol-1-yl)ethyl]amine, Strahlenther. Onkol. 189 (2013) 246–254.
[12] B. Jones, R.G. Dale, A.M. Gaya, Linear quadratic modeling of increased late normal-tissue effects in special clinical situations, Int. J. Radiat. Oncol. Biol. Phys. 64 (2006) 948–953.
[13] T.M. Pawlik, K. Keyomarsi, Role of cell cycle in mediating sensitivity to radiotherapy, Int. J. Radiat. Oncol. Biol. Phys. 59 (2004) 928–942.
[14] F. Pajonk, E. Vlashi, W.H. McBride, Radiation resistance of cancer stem cells: the 4 R's of radiobiology revisited, Stem Cells 28 (2010) 639–648.
[15] L. Cheng, Z. Huang, W. Zhou, Q. Wu, S. Donnola, J.K. Liu, X. Fang, A.E. Sloan, Y. Mao, J.D. Lathia, W. Min, R.E. McLendon, J.N. Rich, S. Bao, Glioblastoma stem cells generate vascular pericytes to support vessel function and tumor growth, Cell 153 (2013) 139–152.
[16] M. Jamal, B.H. Rath, P.S. Tsang, K. Camphausen, P.J. Tofilon, The brain microenvironment preferentially enhances the radioresistance of $CD133^{+}$glioblastoma stem-like cells, Neoplasia 14 (2012) 150–158.
[17] Y. Hara, M. Wakamori, M. Ishii, E. Maeno, M. Nishida, T. Yoshida, H. Yamada, S. Shimizu, E. Mori, J. Kudoh, N. Shimizu, H. Kurose, Y. Okada, K. Imoto, Y. Mori, LTRPC2 Ca^{2+}-permeable channel activated by changes in redox status confers susceptibility to cell death, Mol. Cell 9 (2002) 163–173.
[18] M. Ishii, A. Oyama, T. Hagiwara, A. Miyazaki, Y. Mori, Y. Kiuchi, S. Shimizu, Facilitation of H2O2-induced A172 human glioblastoma cell death by insertion of oxidative stress-sensitive TRPM2 channels, Anticancer Res. 27 (2007) 3987–3992.
[19] M. Naziroglu, A. Luckhoff, A calcium influx pathway regulated separately by oxidative stress and ADP-Ribose in TRPM2 channels: single channel events, Neurochem. Res. 33 (2008) 1256–1262.
[20] M. Naziroglu, A. Luckhoff, Effects of antioxidants on calcium influx through TRPM2 channels in transfected cells activated by hydrogen peroxide, J. Neurol. Sci. 270 (2008) 152–158.
[21] E. Fonfria, I.C. Marshall, C.D. Benham, I. Boyfield, J.D. Brown, K. Hill, J.P. Hughes, S.D. Skaper, S. McNulty, TRPM2 channel opening in response to oxidative stress is dependent on activation of poly(ADP-ribose) polymerase, Br. J. Pharmacol. 143 (2004) 186–192.
[22] F.J. Kuhn, I. Heiner, A. Luckhoff, TRPM2: a calcium influx pathway regulated by oxidative stress and the novel second messenger ADP-ribose, Pflugers Arch. 451 (2005) 212–219.
[23] A.L. Perraud, C.L. Takanishi, B. Shen, S. Kang, M.K. Smith, C. Schmitz, H.M. Knowles, D. Ferraris, W. Li, J. Zhang, B.L. Stoddard, A.M. Scharenberg, Accumulation of free ADP-ribose from mitochondria mediates oxidative stress-induced gating of TRPM2 cation channels, J. Biol. Chem. 280 (2005) 6138–6148.
[24] J. Eisfeld, A. Luckhoff, Trpm2, Handb. Exp. Pharmacol. (2007) 237–252.
[25] K. Inamura, Y. Sano, S. Mochizuki, H. Yokoi, A. Miyake, K. Nozawa, C. Kitada, H. Matsushime, K. Furuichi, Response to ADP-ribose by activation of TRPM2 in the CRI-G1 insulinoma cell line, J. Membr. Biol. 191 (2003) 201–207.
[26] X. Zeng, S.C. Sikka, L. Huang, C. Sun, C. Xu, D. Jia, A.B. Abdel-Mageed, J.E. Pottle, J.T. Taylor, M. Li, Novel role for the transient receptor potential channel TRPM2 in prostate cancer cell proliferation, Prostate Cancer Prostatic Dis. 13 (2010) 195–201.
[27] W. Zhang, I. Hirschler-Laszkiewicz, Q. Tong, K. Conrad, S.C. Sun, L. Penn, D.L. Barber, R. Stahl, D.J. Carey, J.Y. Cheung, B.A. Miller, TRPM2 is an ion channel that modulates hematopoietic cell death through activation of caspases and PARP cleavage, Am. J. Physiol. Cell Physiol. 290 (2006) C1146–C1159.
[28] W. Zhang, X. Chu, Q. Tong, J.Y. Cheung, K. Conrad, K. Masker, B.A. Miller, A novel TRPM2 isoform inhibits calcium influx and susceptibility to cell death, J. Biol. Chem. 278 (2003) 16222–16229.
[29] U. Orfanelli, A.K. Wenke, C. Doglioni, V. Russo, A.K. Bosserhoff, G. Lavorgna, Identification of novel sense and antisense transcription at the TRPM2 locus in cancer, Cell Res. 18 (2008) 1128–1140.
[30] S. McNulty, E. Fonfria, The role of TRPM channels in cell death, Pflugers Arch. 451 (2005) 235–242.
[31] S. Mergler, R. Derckx, P.S. Reinach, F. Garreis, A. Bohm, L. Schmelzer, S. Skosyrski, N. Ramesh, S. Abdelmessih, O.K. Polat, N. Khajavi, A.I. Riechardt, Calcium regulation by temperature-sensitive transient receptor potential channels in human uveal melanoma cells, Cell. Signal. 26 (2014) 56–69.
[32] S. Mergler, M. Skrzypski, M. Sassek, P. Pietrzak, C. Pucci, B. Wiedenmann, M.Z. Strowski, Thermo-sensitive transient receptor potential vanilloid channel-1 regulates intracellular calcium and triggers chromogranin A secretion in pancreatic neuroendocrine BON-1 tumor cells, Cell. Signal. 24 (2012) 233–246.
[33] S. Malagarie-Cazenave, N. Olea-Herrero, D. Vara, C. Morell, I. Diaz-Laviada, The vanilloid capsaicin induces IL-6 secretion in prostate PC-3 cancer cells, Cytokine 54 (2011) 330–337.
[34] C. Amantini, M. Mosca, M. Nabissi, R. Lucciarini, S. Caprodossi, A. Arcella, F. Giangaspero, G. Santoni, Capsaicin-induced apoptosis of glioma cells is mediated by TRPV1 vanilloid receptor and requires p38 MAPK activation, J. Neurochem. 102 (2007) 977–990.
[35] G. Santoni, S. Caprodossi, V. Farfariello, S. Liberati, A. Gismondi, C. Amantini, Antioncogenic effects of transient receptor potential vanilloid 1 in the progression of transitional urothelial cancer of human bladder, ISRN Urol. 2012 (2012) 458238.
[36] C. Amantini, P. Ballarini, S. Caprodossi, M. Nabissi, M.B. Morelli, R. Lucciarini, M.A. Cardarelli, G. Mammana, G. Santoni, Triggering of transient receptor potential vanilloid type 1 (TRPV1) by capsaicin induces Fas/CD95-mediated apoptosis of urothelial cancer cells in an ATM-dependent manner, Carcinogenesis 30 (2009) 1320–1329.
[37] K. Stock, J. Kumar, M. Synowitz, S. Petrosino, R. Imperatore, E.S. Smith, P. Wend, B. Purfurst, U.A. Nuber, U. Gurok, V. Matyash, J.H. Walzlein, S.R. Chirasani, G. Dittmar, B.F. Cravatt, S. Momma, G.R. Lewin, A. Ligresti, L. De Petrocellis, L. Cristino, V. Di Marzo, H. Kettenmann, R. Glass, Neural precursor cells induce cell death of high-grade astrocytomas through stimulation of TRPV1, Nat. Med. 18 (2012) 1232–1238.
[38] S. Li, A.M. Bode, F. Zhu, K. Liu, J. Zhang, M.O. Kim, K. Reddy, T. Zykova, W.Y. Ma, A.L. Carper, A.K. Langfald, Z. Dong, TRPV1-antagonist AMG9810 promotes mouse skin tumorigenesis through EGFR/Akt signaling, Carcinogenesis 32 (2011) 779–785.
[39] K. Masumoto, M. Tsukimoto, S. Kojima, Role of TRPM2 and TRPV1 cation channels in cellular responses to radiation-induced DNA damage, Biochim. Biophys. Acta 1830 (2013) 3382–3390.
[40] N. Heise, D. Palme, M. Misovic, S. Koka, J. Rudner, F. Lang, H.R. Salih, S.M. Huber, G. Henke, Non-selective cation channel-mediated Ca^{2+}-entry and activation of Ca^{2+}/calmodulin-dependent kinase II contribute to G2/M cell cycle arrest and survival of irradiated leukemia cells, Cell. Physiol. Biochem. 26 (2010) 597–608.
[41] D. Palme, M. Misovic, E. Schmid, D. Klumpp, H.R. Salih, J. Rudner, S. Huber, Kv3.4 potassium channel-mediated electrosignaling controls cell cycle and survival of irradiated leukemia cells, Pflugers Arch. (2013), http://dx.doi.org/10.1007/s00424-013-1249-5.
[42] S.S. Kuo, A.H. Saad, A.C. Koong, G.M. Hahn, A.J. Giaccia, Potassium-channel activation in response to low doses of gamma-irradiation involves reactive oxygen intermediates in nonexcitatory cells, Proc. Natl. Acad. Sci. U. S. A. 90 (1993) 908–912.
[43] S.M. Huber, M. Misovic, C. Mayer, H.P. Rodemann, K. Dittmann, EGFR-mediated stimulation of sodium/glucose cotransport promotes survival of irradiated human A549 lung adenocarcinoma cells, Radiother. Oncol. 103 (2012) 373–379.
[44] V. Ganapathy, M. Thangaraju, P.D. Prasad, Nutrient transporters in cancer: relevance to Warburg hypothesis and beyond, Pharmacol. Ther. 121 (2009) 29–40.
[45] J.A. Nelson, R.E. Falk, The efficacy of phloridzin and phloretin on tumor cell growth, Anticancer Res. 13 (1993) 2287–2292.
[46] N. Ishikawa, T. Oguri, T. Isobe, K. Fujitaka, N. Kohno, SGLT gene expression in primary lung cancers and their metastatic lesions, Jpn. J. Cancer Res. 92 (2001) 874–879.
[47] B.M. Helmke, C. Reisser, M. Idzko, G. Dyckhoff, C. Herold-Mende, Expression of SGLT-1 in preneoplastic and neoplastic lesions of the head and neck, Oral Oncol. 40 (2004) 28–35.
[48] L.C. Yu, C.Y. Huang, W.T. Kuo, H. Sayer, J.R. Turner, A.G. Buret, SGLT-1-mediated glucose uptake protects human intestinal epithelial cells against Giardia duodenalis-induced apoptosis, Int. J. Parasitol. 38 (2008) 923–934.
[49] V.F. Casneuf, P. Fonteyne, N. Van Damme, P. Demetter, P. Pauwels, B. de Hemptinne, M. De Vos, C. Van de Wiele, M. Peeters, Expression of SGLT1, Bcl-2 and p53 in primary pancreatic cancer related to survival, Cancer Invest. 26 (2008) 852–859.

[50] Z. Weihua, R. Tsan, W.C. Huang, Q. Wu, C.H. Chiu, I.J. Fidler, M.C. Hung, Survival of cancer cells is maintained by EGFR independent of its kinase activity, Cancer Cell 13 (2008) 385–393.

[51] N. Leiprecht, C. Munoz, I. Alesutan, G. Siraskar, M. Sopjani, M. Foller, F. Stubenrauch, T. Iftner, F. Lang, Regulation of Na^+-coupled glucose carrier SGLT1 by human papillomavirus 18 E6 protein, Biochem. Biophys. Res. Commun. 404 (2011) 695–700.

[52] E.M. Wright, D.D. Loo, B.A. Hirayama, Biology of human sodium glucose transporters, Physiol. Rev. 91 (2011) 733–794.

[53] J. Ren, L.R. Bollu, F. Su, G. Gao, L. Xu, W.C. Huang, M.C. Hung, Z. Weihua, EGFR-SGLT1 interaction does not respond to EGFR modulators, but inhibition of SGLT1 sensitizes prostate cancer cells to EGFR tyrosine kinase inhibitors, Prostate 73 (2013) 1453–1461.

[54] S.M. Huber, L. Butz, B. Stegen, D. Klumpp, N. Braun, P. Ruth, F. Eckert, Ionizing radiation, ion transports, and radioresistance of cancer cells, Frontiers in Physiology | Membrane Physiology and Membrane Biophysics 4 (2013) 212.

[55] A. Sreekumar, M.K. Nyati, S. Varambally, T.R. Barrette, D. Ghosh, T.S. Lawrence, A.M. Chinnaiyan, Profiling of cancer cells using protein microarrays: discovery of novel radiation-regulated proteins, Cancer Res. 61 (2001) 7585–7593.

[56] D.W. Voehringer, D.L. Hirschberg, J. Xiao, Q. Lu, M. Roederer, C.B. Lock, L.A. Herzenberg, L. Steinman, L.A. Herzenberg, Gene microarray identification of redox and mitochondrial elements that control resistance or sensitivity to apoptosis, Proc. Natl. Acad. Sci. U. S. A. 97 (2000) 2680–2685.

[57] X.W. Mao, J.D. Crapo, D.S. Gridley, Mitochondrial oxidative stress-induced apoptosis and radioprotection in proton-irradiated rat retina, Radiat. Res. 178 (2012) 118–125.

[58] M.E. Harper, A. Antoniou, E. Villalobos-Menuey, A. Russo, R. Trauger, M. Vendemelio, A. George, R. Bartholomew, D. Carlo, A. Shaikh, J. Kupperman, E.W. Newell, I.A. Bespalov, S.S. Wallace, Y. Liu, J.R. Rogers, G.L. Gibbs, J.L. Leahy, R.E. Camley, R. Melamede, M.K. Newell, Characterization of a novel metabolic strategy used by drug-resistant tumor cells, FASEB J. 16 (2002) 1550–1557.

[59] W.H. Su, P.C. Chuang, E.Y. Huang, K.D. Yang, Radiation-induced increase in cell migration and metastatic potential of cervical cancer cells operates via the K-Ras pathway, Am. J. Pathol. 180 (2012) 862–871.

[60] A.C. Pickhard, J. Margraf, A. Knopf, T. Stark, G. Piontek, C. Beck, A.L. Boulesteix, E.Q. Scherer, S. Pigorsch, J. Schlegel, W. Arnold, R. Reiter, Inhibition of radiation induced migration of human head and neck squamous cell carcinoma cells by blocking of EGF receptor pathways, BMC Cancer 11 (2011) 388.

[61] J.W. Jung, S.Y. Hwang, J.S. Hwang, E.S. Oh, S. Park, I.O. Han, Ionising radiation induces changes associated with epithelial–mesenchymal transdifferentiation and increased cell motility of A549 lung epithelial cells, Eur. J. Cancer 43 (2007) 1214–1224.

[62] Y.C. Zhou, J.Y. Liu, J. Li, J. Zhang, Y.Q. Xu, H.W. Zhang, L.B. Qiu, G.R. Ding, X.M. Su, S. Mei, G.Z. Guo, Ionizing radiation promotes migration and invasion of cancer cells through transforming growth factor-beta-mediated epithelial–mesenchymal transition, Int. J. Radiat. Oncol. Biol. Phys. 81 (2011) 1530–1537.

[63] S. Biswas, M. Guix, C. Rinehart, T.C. Dugger, A. Chytil, H.L. Moses, M.L. Freeman, C.L. Arteaga, Inhibition of TGF-beta with neutralizing antibodies prevents radiation-induced acceleration of metastatic cancer progression, J. Clin. Invest. 117 (2007) 1305–1313.

[64] D.M. Kambach, V.L. Sodi, P.I. Lelkes, J. Azizkhan-Clifford, M.J. Reginato, ErbB2, FoxM1 and 14-3-3zeta prime breast cancer cells for invasion in response to ionizing radiation, Oncogene 33 (2014) 589–598.

[65] O. Kargiotis, C. Chetty, V. Gogineni, C.S. Gondi, S.M. Pulukuri, A.P. Kyritsis, M. Gujrati, J.D. Klopfenstein, D.H. Dinh, J.S. Rao, uPA/uPAR downregulation inhibits radiation-induced migration, invasion and angiogenesis in IOMM-Lee meningioma cells and decreases tumor growth *in vivo*, Int. J. Oncol. 33 (2008) 937–947.

[66] S. Asuthkar, A.K. Nalla, C.S. Gondi, D.H. Dinh, M. Gujrati, S. Mohanam, J.S. Rao, Gadd45a sensitizes medulloblastoma cells to irradiation and suppresses MMP-9-mediated EMT, Neuro Oncol. 13 (2011) 1059–1073.

[67] C. Wild-Bode, M. Weller, A. Rimner, J. Dichgans, W. Wick, Sublethal irradiation promotes migration and invasiveness of glioma cells: implications for radiotherapy of human glioblastoma, Cancer Res. 61 (2001) 2744–2750.

[68] W. Wick, A. Wick, J.B. Schulz, J. Dichgans, H.P. Rodemann, M. Weller, Prevention of irradiation-induced glioma cell invasion by temozolomide involves caspase 3 activity and cleavage of focal adhesion kinase, Cancer Res. 62 (2002) 1915–1919.

[69] B. Hegedus, J. Zach, A. Czirok, J. Lovey, T. Vicsek, Irradiation and Taxol treatment result in non-monotonous, dose-dependent changes in the motility of glioblastoma cells, J. Neuro Oncol. 67 (2004) 147–157.

[70] S. Rieken, D. Habermehl, A. Mohr, L. Wuerth, K. Lindel, K. Weber, J. Debus, S.E. Combs, Targeting alphanubeta3 and alphanubeta5 inhibits photon-induced hypermigration of malignant glioma cells, Radiat. Oncol. 6 (2011) 132.

[71] A.V. Badiga, C. Chetty, D. Kesanakurti, D. Are, M. Gujrati, J.D. Klopfenstein, D.H. Dinh, J.S. Rao, MMP-2 siRNA inhibits radiation-enhanced invasiveness in glioma cells, PLoS One 6 (2011) e20614.

[72] S.Y. Kwak, J.S. Yang, B.Y. Kim, I.H. Bae, Y.H. Han, Ionizing radiation-inducible miR-494 promotes glioma cell invasion through EGFR stabilization by targeting p190B rhoGAP, Biochim. Biophys. Acta 1843 (2014) 508–516.

[73] A. Canazza, C. Calatozzolo, L. Fumagalli, A. Bergantin, F. Ghielmetti, L. Fariselli, D. Croci, A. Salmaggi, E. Ciusani, Increased migration of a human glioma cell line after *in vitro* CyberKnife irradiation, Cancer Biol. Ther. 12 (2011) 629–633.

[74] M. Steinle, D. Palme, M. Misovic, J. Rudner, K. Dittmann, R. Lukowski, P. Ruth, S.M. Huber, Ionizing radiation induces migration of glioblastoma cells by activating BK K^+ channels, Radiother. Oncol. 101 (2011) 122–126.

[75] W.J. Kil, P.J. Tofilon, K. Camphausen, Post-radiation increase in VEGF enhances glioma cell motility *in vitro*, Radiat. Oncol. 7 (2012) 25.

[76] I. Vanan, Z. Dong, E. Tosti, G. Warshaw, M. Symons, R. Ruggieri, Role of a DNA damage checkpoint pathway in ionizing radiation-induced glioblastoma cell migration and invasion, Cell. Mol. Neurobiol. 32 (2012) 1199–1208.

[77] W.T. Arscott, A.T. Tandle, S. Zhao, J.E. Shabason, I.K. Gordon, C.D. Schlaff, G. Zhang, P.J. Tofilon, K.A. Camphausen, Ionizing radiation and glioblastoma exosomes: implications in tumor biology and cell migration, Transl. Oncol. 6 (2013) 638–648.

[78] W. Zhou, Y. Xu, G. Gao, Z. Jiang, X. Li, Irradiated normal brain promotes invasion of glioblastoma through vascular endothelial growth and stromal cell-derived factor 1alpha, Neuroreport 24 (2013) 730–734.

[79] A. Shankar, S. Kumar, A. Iskander, N.R. Varma, B. Janic, A. Decarvalho, T. Mikkelsen, J.A. Frank, M.M. Ali, R.A. Knight, S. Brown, A.S. Arbab, Subcurative radiation significantly increases proliferation, invasion, and migration of primary GBM *in vivo*, Chin. J. Cancer 33 (2013) 148–158.

[80] S.C. Wang, C.F. Yu, J.H. Hong, C.S. Tsai, C.S. Chiang, Radiation therapy-induced tumor invasiveness is associated with SDF-1-regulated macrophage mobilization and vasculogenesis, PLoS One 8 (2013) e69182.

[81] J. Johnson, M.O. Nowicki, C.H. Lee, E.A. Chiocca, M.S. Viapiano, S.E. Lawler, J.J. Lannutti, Quantitative analysis of complex glioma cell migration on electrospun polycaprolactone using time-lapse microscopy, Tissue Eng. C Methods 15 (2009) 531–540.

[82] S. Watkins, H. Sontheimer, Hydrodynamic cellular volume changes enable glioma cell invasion, J. Neurosci. 31 (2011) 17250–17259.

[83] B.R. Haas, H. Sontheimer, Inhibition of the sodium-potassium-chloride cotransporter isoform-1 reduces glioma invasion, Cancer Res. 70 (2010) 5597–5606.

[84] C.W. Habela, N.J. Ernest, A.F. Swindall, H. Sontheimer, Chloride accumulation drives volume dynamics underlying cell proliferation and migration, J. Neurophysiol. 101 (2009) 750–757.

[85] V.A. Cuddapah, H. Sontheimer, Molecular interaction and functional regulation of ClC-3 by Ca^{2+}/calmodulin-dependent protein kinase II (CaMKII) in human malignant glioma, J. Biol. Chem. 285 (2010) 11188–11196.

[86] V.A. Cuddapah, K.L. Turner, S. Seifert, H. Sontheimer, Bradykinin-induced chemotaxis of human gliomas requires the activation of KCa3.1 and ClC-3, J. Neurosci. 33 (2013) 1427–1440.

[87] C.B. Ransom, H. Sontheimer, BK channels in human glioma cells, J. Neurophysiol. 85 (2001) 790–803.

[88] H. Sontheimer, An unexpected role for ion channels in brain tumor metastasis, Exp. Biol. Med. (Maywood) 233 (2008) 779–791.

[89] K.L. Turner, A. Honasoge, S.M. Robert, M.M. McFerrin, H. Sontheimer, A proinvasive role for the Ca^{2+}-activated K^+ channel KCa3.1 in malignant glioma, Glia 62 (2014) 971–981.

[90] N.J. Ernest, A.K. Weaver, L.B. Van Duyn, H.W. Sontheimer, Relative contribution of chloride channels and transporters to regulatory volume decrease in human glioma cells, Am. J. Physiol. Cell Physiol. 288 (2005) C1451–C1460.

[91] M.B. McFerrin, H. Sontheimer, A role for ion channels in glioma cell invasion, Neuron Glia Biol. 2 (2006) 39–49.

[92] L. Catacuzzeno, F. Aiello, B. Fioretti, L. Sforna, E. Castigli, P. Ruggieri, A.M. Tata, A. Calogero, F. Franciolini, Serum-activated K and Cl currents underlay U87-MG glioblastoma cell migration, J. Cell. Physiol. 226 (2010) 1926–1933.

[93] M. Sciaccaluga, B. Fioretti, L. Catacuzzeno, F. Pagani, C. Bertollini, M. Rosito, M. Catalano, G. D'Alessandro, A. Santoro, G. Cantore, D. Ragozzino, E. Castigli, F. Franciolini, C. Limatola, CXCL12-induced glioblastoma cell migration requires intermediate conductance Ca^{2+}-activated K^+ channel activity, Am. J. Physiol. Cell Physiol. 299 (2010) C175–C184.

[94] V.C. Lui, S.S. Lung, J.K. Pu, K.N. Hung, G.K. Leung, Invasion of human glioma cells is regulated by multiple chloride channels including ClC-3, Anticancer Res. 30 (2010) 4515–4524.

[95] G. Tabatabai, B. Frank, R. Mohle, M. Weller, W. Wick, Irradiation and hypoxia promote homing of haematopoietic progenitor cells towards gliomas by TGF-beta-dependent HIF-1alpha-mediated induction of CXCL12, Brain 129 (2006) 2426–2435.

[96] M. Kioi, H. Vogel, G. Schultz, R.M. Hoffman, G.R. Harsh, J.M. Brown, Inhibition of vasculogenesis, but not angiogenesis, prevents the recurrence of glioblastoma after irradiation in mice, J. Clin. Invest. 120 (2010) 694–705.

[97] S.V. Kozin, W.S. Kamoun, Y. Huang, M.R. Dawson, R.K. Jain, D.G. Duda, Recruitment of myeloid but not endothelial precursor cells facilitates tumor regrowth after local irradiation, Cancer Res. 70 (2010) 5679–5685.

[98] A.K. Weaver, M.L. Olsen, M.B. McFerrin, H. Sontheimer, BK channels are linked to inositol 1,4,5-triphosphate receptors via lipid rafts: a novel mechanism for coupling $[Ca^{2+}]_i$ to ion channel activation, J. Biol. Chem. 282 (2007) 31558–31568.

[99] C. Garcia-Moruja, J.M. Alonso-Lobo, P. Rueda, C. Torres, N. Gonzalez, M. Bermejo, F. Luque, F. Arenzana-Seisdedos, J. Alcami, A. Caruz, Functional characterization of SDF-1 proximal promoter, J. Mol. Biol. 348 (2005) 43–62.

[100] F. Li, P. Sonveaux, Z.N. Rabbani, S. Liu, B. Yan, Q. Huang, Z. Vujaskovic, M.W. Dewhirst, C.Y. Li, Regulation of HIF-1alpha stability through S-nitrosylation, Mol. Cell 26 (2007) 63–74.

[101] B.J. Moeller, Y. Cao, C.Y. Li, M.W. Dewhirst, Radiation activates HIF-1 to regulate vascular radiosensitivity in tumors: role of reoxygenation, free radicals, and stress granules, Cancer Cell 5 (2004) 429–441.

[102] M.J. Kim, R.K. Kim, C.H. Yoon, S. An, S.G. Hwang, Y. Suh, M.J. Park, H.Y. Chung, I.G. Kim, S.J. Lee, Importance of PKCdelta signaling in fractionated-radiation-induced expansion of glioma-initiating cells and resistance to cancer treatment, J. Cell Sci. 124 (2011) 3084–3094.

[103] C. Lagadec, E. Vlashi, L. Della Donna, C. Dekmezian, F. Pajonk, Radiation-induced reprogramming of breast cancer cells, Stem Cells 30 (2012) 833–844.
[104] K. Tamura, M. Aoyagi, N. Ando, T. Ogishima, H. Wakimoto, M. Yamamoto, K. Ohno, Expansion of CD133-positive glioma cells in recurrent de novo glioblastomas after radiotherapy and chemotherapy, J. Neurosurg. 119 (2013) 1145–1155.
[105] M. Gatti, A. Pattarozzi, A. Bajetto, R. Wurth, A. Daga, P. Fiaschi, G. Zona, T. Florio, F. Barbieri, Inhibition of CXCL12/CXCR4 autocrine/paracrine loop reduces viability of human glioblastoma stem-like cells affecting self-renewal activity, Toxicology 314 (2013) 209–220.
[106] G. Liu, X. Yuan, Z. Zeng, P. Tunici, H. Ng, I.R. Abdulkadir, L. Lu, D. Irvin, K.L. Black, J.S. Yu, Analysis of gene expression and chemoresistance of $CD133^{+}$ cancer stem cells in glioblastoma, Mol. Cancer 5 (2006) 67.
[107] M.J. Jung, J.K. Rho, Y.M. Kim, J.E. Jung, Y.B. Jin, Y.G. Ko, J.S. Lee, S.J. Lee, J.C. Lee, M.J. Park, Upregulation of CXCR4 is functionally crucial for maintenance of stemness in drug-resistant non-small cell lung cancer cells, Oncogene 32 (2013) 209–221.
[108] M. Nakada, E. Nambu, N. Furuyama, Y. Yoshida, T. Takino, Y. Hayashi, H. Sato, Y. Sai, T. Tsuji, K.I. Miyamoto, A. Hirao, J.I. Hamada, Integrin alpha3 is overexpressed in glioma stem-like cells and promotes invasion, Br. J. Cancer 108 (2013) 2516–2524.
[109] P. Ruggieri, G. Mangino, B. Fioretti, L. Catacuzzeno, R. Puca, D. Ponti, M. Miscusi, F. Franciolini, G. Ragona, A. Calogero, The inhibition of KCa3.1 channels activity reduces cell motility in glioblastoma derived cancer stem cells, PLoS One 7 (2012) e47825.
[110] S. Rao, R. Sengupta, E.J. Choe, B.M. Woerner, E. Jackson, T. Sun, J. Leonard, D. Piwnica-Worms, J.B. Rubin, CXCL12 mediates trophic interactions between endothelial and tumor cells in glioblastoma, PLoS One 7 (2012) e33005.
[111] J.P. Greenfield, W.S. Cobb, D. Lyden, Resisting arrest: a switch from angiogenesis to vasculogenesis in recurrent malignant gliomas, J. Clin. Invest. 120 (2010) 663–667.
[112] H.S. Jang, S. Lal, J.A. Greenwood, Calpain 2 is required for glioblastoma cell invasion: regulation of matrix metalloproteinase 2, Neurochem. Res. 35 (2010) 1796–1804.
[113] C.M. Park, M.J. Park, H.J. Kwak, H.C. Lee, M.S. Kim, S.H. Lee, I.C. Park, C.H. Rhee, S.I. Hong, Ionizing radiation enhances matrix metalloproteinase-2 secretion and invasion of glioma cells through Src/epidermal growth factor receptor-mediated p38/Akt and phosphatidylinositol 3-kinase/Akt signaling pathways, Cancer Res. 66 (2006) 8511–8519.
[114] D.R. Maddirela, D. Kesanakurti, M. Gujrati, J.S. Rao, MMP-2 suppression abrogates irradiation-induced microtubule formation in endothelial cells by inhibiting alphavbeta3-mediated SDF-1/CXCR4 signaling, Int. J. Oncol. 42 (2011) 1279–1288.
[115] X.Z. Ye, S.L. Xu, Y.H. Xin, S.C. Yu, Y.F. Ping, L. Chen, H.L. Xiao, B. Wang, L. Yi, Q.L. Wang, X.F. Jiang, L. Yang, P. Zhang, C. Qian, Y.H. Cui, X. Zhang, X.W. Bian, Tumor-associated microglia/macrophages enhance the invasion of glioma stem-like cells via TGF-beta1 signaling pathway, J. Immunol. 189 (2012) 444–453.
[116] S. Bao, Q. Wu, S. Sathornsumetee, Y. Hao, Z. Li, A.B. Hjelmeland, Q. Shi, R.E. McLendon, D.D. Bigner, J.N. Rich, Stem cell-like glioma cells promote tumor angiogenesis through vascular endothelial growth factor, Cancer Res. 66 (2006) 7843–7848.
[117] R. Wang, K. Chadalavada, J. Wilshire, U. Kowalik, K.E. Hovinga, A. Geber, B. Fligelman, M. Leversha, C. Brennan, V. Tabar, Glioblastoma stem-like cells give rise to tumour endothelium, Nature 468 (2010) 829–833.

frontiers in
PHYSIOLOGY

REVIEW ARTICLE
published: 14 August 2013
doi: 10.3389/fphys.2013.00212

Ionizing radiation, ion transports, and radioresistance of cancer cells

Stephan M. Huber[1]*, Lena Butz[2], Benjamin Stegen[1], Dominik Klumpp[1], Norbert Braun[1], Peter Ruth[2] and Franziska Eckert[1]

[1] Department of Radiation Oncology, University of Tübingen, Tübingen, Germany
[2] Department of Pharmacology, Toxicology and Clinical Pharmacy, Institute of Pharmacy, University of Tübingen, Tübingen, Germany

Edited by:
Andrea Becchetti, University of Milano-Bicocca, Italy

Reviewed by:
Ildikò Szabò, University of Padova, Italy
Yinsheng Wan, Providence College, USA

***Correspondence:**
Stephan M. Huber, Department of Radiation Oncology, University of Tübingen, Hoppe-Seyler-Str. 3, 72076 Tübingen, Germany
e-mail: stephan.huber@uni-tuebingen.de

The standard treatment of many tumor entities comprises fractionated radiation therapy which applies ionizing radiation to the tumor-bearing target volume. Ionizing radiation causes double-strand breaks in the DNA backbone that result in cell death if the number of DNA double-strand breaks exceeds the DNA repair capacity of the tumor cell. Ionizing radiation reportedly does not only act on the DNA in the nucleus but also on the plasma membrane. In particular, ionizing radiation-induced modifications of ion channels and transporters have been reported. Importantly, these altered transports seem to contribute to the survival of the irradiated tumor cells. The present review article summarizes our current knowledge on the underlying mechanisms and introduces strategies to radiosensitize tumor cells by targeting plasma membrane ion transports.

Keywords: radiation therapy, cell cycle, DNA repair, ion channels

INTRODUCTION

Increasing pieces of evidence strongly indicate that ion transports across biological membranes fulfill functions beyond those described by classical physiology such as epithelial transports and neuronal or muscle excitability. More and more, it turns out that ion transports are involved in virtually all cell-biological processes. By modifying the chemistry, electricity and mechanics of cells, ion transports directly interact with cellular biochemistry and constitute signaling modules that are capable of altering protein function, gene expression (Tolon et al., 1996) and epigenetics (Lobikin et al., 2012). Moreover, ion transport-generating proteins such as ion channels have been identified to directly signal in macromolecular complexes with, e.g., surface receptors and downstream kinases (Arcangeli, 2011), or to directly bind to DNA as transcription factors (Gomez-Ospina et al., 2006).

Over the past two decades, ion transports came more and more in the focus of oncological research. Increasingly, data accumulate indicating tumor-suppressing as well as oncogenic functions of ion transport processes. In particular, ion transports have been identified as key regulators of neoplastic transformation, malignant progression, tissue invasion and metastasis (for review see Huber, 2013). Most recent data suggest that ion transports may also contribute to therapy resistance especially to radioresistance of tumor cells. The second chapter of this review article aims at giving an overview of those data. Since worldwide, only a handful of laboratories including ours are working in this research field only few data on ion transports in radioresistance are available and in most cases, the underlying molecular mechanisms of the observed phenomena remain ill-defined. Because tumor hypoxia is a major obstacle in radiotherapy, the second chapter also includes ion transports in the mitochondria that confer hypoxia resistance to normal tissue and probably also to tumor cells. At the end, this article provides some ideas how the acquired knowledge might be harnessed in the future for new strategies of anti-cancer therapy that combine ion transport-targeting and radiotherapy. To begin with, a brief introduction into radiotherapy and its radiobiological principles is given in the next paragraphs.

RADIOTHERAPY

According to the German Cancer Aid, 490,000 people in Germany are diagnosed with cancer every year (German-Cancer-Aid, 2013a) (data originating from February 2012), 218,000 die from their disease. About half of all cancer patients receive radiation treatment, half of all cures from cancer include radiotherapy (German-Cancer-Aid, 2013b). Radiotherapy is one of the main pillars of cancer treatment together with surgery and systemic therapy, mainly chemotherapy. Examples for curative radiotherapy without surgery are prostate (Eckert et al., 2013; Kotecha et al., 2013) and head and neck cancer (Glenny et al., 2010). Preoperative radiotherapy is applied in rectal cancer (Sauer et al., 2012), postoperative treatment in breast cancer (Darby et al.). Yet, also rare tumor entities like sarcoma and small cell carcinoma are treated with radiotherapy (Eckert et al., 2010a,b; Muller et al., 2012). Despite modern radiation techniques and advanced multimodal treatments local failures and distant metastases often limit the prognosis, especially due to limited salvage treatments (Muller et al., 2011; Zhao et al., 2012).

INTRINSIC AND HYPOXIC RADIORESISTANCE

Radiation therapy impairs the clonogenic survival of tumor cells mainly by causing double strand breaks in the DNA backbone. The number of double strand breaks increases linearly with the absorbed radiation dose (unit Gray, Gy). The intrinsic capacity

to repair these DNA damages by non-homologous end joining or homologous recombination determines how radio resistant a given tumor cell is. Irradiated tumor cells which leave residual DNA double strand breaks unrepaired lose their clonogenicity meaning that these cells cannot restore tumor mass. Ion transports may directly be involved in the cellular stress response to DNA damage by controlling cell cycle, metabolic adaptations or DNA repair and, thus, contribute to intrinsic radioresistance and the survival of the tumor cell.

Besides intrinsic factors, the microenvironment influences the radiosensitivity of a tumor. Hypoxic areas frequently occur in solid tumors. Hypoxic tumor cells, however, are somehow "protected" from radiotherapy [reviewed in Harada (2011)]. This is because ionizing radiation generates directly or indirectly radicals in the deoxyribose moiety of the DNA backbone. In a hypoxic atmosphere, thiols can react with those DNA radicals by hydrogen atom donation which results in chemical DNA repair. In the presence of oxygen, in contrast, oxygen fixes radicals of the deoxyribose moiety to strand break precursors (Cullis et al., 1987). This so called oxygen effect radiosensitizes tumor cells by a factor of two to three (oxygen enhancement ratio) as compared to the hypoxic situation (Langenbacher et al., 2013). Accordingly, patients with hypoxic tumors who undergo radiotherapy have a worse prognosis than those with normoxic tumors [e.g., cervical cancer (Fyles et al., 2002, 2006)]. Notably, ion transport processes have been identified as important players in the adaptation of tumor cells to a hypoxic microenvironment. Hence, ion transports via adaptation to hypoxia also indirectly contribute to the radioresistance of tumors.

In radiotherapy, fractionated treatment regimens have been established which may reoxygenate and thereby radiosensitize the irradiated tumor during therapy time. In addition, fractionated radiotherapy spaces out the single fractions in a way that allows DNA repair of normal tissue, that re-distribute cell cycle of the tumor cells in more sensitive phases and that minimize repopulation of the tumor during therapy. The next paragraphs will give an introduction to the underlying radiobiology.

FRACTIONATED RADIATION THERAPY. REPAIR, REOXYGENATION, REDISTRIBUTION, AND REPOPULATION

Early in historic development of radiotherapy fractionation was introduced as a means to limit side effects when giving therapeutic radiation doses (Bernier et al., 2004). Standard fractionation is defined as single doses of 1.8–2 Gy, once daily, 5 days per week.

The principal rationale for fractionation is based on the fact that recovery after radiation is better in normal tissue than in tumors, especially concerning late reacting tissues responsible for late side effects of radiotherapy (Jones et al., 2006) such as fibrosis, damage of spinal cord and brain, as well as most inner organs. Radiation with high single doses is only possible without increased side effects if the radiation field can be confined to the tumor (e.g., stereotactic radiotherapy of brain metastases [Rodrigues et al., 2013) and SBRT, stereotactic body radiation therapy (Grills et al., 2012)]. Yet, many situations in radiation oncology such as adjuvant treatment or irradiation of nodal regions require irradiation of significant volumes of normal tissue.

Alpha-beta ratios

Acute effects of ionizing irradiation on clonogenic cell survival *in vitro* as well as on late toxicity of the normal tissue in patients which underwent radiotherapy are described by the linear-quadratic model (Barendsen, 1982; Dale, 1985). The mathematical fit of the clonogenic survival (late toxicity) is calculated as follows: $N = N_0 \times E^{-(\alpha D - \beta D\hat{}2)}$ with N being the number of surviving cells (patients without late toxicity), N_0 being the initial number of cells (number of patients receiving radiotherapy), α [1/Gy] and β [1/Gy^2] being cell (tissue)-specific constants and D the delivered radiation dose. Low alpha-beta ratios (α/β) [Gy] as determined for many normal tissues indicate that dose fractionation in daily fractions of usually 2 Gy increases survival and decreases late toxicity as compared to a single equivalent dose. Tumors with high alpha-beta ratios, in contrast do not benefit from fractionation. For some tumors such as squamous cell carcinoma of the head and neck there is even a rationale for hyperfractionated radiotherapy with twice daily irradiation of 1.2–1.4 Gy per fraction [reviewed in Nguyen and Ang (2002)]. The theoretical advantage has been confirmed in clinical trials [e.g., EORTC trial 22791 in advanced head and neck cancer Horiot et al. (1992)]. Different fractionation schedules for distinct clinical situations are applied for example in whole-brain radiotherapy. In prophylactic radiation 2–2.5 Gy fractions are applied to limit neurocognitive deficits (Auperin et al., 1999; Le Pechoux et al., 2011; Eckert et al., 2012). For therapeutic radiation 3 Gy fractions or even 4 Gy fractions are preferred in a palliative setting and limited life expectancy to shorten the treatment time to 5 or 10 days (Lutz, 2007; Rades et al., 2007a,b).

Reoxygenation

As mentioned above, fractionated radiation may also lead to reoxygenation of the tumor during therapy (Withers, 1975; Pajonk et al., 2010). Blood vessels of tumors lack normal architecture and are prone to collapse whenever tissue pressure of the expanding tumor mass increases. This aggravates tumor malperfusion and accelerates intermittent or chronic tumor hypoxia. Being sublethal as related to the whole tumor, single radiation fractions in the range of 2 Gy kill a significant percentage of the tumor cells which give rise to tumor shrinkage. Shrinkage, in turn, is thought to increase blood and oxygen supply of the tumor by improving vessel perfusion and by increasing the ratio of vascularization and the residual tumor mass (Maftei et al., 2011; Narita et al., 2012). Increased oxygenation then reverses hypoxic radioresistance of the tumor and improves the therapeutic outcome of radiotherapy.

Redistribution and repopulation

The sensitivity to radiotherapy during cell cycle differs, being highest in M and lowest in late S phase of cell cycle (Pawlik and Keyomarsi, 2004). Often depending on p53 function, irradiated tumor cells accumulate in G_1 or G_2 phase of cell cycle to repair their DNA damages. In a radiation dose-dependent manner, irradiated cells are released from cell cycle arrest and re-enter cell

cycling and tumor repopulation. Importantly, repopulation after irradiation is often accelerated probably due to selection of more aggressive tumor cells (Marks and Dewhirst, 1991). Fractionated radiation regimes aim to re-distribute tumor cells in a more vulnerable phase of the cell cycle in the time intervals between two fractions and to impair repopulation (Pawlik and Keyomarsi, 2004).

CANCER STEM CELLS (CSCs)

Cancer stem cells (CSCs) may resist radiation therapy [for review see Pajonk et al. (2010)]. Mechanisms that might contribute to the relative resistance of CSCs as compared to the non-CSC cells of a given tumor include (i) higher oxidative defense and, therefore, lower radiation-induced insults, (ii) activated DNA checkpoints resulting in faster DNA repair, and (iii) an attenuated radiation-induced cell cycle redistribution. Fractionation regimes are designed that way that the macroscopically visible bulk of tumor cells (i.e., the non CSCs) and not the rare CSCs become redistributed into a more vulnerable phase of cell cycle between two consecutive fractions of radiotherapy. Finally, radiation therapy is thought to switch CSCs from an asymmetrical into a symmetrical mode of cell division; i.e., a CSC which normally divides into a daughter CSC and a lineage-committed progenitor cell is induced by the radiotherapy to divide symmetrically into two proliferative stem daughter cells. This is thought to accelerate repopulation of the tumor after end of radiotherapy (Pajonk et al., 2010).

In summary, fractionated radiotherapy may radio sensitize tumor cells by reoxygenation of the tumor and redistribution of the tumor cells in more vulnerable phases of cell cycle while protecting at the same time normal tissue if the alpha-beta ratio of the tumor exceeds that of the normal tissue. On the other hand, the applied fractionation protocols might spare CSCs due to their radiobiology that differs from that of the bulk of non-CSCs. Furthermore, single radiation fractions apply sublethal doses of ionizing radiation. Data from *in vitro* and animal studies suggest that sublethal doses of ionizing radiation may stimulate migration and tissue invasion of the tumor cells. Translated into the *in vivo* situation, this might imply that cells at the edge of solid tumors might be stimulated by the first radiation fractions to migrate out of the target volume of radiation resulting in survival of the evaded cells and tumor relapse. Moreover, if radiation fractions further induce tumor cell invasion into blood or lymph vessels, fractionated radiotherapy regimes might also boost metastases. As described in the next paragraphs, ion transports fulfill pivotal functions in cell migration especially in radiation-induced migration.

ION TRANSPORTS AND RADIORESISTANCE

Ion transports can be assessed by tracer-flux measurements, fluorescence microscopy/photometry using ion species-specific fluorescence dyes such as the Ca^{2+}-specific fluorochrome fura-2, as well as by electrophysiological means. The latter can be applied if ion transports are electrogenic. Measurements of ion transports during treatment with ionizing radiation are hardly feasible. Reported electrophysiological *in vitro* data on irradiated tumor cells indicate that radiation-induced transport modifications may occur instantaneously and may last up to 24 h post irradiation (Kuo et al., 1993). They further suggest that these modifications may be induced by doses used for single fractions in the clinic (Steinle et al., 2011). The following paragraphs summarize radiation-induced transport modifications as observed in *in vitro* studies on tumor cell lines and their putative contribution to the radioresistance of tumor cells. Whether these processes may indeed underlie therapy failure in tumor patients can only be answered if more data from tumor mouse models and clinical trials become available.

Tumor cells have been proposed to adapt either a "Grow" or a "Go" phenotype in dependence on changes in their microenvironment. When developing a certain mass, growing solid tumors are prone to become malperfused because of the insufficient tumor vasculature. As a consequence of malperfusion, microenvironmental stress by hypoxia, interstitial nutrient depletion, and low pH increases (Stock and Schwab, 2009; Hatzikirou et al., 2012) which is thought to trigger at a certain point the induction of the "Go" phenotype. By migration and tissue invasion "Go" tumor cells may evade the locally reined stress burden and resettle in distant and less hostile regions. Once re-settled, tumor cells may readapt the "Grow" phenotype by reentering cell cycling and may establish tumor satellites in more or less close vicinity of the primary focus. Moreover, this stress evasion may lead to metastases if the "Go" cells invade into blood or lymph vessels.

Migration and tissue invasion are directed by extracellular hapto- and chemotactic signals which trigger preset "Go" programs (Schwab et al., 2007, 2012). The latter comprise intracellular signaling, cellular motor functions including cell volume changes and cytoskeletal dynamics, as well as extracellular matrix digestion and reorganization. Ion transports have been suggested to contribute to all of these processes (Schwab et al., 2007, 2012). As a matter of fact, highly invasive and metastatic phenotypes of tumor cells often show aberrant activity of certain ion transports. The following paragraphs describe the role of these ion transports in particular of those across the plasma membrane using the example of glioblastoma cells.

MOTOR FUNCTION

Glioblastoma cells exhibit a highly migrative phenotype and "travel" long distances throughout the brain (Johnson et al., 2009). Primary foci of glioblastoma show, therefore, even at early stages of diagnosis a characteristic diffuse and net-like brain infiltration (Niyazi et al., 2011). Tumor margins are often not definable and complete surgical tumor resection as well as capture of all residual tumor cells by the radiation target volume is hardly possible (Weber et al., 2009). This results in therapy failure accompanied by very bad prognosis for the survival of the patient in almost all cases of glioblastoma (Niyazi et al., 2011). Glioblastoma cells typically migrate into the surrounding brain parenchyma primarily by using nerve bundles and the vasculature as tracks. The close vicinity to the vasculature has the advantage for the migrating glioblastoma cell of a continuous and sufficient supply of oxygen, nutrients, growth factors, chemokines, and cytokines (Montana and Sontheimer, 2011). Glioblastoma cells have to squeeze through very narrow interstitial spaces during their brain invasion along those tracks. This

requires highly effective local cell volume decrease and re-increase procedures. Notably, glioblastoma cells are capable to lose all unbound cell water leading to maximal cell shrinkage (Watkins and Sontheimer, 2011). Unusually high cytosolic Cl^- concentrations (100 mM) provide the electrochemical driving force for this tremendous cell volume decrease. The cytosolic Cl^- concentration is built up highly above its electrochemical equilibrium concentration by the Na/K/2Cl cotransporter NKCC1 (Haas and Sontheimer, 2010; Haas et al., 2011) allowing glioblastoma cells to utilize Cl^- as an osmolyte.

Local regulatory volume increase and decrease have been proposed to drive migration mechanics. The latter is generated by the loss of Cl^- and K^+ ions along their electrochemical gradients followed by osmotically obliged water fluxes. Involved transporters probably are ClC-3 Cl^- channels (Olsen et al., 2003; Cuddapah and Sontheimer, 2010; Lui et al., 2010), Ca^{2+}-activated high conductance BK (Ransom and Sontheimer, 2001; Ransom et al., 2002; Sontheimer, 2008) as well as intermediate conductance IK K^+ channels (Catacuzzeno et al., 2010; Sciaccaluga et al., 2010; Ruggieri et al., 2012) and AQP-1 water channels (Mccoy and Sontheimer, 2007; Mccoy et al., 2010). To a lower extent, K^+ and Cl^- efflux is probably also mediated by KCC1-generated cotransport (Ernest et al., 2005). These transports are crucial for glioblastoma migration since either transport blockade inhibits glioblastoma cell migration and invasion (Ernest et al., 2005; Mcferrin and Sontheimer, 2006; Catacuzzeno et al., 2010; Haas and Sontheimer, 2010; Lui et al., 2010; Sciaccaluga et al., 2010).

Notably, Ca^{2+}-activated BK (Ransom and Sontheimer, 2001; Liu et al., 2002; Ransom et al., 2002; Weaver et al., 2006) and IK K^+ channels (Ruggieri et al., 2012) are ontogenetically down-regulated or absent in mature glial cells but up-regulated with neoplastic transformation and malignant tumor progression as shown in expression studies in human glioma tissue. Moreover, glioblastoma cells up-regulate a unique splice variant of the BK channel (Liu et al., 2002) which exhibits a higher Ca^{2+} sensitivity than the other isoforms (Ransom et al., 2002) and is indispensable for glioblastoma proliferation *in vitro*. Similarly, ClC-3 Cl^- channels are mal-expressed in glioblastoma tissue where they traffic, in contrast to normal tissue, to the plasma membrane (Olsen et al., 2003). The predominant (surface) expression of ClC-3 and the BK splice variant by glioblastoma cells renders both channel types putative glioblastoma-specific therapeutic targets.

EVASION FROM RADIATION STRESS

External beam radiation may induce the "Go" phenotype in tumor cells similarly to the situation described for stress arising from an adverse tumor microenvironment (**Figure 1**). Ionizing radiation at doses used in single fractions during fractionated radiotherapy has been demonstrated *in vitro* and by a mouse study (Wild-Bode et al., 2001) to induce migration, invasion and spreading of head and neck squamous carcinoma (Pickhard et al., 2011), lung adenocarinoma (Jung et al., 2007; Zhou et al., 2011), meningioma (Kargiotis et al., 2008), medulloblastoma (Asuthkar et al., 2011), and glioblastoma cells (Wild-Bode et al., 2001; Wick et al., 2002; Badiga et al., 2011; Canazza et al., 2011; Rieken et al., 2011; Steinle et al., 2011; Kil et al., 2012; Vanan et al., 2012). The phenomenon of radiation-stimulated migration might be particularly relevant for highly migrating and brain-infiltrating glioblastoma cells.

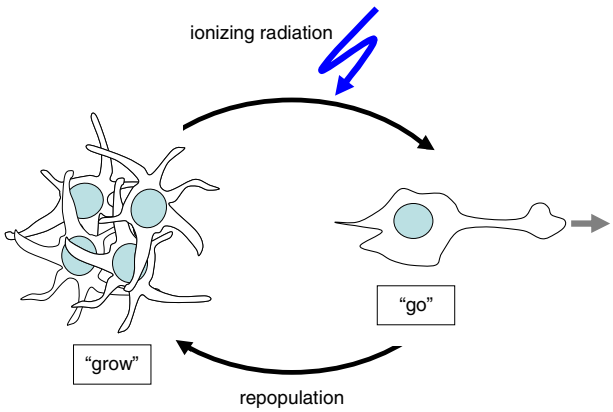

FIGURE 1 | Cellular stress such as ionizing radiation induces the switch from "Grow" to "Go" phenotype.

After macroscopic complete resection glioblastoma is usually treated by adjuvant radiotherapy of the tumor bed applying 54–60 Gy in daily fractions of 1.8–2 Gy combined with temozolomide (Stupp et al., 2005). The median progression-free survival after therapy ranges between 5 and 7 months (Stupp et al., 2005). The recurrence of glioblastoma is typically observed within the former target volume of the adjuvant fractionated radiotherapy. This might be due either to a high intrinsic radioresistance of the glioblastoma cells or to re-invasion of tumor cells into the area of the irradiated primary. One might speculate that this necrotic area, meanwhile cleared by phagocytes, offers optimal growth conditions for such re-invading tumor cells. In this latter scenario, re-invading cells might be recruited from glioblastoma (stem) cells pre-spreaded prior to radiotherapy onset in areas outside the target volume, or from cells that successfully evaded during radiation therapy.

Radiation-induced up-regulation of integrin- (Wild-Bode et al., 2001; Nalla et al., 2010; Canazza et al., 2011; Rieken et al., 2011), VEGF- (Sofia Vala et al., 2010; Badiga et al., 2011; Kil et al., 2012), EGF- (Kargiotis et al., 2008; Pickhard et al., 2011) or/and TGFbeta signaling (Canazza et al., 2011; Zhou et al., 2011) has been proposed to promote tumor cell migration. Downstream ion transport processes have been reported for glioblastoma cells (Steinle et al., 2011). In this study, BK K^+ channel activation and subsequent BK-dependent activation of the CaMKII kinase were identified as key triggers of radiation-induced migration (Steinle et al., 2011). Additionally, ClC-3 anion channels were identified as downstream targets of radiation-induced CaMKII activity (Huber, 2013). This suggests on the one hand motor function (i.e., volume decrease) of radiation-induced BK and ClC-3 currents, on the other hand, it points to a signaling function of BK channels in the programming of radiation-stimulated glioblastoma migration (**Figure 2**). Similar to the situation in migrating glioblastoma cells, radiation-induced plasma membrane K^+ currents and downstream CaMKII activation have been defined as key signaling events in cell cycle control of irradiated leukemia cells as introduced in the following paragraphs.

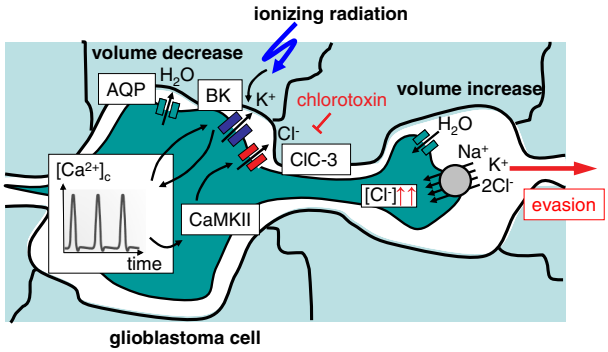

FIGURE 2 | Ionizing radiation (IR)-induced activation of BK K^+ channels results in evasion of glioblastoma cells from radiation stress. Activation of BK channels occurs upstream of CaMKII and ClC-3 Cl^- channels. The $Na^+/K^+/2Cl^-$ cotransporter accumulates Cl^- above its electrochemical equilibrium. Cl^- is used as osmolyte for volume decrease.

DNA REPAIR

Survival of irradiated tumor cells critically depends on DNA repair. This involves cell cycle arrest, elevated energy consumption, chromatin relaxation, and formation of repair complexes at the site of DNA damage. Recent *in vitro* observations suggest that radiation-induced ion transports may contribute to these processes in an indirect manner.

Cell cycle control

Survival of irradiated human leukemia cells depends on Ca^{2+} signaling. Radiation reportedly stimulates Ca^{2+} entry through TRPV5/6-like channels and subsequently activates CaMKII, which in turn fosters G_1/S transition, S progression and accumulation in G_2 phase of the cell cycle (Heise et al., 2010). Moreover, Ca^{2+} signaling in human leukemia cells has been demonstrated to be tightly regulated by voltage-gated $K_v3.4$ K^+ channels and translates into G_2/M cell cycle arrest by CaMKII-mediated inhibitory phosphorylation of the phosphatase cdc25B resulting in inactivation of the mitosis promoting factor and G_2/M arrest. Radiation activates Kv3.4 currents without changing the surface expression of the channel protein. Most importantly, inhibition of $K_v3.4$ by tetraethylammonium and blood-depressing substance-1 and substance-2 or silencing of the $K_v3.4$ channels by RNA interference prevents TRPV5/6-mediated Ca^{2+} entry, CaMKII activation, as well as cdc25B inactivation which results in release from radiation-induced G_2/M arrest, increased apoptosis, and decreased clonogenic survival. Thus, targeting of $K_v3.4$ radiosensitizes the leukemia cells demonstrating the pivotal role of this channel in cell cycle arrest required for DNA repair (Palme et al., 2013). Similar results have been obtained in prostate cancer cells, where TRPV6 inhibition by capsaicin resulted in radiosensitization (Klotz et al., 2011).

Glucose fueling and chromatin relaxation

In addition to cell cycle control, radiation-induced ion transports are proposed to improve glucose fueling of irradiated tumor cells. Fast proliferating tumor cells have a high metabolism at low external glucose and oxygen concentration in the usually chronically under-perfused growing tumor tissue. At the same time, many tumor cells cover their high energy requirements by anaerobic glycolysis with low ATP yield per metabolized glucose even under normoxic conditions. To sustain sufficient glucose fueling, tumor cells may up-regulate the Na^+/glucose cotransporter (SGLT). SGLTs are capable to take up glucose into the tumor cell even against a high chemical gradient (Ganapathy et al., 2009). Several tumor entities such as colorectal, pancreatic, lung, head and neck, prostate, kidney, cervical, mammary, and bladder cancer as well as chondrosarcomas and leukemia have indeed been shown to up-regulate SGLTs (Nelson and Falk, 1993; Ishikawa et al., 2001; Helmke et al., 2004; Casneuf et al., 2008; Weihua et al., 2008; Yu et al., 2008; Leiprecht et al., 2011; Wright et al., 2011). The inwardly directed Na^+ gradient and the voltage across the plasma membrane drive the electrogenic SGLT-generated glucose transport into the cell. The membrane voltage is tightly regulated by the activity of voltage gated K^+ channels which counteract SGLT-mediated depolarization.

Ionizing radiation has been demonstrated to activate EGF receptors (Dittmann et al., 2009). In addition, SGLT1 reportedly is in complex with and under the direct control of the EGF receptor (Weihua et al., 2008) suggesting radiation-induced SGLT1 modifications. As a matter of fact, ionizing radiation stimulates a long lasting EGFR-dependent and SGLT-mediated glucose uptake in A549 lung adenocarcinoma and head and neck squamous carcinoma cell lines (but not in non-transformed fibroblasts) as shown by ^{3}H-glucose uptake and patch-clamp, current clamp recordings (Huber et al., 2012). In the latter experiments, radiation-induced and SGLT-mediated depolarization of membrane potential was preceded by a transient hyperpolarization of the plasma membrane indicative of radiation-induced K^+ channel activation (Huber et al., 2012). Such radiation-induced increase in K^+ channel activity has been reported for several tumor cell lines including A549 lung adenocarcinoma cells (Kuo et al., 1993). In this cell line, radiation at doses between 0.1 and 6 Gy stimulates the activity of voltage gated K^+ channels within 5 min, which gradually declines thereafter. It is tempting to speculate that this radiation-stimulated K^+ channel activity counteracts the depolarization of the membrane potential caused by the SGLT activity shortly after radiation and sustains the driving force for Na^+-coupled glucose uptake (Huber et al., 2012).

Ionizing radiation may lead to necrotic as well as apoptotic cell death depending on cell type, dose, and fractionation (Verheij, 2008). In particular, necrotic cell death may be associated with ATP depletion (Dorn, 2013). Increased SGLT activity in irradiated tumor cells might contribute to ATP replenishment counteracting necrotic cell death. Such function has been suggested in irradiated A549 cells by experiments analyzing cellular ATP concentrations, chromatin remodeling, residual DNA damage, and clonogenic survival of irradiated tumor cells (Dittmann et al., 2013). The data demonstrate that radiation of A549 lung adenocarcinoma cells leads to a transient intracellular ATP depletion and to histone H3 modifications crucial

for both chromatin remodeling and DNA repair in response to irradiation.

Importantly, recovery from radiation-induced ATP crisis was EGFR/SGLT-dependent and associated with improved DNA-repair and increased clonogenic cell survival. The blockade of either EGFR or SGLT inhibited ATP level recovery and histone H3 modifications. *Vice versa*, inhibition of the acetyltransferase TIP60, which is essential for histone H3 modification, prevented chromatin remodeling as well as ATP crisis (Dittmann et al., 2013). Together, these data suggest that radiation-associated interactions between SGLT1 and EGFR result in increased glucose uptake, which counteracts the ATP crisis in tumor cells caused by chromatin remodeling. Importantly, the blockade of recovery from ATP crisis by SGLT1 inhibition may radio-sensitize tumor cells as demonstrated in lung adenocarcinoma and head and neck squamous carcinoma cell lines (Huber et al., 2012; Dittmann et al., 2013).

Formation of repair complexes

In addition to SGLT-generated glucose uptake, radiation-induced electrosignaling via transient receptor potential melastatin 2 (TRPM2) and vanilloid 1 (TRPV1) cation channels, has been shown to stimulate Ataxia telangiectasia mutated (ATM) kinase activation, histone 2AX (H2AX) phosphorylation, and γH2AX focus formation in A549 lung adenocarcinoma cells, processes required to recruit further repair proteins to the DNA double strand break (Masumoto et al., 2013). Furthermore, radiation-induced TRPM2 induces ATP release and P2Y signaling in A549 cells (Masumoto et al., 2013). Radiation-stimulated and $P2X_7$ receptor- and gap junction hemichannel connexin43-mediated ATP release has been suggested to signal in a paracrine manner to unirradiated bystander cells in the B16 melanoma model (Ohshima et al., 2012).

Combined, these recent data indicate that ion transports may regulate processes that mediate intrinsic radioresistance. The investigation of ion transports in radiobiology is at its very beginning and the few data available are mostly phenomenological in nature. The molecular mechanisms that underlie, e.g., regulation of DNA repair by ion transports are ill-defined. Nevertheless, the data prove functional significance of ion transports and electrosignaling for the survival of irradiated tumor cells and might have translational implications for radiotherapy in the future.

Similar to intrinsic radioresistance, the function of ion transports in hypoxia resistance and associated hypoxic radioresistance of tumor cells is not well-defined. The following paragraphs give a summary of what is known about mitochondrial transports and hypoxia resistance of normal tissue and how these findings might also apply for tumor cells.

MITOCHONDRIAL UNCOUPLING AND RESISTANCE TO HYPOXIA, CHEMO-, AND RADIOTHERAPY

Intermittent hypoxia is a common feature of vascularized solid tumors. The pathophysiologial aspects of hypoxia and reoxygenation are well-known from ischemia-reperfusion injuries observed in normal tissue. Reoxygenation-associated production of reactive oxygen species (ROS) is a major cause of the hypoxia/reoxygenation injury after myocardial, hepatic, intestinal, cerebral, renal and other ischemia and mitochondria have been identified as one of the main sources of ROS formation herein (Li and Jackson, 2002). Mitochondrial ROS formation mutually interacts with hypoxia/reoxygenation-associated cellular Ca^{2+} overload. Brief hypoxic periods induce an adaptation to hypoxia in several tissues which lowers ischemia-reperfusion injuries of subsequent ischemic insults (so-called ischemic preconditioning). Similar adaptations which involve alterations in mitochondrial ion transport have been proposed to confer hypoxia resistance of tumor cells.

Mitochondrial ROS formation

Activity and efficacy of the mitochondrial respiration chain are fine-tuned by the dependence of the ATP synthase (complex V) on the membrane potential $\Delta\Psi_m$, by the ATP/ADP ratio, as well as by reversible phosphorylation of the complexes I and IV (**Figure 3**) (Kadenbach, 2003). It is suggested that under physiological conditions (high ATP/ADP ratios), the membrane potential $\Delta\Psi_m$ is kept low [around −100 to −150 mV (Kadenbach, 2003)]. The efficacy of the respiratory chain at low $\Delta\Psi_m$ is high. At higher ATP demand or decreasing cellular ATP levels, cytochrome c oxidase (complex IV) is relieved from ATP blockade and $\Delta\Psi_m$ increases. High $\Delta\Psi_m$ values (up to −180 mV), however, lower the efficacy of cytochrome c oxidase (Kadenbach, 2003) and increase the probability of single electron leakage at complex I and III to molecular oxygen resulting in an increased $O_2{\cdot}^-$ production (**Figure 3**) (Korshunov et al., 1997; Skulachev, 1998; Kadenbach, 2003).

The respiratory chain is also regulated by the cytosolic ($[Ca^{2+}]_i$) and mitochondrial matrix free Ca^{2+} concentration ($[Ca^{2+}]_m$) in a complex manner (for review see Pizzo et al., 2012). The phosphatases that dephosphorylate (and thereby switch-off) the NADH oxidase and that relieve the ATP blockade of complex IV are inhibited by $[Ca^{2+}]_m$ and activated by $[Ca^{2+}]_i$, respectively (**Figure 3**). As a consequence, increase in $[Ca^{2+}]_m$ and $[Ca^{2+}]_i$ results in a higher $\Delta\Psi_m$ and a concurrently increased production of reactive oxygen species (Kadenbach, 2003).

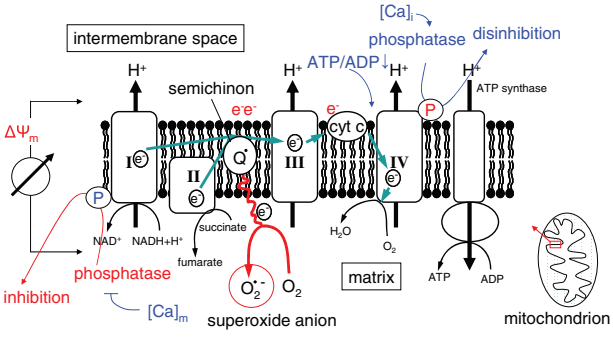

FIGURE 3 | Mitochondrial ROS formation in dependence on $\Delta\Psi_m$ (I, II, III, and IV, electron transport complexes I, II, III, and IV; Q: semiquinone radical; cyt C: cytochrome C). Ca^{2+} and the ATP/ADP ratio regulate the electron chain at complexes I and IV.

Hypoxia decreases the activity of the mitochondrial manganese superoxide dismutase (Mn-SOD) and of the cytochrome c oxidase. Depletion of the final electron acceptor, however, increases the formation of $O_2{\cdot}^-$ during reoxygenation by the enhanced leakage of single electrons from more proximal complexes of the respiration chain (for review see Li and Jackson, 2002; Sack, 2006). Lowered $O_2{\cdot}^-$-detoxifying capability combined with simultaneous elevated $O_2{\cdot}^-$ production results in a highly elevated $O_2{\cdot}^-$ concentration which, e.g., in hepatocytes increases 15-fold within 15 min of reoxygenation (Caraceni et al., 1995).

Hypoxia/reoxygenation-associated Ca^{2+} overload

Hypoxia-associated energy depletion and the concomitant impairment of plasma membrane Na^+ and Ca^{2+} pump activity lead to a decline of the chemical Na^+, Ca^{2+} and K^+ gradients across the plasma membrane and to the depolarization of the plasma membrane potential. In parallel, increased lactic acid fermentation during hypoxia increases the cytosolic proton concentration and lowers the intracellular pH. The proton extrusion machinery that is already active during hypoxia becomes massively activated during reoxygenation and restores a physiological pH by wash-out of lactic acid and activation of the sodium/hydrogen exchanger and sodium/bicarbonate symporter. The latter, Na^+-coupled transports, in turn, further increase the cytosolic Na^+ concentration to a level, where the low affinity high capacity sodium/calcium exchanger in the plasma membrane starts to operate in the reverse mode (i.e., to extrude Na^+ at the expense of Ca^{2+} uptake). At that time, reoxygenation-mediated oxidative stress (see above) stimulates further Ca^{2+} entry through Ca^{2+}-permeable channels in the plasma membrane and the release of Ca^{2+} from the endoplasmic reticulum resulting in an abrupt rise in $[Ca^{2+}]_i$ during the first minutes of reoxygenation. Cytosolic Ca^{2+} is buffered by $\Delta\Psi_m$-driven and uniporter-mediated Ca^{2+} uptake into the mitochondrial matrix which increases $[Ca^{2+}]_m$. Elevated $[Ca^{2+}]_m$ and $[Ca^{2+}]_i$ values, in turn, signal back to the respiratory chain by further increasing $\Delta\Psi_m$ (see above). Exceeding the Ca^{2+} threshold concentration in the matrix, $[Ca^{2+}]_m$ activates the permeability transition pore which leads to breakdown of $\Delta\Psi_m$, swelling of the mitochondrial matrix and eventually release of cytochrome c from the intermembrane space into the cytosol (Crompton, 1999; Rasola and Bernardi, 2011). By reversing the ATP synthase activity, into the ATPase proton pump mode, the F_0/F_1 complex in the inner mitochondrial delays the break-down of $\Delta\Psi_m$ at the expense of ATP hydrolysis. In addition to this ATP depletion, the loss of cytochrome c and the concurrent decline of the final electron acceptor (cytochrome c oxidase of complex IV) further increases the formation of $O_2{\cdot}^-$ by more proximal complexes. The pivotal role of membrane transports in this process is illustrated by the fact that inhibition of the sodium/hydrogen antiporter in the plasma membrane, the Ca^{2+} uniporter in the inner mitochondrial membrane, or Ca^{2+} channels in the endoplasmic reticulum (ER) decreases the hypoxia/reoxygenation injury *in vitro* (for review see Crompton, 1999; Li and Jackson, 2002; Sack, 2006; Yellon and Hausenloy, 2007).

Ischemic pre-conditioning

Cells can also adapt to repetitive periods of hypoxia. This so-called ischemic preconditioning has been demonstrated in the myocardium where it reduces ischemia-caused infarct size, myocardial stunning, and incidence of cardiac arrhythmias (Gross and Peart, 2003). Since mitochondrial ROS formation increases with increasing $\Delta\Psi_m$ (Korshunov et al., 1997; Skulachev, 1998; Kadenbach, 2003) lowering of the mitochondrial $\Delta\Psi_m$ is proposed to be a key adaptation event in ischemic preconditioning (Sack, 2006). Lowering of $\Delta\Psi_m$ reduces not only mitochondrial $O_2{\cdot}^-$ production but also the mitochondrial Ca^{2+} overload during reoxygenation (Gross and Peart, 2003; Prasad et al., 2009). The hypoxic preconditioning-associated reduction of $\Delta\Psi_m$ is in part achieved by up-regulation of ATP-sensitive (mitoKATP) and Ca^{2+}-activated (mitoKCa) K^+ channels in the inner mitochondrial membrane which short-circuit $\Delta\Psi_m$ (Murata et al., 2001; Gross and Peart, 2003; Prasad et al., 2009; Singh et al., 2012; Szabo et al., 2012). The uncoupling proteins-2 and -3 (UCP-2, -3) constitute two further proteins that have been suggested to play a role in counteracting cardiac hypoxia/reoxygenation injury and in hypoxic preconditioning in heart and brain (Mcleod et al., 2005; Sack, 2006; Ozcan et al., 2013). Activation of these proteins results in a modest depolarization of $\Delta\Psi_m$ by maximally 15 mV (Fink et al., 2002). High expression of UCP-3 has also been demonstrated in skeletal muscle where it suppresses mitochondrial oxidant emission during fatty acid-supported respiration (Anderson et al., 2007). Accordingly, overexpression of UCP-3 in cultured human muscle cells lowers $\Delta\Psi_m$, raises the ATP/ADP ratio, and favors fatty acid vs. glucose oxidation (Garcia-Martinez et al., 2001). Conversely, knockdown of UCP-3 increased the coupling between electron and proton transfer across the inner mitochondrial membrane and ROS production (Vidal-Puig et al., 2000; Talbot and Brand, 2005). UCP-3 protein is robustly up-regulated in chondrocytes (Watanabe et al., 2008) and skeletal muscle during hypoxia and the absence of UCP-3 exacerbates hypoxia-induced ROS (Lu and Sack, 2008). UCP-3 is not constitutively active. $O_2{\cdot}^-$ has been demonstrated to stimulate the activity of UCP-3 in skeletal muscle suggesting that UCP-3 is the effector of a feed back loop which restricts overshooting ROS production (Echtay et al., 2002).

Mitochondrial uncoupling in tumor cells

Recent studies suggest that UCPs are upregulated in a number of aggressive human cancers. In particular, over-expression of UCP2 has been reported in leukemia as well as in breast, colorectal, ovarian, bladder, esophagus, testicular, kidney, pancreatic, lung, and prostate cancer (Ayyasamy et al., 2011; Su et al., 2012). In human colon cancer, UCP2 mRNA and protein expression reportedly is increased by factor of 3–4 as compared to peritumoral normal epithelium. In addition, UCP2 expression gradually increases during the colon adenoma-carcinoma sequence (Horimoto et al., 2004) and is higher in clinical stages III and IV colon cancer than in stage I and II (Kuai et al., 2010). Similarly, UCP4 expression has been shown to correlate with lymph node metastases in breast cancer (Gonidi et al., 2011) and UCP1 expression in prostate cancer with disease progression from primary to bone metastatic cancers (Zhau et al., 2011). Moreover, postmenopausal breast

tumors with low estrogen receptor (ER) alpha to ER beta ratios that associate with higher UCP5 expression and higher oxidative defense have a poor prognosis (Sastre-Serra et al., 2013). Finally, ectopic expression of UCP2 in MCF7 breast cancer cells has been demonstrated to enhance proliferation, migration and matrigel invasion *in vitro* and to promote tumor growth *in viv*o (Ayyasamy et al., 2011). Together, these observations suggest that UCPs may contribute to the malignant progression of tumor cells.

In addition to malignant progression, UCPs may alter the therapy sensitivity of tumor cells. In specimens of human ovarian cancers carboplatin/paclitaxel-resistant cancers showed decreased UCP2 protein abundances as compared to the sensitive ones (Pons et al., 2012). Likewise, progression-free and overall survival of patients with inoperable lung cancer who received cisplatin-based chemotherapy was higher when tumors expressed high levels of UCP2 as compared to tumors with low UCP2 levels (Su et al., 2012). A possible explanation of the latter observation is that especially in lung tumors with mutated p53, cisplatin elicits oxidative stress that induces pro-survival signaling. High UCP2 expression, however, diminishes cisplatin-evoked oxidative stress and, in turn, decreases the pro-survival signals (Su et al., 2012).

In lung cancer cell lines with wildtype p53, in contrast, down-regulation of UCP2 results in significantly increased paclitaxel-induced cell death (Su et al., 2012). Similarly, overexpression of UCP2 in a human colon cancer cell line has been shown to blunt topoisomerase I inhibitor CPT-11-induced accumulation of reactive oxygen species and apoptosis *in vitro* and to confer CPT-11 resistance of tumor *xeno*grafts (Derdak et al., 2008). In addition, in pancreatic adenocarcinoma, non-small cell lung adenocarcinoma, and bladder carcinoma cell lines IC_{50} values of the anticancer drug gemcitabine increase with intrinsic UCP2 mRNA abundance. Furthermore, UCP2 overexpression strongly decreases gemcitabine-induced mitochondrial superoxide formation and protects cancer cells from apoptosis (Dalla Pozza et al., 2012). Finally, metabolic changes including UCP2 up-regulation and UCP2-mediated uncoupling of oxidative phosphorylation have been demonstrated in multidrug-resistant subclones of various tumor cell lines (Harper et al., 2002). Similarly, in acute myeloid leukemia cells, UCP2 up-regulation has been shown to foster the Warburg effect (i.e., anaerobic glycolysis in the absence of respiratory impairment) (Samudio et al., 2008).

UCP2 expression is stimulated by co-culturing of these leukemia cells with bone marrow-derived mesenchymal stromal cells (Samudio et al., 2008). Other stimuli of UCP expression/activity are hydrogen peroxide as shown for UCP5 in colon cancer cells (Santandreu et al., 2009) and gemcitabine chemotherapy as reported for UCP2 in pancreatic, lung and bladder cancer cell lines (Dalla Pozza et al., 2012). Collectively, these data suggest that tumor cells may acquire resistance to chemotherapy by up-regulation of UCPs and lowering of the therapy-evoked mitochondrial formation of reactive oxygen species (Robbins and Zhao, 2011).

Accordingly, experimental targeting of UCPs has been demonstrated to sensitize tumor cells to chemotherapy *in vitro*. For instance, genipin-induced inhibition or glutathionylation of UCP2 sensitizes drug-resistant leukemia subclones to chemotherapy with menadione, doxorubicin, or epirubicin (Mailloux et al., 2010; Pfefferle et al., 2012). Likewise, UCP2 inhibition by genipin or UCP2 mRNA silencing strongly enhances gemcitabine-induced mitochondrial superoxide generation and apoptotic cell death of pancreatic, lung and bladder cancer cell lines (Dalla Pozza et al., 2012). Moreover, UCP2 inhibition has been reported to trigger reactive oxygen species-dependent nuclear translocation of GAPDH and autophagic cell death in pancreatic adenocarcinoma cells (Dando et al., 2013) Together, this suggests that targeting UCPs might be a promising strategy to overcome resistance to anti-cancer therapies in the clinic. Notably, in an acute myeloid leukemia cell line, the cytotoxicity of cisplatin has been proposed to be in part mediated by cisplatin-dependent down-regulation of UCPs (Samudio et al., 2008) suggesting that established chemotherapy regimes already may co-target UCPs.

It is tempting to speculate that UCPs may also confer resistance to radiotherapy. One could hypothesize that UCPs adapt the tumor cells to a "relatively radioprotected" hypoxic microenvironment by decreasing hypoxia-associated mitochondrial formation of reactive oxygen species. Such UCP function in hypoxia resistance has been demonstrated for a lung adenocarcinoma cell line (Deng et al., 2012). Notably, radiation induces up-regulation of UCP2 expression as shown in colon carcinoma cells (Sreekumar et al., 2001) and in a radiosensitive subclone of B cell lymphoma (Voehringer et al., 2000). On the one hand, this UCP2 up-regulation might facilitate radiation-induced apoptosis induction by accelerating the break-down of $\Delta\Psi_m$ as proposed by the authors of these studies. On the other hand, radiation-induced UCP2 upregulation might be radioprotective by lowering the radiation-induced burden of reactive oxygen species. As a matter of fact, multi-resistant subclones of leukemia cells show higher UCP2 protein expression, lower $\Delta\Psi_m$, lower radiation induced formation of reactive oxygen species and decreased DNA damage as compared to their parental sensitive cells (Harper et al., 2002).

In summary, UCPs suppress the formation of $O_2{\cdot}^-$, a byproduct of the mitochondrial respiration chain and a major source of oxidative stress. In some cancers UCPs in particular UCP2 are highly upregulated and may contribute to the reprogramming of the cell metabolism that results in chemoresistance (for review see Baffy, 2010; Baffy et al., 2011) or even radioresistance. Moreover, recent studies imply that UCP2 may repress p53-mediated apoptosis providing a potential new mechanism of how UCP2 contributes to cancer development (Robbins and Zhao, 2011).

Together, these observations suggest that ion transport processes are critically involved in evasion from radiation stress, and intrinsic or hypoxic radioresistance. Since ion transport-mediated radioresistance might underlie failure of radiotherapy, concepts which combine ion transport targeting with radiotherapy hold promise for new therapy strategies in the future. A summary of how ion transport can be harnessed for anticancer therapy and how these therapy strategies might be combined with radiotherapy is given in the next paragraphs.

TARGETING ION TRANSPORTS IN RADIOTHERAPY

An important reason for the study of ion transports in the context of radiotherapy is the possible translation of the acquired knowledge into anti-cancer therapy. Many pharmacological modulators

of ion transports are already in clinical use or currently tested in clinical trials (Wulff and Castle, 2010). Moreover, tumors often over-express certain types of transport proteins.

These proteins such as the transient receptor melastatin 8 (TRPM8) non-selective cation channel in prostate cancer have been used in clinical trials as tumor-associated antigen for anti-tumor vaccination (Fuessel et al., 2006). Tumor promoting inflammation and anti-tumor immune effects are evolving fields of preclinical and clinical research (Hanahan and Weinberg, 2011). Preclinical evidence supports the thesis that tumors have to develop immune-evading capacities in order to grow into macroscopic, clinically detectable lesions (Koebel et al., 2007; Teng et al., 2008). Possible mechanisms are the secretion of cytokines and chemokines by cancer and tumor stroma cells (Vianello et al., 2006; Shields et al., 2010), the priming of infiltrating T-lymphocytes toward immunosuppressive regulatory T-cells and the recruitment of myeloid-derived suppressor cells and tumor-associated macrophages (Tanchot et al., 2013; Oleinika et al., 2013). Irradiation of tumors has been shown to impair on the one hand the immunosuppressive action of the tumor and on the other to induce so-called "immunogenic" cell death within the tumor with translocation of calreticulin to the plasma membrane, release of HMGB1 or ATP (Formenti and Demaria, 2013). Preclinical studies showed a synergistic effect of irradiation and several immunotherapeutic approaches such as dendritic cell injection (Finkelstein et al., 2012), anti-CTLA-4-antibody (Grosso and Jure-Kunkel, 2013), and vaccines (Chakraborty et al., 2004). Interestingly, for combination with anti-CTLA-4 antibody a synergistic effect could only be demonstrated for fractionated but not for single-dose irradiation (Demaria and Formenti, 2012).

In addition, over-expressed transport proteins in tumors can be harnessed to target drugs, cytokines, or radioactivity to the tumor cells (Hartung et al., 2011). One example is the specific surface expression of ClC-3 Cl^- channels by glioblastoma (and other tumor entities) which suggests ClC-3 as an excellent and highly specific target for anti-glioblastoma therapy. Chlorotoxin which is a 36 amino acid-long peptide from the venom of the scorpion *Leiurus quinquestriatus* has been found to inhibit ClC-3 and to preferentially bind to the cell surface of a variety of human malignancies. This specificity probably comes from the highly affine binding of chlorotoxin to a lipid raft-anchored complex of matrix metalloproteinase-2, membrane type-I MMP, and transmembrane inhibitor of metalloproteinase-2, as well as ClC-3 (Veiseh et al., 2007). Ongoing clinical trials successfully used ^{131}I-labeled chlorotoxin as glioblastoma-specific PET-tracer (Hockaday et al., 2005) and for targeted radiation of glioblastoma cells (Mamelak and Jacoby, 2007). Due to the low surface expression of ClC-3 in normal tissue, chlorotoxin exhibits little or no affinity to normal cells (Lyons et al., 2002). If the *in vitro* and mouse data on radiation-stimulated glioblastoma migration reflect indeed the *in vivo* situation in glioblastoma patients, a clinical setting might be envisaged in which radiation-induced glioblastoma spreading is prevented by combining radiotherapy with chlorotoxin blockade of ClC-3 channels.

CONCLUDING REMARKS

Interdisciplinary approaches linking radiobiology with physiology brought about the first peaces of evidence suggesting a functional significance of ion transport processes for the survival of irradiated tumor cells. The few reports published up to now on this topic are confined to phenomena occurring in the plasma membrane due to the methodological restrictions of studying these processes in the membranes of mitochondria, endoplasmic reticulum, or nuclear envelope. Intracellular membrane transports, however, might similarly impact tumor cell radiosensitivity. This is suggested by the notion that intracellular Cl^- channel CLIC1 protein expression regulates radiosensitivity in laryngeal cancer cells (Kim et al., 2010). However, the molecular mechanisms underlying, e.g., radiation-induced transport modifications, or downstream signaling events are far from being understood. Despite all these limitations, our current knowledge already clearly indicates that the observed transport processes may be crucial for the survival of the tumor and, thus, are worthwhile to spend further and more effort in this field which might lead to new strategies for cancer treatment in the future.

ACKNOWLEDGMENTS

This work has been supported by the Wilhelm-Sander-Stiftung (2011.083.1). Dominik Klumpp and Benjamin Stegen were supported by the DFG International Graduate School 1302 (TP T9).

REFERENCES

Anderson, E. J., Yamazaki, H., and Neufer, P. D. (2007). Induction of endogenous uncoupling protein 3 suppresses mitochondrial oxidant emission during fatty acid-supported respiration. *J. Biol. Chem.* 282, 31257–31266. doi: 10.1074/jbc.M706129200

Arcangeli, A. (2011). Ion channels and transporters in cancer. 3. Ion channels in the tumor cell-microenvironment cross talk. *Am. J. Physiol. Cell Physiol.* 301, C762–C771.

Asuthkar, S., Nalla, A. K., Gondi, C. S., Dinh, D. H., Gujrati, M., Mohanam, S., et al. (2011). Gadd45a sensitizes medulloblastoma cells to irradiation and suppresses MMP-9-mediated EMT. *Neuro Oncol.* 13, 1059–1073. doi: 10.1093/neuonc/nor109

Auperin, A., Arriagada, R., Pignon, J. P., Le Pechoux, C., Gregor, A., Stephens, R. J., et al. (1999). Prophylactic cranial irradiation for patients with small-cell lung cancer in complete remission. prophylactic cranial irradiation overview collaborative group. *N. Engl. J. Med.* 341, 476–484. doi: 10.1056/NEJM199908123410703

Ayyasamy, V., Owens, K. M., Desouki, M. M., Liang, P., Bakin, A., Thangaraj, K., et al. (2011). Cellular model of Warburg effect identifies tumor promoting function of UCP2 in breast cancer and its suppression by genipin. *PLoS ONE* 6:e24792. doi: 10.1371/journal.pone.0024792

Badiga, A. V., Chetty, C., Kesanakurti, D., Are, D., Gujrati, M., Klopfenstein, J. D., et al. (2011). MMP-2 siRNA inhibits radiation-enhanced invasiveness in glioma cells. *PLoS ONE* 6:e20614. doi: 10.1371/journal.pone.0020614

Baffy, G. (2010). Uncoupling protein-2 and cancer. *Mitochondrion* 10, 243–252. doi: 10.1016/j.mito.2009.12.143

Baffy, G., Derdak, Z., and Robson, S. C. (2011). Mitochondrial recoupling: a novel therapeutic strategy for cancer. *Br. J. Cancer* 105, 469–474.

Barendsen, G. W. (1982). Dose fractionation, dose rate and iso-effect relationships for normal tissue responses. *Int. J. Radiat. Oncol. Biol. Phys.* 8, 1981–1997. doi: 10.1016/0360-301690459-X

Bernier, J., Hall, E. J., and Giaccia, A. (2004). Radiation oncology: a century of achievements. *Nat. Rev. Cancer* 4, 737–747. doi: 10.1038/nrc1451

Canazza, A., Calatozzolo, C., Fumagalli, L., Bergantin, A., Ghielmetti,

F., Fariselli, L., et al. (2011). Increased migration of a human glioma cell line after *in vitro* CyberKnife irradiation. *Cancer Biol. Ther.* 12, 629–633. doi: 10.4161/cbt.12.7.16862

Caraceni, P., Ryu, H. S., Van Thiel, D. H., and Borle, A. B. (1995). Source of oxygen free radicals produced by rat hepatocytes during postanoxic reoxygenation. *Biochim. Biophys. Acta* 1268, 249–254. doi: 10.1016/0167-488900077-6

Casneuf, V. F., Fonteyne, P., Van Damme, N., Demetter, P., Pauwels, P., De Hemptinne, B., et al. (2008). Expression of SGLT1, Bcl-2 and p53 in primary pancreatic cancer related to survival. *Cancer Invest.* 26, 852–859. doi: 10.1080/07357900801956363

Catacuzzeno, L., Aiello, F., Fioretti, B., Sforna, L., Castigli, E., Ruggieri, P., et al. (2010). Serum-activated K and Cl currents underlay U87-MG glioblastoma cell migration. *J. Cell Physiol.* 226, 1926–1933. doi: 10.1002/jcp.22523

Chakraborty, M., Abrams, S. I., Coleman, C. N., Camphausen, K., Schlom, J., and Hodge, J. W. (2004). External beam radiation of tumors alters phenotype of tumor cells to render them susceptible to vaccine-mediated T-cell killing. *Cancer Res.* 64, 4328–4337. doi: 10.1158/0008-5472.CAN-04-0073

Crompton, M. (1999). The mitochondrial permeability transition pore and its role in cell death. *Biochem. J.* 341, 233–249.

Cuddapah, V. A., and Sontheimer, H. (2010). Molecular interaction and functional regulation of ClC-3 by Ca2+/calmodulin-dependent protein kinase II (CaMKII) in human malignant glioma. *J. Biol. Chem.* 285, 11188–11196. doi: 10.1074/jbc.M109.097675

Cullis, P. M., Jones, G. D. D., Lea, J., Symons, M. C. R., and Sweeney, M. (1987). The effects of ionizing radiation on deoxyribonucleic acid. Part 5. The role of thiols in chemical repair. *J. Chem. Soc., Perkin Trans. 2,* 1907–1914. doi: 10.1039/p29870001907

Dale, R. G. (1985). The application of the linear-quadratic dose-effect equation to fractionated and protracted radiotherapy. *Br. J. Radiol.* 58, 515–528. doi: 10.1259/0007-1285-58-690-515

Dalla Pozza, E., Fiorini, C., Dando, I., Menegazzi, M., Sgarbossa, A., Costanzo, C., et al. (2012). Role of mitochondrial uncoupling protein 2 in cancer cell resistance to gemcitabine. *Biochim. Biophys. Acta* 1823, 1856–1863. doi: 10.1016/j.bbamcr.2012.06.007

Dando, I., Fiorini, C., Pozza, E. D., Padroni, C., Costanzo, C., Palmieri, M., et al. (2013). UCP2 inhibition triggers ROS-dependent nuclear translocation of GAPDH and autophagic cell death in pancreatic adenocarcinoma cells. *Biochim. Biophys. Acta* 1833, 672–679. doi: 10.1016/j.bbamcr.2012.10.028

Darby, S., Mcgale, P., Correa, C., Taylor, C., Arriagada, R., Clarke, M., et al. (2011). Effect of radiotherapy after breast-conserving surgery on 10-year recurrence and 15-year breast cancer death: meta-analysis of individual patient data for 10, 801 women in 17 randomised trials. *Lancet* 378, 1707–1716. doi: 10.1016/S0140-673661629-2

Demaria, S., and Formenti, S. C. (2012). Radiation as an immunological adjuvant: current evidence on dose and fractionation. *Front. Oncol.* 2:153. doi: 10.3389/fonc.2012.00153

Deng, S., Yang, Y., Han, Y., Li, X., Wang, X., Li, X., et al. (2012). UCP2 inhibits ROS-mediated apoptosis in A549 under hypoxic conditions. *PLoS ONE* 7:e30714. doi: 10.1371/journal.pone.0030714

Derdak, Z., Mark, N. M., Beldi, G., Robson, S. C., Wands, J. R., and Baffy, G. (2008). The mitochondrial uncoupling protein-2 promotes chemoresistance in cancer cells. *Cancer Res.* 68, 2813–2819. doi: 10.1158/0008-5472.CAN-08-0053

Dittmann, K., Mayer, C., Kehlbach, R., Rothmund, M. C., and Peter Rodemann, H. (2009). Radiation-induced lipid peroxidation activates src kinase and triggers nuclear EGFR transport. *Radiother. Oncol.* 92, 379–382. doi: 10.1016/j.radonc.2009.06.003

Dittmann, K., Mayer, C., Rodemann, H. P., and Huber, S. M. (2013). EGFR cooperates with glucose transporter SGLT1 to enable chromatin remodeling in response to ionizing radiation. *Radiother. Oncol.* 107, 247–251. doi: 10.1016/j.radonc.2013.03.016

Dorn, G. W. 2nd. (2013). Molecular mechanisms that differentiate apoptosis from programmed necrosis. *Toxicol. Pathol.* 41, 227–234. doi: 10.1177/0192623312466961

Echtay, K. S., Roussel, D., St-Pierre, J., Jekabsons, M. B., Cadenas, S., Stuart, J. A., et al. (2002). Superoxide activates mitochondrial uncoupling proteins. *Nature* 415, 96–99. doi: 10.1038/415096a

Eckert, F., Alloussi, S., Paulsen, F., Bamberg, M., Zips, D., Spillner, P. et al. (2013). Prospective evaluation of a hydrogel spacer for rectal separation in dose-escalated intensity-modulated radiotherapy for clinically localized prostate cancer. *BMC Cancer* 13:27. doi: 10.1186/1471-2407-13-27

Eckert, F., Fehm, T., Bamberg, M., and Muller, A. C. (2010a). Small cell carcinoma of vulva: curative multimodal treatment in face of resistance to initial standard chemotherapy. *Strahlenther. Onkol.* 186, 521–524.

Eckert, F., Matuschek, C., Mueller, A. C., Weinmann, M., Hartmann, J. T., Belka, C., et al. (2010b). Definitive radiotherapy and single-agent radiosensitizing ifosfamide in patients with localized, irresectable soft tissue sarcoma: a retrospective analysis. *Radiat. Oncol.* 5, 55.

Eckert, F., Gani, C., Bamberg, M., and Muller, A. C. (2012). Cerebral metastases in extrapulmonary cell carcinoma: implications for the use of prophylactic cranial irradiation. *Strahlenther. Onkol.* 188, 478–483. doi: 10.1007/s00066-012-0084-5

Ernest, N. J., Weaver, A. K., Van Duyn, L. B., and Sontheimer, H. W. (2005). Relative contribution of chloride channels and transporters to regulatory volume decrease in human glioma cells. *Am. J. Physiol. Cell Physiol.* 288, C1451–1460. doi: 10.1152/ajpcell.00503.2004

Fink, B. D., Hong, Y. S., Mathahs, M. M., Scholz, T. D., Dillon, J. S., and Sivitz, W. I. (2002). UCP2-dependent proton leak in isolated mammalian mitochondria. *J. Biol. Chem.* 277, 3918–3925. doi: 10.1074/jbc.M107955200

Finkelstein, S. E., Iclozan, C., Bui, M. M., Cotter, M. J., Ramakrishnan, R., Ahmed, J., et al. (2012). Combination of external beam radiotherapy (EBRT) with intratumoral injection of dendritic cells as neo-adjuvant treatment of high-risk soft tissue sarcoma patients. *Int. J. Radiat. Oncol. Biol. Phys.* 82, 924–932. doi: 10.1016/j.ijrobp.2010.12.068

Formenti, S. C., and Demaria, S. (2013). Combining radiotherapy and cancer immunotherapy: a paradigm shift. *J. Natl. Cancer Inst.* 105, 256–265. doi: 10.1093/jnci/djs629

Fuessel, S., Meye, A., Schmitz, M., Zastrow, S., Linne, C., Richter, K., et al. (2006). Vaccination of hormone-refractory prostate cancer patients with peptide cocktail-loaded dendritic cells: results of a phase I clinical trial. *Prostate* 66, 811–821. doi: 10.1002/pros.20404

Fyles, A., Milosevic, M., Hedley, D., Pintilie, M., Levin, W., Manchul, L., et al. (2002). Tumor hypoxia has independent predictor impact only in patients with node-negative cervix cancer. *J. Clin. Oncol.* 20, 680–687. doi: 10.1200/JCO.20.3.680

Fyles, A., Milosevic, M., Pintilie, M., Syed, A., Levin, W., Manchul, L., et al. (2006). Long-term performance of interstial fluid pressure and hypoxia as prognostic factors in cervix cancer. *Radiother. Oncol.* 80, 132–137. doi: 10.1016/j.radonc.2006.07.014

Ganapathy, V., Thangaraju, M., and Prasad, P. D. (2009). Nutrient transporters in cancer: relevance to Warburg hypothesis and beyond. *Pharmacol. Ther.* 121, 29–40. doi: 10.1016/j.pharmthera.2008.09.005

Garcia-Martinez, C., Sibille, B., Solanes, G., Darimont, C., Mace, K., Villarroya, F., et al. (2001). Overexpression of UCP3 in cultured human muscle lowers mitochondrial membrane potential, raises ATP/ADP ratio, and favors fatty acid vs. glucose oxidation. *FASEB J.* 15, 2033–2035.

German-Cancer-Aid. (2013a). *Homepage*. Available online at: http://www.krebshilfe.de/krebszahlen.html

German-Cancer-Aid. (2013b). *Information Booklet*. Available online at: http://www.krebshilfe.de/fileadmin/Inhalte/Downloads/PDFs/Blaue_Ratgeber/053_strahlen.pdf.

Glenny, A. M., Furness, S., Worthington, H. V., Conway, D. I., Oliver, R., Clarkson, J. E., et al. (2010). Interventions for the treatment of oral cavity and oropharyngeal cancer: radiotherapy. *Cochrane Database Syst. Rev.* CD006387. doi: 10.1002/14651858.CD006387.pub2

Gomez-Ospina, N., Tsuruta, F., Barreto-Chang, O., Hu, L., and Dolmetsch, R. (2006). The C terminus of the L-type voltage-gated calcium channel Ca(V)1.2 encodes a transcription factor. *Cell* 127, 591–606. doi: 10.1016/j.cell.2006.10.017

Gonidi, M., Athanassiadou, A. M., Patsouris, E., Tsipis, A., Dimopoulos, S., Kyriakidou, V., et al. (2011). Mitochondrial UCP4 and bcl-2 expression in imprints of breast carcinomas: relationship with DNA ploidy and classical prognostic factors.

Pathol. Res. Pract. 207, 377–382. doi: 10.1016/j.prp.2011.03.007

Grills, I. S., Hope, A. J., Guckenberger, M., Kestin, L. L., Werner-Wasik, M., Yan, D., et al. (2012). A collaborative analysis of stereotactic lung radiotherapy outcomes for early-stage non-small-cell lung cancer using daily online cone-beam computed tomography image-guided radiotherapy. *J. Thorac. Oncol.* 7, 1382–1393. doi: 10.1097/JTO.0b013e318260e00d

Gross, G. J., and Peart, J. N. (2003). KATP channels and myocardial preconditioning: an update. *Am. J. Physiol. Heart Circ. Physiol.* 285, H921–H930.

Grosso, J. F., and Jure-Kunkel, M. N. (2013). CTLA-4 blockade in tumor models: an overview of preclinical and translational research. *Cancer Immun.* 13, 5.

Haas, B. R., Cuddapah, V. A., Watkins, S., Rohn, K. J., Dy, T. E., and Sontheimer, H. (2011). With-No-Lysine Kinase 3 (WNK3) stimulates glioma invasion by regulating cell volume. *Am. J. Physiol. Cell Physiol.* 301, C1150–C1160. doi: 10.1152/ajpcell.00203.2011

Haas, B. R., and Sontheimer, H. (2010). Inhibition of the sodium-potassium-chloride cotransporter isoform-1 reduces glioma invasion. *Cancer Res.* 70, 5597–5606. doi: 10.1158/0008-5472.CAN-09-4666

Hanahan, D., and Weinberg, R. A. (2011). Hallmarks of cancer: the next generation. *Cell* 144, 646–674. doi: 10.1016/j.cell.2011.02.013

Harada, H. (2011). How can we overcome tumor hypoxia in radiation therapy. *J. Radiat. Res.* 52, 545–556.

Harper, M. E., Antoniou, A., Villalobos-Menuey, E., Russo, A., Trauger, R., Vendemelio, M., et al. (2002). Characterization of a novel metabolic strategy used by drug-resistant tumor cells. *FASEB J.* 16, 1550–1557. doi: 10.1096/fj.02-0541com

Hartung, F., Stuhmer, W., and Pardo, L. A. (2011). Tumor cell-selective apoptosis induction through targeting of K(V)10.1 via bifunctional TRAIL antibody. *Mol. Cancer* 10, 109.

Hatzikirou, H., Basanta, D., Simon, M., Schaller, K., and Deutsch, A. (2012). 'Go or Grow': the key to the emergence of invasion in tumour progression. *Math. Med. Biol.* 29, 49–65. doi: 10.1093/imammb/dqq011

Heise, N., Palme, D., Misovic, M., Koka, S., Rudner, J., Lang, F., et al. (2010). Non-selective cation channel-mediated Ca2+-entry and activation of Ca2+/calmodulin-dependent kinase II contribute to G2/M cell cycle arrest and survival of irradiated leukemia cells. *Cell Physiol. Biochem.* 26, 597–608. doi: 10.1159/000322327

Helmke, B. M., Reisser, C., Idzko, M., Dyckhoff, G., and Herold-Mende, C. (2004). Expression of SGLT-1 in preneoplastic and neoplastic lesions of the head and neck. *Oral Oncol.* 40, 28–35. doi: 10.1016/S1368-837500129-5

Hockaday, D. C., Shen, S., Fiveash, J., Raubitschek, A., Colcher, D., Liu, A., et al. (2005). Imaging glioma extent with 131I-TM-601. *J. Nucl. Med.* 46, 580–586.

Horimoto, M., Resnick, M. B., Konkin, T. A., Routhier, J., Wands, J. R., and Baffy, G. (2004). Expression of uncoupling protein-2 in human colon cancer. *Clin. Cancer Res.* 10, 6203–6207. doi: 10.1158/1078-0432.CCR-04-0419

Horiot, J. C., Le Fur, R., N'guyen, T., Chenal, C., Schraub, S., Alfonsi, S., et al. (1992). Hyperfractionation versus conventional fractionation in oropharyngeal carcinoma: final analysis of a randomized trial of the EORTC cooperative group of radiotherapy. *Radiother. Oncol.* 25, 231–241. doi: 10.1016/0167-814090242-M

Huber, S. M. (2013). Oncochannels. *Cell Calcium*. 53, 241–255. doi: 10.1016/j.ceca.2013.01.001

Huber, S. M., Misovic, M., Mayer, C., Rodemann, H. P., and Dittmann, K. (2012). EGFR-mediated stimulation of sodium/glucose cotransport promotes survival of irradiated human A549 lung adenocarcinoma cells. *Radiother. Oncol.* 103, 373–379. doi: 10.1016/j.radonc.2012.03.008

Ishikawa, N., Oguri, T., Isobe, T., Fujitaka, K., and Kohno, N. (2001). SGLT gene expression in primary lung cancers and their metastatic lesions. *Jpn. J. Cancer Res.* 92, 874–879. doi: 10.1111/j.1349-7006.2001.tb01175.x

Johnson, J., Nowicki, M. O., Lee, C. H., Chiocca, E. A., Viapiano, M. S., Lawler, S. E., et al. (2009). Quantitative analysis of complex glioma cell migration on electrospun polycaprolactone using time-lapse microscopy. *Tissue Eng. Part C Methods* 15, 531–540. doi: 10.1089/ten.tec.2008.0486

Jones, B., Dale, R. G., and Gaya, A. M. (2006). Linear quadratic modeling of increased late normal-tissue effects in special clinical situations. *Int. J. Radiat. Oncol. Biol. Phys.* 64, 948–953. doi: 10.1016/j.ijrobp.2005.10.016

Jung, J. W., Hwang, S. Y., Hwang, J. S., Oh, E. S., Park, S., and Han, I. O. (2007). Ionising radiation induces changes associated with epithelial-mesenchymal transdifferentiation and increased cell motility of A549 lung epithelial cells. *Eur. J. Cancer* 43, 1214–1224. doi: 10.1016/j.ejca.2007.01.034

Kadenbach, B. (2003). Intrinsic and extrinsic uncoupling of oxidative phosphorylation. *Biochim. Biophys. Acta* 1604, 77–94. doi: 10.1016/S0005-272800027-6

Kargiotis, O., Chetty, C., Gogineni, V., Gondi, C. S., Pulukuri, S. M., Kyritsis, A. P., et al. (2008). uPA/uPAR downregulation inhibits radiation-induced migration, invasion and angiogenesis in IOMM-Lee meningioma cells and decreases tumor growth *in vivo*. *Int. J. Oncol.* 33, 937–947.

Kil, W. J., Tofilon, P. J., and Camphausen, K. (2012). Post-radiation increase in VEGF enhances glioma cell motility *in vitro*. *Radiat. Oncol.* 7, 25. doi: 10.1186/1748-717X-7-25

Kim, J. S., Chang, J. W., Yun, H. S., Yang, K. M., Hong, E. H., Kim, D. H., et al. (2010). Chloride intracellular channel 1 identified using proteomic analysis plays an important role in the radiosensitivity of HEp-2 cells via reactive oxygen species production. *Proteomics* 10, 2589–2604. doi: 10.1002/pmic.200900523

Klotz, L., Venier, N., Colquhoun, A. J., Sasaki, H., Loblaw, D. A., Fleshner, N., et al. (2011). Capsaicin, a novel radiosensitizer, acts via a TRPV6 mediated phenomenon. *J. Clin. Oncol.* 29(Suppl. 7; Abstr. 23).

Koebel, C. M., Vermi, W., Swann, J. B., Zerafa, N., Rodig, S. J., Old, L. J., et al. (2007). Adaptive immunity maintains occult cancer in an equilibrium state. *Nature* 450, 903–907. doi: 10.1038/nature06309

Korshunov, S. S., Skulachev, V. P., and Starkov, A. A. (1997). High protonic potential actuates a mechanism of production of reactive oxygen species in mitochondria. *FEBS Lett.* 416, 15–18. doi: 10.1016/S0014-579301159-9

Kotecha, R., Yamada, Y., Pei, X., Kollmeier, M. A., Cox, B., Cohen, G. N., et al. (2013). Clinical outcomes of high-dose-rate brachytherapy and external beam radiotherapy in the management of clinically localized prostate cancer. *Brachytherapy* 12, 44–49. doi: 10.1016/j.brachy.2012.05.003

Kuai, X. Y., Ji, Z. Y., and Zhang, H. J. (2010). Mitochondrial uncoupling protein 2 expression in colon cancer and its clinical significance. *World J. Gastroenterol.* 16, 5773–5778. doi: 10.3748/wjg.v16.i45.5773

Kuo, S. S., Saad, A. H., Koong, A. C., Hahn, G. M., and Giaccia, A. J. (1993). Potassium-channel activation in response to low doses of gamma-irradiation involves reactive oxygen intermediates in nonexcitatory cells. *Proc. Natl. Acad. Sci. U.S.A.* 90, 908–912. doi: 10.1073/pnas.90.3.908

Langenbacher, M., Abdel-Jalil, R. J., Voelter, W., Weinmann, M., and Huber, S. M. (2013). *In vitro* hypoxic cytotoxicity and hypoxic radiosensitization. Efficacy of the novel 2-nitroimidazole N, N, N-tris[2-(2-nitro-1H-imidazol-1-yl)ethyl]amine. *Strahlenther. Onkol.* 189, 246–254. doi: 10.1007/s00066-012-0273-2

Le Pechoux, C., Laplanche, A., Faivre-Finn, C., Ciuleanu, T., Wanders, R., Lerouge, D., et al. (2011). Clinical neurological outcome and quality of life among patients with limited small-cell cancer treated with two different doses of prophylactic cranial irradiation in the intergroup phase III trial (PCI99-01, EORTC 22003-08004, RTOG (0212). and IFCT 99-01). *Ann. Oncol.* 22, 1154–1163. doi: 10.1093/annonc/mdq576

Leiprecht, N., Munoz, C., Alesutan, I., Siraskar, G., Sopjani, M., Foller, M., et al. (2011). Regulation of Na(+)-coupled glucose carrier SGLT1 by human papillomavirus 18 E6 protein. *Biochem. Biophys. Res. Commun.* 404, 695–700. doi: 10.1016/j.bbrc.2010.12.044

Li, C., and Jackson, R. M. (2002). Reactive species mechanisms of cellular hypoxia-reoxygenation injury. *Am. J. Physiol. Cell Physiol.* 282, C227–241. doi: 10.1152/ajpcell.00112.2001

Liu, X., Chang, Y., Reinhart, P. H., Sontheimer, H., and Chang, Y. (2002). Cloning and characterization of glioma BK, a novel BK channel isoform highly expressed in human glioma cells. *J. Neurosci.* 22, 1840–1849.

Lobikin, M., Chernet, B., Lobo, D., and Levin, M. (2012). Resting potential, oncogene-induced tumorigenesis, and metastasis: the bioelectric basis of cancer *in vivo*. *Phys. Biol.* 9, 065002. doi: 10.1088/1478-3975/9/6/065002

Lu, Z., and Sack, M. N. (2008). ATF-1 is a hypoxia-responsive transcriptional activator of skeletal muscle mitochondrial-uncoupling protein 3. *J. Biol. Chem.* 283, 23410–23418. doi: 10.1074/jbc.M801236200

Lui, V. C., Lung, S. S., Pu, J. K., Hung, K. N., and Leung, G. K. (2010). Invasion of human glioma cells is regulated by multiple chloride channels including ClC-3. *Anticancer Res.* 30, 4515–4524.

Lutz, S. (2007). Palliative whole-brain radiotherapy fractionation: convenience versus cognition. *Cancer* 110, 2363–2365.

Lyons, S. A., O'neal, J., and Sontheimer, H. (2002). Chlorotoxin, a scorpion-derived peptide, specifically binds to gliomas and tumors of neuroectodermal origin. *Glia* 39, 162–173. doi: 10.1002/glia.10083

Maftei, C. A., Bayer, C., Shi, K., Astner, S. T., and Vaupel, P. (2011). Changes in the fraction of total hypoxia and hypoxia subtypes in human squamous cell carcinomas upon fractionated irradiation: evaluation using pattern recognition in microcirculatory supply units. *Radiother. Oncol.* 101, 209–216. doi: 10.1016/j.radonc.2011.05.023

Mailloux, R. J., Adjeitey, C. N., and Harper, M. E. (2010). Genipin-induced inhibition of uncoupling protein-2 sensitizes drug-resistant cancer cells to cytotoxic agents. *PLoS ONE* 5:e13289. doi: 10.1371/journal.pone.0013289

Mamelak, A. N., and Jacoby, D. B. (2007). Targeted delivery of antitumoral therapy to glioma and other malignancies with synthetic chlorotoxin (TM-601). *Expert Opin. Drug Deliv.* 4, 175–186. doi: 10.1517/17425247.4.2.175

Marks, L. B., and Dewhirst, M. (1991). Accelerated repopulation: friend or foe. Exploiting changes in tumor growth characteristics to improve the "efficiency" of radiotherapy. *Int. J. Radiat. Oncol. Biol. Phys.* 21, 1377–1383. doi: 10.1016/0360-301690301-J

Masumoto, K., Tsukimoto, M., and Kojima, S. (2013). Role of TRPM2 and TRPV1 cation channels in cellular responses to radiation-induced DNA damage. *Biochim. Biophys. Acta* 1830, 3382–3390. doi: 10.1016/j.bbagen.2013.02.020

Mccoy, E. S., Haas, B. R., and Sontheimer, H. (2010). Water permeability through aquaporin-4 is regulated by protein kinase C and becomes rate-limiting for glioma invasion. *Neuroscience* 168, 971–981. doi: 10.1016/j.neuroscience.2009.09.020

Mccoy, E., and Sontheimer, H. (2007). Expression and function of water channels (aquaporins) in migrating malignant astrocytes. *Glia* 55, 1034–1043. doi: 10.1002/glia.20524

Mcferrin, M. B., and Sontheimer, H. (2006). A role for ion channels in glioma cell invasion. *Neuron Glia Biol.* 2, 39–49. doi: 10.1017/S1740925X06000044

Mcleod, C. J., Aziz, A., Hoyt, R. F. Jr., Mccoy, J. P. Jr., and Sack, M. N. (2005). Uncoupling proteins 2 and 3 function in concert to augment tolerance to cardiac ischemia. *J. Biol. Chem.* 280, 33470–33476. doi: 10.1074/jbc.M505258200

Montana, V., and Sontheimer, H. (2011). Bradykinin promotes the chemotactic invasion of primary brain tumors. *J. Neurosci.* 31, 4858–4867. doi: 10.1523/JNEUROSCI.3825-10.2011

Muller, A. C., Eckert, F., Heinrich, V., Bamberg, M., Brucker, S., and Hehr, T. (2011). Re-surgery and chest wall re-irradiation for recurrent breast cancer: a second curative approach. *BMC Cancer* 11:197. doi: 10.1186/1471-2407-11-197

Muller, A. C., Gani, C., Weinmann, M., Mayer, F., Sipos, B., Bamberg, M., et al. (2012). Limited disease of extra-pulmonary small cell carcinoma. Impact of local treatment and nodal status, role of cranial irradiation. *Strahlenther. Onkol.* 188, 269–273. doi: 10.1007/s00066-011-0045-4

Murata, M., Akao, M., O'rourke, B., and Marban, E. (2001). Mitochondrial ATP-sensitive potassium channels attenuate matrix Ca(2+) overload during simulated ischemia and reperfusion: possible mechanism of cardioprotection. *Circ. Res.* 89, 891–898. doi: 10.1161/hh2201.100205

Nalla, A. K., Asuthkar, S., Bhoopathi, P., Gujrati, M., Dinh, D. H., and Rao, J. S. (2010). Suppression of uPAR retards radiation-induced invasion and migration mediated by integrin beta1/FAK signaling in medulloblastoma. *PLoS ONE* 5:e13006. doi: 10.1371/journal.pone.0013006

Narita, T., Aoyama, H., Hirata, K., Onodera, S., Shiga, T., Kobayashi, H., et al. (2012). Reoxygenation of glioblastoma multiforme treated with fractionated radiotherapy concomitant with temozolomide: changes defined by 18F-fluoromisonidazole positron emission tomography: two case reports. *Jpn. J. Clin. Oncol.* 42, 120–123. doi: 10.1093/jjco/hyr181

Nelson, J. A., and Falk, R. E. (1993). The efficacy of phloridzin and phloretin on tumor cell growth. *Anticancer Res.* 13, 2287–2292.

Nguyen, L. N., and Ang, K. K. (2002). Radiotherapy for cancer of the head and neck: altered fractionation regimens. *Lancet Oncol.* 3, 693–701. doi: 10.1016/S1470-204500906-3

Niyazi, M., Siefert, A., Schwarz, S. B., Ganswindt, U., Kreth, F. W., Tonn, J. C., et al. (2011). Therapeutic options for recurrent malignant glioma. *Radiother. Oncol.* 98, 1–14. doi: 10.1016/j.radonc.2010.11.006

Ohshima, Y., Tsukimoto, M., Harada, H., and Kojima, S. (2012). Involvement of connexin43 hemichannel in ATP release after gamma-irradiation. *J. Radiat. Res.* 53, 551–557. doi: 10.1093/jrr/rrs014

Oleinika, K., Nibbs, R. J., Graham, G. J., and Fraser, A. R. (2013). Suppression, subversion and escape: the role of regulatory T cells in cancer progression. *Clin. Exp. Immunol.* 171, 36–45. doi: 10.1111/j.1365-2249.2012.04657.x

Olsen, M. L., Schade, S., Lyons, S. A., Amaral, M. D., and Sontheimer, H. (2003). Expression of voltage-gated chloride channels in human glioma cells. *J. Neurosci.* 23, 5572–5582.

Ozcan, C., Palmeri, M., Horvath, T. L., Russell, K. S., and Russell, R. R. (2013). Role of uncoupling protein 3 in ischemia-reperfusion injury, arrhythmias and preconditioning. *Am. J. Physiol. Heart Circ. Physiol.* 304, H1192–H1200. doi: 10.1152/ajpheart.00592.2012

Pajonk, F., Vlashi, E., and Mcbride, W. H. (2010). Radiation resistance of cancer stem cells: the 4 R's of radiobiology revisited. *Stem Cells* 28, 639–648. doi: 10.1002/stem.318

Palme, D., Misovic, M., Schmid, E., Klumpp, D., Salih, H. R., Rudner, J., et al. (2013). Kv3.4 potassium channel-mediated electrosignaling controls cell cycle and survival of irradiated leukemia cells. *Pflugers Archiv* 465, 1209–1221. doi 10.1007/s00424-013-1249-5

Pawlik, T. M., and Keyomarsi, K. (2004). Role of cell cycle in mediating sensitivity to radiotherapy. *Int. J. Radiat. Oncol. Biol. Phys.* 59, 928–942. doi: 10.1016/j.ijrobp.2004.03.005

Pfefferle, A., Mailloux, R. J., Adjeitey, C. N., and Harper, M. E. (2012). Glutathionylation of UCP2 sensitizes drug resistant leukemia cells to chemotherapeutics. *Biochim. Biophys. Acta* 1833, 80–89. doi: 10.1016/j.bbamcr.2012.10.006

Pickhard, A. C., Margraf, J., Knopf, A., Stark, T., Piontek, G., Beck, C., et al. (2011). Inhibition of radiation induced migration of human head and neck squamous cell carcinoma cells by blocking of EGF receptor pathways. *BMC Cancer* 11:388. doi: 10.1186/1471-2407-11-388

Pizzo, P., Drago, I., Filadi, R., and Pozzan, T. (2012). Mitochondrial Ca(2)(+) homeostasis: mechanism, role, and tissue specificities. *Pflugers Arch.* 464, 3–17. doi: 10.1007/s00424-012-1122-y

Pons, D. G., Sastre-Serra, J., Nadal-Serrano, M., Oliver, A., Garcia-Bonafe, M., Bover, I., et al. (2012). Initial activation status of the antioxidant response determines sensitivity to carboplatin/paclitaxel treatment of ovarian cancer. *Anticancer Res.* 32, 4723–4728.

Prasad, A., Stone, G. W., Holmes, D. R., and Gersh, B. (2009). Reperfusion injury, microvascular dysfunction, and cardioprotection: the "dark side" of reperfusion. *Circulation* 120, 2105–2112. doi: 10.1161/CIRCULATIONAHA.108.814640

Rades, D., Kieckebusch, S., Lohynska, R., Veninga, T., Stalpers, L. J., Dunst, J., et al. (2007a). Reduction of overall treatment time in patients irradiated for more than three brain metastases. *Int. J. Radiat. Oncol. Biol. Phys.* 69, 1509–1513.

Rades, D., Lohynska, R., Veninga, T., Stalpers, L. J., and Schild, S. E. (2007b). Evaluation of 2 whole-brain radiotherapy schedules and prognostic factors for brain metastases in breast cancer patients. *Cancer* 110, 2587–2592.

Ransom, C. B., Liu, X., and Sontheimer, H. (2002). BK channels in human glioma cells have enhanced calcium sensitivity. *Glia* 38, 281–291. doi: 10.1002/glia.10064

Ransom, C. B., and Sontheimer, H. (2001). BK channels in human glioma cells. *J. Neurophysiol.* 85, 790–803.

Rasola, A., and Bernardi, P. (2011). Mitochondrial permeability transition in Ca(2+)-dependent apoptosis and necrosis. *Cell Calcium* 50, 222–233. doi: 10.1016/j.ceca.2011.04.007

Rieken, S., Habermehl, D., Mohr, A., Wuerth, L., Lindel, K., Weber, K., et al. (2011). Targeting alphanubeta3 and alphanubeta5 inhibits photon-induced hypermigration of malignant glioma cells. *Radiat. Oncol.* 6, 132. doi: 10.1186/1748-717X-6-132

Robbins, D., and Zhao, Y. (2011). New aspects of mitochondrial uncoupling proteins (UCPs) and their roles in tumorigenesis. *Int. J. Mol. Sci.* 12, 5285–5293. doi: 10.3390/ijms12085285

Rodrigues, G., Zindler, J., Warner, A., and Lagerwaard, F. (2013). Recursive partitioning analysis for the prediction of stereotactic radiosurgery brain metastases lesion

control. *Oncologist* 18, 330–335. doi: 10.1634/theoncologist.2012-0316

Ruggieri, P., Mangino, G., Fioretti, B., Catacuzzeno, L., Puca, R., Ponti, D., et al. (2012). The inhibition of KCa3.1 channels activity reduces cell motility in glioblastoma derived cancer stem cells. *PLoS ONE* 7:e47825. doi: 10.1371/journal.pone.0047825

Sack, M. N. (2006). Mitochondrial depolarization and the role of uncoupling proteins in ischemia tolerance. *Cardiovasc. Res.* 72, 210–219. doi: 10.1016/j.cardiores.2006.07.010

Samudio, I., Fiegl, M., Mcqueen, T., Clise-Dwyer, K., and Andreeff, M. (2008). The warburg effect in leukemia-stroma cocultures is mediated by mitochondrial uncoupling associated with uncoupling protein 2 activation. *Cancer Res.* 68, 5198–5205. doi: 10.1158/0008-5472.CAN-08-0555

Santandreu, F. M., Valle, A., Fernandez De Mattos, S., Roca, P., and Oliver, J. (2009). Hydrogen peroxide regulates the mitochondrial content of uncoupling protein 5 in colon cancer cells. *Cell Physiol. Biochem.* 24, 379–390. doi: 10.1159/000257430

Sastre-Serra, J., Nadal-Serrano, M., Pons, D. G., Valle, A., Garau, I., Garcia-Bonafe, M., et al. (2013). The oxidative stress in breast tumors of postmenopausal women is ERalpha/ERbeta ratio dependent. *Free Radic. Biol. Med.* 61C, 11–17. doi: 10.1016/j.freeradbiomed.2013.03.005

Sauer, R., Liersch, T., Merkel, S., Fietkau, R., Hohenberger, W., Hess, C., et al. (2012). Preoperative versus postoperative chemoradiotherapy for locally advanced rectal cancer: results of the German CAO/ARO/AIO-94 randomized phase III trial after a median follow-up of 11 years. *J. Clin. Oncol.* 30, 1926–1933. doi: 10.1200/JCO.2011.40.1836

Schwab, A., Fabian, A., Hanley, P. J., and Stock, C. (2012). Role of ion channels and transporters in cell migration. *Physiol. Rev.* 92, 1865–1913. doi: 10.1152/physrev.00018.2011.

Schwab, A., Nechyporuk-Zloy, V., Fabian, A., and Stock, C. (2007). Cells move when ions and water flow. *Pflugers Arch.* 453, 421–432. doi: 10.1007/s00424-006-0138-6

Sciaccaluga, M., Fioretti, B., Catacuzzeno, L., Pagani, F., Bertollini, C., Rosito, M., et al. (2010). CXCL12-induced glioblastoma cell migration requires intermediate conductance Ca2+-activated K+ channel activity. *Am. J. Physiol. Cell Physiol.* 299, C175–C184. doi: 10.1152/ajpcell.00344.2009

Shields, J. D., Kourtis, I. C., Tomei, A. A., Roberts, J. M., and Swartz, M. A. (2010). Induction of lymphoidlike stroma and immune escape by tumors that express the chemokine CCL21. *Science* 328, 749–752. doi: 10.1126/science.1185837

Singh, H., Stefani, E., and Toro, L. (2012). Intracellular BK(Ca) (iBK(Ca)) channels. *J. Physiol.* 590, 5937–5947. doi: 10.1113/jphysiol.2011.215533

Skulachev, V. P. (1998). Uncoupling: new approaches to an old problem of bioenergetics. *Biochim. Biophys. Acta* 1363, 100–124. doi: 10.1016/S0005-272800091-1

Sofia Vala, I., Martins, L. R., Imaizumi, N., Nunes, R. J., Rino, J., Kuonen, F., et al. (2010). Low doses of ionizing radiation promote tumor growth and metastasis by enhancing angiogenesis. *PLoS ONE* 5:e11222. doi: 10.1371/journal.pone.0011222

Sontheimer, H. (2008). An unexpected role for ion channels in brain tumor metastasis. *Exp. Biol. Med. (Maywood)* 233, 779–791. doi: 10.3181/0711-MR-308

Sreekumar, A., Nyati, M. K., Varambally, S., Barrette, T. R., Ghosh, D., Lawrence, T. S., et al. (2001). Profiling of cancer cells using protein microarrays: discovery of novel radiation-regulated proteins. *Cancer Res.* 61, 7585–7593.

Steinle, M., Palme, D., Misovic, M., Rudner, J., Dittmann, K., Lukowski, R., et al. (2011). Ionizing radiation induces migration of glioblastoma cells by activating BK K(+) channels. *Radiother. Oncol.* 101, 122–126. doi: 10.1016/j.radonc.2011.05.069

Stock, C., and Schwab, A. (2009). Protons make tumor cells move like clockwork. *Pflugers Arch.* 458, 981–992. doi: 10.1007/s00424-009-0677-8

Stupp, R., Van Den Bent, M. J., and Hegi, M. E. (2005). Optimal role of temozolomide in the treatment of malignant gliomas. *Curr. Neurol. Neurosci. Rep.* 5, 198–206. doi: 10.1007/s11910-005-0047-7

Su, W. P., Lo, Y. C., Yan, J. J., Liao, I. C., Tsai, P. J., Wang, H. C., et al. (2012). Mitochondrial uncoupling protein 2 regulates the effects of paclitaxel on Stat3 activation and cellular survival in lung cancer cells. *Carcinogenesis* 33, 2065–2075. doi: 10.1093/carcin/bgs253

Szabo, I., Leanza, L., Gulbins, E., and Zoratti, M. (2012). Physiology of potassium channels in the inner membrane of mitochondria. *Pflugers Arch.* 463, 231–246. doi: 10.1007/s00424-011-1058-7

Talbot, D. A., and Brand, M. D. (2005). Uncoupling protein 3 protects aconitase against inactivation in isolated skeletal muscle mitochondria. *Biochim. Biophys. Acta* 1709, 150–156.

Tanchot, C., Terme, M., Pere, H., Tran, T., Benhamouda, N., Strioga, M., et al. (2013). Tumor-infiltrating regulatory T cells: phenotype, role, mechanism of expansion in situ and clinical significance. *Cancer Microenviron.* 6, 147–157. doi: 10.1007/s12307-012-0122-y

Teng, M. W., Swann, J. B., Koebel, C. M., Schreiber, R. D., and Smyth, M. J. (2008). Immune-mediated dormancy: an equilibrium with cancer. *J. Leukoc. Biol.* 84, 988–993. doi: 10.1189/jlb.1107774

Tolon, R. M., Sanchez-Franco, F., Lopez Fernandez, J., Lorenzo, M. J., Vazquez, G. F., and Cacicedo, L. (1996). Regulation of somatostatin gene expression by veratridine-induced depolarization in cultured fetal cerebrocortical cells. *Brain Res. Mol. Brain Res.* 35, 103–110. doi: 10.1016/0169-328X(95)00188-X

Vanan, I., Dong, Z., Tosti, E., Warshaw, G., Symons, M., and Ruggieri, R. (2012). Role of a DNA damage checkpoint pathway in ionizing radiation-induced glioblastoma cell migration and invasion. *Cell Mol. Neurobiol.* doi: 10.1007/s10571–012-9846-y

Veiseh, M., Gabikian, P., Bahrami, S. B., Veiseh, O., Zhang, M., Hackman, R. C., et al. (2007). Tumor paint: a chlorotoxin:Cy5.5 bioconjugate for intraoperative visualization of cancer foci. *Cancer Res.* 67, 6882–6888. doi: 10.1158/0008-5472.CAN-06-3948

Verheij, M. (2008). Clinical biomarkers and imaging for radiotherapy-induced cell death. *Cancer Metastasis Rev.* 27, 471–480. doi: 10.1007/s10555-008-9131-1

Vianello, F., Papeta, N., Chen, T., Kraft, P., White, N., Hart, W. K., et al. (2006). Murine B16 melanomas expressing high levels of the chemokine stromal-derived factor-1/CXCL12 induce tumor-specific T cell chemorepulsion and escape from immune control. *J. Immunol.* 176, 2902–2914.

Vidal-Puig, A. J., Grujic, D., Zhang, C. Y., Hagen, T., Boss, O., Ido, Y., et al. (2000). Energy metabolism in uncoupling protein 3 gene knockout mice. *J. Biol. Chem.* 275, 16258–16266. doi: 10.1074/jbc.M910179199

Voehringer, D. W., Hirschberg, D. L., Xiao, J., Lu, Q., Roederer, M., Lock, C. B., et al. (2000). Gene microarray identification of redox and mitochondrial elements that control resistance or sensitivity to apoptosis. *Proc. Natl. Acad. Sci. U.S.A.* 97, 2680–2685. doi: 10.1073/pnas.97.6.2680

Watanabe, H., Bohensky, J., Freeman, T., Srinivas, V., and Shapiro, I. M. (2008). Hypoxic induction of UCP3 in the growth plate: UCP3 suppresses chondrocyte autophagy. *J. Cell Physiol.* 216, 419–425. doi: 10.1002/jcp.21408

Watkins, S., and Sontheimer, H. (2011). Hydrodynamic cellular volume changes enable glioma cell invasion. *J. Neurosci.* 31, 17250–17259. doi: 10.1523/JNEUROSCI.3938-11.2011

Weaver, A. K., Bomben, V. C., and Sontheimer, H. (2006). Expression and function of calcium-activated potassium channels in human glioma cells. *Glia* 54, 223–233. doi: 10.1002/glia.20364

Weber, D. C., Casanova, N., Zilli, T., Buchegger, F., Rouzaud, M., Nouet, P., et al. (2009). Recurrence pattern after [(18)F]fluoroethyltyrosine-positron emission tomography-guided radiotherapy for high-grade glioma: a prospective study. *Radiother. Oncol.* 93, 586–592. doi: 10.1016/j.radonc.2009.08.043

Weihua, Z., Tsan, R., Huang, W. C., Wu, Q., Chiu, C. H., Fidler, I. J., et al. (2008). Survival of cancer cells is maintained by EGFR independent of its kinase activity. *Cancer Cell* 13, 385–393. doi: 10.1016/j.ccr.2008.03.015

Wick, W., Wick, A., Schulz, J. B., Dichgans, J., Rodemann, H. P., and Weller, M. (2002). Prevention of irradiation-induced glioma cell invasion by temozolomide involves caspase 3 activity and cleavage of focal adhesion kinase. *Cancer Res.* 62, 1915–1919.

Wild-Bode, C., Weller, M., Rimner, A., Dichgans, J., and Wick, W. (2001). Sublethal irradiation promotes migration and invasiveness of glioma cells: implications for radiotherapy of human glioblastoma. *Cancer Res.* 61, 2744–2750.

Withers, H. R. (Ed). (1975). "The four R's of radiotherapy," in *Advances in Radiation Biology,* Vol. 5, ed J. T. A. H. Lett (New York, NY: Academic Press).

Wright, E. M., Loo, D. D., and Hirayama, B. A. (2011). Biology of human sodium glucose transporters. *Physiol. Rev.* 91, 733–794. doi: 10.1152/physrev.00055.2009

Wulff, H., and Castle, N. A. (2010). Therapeutic potential of KCa3.1 blockers: recent advances and promising trends. *Expert Rev. Clin. Pharmacol.* 3, 385–396. doi: 10.1586/ecp.10.11

Yellon, D. M., and Hausenloy, D. J. (2007). Myocardial reperfusion injury. *N. Engl. J. Med.* 357, 1121–1135. doi: 10.1056/NEJMra071667

Yu, L. C., Huang, C. Y., Kuo, W. T., Sayer, H., Turner, J. R., and Buret, A. G. (2008). SGLT-1-mediated glucose uptake protects human intestinal epithelial cells against Giardia duodenalis-induced apoptosis. *Int. J. Parasitol.* 38, 923–934. doi: 10.1016/j.ijpara.2007.12.004

Zhao, J., Du, C. Z., Sun, Y. S., and Gu, J. (2012). Patterns and prognosis of locally recurrent rectal cancer following multidisciplinary treatment. *World J. Gastroenterol.* 18, 7015–7020. doi: 10.3748/wjg.v18.i47.7015

Zhau, H. E., He, H., Wang, C. Y., Zayzafoon, M., Morrissey, C., Vessella, R. L., et al. (2011). Human prostate cancer harbors the stem cell properties of bone marrow mesenchymal stem cells. *Clin. Cancer Res.* 17, 2159–2169. doi: 10.1158/1078-0432.CCR-10-2523

Zhou, Y. C., Liu, J. Y., Li, J., Zhang, J., Xu, Y. Q., Zhang, H. W., et al. (2011). Ionizing radiation promotes migration and invasion of cancer cells through transforming growth factor-beta-mediated epithelial-mesenchymal transition. *Int. J. Radiat. Oncol. Biol. Phys.* 81, 1530–1537. doi: 10.1016/j.ijrobp.2011.06.1956

Conflict of Interest Statement: The authors declare that the research was conducted in the absence of any commercial or financial relationships that could be construed as a potential conflict of interest.

Received: 30 April 2013; paper pending published: 28 May 2013; accepted: 24 July 2013; published online: 14 August 2013.

*Citation: Huber SM, Butz L, Stegen B, Klumpp D, Braun N, Ruth P and Eckert F (2013) Ionizing radiation, ion transports, and radioresistance of cancer cells. Front. Physiol. **4**:212. doi: 10.3389/fphys.2013.00212*

This article was submitted to Frontiers in Membrane Physiology and Membrane Biophysics, a specialty of Frontiers in Physiology.

Pflugers Arch - Eur J Physiol (2013) 465:1209–1221
DOI 10.1007/s00424-013-1249-5

SIGNALING AND CELL PHYSIOLOGY

Kv3.4 potassium channel-mediated electrosignaling controls cell cycle and survival of irradiated leukemia cells

Daniela Palme · Milan Misovic · Evi Schmid · Dominik Klumpp · Helmut R. Salih · Justine Rudner · Stephan M. Huber

Received: 16 October 2012 / Revised: 29 January 2013 / Accepted: 8 February 2013 / Published online: 27 February 2013

Abstract Aberrant ion channel expression in the plasma membrane is characteristic for many tumor entities and has been attributed to neoplastic transformation, tumor progression, metastasis, and therapy resistance. The present study aimed to define the function of these "oncogenic" channels for radioresistance of leukemia cells. Chronic myeloid leukemia cells were irradiated (0–6 Gy X ray), ion channel expression and activity, Ca^{2+}- and protein signaling, cell cycle progression, and cell survival were assessed by quantitative reverse transcriptase-polymerase chain reaction, patch-clamp recording, fura-2 Ca^{2+}-imaging, immunoblotting, flow cytometry, and clonogenic survival assays, respectively. Ionizing radiation-induced G_2/M arrest was preceded by activation of K_v3.4-like voltage-gated potassium channels. Channel activation in turn resulted in enhanced Ca^{2+} entry and subsequent activation of Ca^{2+}/calmodulin-dependent kinase-II, and inactivation of the phosphatase cdc25B and the cyclin-dependent kinase cdc2. Accordingly, channel inhibition by tetraethylammonium and blood-depressing substance-1 and substance-2 or downregulation by RNA interference led to release from radiation-induced G_2/M arrest, increased apoptosis, and decreased clonogenic survival. Together, these findings indicate the functional significance of voltage-gated K^+ channels for the radioresistance of myeloid leukemia cells.

Keywords K562 human erythroid leukemia cells · Primary chronic myeloid leukemia cells · Patch-clamp whole-cell recording · Ion channels · Calcium signaling · Cell cycle

D. Palme · M. Misovic · D. Klumpp · J. Rudner · S. M. Huber (✉)
Department of Radiation Oncology, University of Tübingen,
Hoppe-Seyler-Str. 3,
72076 Tübingen, Germany
e-mail: stephan.huber@uni-tuebingen.de

E. Schmid
Department of Physiology, University of Tübingen,
Tübingen, Germany

H. R. Salih
Department of Hematology/Oncology, University of Tübingen,
Tübingen, Germany

Present Address:
J. Rudner
Institute of Cell Biology, University Hospital Essen,
Essen, Germany

Introduction

Cell cycle progression of proliferating cells requires Ca^{2+} signals to enter and accomplish the S and the M phase of the cycle [58, 60]. Fast-proliferating tumor cells have been postulated to remodel their Ca^{2+} signalosome. For instance, many tumor entities such as prostate cancer [34], breast cancer [9], and primary chronic myeloid leukemia (CML) [53] upregulate TRPV5/6 Ca^{2+}-permeable channels. In addition, many tumor entities are endowed with K^+ channels that are different from those of normal cells [30]. K^+ channel-mediated changes of the membrane potential directly participate in the generation of cytosolic Ca^{2+} signals by modulating the activity of voltage-dependent Ca^{2+} entry pathways and/or altering the electrochemical driving force for both, Ca^{2+} entry through channels, and Ca^{2+} extrusion via Na/Ca antiport. Among those "oncogenic" K^+ channels [24] that are upregulated by tumor cells are human ether-à-gogo-related (hERG) [3] and further voltage-gated K_v channels [22, 46], or two-pore domain K^+ channels such as TASK-3 [33, 47] and TREK-1 [62]. In particular, hERG

channels are reportedly overexpressed in leukemias where they promote cell proliferation [36, 49, 50, 55].

Previously, we reported that survival of erythroleukemic K562 cells treated with ionizing radiation (IR) critically depends on Ca^{2+} signaling [39]. Specifically, IR stimulates Ca^{2+}-entry through TRPV5/6-like channels and subsequent activation of Ca^{2+}/calmodulin-dependent kinase-II (CaMKII), which in turn fosters G_1/S transition, S progression, and accumulation in G_2 phase of the cell cycle, resulting in an increased survival of these leukemia cells [21]. Besides TRPV5/6, IR reportedly activates K^+ channels in A549 lung adenocarcinoma cells [25, 31] and in glioblastoma cell lines [59]. IR-induced K^+ channel activity has been proposed to contribute to the stress response in these tumor cells by improving energy supply [25] or inducing stress evasion [59]. The present study, therefore, tested for an involvement of K^+ channels in the stress response of irradiated leukemia cells. To this end, K562 cells which were originally isolated from a patient with CML [39] and primary CML cells were subjected to ionizing radiation. Afterward, K^+ channel activity, Ca^{2+}- and biochemical signaling, cell cycle control, and cell survival were analyzed by whole-cell patch clamp recording, ratiometric Ca^{2+} imaging and immunoblotting, flow cytometry, and colony-forming assays, respectively. Our data suggest that ionizing radiation activates $K_v3.4$ voltage-gated K_v channels, which in turn, via activation of CaMKII isoforms, leads to inactivation of cdc25B and consequently to inactivation of the mitosis-promoting factor, resulting in G_2/M cell cycle arrest. Inhibition or experimental downregulation of $K_v3.4$ overrides G_2/M cell cycle arrest and decreases the survival of the leukemia cells.

Materials and methods

Cell culture Primary CML cells from patients were isolated by density gradient centrifugation after obtaining informed consent in accordance with the Helsinki protocol, and the study was performed according to the guidelines of the local ethics committee. Primary CML cells and K562 human erythroleukemia cells were cultivated in RPMI 1640 medium containing L-glutamine (Gibco, Karlsruhe, Germany) supplemented with 10 % fetal calf serum (FCS) and penicillin (100 U/ml)/streptomycin (100 μg/ml). Ionizing X-ray radiation (IR, single dose of 1–6 Gy) was applied by using a linear accelerator (LINAC SL25 Philips) at a dose rate of 4 Gy/min at room temperature. Following irradiation, cells were post-incubated in supplemented RPMI 1640 medium for 1–48 h (patch-clamp, fura-2 Ca^{2+}-imaging, flow cytometry) and 2 weeks (colony formation).

Patch-clamp recording K562, K562 cells transfected with $K_v3.4$ siRNA or nontargeting RNA (1 μM each, 48–72 h after transfection, see below), and primary CML cells were irradiated with 0, 1, or 5 Gy. Whole-cell currents were evoked by 11–33 voltage pulses (700 ms each) from −50 mV holding potential (−65 and −52 mV after correcting the liquid junction potential in NaCl and Na-D-gluconate bath solution, respectively) to voltages between −100 mV (−115 and −102 mV, respectively) and +60 mV (+45 mV), +80 mV (+78 mV), or +100 mV (+85 mV) delivered in 5–20-mV increments. Peak current values were analyzed 1–5 h post-IR. The liquid junction potentials between the pipette and the bath solutions were estimated according to Barry and Lynch [5], and data were corrected for the estimated liquid junction potentials. Membrane potential was recorded in the whole-cell 0 pA current-clamp mode. Cells were superfused at 37 °C temperature with NaCl solution (in millimolars—125 NaCl, 32 *N*-2-hydroxyethylpiperazine-*N*-2-ethanesulfonic acid (HEPES), 5 KCl, 5 D-glucose, 1 $MgCl_2$, 1 $CaCl_2$, titrated with NaOH to pH 7.4). Upon GΩ-seal formation and entry into the whole-cell recording mode, cells were recorded with NaCl bath solution, KCl bath solution (in millimolars—130 KCl, 32 HEPES, 5 D-glucose, 1 $MgCl_2$, 1 $CaCl_2$, titrated with KOH to pH 7.4), or Na-D-gluconate bath solution (in millimolars—150 Na-D-gluconate, 10 HEPES, 1 Ca-D-gluconate$_2$, titrated with NaOH to pH 7.4). The K-D-gluconate pipette solution contained (in millimolars)—140 K-D-gluconate, 5 HEPES, 5 $MgCl_2$, 1 K_2-EGTA, 1 K_2-ATP, titrated with KOH to pH 7.4. To inhibit Kv3.4 currents, blood-depressing substance 2 (BDS-II, Sigma, Taufkirchen, Germany) was added at a concentration of 2 μM to the NaCl bath solution.

Quantitative RT-PCR Messenger RNAs of irradiated K562 cells (0 and 5 Gy, 2 h post-IR) were isolated (Qiagen RNA extraction kit, Hilden, Germany) and reversely transcribed in cDNA (RT^2 First Strand Kit, SABiosciences, Qiagen). K^+ channel-specific fragments were amplified by the use of a polymerase chain reaction (PCR) array (SABiosciences #PAHS-036F, Qiagen, Hilden, Germany) and a Roche Light Cycler 480. C_t (threshold cycle) values of the PCR amplifications were normalized to that of a housekeeper.

Western blotting Irradiated K562 and primary CML cells (0 and 5 Gy, 2–6 h post-IR) were lysed in a buffer (containing in millimolars—50 HEPES pH 7.5, 150 NaCl, 1 EDTA, 10 sodium pyrophosphate, 10 NaF, 2 Na_3VO_4, 1 phenylmethylsulfonylfluorid additionally containing 1 % triton X-100, 5 μg/ml aprotinin, 5 μg/ml leupeptin, and 3 μg/ml pepstatin) and separated by sodium dodecyl sulfate-polyacrylamide gel electrophoresis (SDS-PAGE) under reducing condition. In some experiments, cells were pre-incubated (0.5 h), irradiated, and post-incubated (6 h) in the presence of the K_v channel inhibitor tetraethylammonium (TEA, 0 or 3 mM) or the CaMKII inhibitor KN-93 (0 or 30 μM).

Surface proteins of irradiated (0 and 5 Gy, 2 h post-IR) K562 cells were enriched by the use of a cell surface protein isolation kit (Pierce, Rockford, IL, USA) according to the supplied protocol and separated by SDS-PAGE under reducing condition. Segregated proteins were electro-transferred onto PVDF membranes (Roth, Karlsruhe, Germany). Blots were blocked in TBS buffer containing 0.05 % Tween 20 and 5 % non-fat dry milk for 1 h at room temperature. The membrane was incubated overnight at 4°C with the following primary antibodies: rabbit anti-phospho-CaMKII (Thr286) antibody (Cell Signaling #3361, New England Biolabs, Frankfurt, Germany, 1:1,000), rabbit anti-CaMKII (pan) antibody (Cell Signaling #3362, 1:1,000), rabbit anti-phospho-cdc25B (Ser187) antibody (Epitomics #T1162, Biomol Hamburg, Germany, 1:1,000), rabbit anti-cdc25B antibody (Cell Signaling #9525, 1:1,000), rabbit-anti $K_v3.4$ (Alomone, # APC-019, Jerusalem, Israel, 1:200), or rabbit anti-Na/K-ATPase (α1-subunit) antibody (cell signaling #3010, 1:1,000). Antibody binding was detected with a horseradish peroxidase-linked goat anti-rabbit or horse anti-mouse IgG antibody (Cell Signaling #7074 and #7076, respectively; 1:1,000–1:2,000 dilution in TBS–Tween/5% milk) incubated for 1 h at room temperature and enhanced chemiluminescence (ECL Western blotting analysis system, GE Healthcare/Amersham-Biosciences, Freiburg, Germany). Equal gel loading was verified by an antibody against β-actin (mouse anti-β-actin antibody, clone AC-74, Sigma #A2228 1:20,000). Where indicated, protein levels were quantified by densitometry using ImageJ software (ImageJ 1.40 g NIH, USA).

Fura-2 Ca^{2+} imaging Fluorescence measurements were performed using an inverted phase-contrast microscope (Axiovert 100; Zeiss, Oberkochen, Germany). Fluorescence was evoked by a filter wheel (Visitron Systems, Puchheim, Germany)-mediated alternative excitation at 340/26 or 387/11 nm (AHF, Analysentechnik, Tübingen, Germany). Excitation and emission light was deflected by a dichroic mirror (409/LP nm beamsplitter, AHF) into the objective (Fluar ×40/1.30 oil; Zeiss) and transmitted to the camera (Visitron Systems), respectively. Emitted fluorescence intensity was recorded at 587/35 nm (AHF). Excitation was controlled and data acquired by Metafluor computer software (Universal Imaging, Downingtown, PA, USA). The 340/380-nm fluorescence ratio was used as a measure of cytosolic free Ca^{2+} concentration ($[Ca^{2+}]_i$), the slope of the increase in the 340/380 nm-ratio as a measure of Ca^{2+} entry into the cells. The cells were irradiated (0 or 5 Gy) and loaded with fura-2/AM (2 μM for 30 min at 37 °C; Molecular Probes, Goettingen, Germany) in supplemented RPMI medium. $[Ca^{2+}]_i$ was determined 2–3 h post-IR at 37 °C during superfusion with NaCl solution, during extracellular Ca^{2+} removal in EGTA-buffered NaCl solution (in millimolars—125 NaCl, 32 HEPES, 5 KCl, 5 D-glucose, 1 $MgCl_2$, 0.5 EGTA, titrated with NaOH to pH 7.4), and Ca^{2+} re-addition in NaCl solution additionally containing TEA or, for control, NaCl (3 mM each).

Transfection with siRNA K562 cells were cultured at a low density to ensure log phase growth. For transfection, cells (3×10^6) were resuspended in 300 μl RPMI 1640 without phenol red. After adding siRNAs (1 μM), cells were electroporated at 340 V for 5 ms, using an EPI2500 electroporator (Fischer, Heidelberg, Germany). Immediately after transfection, cells were re-suspended in pre-warmed medium and continued to be cultured. Transfection efficiency and viability was determined by transfecting the cells with 400 nM green fluorescence siGLO siRNA followed by propidium iodide exclusion dye and flow cytometric analysis. $K_v3.4$ ON-TARGET SMARTpool, siCONTROL NON-TARGETING pool, and siGLO siRNA were purchased from Dharmacon (Chicago, IL, USA). Downregulation of $K_v3.4$ was controlled by immunoblotting (data not shown) and patch-clamp recording.

Flow cytometry K562 cells were pre-incubated (30 min), irradiated (0 or 5 Gy), and incubated for further 24 or 48 h in supplemented RPMI 1640 medium additionally containing either TEA or NaCl (3 mM each), or blood-depressing substance-1 (BDS-I) (0 or 5 μM, Sigma). In further experiments, K562 cells were irradiated (0 or 5 Gy) 24 h after transfection with either $K_v3.4$ or non-targeting siRNA and grown for 48 h in supplemented RPMI 1640 medium. For cell cycle analysis, cells were permeabilized and stained (30 min at room temperature) with propidium iodide (PI) solution (containing 0.1% Na-citrate, 0.1% triton X-100, 10 μg/ml PI in phosphate-buffered saline, PBS), and the DNA amount was analyzed by flow cytometry (FACS Calibur, Becton Dickinson, Heidelberg, Germany, 488 nm excitation wavelength) in fluorescence channel FL-3 (linear scale, >670 nm emission wavelength). In parallel, cells with degraded DNA were defined by the $subG_1$ population of the PI histogram recorded in fluorescence channel FL-2 (logarithmic scale, 564–606 nm emission wavelength). For determination of phosphatidylserine exposure (which results from break-down of the phospholipids asymmetry of the plasma membrane) and (secondary) necrosis, cells were resuspended in NaCl solution containing annexin V fluos (1:80 dilution; BD Biosciences, Heidelberg, Germany) and PI (10 μg/ml). After 30 min of staining, annexin-V binding and PI staining were measured by flow cytometry in fluorescence channels FL-1 (515–545 nm emission wavelength) and FL-3, respectively. Data were analyzed with the FCS Express 3 software (De Novo Software, Los Angeles, CA, USA).

BrdU incorporation To test for DNA synthesis/repair by bromodeoxyuridine (BrdU) incorporation, the cells were

resuspended in supplemented RPMI 1640 medium containing BrdU (20 μM) and TEA or NaCl (3 mM each), irradiated with 0 or 5 Gy, post-incubated for 8 h at 37 °C, washed, and fixed with 70% ethanol and consecutively treated with RNase A (0.1 mg/ml in PBS for 10 min at 37 °C), pepsin (0.5 mg/ml in 0.05 N HCl for 10 min at 37 °C), and 2 N HCl (for 10 min at room temperature). For immunolabelling, cells were incubated (30 min at room temperature) with a monoclonal mouse anti-BrdU antibody (1:67 dilution in PBS/1 % bovine serum albumin (BSA), Becton Dickinson, Pharmingen, Freiburg, Germany) and post-incubated (30 min at room temperature) with a fluoresceinisothiocyanat-conjugated rabbit anti-mouse IgG antibody (1:100 in PBS/1 % BSA, DAKO, Hamburg, Germany). Thereafter, cells were stained (15 min at 4 °C) with PI solution (25 μg/ml PI and 20 μg/ml RNAse A in PBS/1% BSA). BrdU- and PI-specific fluorescence was analyzed by flow cytometry in fluorescence channels FL-1 and FL-3, respectively.

Colony-formation assay To test for clonogenic survival, cultures of K562 cells were diluted to 100 or 200 cells/ml with supplemented RPMI 1640 medium additionally containing TEA (3 mM) or, for control, NaCl (3 mM), and seeded out in six-well plates (5 ml/well). In a second series of experiments, 100 cells were seeded in 96-well plates in 200 μl supplemented RPMI 1640 medium additionally containing BDS-I (0 or 5 μM) or BDS-II (0 or 5 μM). Thereafter, cells of both experimental series were irradiated (0–5 Gy) and grown for 2 weeks. In further experiments, K562 cells were seeded 48 h after transfection with either $K_v3.4$ or non-targeting siRNA in supplemented RPMI 1640 medium, irradiated (0–6 Gy), and grown for 2 weeks. K562 cells formed round colonies that adhered to the bottom. The plating efficiency was defined by dividing the number of colonies by the number of plated cells. Survival fraction was calculated by dividing the plating efficiency of the treated cells by that of the untreated controls.

Results

To test for IR-induced changes in ion channel activity, irradiated (0, 1, or 5 Gy) K562 cells were recorded with the patch-clamp technique in whole-cell mode using physiological intra- (i.e., pipette) and extracellular (i.e., bath) solutions. K562 cells exhibited a membrane potential of around −50 mV (Fig. 1a, b) which tended to hyperpolarize upon irradiation with 5 Gy (Fig. 1a, b). This slight hyperpolarization was accompanied by a change in whole-cell currents (Fig. 1c). In particular, IR (5 Gy) induced within 1–3 h an increase in outward current (Fig. 1c, *right*) that showed fast voltage-dependent activation (time constant $T\approx$ 1 ms at +25 mV), time-dependent inactivation at voltages more positive than 0 mV ($T\approx$40 ms at +25 mV). The IR-stimulated current fraction (ΔI, grey curve in Fig. 1d) was K^+-selective as deduced from a reversal potential of the current voltage relationship (*I/V* curve) that was close to K^+ equilibrium potential (E_K=−89 mV). Together, K^+-selectivity, voltage-dependent activation, and time-dependent inactivation (Fig. 1c, *right*) classify the IR-induced current as voltage-gated K_v current. The peak current densities (Fig. 1e, *left*) and peak current conductances (Fig. 1e, *right*) of individual control (0 Gy), 1 Gy-, and 5 Gy-irradiated K562 cells show the dependence of the K_v current on the IR dose. To closer define the gating behavior, an extended pulse protocol (Fig. 1f, insert) was applied to irradiated (5 Gy) K562 cells. From the recorded currents (Fig. 1f), the voltage-gated current fraction (I_{volt}, Fig. 1g) was isolated by subtracting the "non-gating," linear current fraction, and the normalized conductance ($G_{volt}/G_{volt\ max}$; Fig. 1h) was calculated. As shown for the mean curve in Fig. 1g, a half-maximal voltage of activation of $V_{1/2}$=−44±5 mV (n=5)

Fig. 1 IR stimulates voltage-gated (K_v) K^+ channels in K562 cells. **a**, **b** Membrane voltage of control (*black line* in **a** and *open circles* in **b**, n=12) and irradiated (5 Gy) K562 cells (1.7±0.2 h post-IR, *red line* in **a** and *closed triangles* in **b**, n=8) recorded in current-clamp mode with K-D-gluconate pipette combined with NaCl (**a**, **b**) and KCl bath solution (**a**). *Red marks* in **b** indicate the median voltages (p=0.06, two-tailed $t$test) **c** Current tracings from a control K562 cell (0 Gy, *first tracings*) and cells irradiated with 1 Gy (*second tracings*) or 5 Gy (*third tracings*). Records were obtained with K-D-gluconate pipette and Na-D-gluconate bath solution. The *insert* shows the holding potential and the applied voltage pulse protocol. Applied voltages refer to the cytoplasmic face of the membrane with respect to the extracellular space. In the current tracings, the individual current sweeps recorded at the different voltages are superimposed. Outward currents, defined as flow of positive charge (here: K^+) from the cytoplasmic to the extracellular membrane face, are positive currents and depicted as upward deflections of the original current tracings. The zero current value is indicated by the *red line*. **d** Relationships between mean peak current densities and voltage (±SE, n=9–26) of control (0 Gy) and irradiated K562 cells (5 Gy, 2.8±0.4 h post-IR) recorded as in (**c**, *first* and *third tracings*). The *grey curve* (ΔI) resulted from subtracting the mean current densities of the 0 Gy- from the 5 Gy-irradiated cells. **e** Densities of the peak outward current (*left*) and conductance (*right*) of control K562 cells (0 Gy, *open circles*) and cells irradiated with 1 Gy (*closed diamonds*) or 5 Gy (*closed triangles*). Peak currents were analyzed at 0 mV and conductances between −40 and 0 mV. Shown are individual cells (n=7–26) and the median value (*red line*) recorded as in **c** 3.2± 0.6 h and 2.8±0.4 h post-IR with 0 Gy and 5 Gy, respectively. *Asterisk* indicates significant difference ($p\leq$0.05), Kruskal–Wallis test (non-parametric ANOVA). **f** Relationships between mean normalized peak current and voltage (±SE, n=5) of irradiated K562 cells (5 Gy, 1.8±0.6 h post-IR) recorded with the indicated pulse protocol with K-D-gluconate in the pipette and NaCl in the bath. **g** Mean current voltage relationship of the voltage-gated-current fraction (±SE, n=5) isolated from the recordings shown in **f** by subtracting the linear current fraction. **h** Relationship between mean normalized conductance ($G_{volt}/G_{volt\ max}$, ±SE, n=5), and the voltage as calculated from the data in **g**. The Boltzmann fit of the mean normalized conductances is indicated by the *red line*, the half-maximal voltage of activation ($V_{1/2}$) by the *vertical blue line*

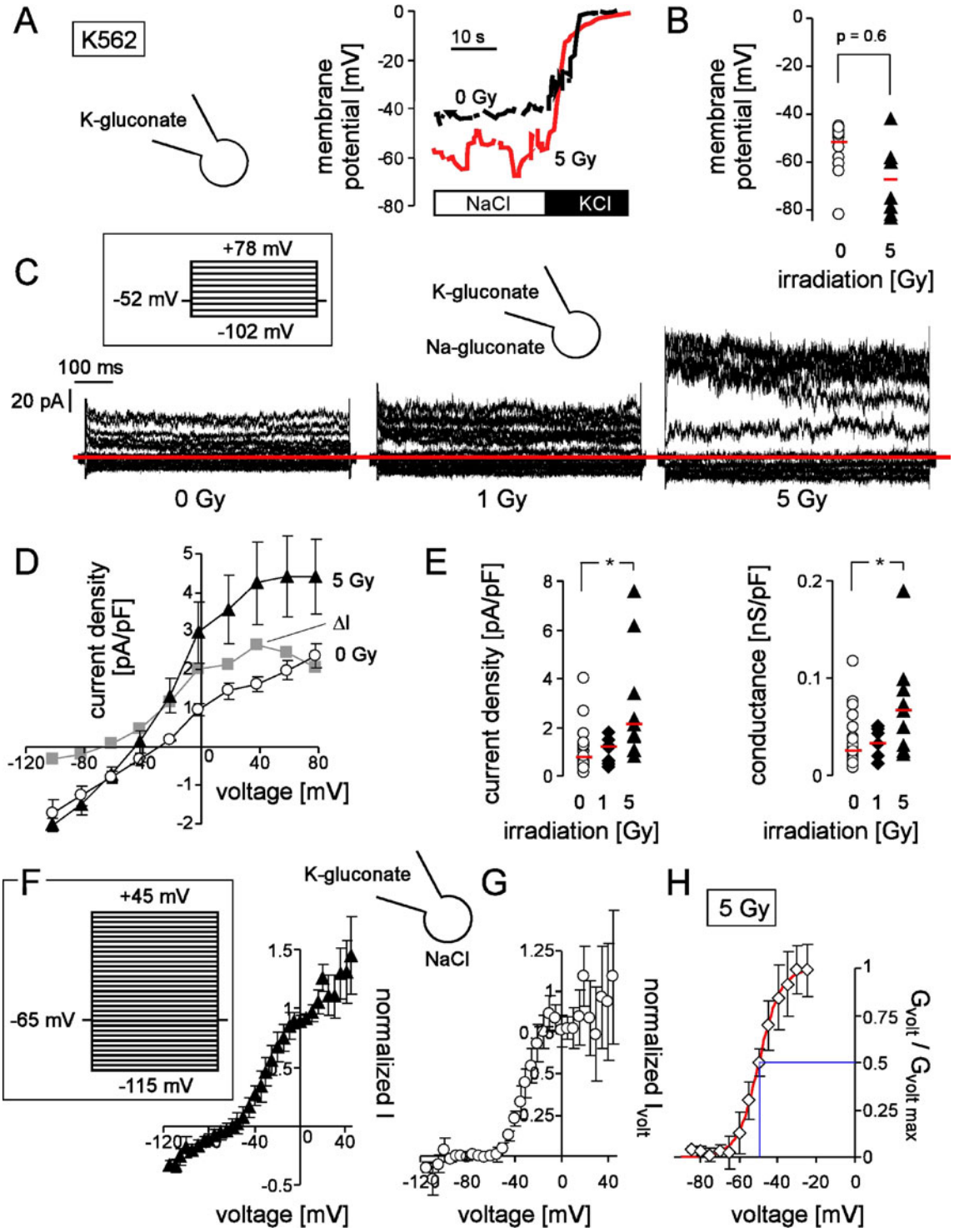

was deduced by fitting the individual normalized conductance voltage relationship with the Boltzmann equation.

To narrow down potential molecular correlates of the IR-induced K_v current, K^+ channel mRNA abundance of irradiated (0 and 5 Gy) K562 cells was analyzed 2 h post-IR by a quantitative reverse transcriptase-polymerase chain reaction (RT-PCR) micro-array. As shown in Fig. 2a, transcripts specific for KCNH2 (hERG), KCNN4 (KCa3.1), KCNC4 (K_v3.4), and KCNQ4 (K_vLQT4) could be identified. The latter two channel types have biophysical signatures similar to the IR-stimulated current of the present study. IR induced a decrease in hERG-, K_v3.4-, and K_vLQT4 mRNA abundance (compare open and closed bars in Fig. 2a). In addition to the mRNA, K_v3.4 protein could be detected in total cell

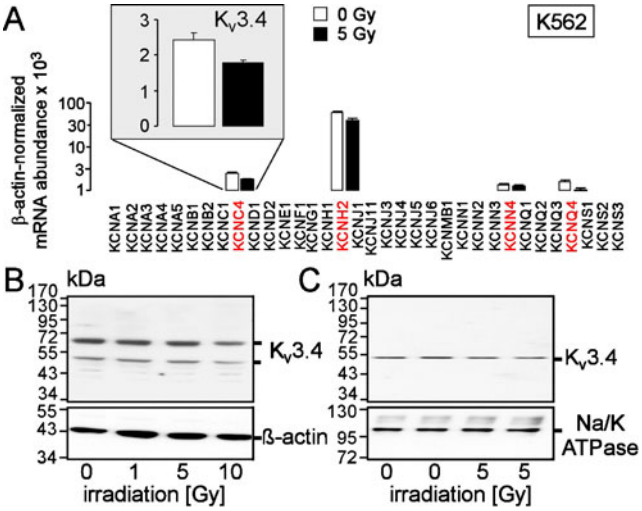

Fig. 2 IR does not affect $K_v3.4$ (KCNC4) mRNA protein or surface expression. **a** Mean housekeeper-normalized K^+ channel mRNA abundance (±SE, $n=3$) as determined in control (*open bars*) and irradiated K562 cells (2 h post-IR) by quantitative RT-PCR array. The *insert* shows the $K_v3.4$ (KCNC4) mRNA abundance in higher power. **b**, **c** Immunoblots of total lysates (**b**) and surface proteins (**c**) of control (0 Gy) and irradiated K562 cells (5 Gy, 2 h post-IR) probed against $K_v3.4$ (*upper blots*). For loading control, β-actin (**b**) and Na/K-ATPase α-subunit (**c**) immunoblots were performed

lysates (Fig. 2b) and in enriched surface proteins (Fig. 2c) by immunoblotting. Two $K_v3.4$ immunoreactive bands (50 and 70 kDa) were suggestive of Kv3.4 splice isoforms as previously described [63]. On the cell surface of K562 cells, only the 50 kDa protein was detectable (Fig. 2c). IR did not alter the abundance of $K_v3.4$-immunoreactive total (Fig. 2a) or surface protein (Fig. 2c). Together, these data suggest that the IR-stimulated K_v current did not result from a change in (surface) expression of the channels.

In order to estimate whether IR-induced K_v current activation is peculiar to the K562 leukemia model or a more general phenomenon, $K_v3.4$ protein abundance and function was analyzed in primary CML cells upon IR with 0 or 5 Gy. Primary CML cells exhibited $K_v3.4$ protein (70 kDa) expression, which was not altered 2 h post-IR (Fig. 3a). K_v channel activity, in contrast, was stimulated by IR within 1–3 h post-IR (Fig. 3b, c) suggesting that IR-induced K_v channel activation is a general phenomenon and not restricted to K562 cells. The K_v current fraction of primary CML cells activated very fast (time constants of $T=6\pm1$ ms, 3 ± 0.5 ms, 1 ± 0.3 s, and 0.6 ± 0.1 ms after stepping the voltage from −65 mV to −35, −15, +5, and +25 mV, respectively) with a $V_{1/2}$ for activation of -48 ± 2 mV ($n=5$, data not shown). Notably, K_v current inactivation in irradiated primary CML cells was faster ($T=13\pm7$ ms at 25 mV) than that in irradiated K562 cells (see above).

K^+ channels participate in the generation of cytosolic Ca^{2+} signals. The effect of IR-induced K^+ channel activity on Ca^{2+} entry was tested in K562 cells by Fura-2 Ca^{2+}-imaging. K^+ channels were inhibited by the K_v channel blocker tetraethylammonium (TEA, 3 mM), which exerts an inhibitory potency among the identified K^+ channels of $K_v3.4$ ($IC_{50}=0.3$ mM [52])>K_vLQT4 ($IC_{50}=3.0$ mM [20]) >>hERG1 ($IC_{50}=46$ mM [11]) and KCa3.1 ($Kd=30$ mM [38]). IR (5 Gy) stimulated the Ca^{2+} entry upon removal and re-addition of external Ca^{2+} (Fig. 4a). Importantly, TEA abolished the IR-induced Ca^{2+} entry (compare first and third bars in Fig. 4b). Surprisingly, TEA stimulated the Ca^{2+}-entry in unirradiated cells (compare first and second bars in Fig. 4b), a phenomenon which was not further studied.

Ca^{2+}/calmodulin-dependent kinase II (CaMKII) isoforms are reportedly activated in K562 cells by IR-stimulated Ca^{2+} signaling [21]. In the present study, K^+ channel blockade by TEA (3 mM) as well as the kinase inhibitor KN-93 (30 μM) alleviated IR (5 Gy)-induced CaMKII activation as evidenced by decreased auto-phosphorylation at Thr286 (Fig. 4c, d). Phosphorylation of the phosphatase cdc25B at Ser187 has been demonstrated to decrease cdc25 activity [10]. Since cdc25 isoforms are reported downstream targets of CaMKII (see "Discussion"), cdc25B phosphorylation at Ser187 was assessed in irradiated K562 cells. IR increased phosphorylation of cdc25B at Ser187 in a KN-93- and TEA-sensitive manner (Fig. 4e). Active cdc25B reportedly dephosphorylates and thereby activates cdc2, a subunit of the mitosis-promoting factor. In line with the observed KN-93 and TEA-mediated attenuation of the IR-mediated cdc25B inhibition, KN93 and TEA also decreased the IR-stimulated inhibitory phosphorylation of cdc2 at Tyr15 (Fig. 4f). Together, these data suggest that IR induces K^+-channel-regulated Ca^{2+} signals which inhibit the mitosis-promoting factor via activation of CaMKII isoforms and subsequent inactivation of cdc25B. Blockage of the voltage-gated K^+ channels and the CaMKII isoforms by TEA and KN-93, respectively, attenuates the IR-induced inhibition of the mitosis-promoting factor.

Next, the effect of voltage-gated K^+ channel inhibition on the cell cycle was studied in irradiated (0 and 5 Gy) K562 cells by flow cytometry. Within 48 h, IR (5 Gy) induced a redistribution of the cells from G_1 to G_2 phase of the cell cycle, which is indicative of an IR-induced accumulation in G_2/M arrest (Fig. 5, black histograms in A and open bars in B). In line with the observed K_v channel blocker-mediated disinhibition of the mitosis-promoting factor (Fig. 4f), TEA (3 mM) blunted the IR-induced accumulation in G_2 (Fig. 5, red histograms in A and closed bars in B). In theory, this TEA effect might be also a consequence of a putative TEA-mediated block of the previously reported [21] IR-stimulated G_1/S transition and S progression. To exclude this possibility, incorporation of the thymidine analogue bromodeoxyuridine (BrdU) was measured in irradiated (0 or 5 Gy) K562 cells. As shown in Fig. 6, TEA even promoted the G_1/S transition within the first 8 h post-IR.

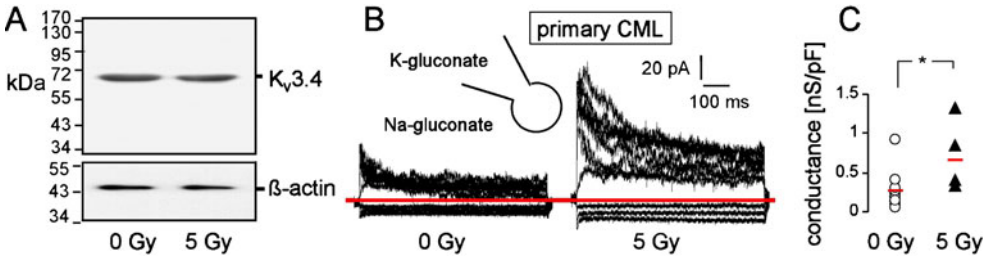

Fig. 3 Primary chronic myeloid leukemia (CML) cells express K_v3.4 protein and activate voltage-gated K^+ channels upon irradiation. **a** Immunoblots of total lysates from control (0 Gy) and irradiated CML cells (5 Gy, 2 h post-IR) probed against K_v3.4 (*top*) and for loading control against β-actin (*bottom*). **b** Current tracings from a control (0 Gy, *first tracings*) and an irradiated CML cell (5 Gy, *second tracings*). Records were obtained with K-D-gluconate pipette and Na-D-gluconate bath solution. **c** Conductance density of control (0 Gy, *open circles*) and irradiated CML cells (5 Gy, *closed triangles*). Conductances were calculated for the peak outward current between 0 and 40 mV voltage. Shown are individual cells (n=5–11) and the median value (*red line*) recorded as in **b** 1.8±0.2 h post-IR with 0 and 5 Gy. *Asterisk* indicates significant difference ($p \leq 0.05$), two-tailed t test

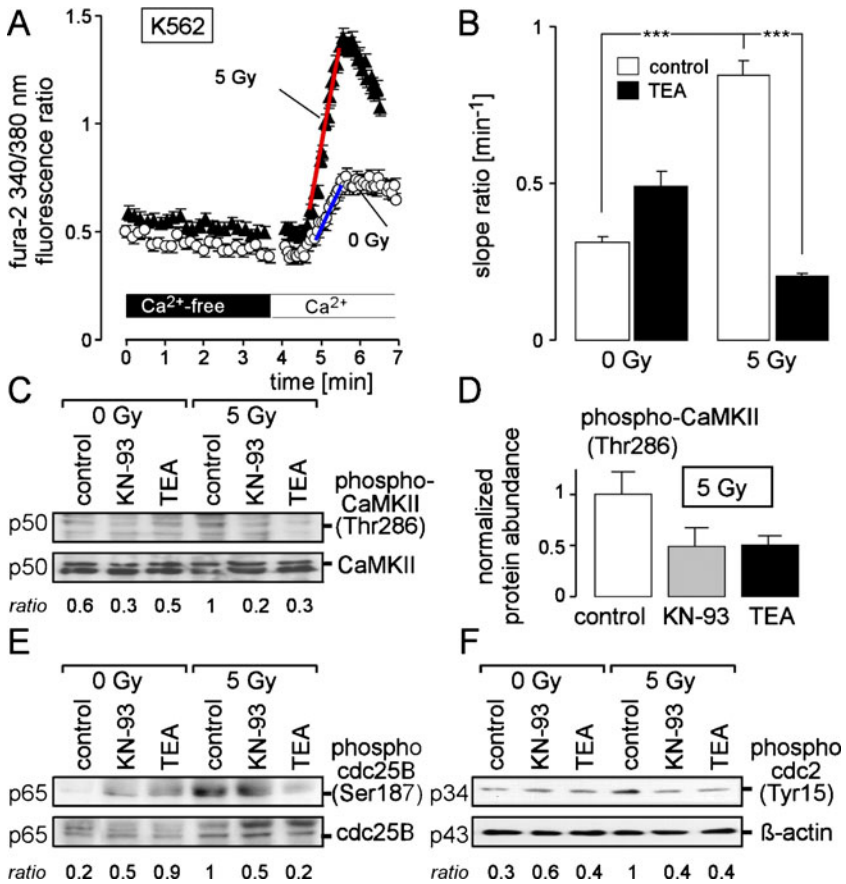

Fig. 4 K_v channels stimulate Ca^{2+} entry, CaMKII activity, cdc25B, and cdc2 phosphorylation in irradiated K562 cells. **a** Time course of the mean ratio between the 340 and the 380 nm excited fura-2 fluorescence as a measure of the cytosolic free Ca^{2+} concentration. Ratios were recorded 80 min post-irradiation with 0 Gy (*open circles*; n=25) or 5 Gy (*closed triangles* n=34) during removal and re-addition of external Ca^{2+}. **b** Mean slope of ratio increase upon Ca^{2+} re-addition. Slopes for the linear course of ratio increase upon Ca^{2+} re-addition (as indicated by *blue* and *red lines* in **a**) were calculated for K562 cells 1–3 post-irradiation with 0 and 5 Gy. Cells were irradiated and post-incubated in the absence (*open bars*) or presence (*closed bars*) of the K_v channel blocker tetraethylammonium (TEA, 3 mM). Given are means ±SE (n=102–378, *** indicates $p \leq 0.001$, ANOVA). **c** Immunoblots showing the abundance of phosphorylated (Thr286, *upper panel*) and total CaMKII isoforms (*lower panel*) of K562 lysed 6 h after irradiation with 0 and 5 Gy. Cells were irradiated and post-incubated in the absence or presence of the CaMKII inhibitor KN-93 (30 μM) or TEA (3 mM). **d** Mean (±SE, n=3 lysates) protein abundance of phospho-CaMKII (Thr286) analyzed and normalized to that of the 5 Gy-irradiated cells which were irradiated and post-incubated in the absence of KN-93 and TEA as in (**c**). **e**, **f** Immunoblots probed against phospho-cdc25B (Ser187), cdc25B, phospho-cdc2 (Tyr15), or ß-actin. Numbers (*ratio*) in (**c**, **e**, **f**) indicate the normalized ratio between the densitometry values of the *band in the upper* and *lower plot*

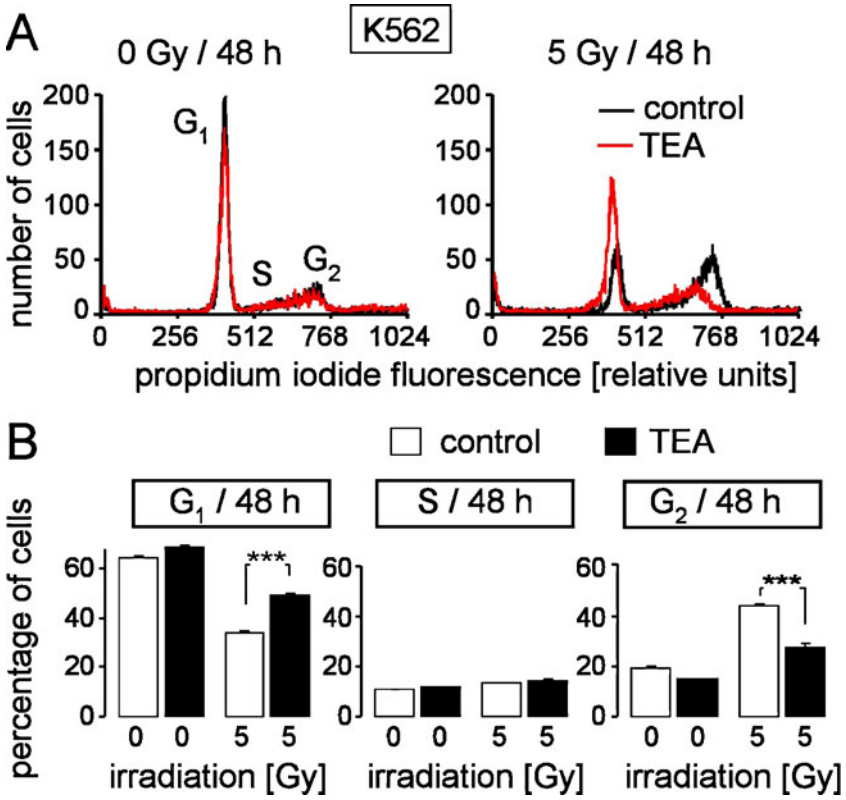

Fig. 5 Increase in K_v channel activity induces G_2/M arrest in irradiated K562 cells. **a** Histograms of propidium iodide-stained K562 cells (Nicoletti protocol) recorded by flow cytometry 48 h post-IR with 0 Gy (*left*) or 5 Gy (*right*). Cells were pre-incubated (0.5 h), irradiated, and post-incubated in the absence (control, *black line*) or presence of TEA (3 mM, *red line*). **b** Mean percentage (n=6) of 0 Gy (control, *first* and *second bars*) and 5 Gy- irradiated cells (*third* and *fourth bars*) residing in G_1 (*upper line*), S (*middle line*), or G_2 phase of cell cycle (*lower line*) recorded as in (**a**) 48 h post-IR. *** indicates $p \leq 0.001$, ANOVA

Together, these experiments suggest that inhibition of the K_v channels by TEA results in an override of the G_2/M arrest in irradiated cells.

Finally, the involvement of the K_v channels in survival of irradiated K562 cells was determined. To this end, breakdown of the phospholipid asymmetry across the plasma membrane and clonogenic survival of irradiated (0 or 5 Gy) K562 cells was assessed in the presence or absence of TEA by annexin V binding in flow cytometry and colony formation assays, respectively. TEA augmented the IR-induced breakdown of the phospholipid asymmetry (Fig. 7a, b) and decreased clonogenic survival of K562 cells (Fig. 7c), strongly suggesting that K_v channel targeting radiosensitizes K562 leukemia cells. Besides radiosensitization, TEA decreased the plating efficacy of unirradiated K562 cells (from 0.4 to 0.08) suggesting a cytotoxic effect of TEA also in unirradiated cells.

Since TEA inhibits also K_vLQT4 (albeit with much lower efficacy) and potentially also other yet unidentified K^+ channels in K562 cells, the effects of the more K_v3.4-specific inhibitors BDS-I and BDS-II [14, 65] were tested on radiation-induced whole-cell current, on cell cycle control, cell death, and clonogenic survival in irradiated (0 or 5 Gy) K562 cells. BDS-II (2 μM) inhibited in irradiated K562 cells a current fraction that resembled the irradiation-induced current (grey curve in Fig. 1d) in K^+ selectivity and voltage-dependent activation (Fig. 8a, b). Similar to TEA, BDS-I (5 μM) decreased the number of irradiated cells accumulating 48 h post-IR in the G_2 phase of cell cycle (Fig. 8c, right). In contrast to TEA, BDS-I significantly decreased and increased the number of unirradiated cells residing in the G_1 and S phase of cell cycle, respectively (Fig. 8c, left and middle). In addition, BDS-1 induced cell death which was more pronounced in irradiated cells (Fig. 8d). Moreover, BDS-1 and BDS-2 (5 μM) decreased the clonogenic survival of irradiated K562 cells (without decreasing the plating efficiencies). Together, the data indicate a radiosensitizing effect of the more specific K_v3.4 inhibitors BDS-I and BDS-II. Like TEA, BDS-I exhibited cytotoxicity also in unirradiated cells.

In a last series of experiments, K_v3.4 was downregulated in K562 cells by RNA interference, and whole-cell currents, cell cycle, cell death, and clonogenic survival were determined in irradiated (0 or 5 Gy) K562 cells. K_v3.4 silencing decreased whole-cell currents of irradiated cells (Fig. 9a, b). The downregulated current fraction (ΔI, grey curve in Fig. 9b) was similar to the radiation-stimulated current fraction (grey curve in Fig. 1d) and the BDS-II-sensitive current fraction of irradiated K562 cells (grey curve in Fig. 8b) suggesting Kv3.4 channels generated at significant part of the radiation-stimulated BDS-II-sensitive currents in K562 cells. Like TEA (Fig. 5) and BDS-I (Fig. 8c) treatment, K_v3.4 silencing increased the percentage of irradiated cells that accumulated in the G_2 phase of the cell cycle 48 h post-IR (Fig. 9c, d). Like TEA- (Fig. 7a, b) and BDS-I treatment (Fig. 8d), K_v3.4 silencing increased cell death in the irradiated cells as revealed by the higher number of cells with

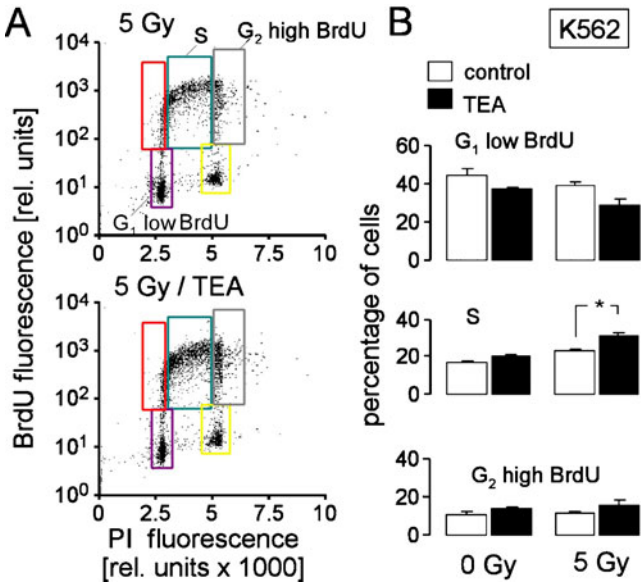

Fig. 6 Inhibition of K_v channels fosters radiation-induced G_1/S transition. **a** *Dot plots* showing the DNA-synthesis by bromdesoxyuridin (BrdU) incorporation and DNA amount by propidium iodide (PI) staining after incubation for 8 h in the absence (*top*) and presence of TEA (3 mM, *bottom*) following irradiation with 5 Gy. BrdU-positive cells in S-phase of cell cycle are outlined in *turquoise*, cells which reside in G_1 and G_2 and which did not accumulate BrdU (low BrdU) are outlined in *violet* and *yellow*, respectively. The BrdU-positive cells (high BrdU) in G_1 and G_2 are indicated by the *red* and *grey boxes*, respectively. **b** Mean percentage (±SE) of control (0 Gy) and irradiated (5 Gy) cells residing in the G_1 low BrdU, S, or G_2 high BrdU, population as defined in (**a**). Shown is a representative experiment performed in triplicates, * indicates $p \leq 0.05$, ANOVA

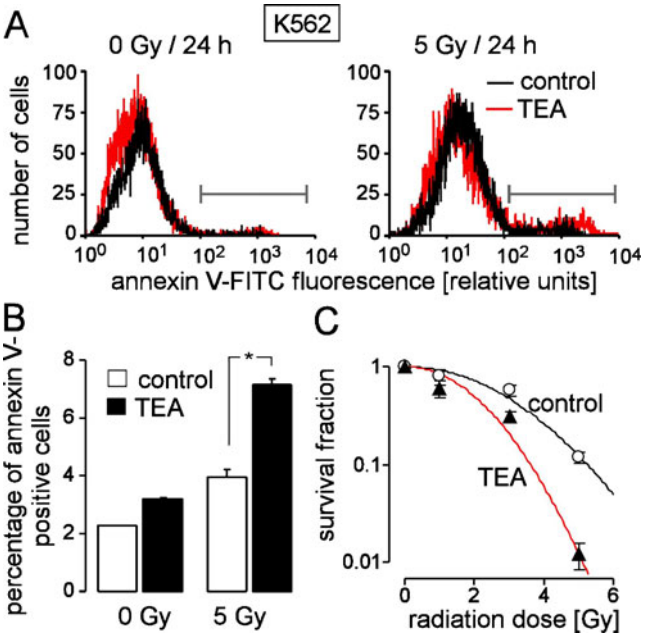

Fig. 7 Inhibition of K_v channels by TEA radiosensitizes K562 cells. **a** Histograms showing annexin V-binding to K562 cells which were irradiated (0 Gy, *left* and 5 Gy, *right*) and post-incubated (24 h) in the absence (*black line*) or presence (*red line*) of TEA (3 mM) before recording by flow cytometry. **b** Mean percentage of annexin V-binding cells (±SE, $n=12$) 24 h post-IR with 0 (*first* and *second* bars) and 5 Gy (*third* and *fourth bars*). Cells were irradiated and post-incubated in the absence (control, *open bars*) or presence of TEA (3 mM, *closed triangles*). **c** Mean survival fraction (±SE, $n=3$) of irradiated (0, 1, 3, or 5 Gy) K562 cells. Cells were irradiated and post-incubated in the absence (control, *open bars*) or presence of TEA (3 mM, *closed triangles*). Mean plating efficiencies were 0.4 and 0.08 for the non-irradiated control and TEA-treated group, respectively. *Asterisk* indicates $p \leq 0.05$, Kruskal–Wallis test (nonparametric ANOVA)

degraded DNA ($_{sub}G_1$ fraction, Fig. 9c, e). Finally, $K_v3.4$ silencing decreased clonogenic survival of irradiated K562 cells (Fig. 9f). The effect of $K_v3.4$ silencing was not as pronounced as treatment with the Kv3.4 inhibitors TEA or BDS-1 and BDS-II hinting to a significant residual activity of $K_v3.4$ in the silenced cells. Together, these data on cell cycling and survival suggest that K_v channels including $K_v3.4$ indeed control cell cycle and foster survival of irradiated K562 cells.

Discussion

Aberrant ion channel expression is a hallmark of cancer cells. "Oncogenic" channels [24] have been shown to participate in multiple processes of tumor biology. They regulate cell proliferation, malignant progression, invasion and metastasis, adaptation to the microenvironment, and tumor neovascularization (for review, see [4, 6, 12, 17, 24, 32, 35]. In particular, voltage-gated K^+ channels such as shaker- ($K_v1.x$), shaw- ($K_v3.x$), or shal-related ($K_v4.x$) channels have been reported to promote cell proliferation of breast [27], colon [57], gastric [29], lung [28], ovarian [67], and squamous head and neck cancer [44], as well as leiomyosarcoma [8]. Similarly, hERG ($K_v11.1$) voltage-gated K^+ channels are upregulated in many tumor entities [3] including leukemia where they regulate cell cycle and cell proliferation [36]. In line with this observation, hERG mRNA was most abundant among the four K^+ channel types identified in K562 cells in the present study.

Similarly to K562, hERG protein is highly abundant and functional in the primary CML cells used in this study (own unpublished results). Further common features of K562 and the primary cells are the reported radiation-induced Ca^{2+} entry [21] and the radiation-induced K_v channel activation observed in the present study. Together, these suggest that K562 can be used as CML cell model to study regulation of radiation-induced Ca^{2+} signaling by K_v channels.

The present study identified a functional significance of $K_v3.4$ for the survival of irradiated K562 cells. Reported biophysical features of $K_v3.4$ channels comprise (1) high voltage of activation when heterologously expressed, (2) a shift of the activation voltage to highly negative values (half-maximal voltage of activation, $V_{1/2}=-44$ mV) when

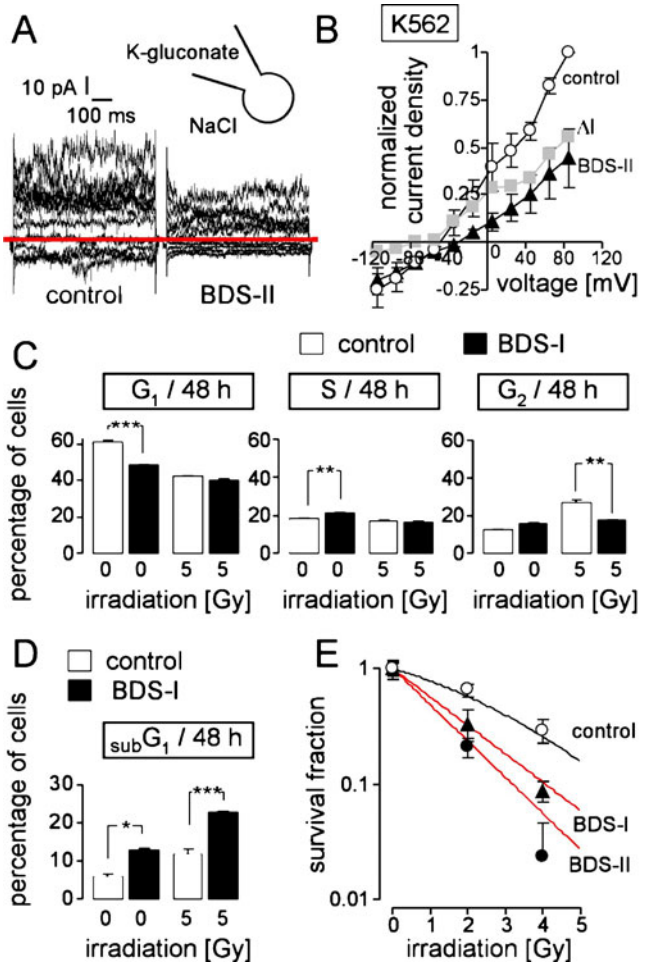

Fig. 8 $K_v3.4$ inhibitors BDS-I and BDS-II mimic the effect of TEA. **a**, **b** Current tracings (**a**) and mean (±SE, $n=3$) normalized current density voltage relationships (**b**) recorded in paired experiments from irradiated K562 cells (5 Gy, 2.6±0.8 h post-IR) with Na-D-gluconate pipette- and NaCl bath solution before (control, **a**, *left* and **b**, *open circles*) and after application of BDS-II (2 μM, **a** *right* and **b** *closed triangles*) to the bath solution. The *grey curve* in **b** shows the BDS-II-sensitive current fraction ΔI. **c** Mean percentage of cells (±SE, $n=4$–15) treated with BDS-I (0 and 5 μM) residing in G_1 (*left*), S (*middle*), and G_2 (*right*) phase of cell cycle, respectively, 48 h post-IR with 0 or 5 Gy. **d** Mean percentage (±SE, $n=4$–15) of dead cells ($subG_1$ population) treated with BDS-1 (0 or 5 μM) 48 h post-IR.*, **, and *** indicate $p\leq0.05$, $p\leq0.01$, and $p\leq0.001$, respectively, ANOVA. **e** Mean survival fraction (±SE, $n=3$–9) of irradiated (0, 2, or 4 Gy) BDS-1 or BDS-2 (0 or 5 μM, each)-treated cells. Mean plating efficiencies were 0.09, 0.19, and 0.14 for control, BDS-1-, and BDS-2-treated cells, respectively

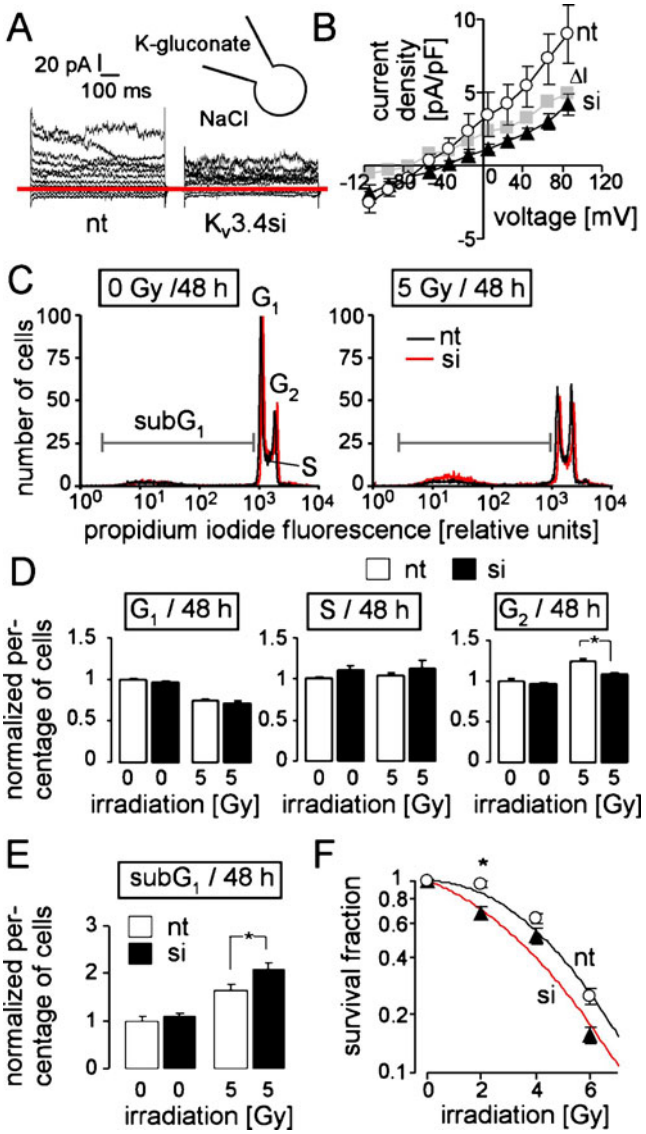

Fig. 9 $K_v3.4$ RNA interference overrides G_2/M arrest in irradiated K562 cells. **a, b** Current tracings (**a**) and mean (±SE) current densities voltage relationships (**b**) recorded from irradiated K562 cells (5 Gy, 2.1±0.4 and 2.1±0.3 h post-IR, respectively) pre-treated either with non-targeting RNA (*nt*, **a** *left* and **b** *open circles*, $n=11$) or $K_v3.4$ siRNA (*si*, **a** *right* and b *closed triangles*, $n=9$). Records were obtained as in Fig. 8a, b with K-D-gluconate pipette and NaCl bath solution. The *grey curve* in **b** indicates the current fraction ΔI that was sensitive to $K_v3.4$ downregulation. **c** Histograms of propidium iodide-stained K562 cells (Nicoletti protocol) recorded by flow cytometry 48 h post-IR with 0 Gy (*left*) or 5 Gy (*right*). Cells were transfected with non-targeting (*nt*, *black line*) or Kv3.4 siRNA (*si*, *red line*) 24 h prior to IR. **d** Normalized percentage of cells treated with non-targeting RNA (*nt*, open bars) or $K_v3.4$ siRNA (*si*, *closed bars*) residing in G_1 (*left*), S (*middle*), and G_2 (*right*) phase of cell cycle, respectively, 48 h post-IR with 0 or 5 Gy (recorded as in (**c**)). **e** Normalized percentage of dead cells ($subG_1$ population) treated with non-targeting RNA (*nt*, *open bar*) or $K_v3.4$ siRNA (*si*, *closed bar*) 48 h post-IR with 0 or 5 Gy (recorded as in (**c**)). **f** Mean survival fraction (±SE, $n=10$–14) of irradiated (0, 2, 4, or 6 Gy) MOCK-, non-targeting RNA-, and $K_v3.4$ siRNA (*si*, *closed triangles*)-transfected K562 cells. Data from MOCK- ($n=4$) and non-targeting RNA-transfected cells ($n=10$) did not differ and were pooled (*nt*, *open circles*). Mean plating efficiencies were 0.4 and 0.5 for the MOCK-/non-targeting RNA-, and $K_v3.4$ siRNA-transfected cells, respectively. *Asterisk* indicates $p\leq0.05$, ANOVA

coexpressed with MinK-related peptide 2 (MiRP2, KCNE3), (3) very fast activation, and (4) fast inactivation, as well as sensitivity to BDS-II with IC_{50}s of 0.3 μM (Kv3.4) and 7 μM ($K_v3.4$/MiRP2) [1]. Similarly to $K_v3.4$/MiRP2, the $K_v3.4$ currents of K562 cells and the K_v currents of primary CML cells observed in the present study exhibited mean $V_{1/2}$s of −44 and −48 mV, respectively. In addition, K_v currents of the irradiated primary CML cells activated and inactivated fast with time constants reported for $K_v3.4$

channels [65]. The $K_v3.4$ currents in irradiated K562 cells, however, inactivated slower (compare Figs. 1c (right) with 3b (right)). Alternative splicing and alternative transcription start sites have been reported for mammalian $K_v3.4$ channels [63]. In particular, variant $K_v3.4d$ lacks N-terminal amino acids which might be involved in the N-terminal "ball and chain" inactivation. In K562 cells, only surface expression of an about 50 kDa $K_v3.4$-immunoreactive protein could be detected (see Fig. 2c) while primary CML cells expressed only the 70 kDa $K_v3.4$ full-length protein. Moreover, protein kinase C-dependent posphorylation of NH_2-terminal serines S8, S9, S15, and S21 has been shown to slow down $K_v3.4$ inactivation [7]. It is therefore tempting to speculate that the difference in inactivation kinetics between the primary CML and the K562 cell line might reflect either expression of different isoforms, or different phosphorylation states of the $K_v3.4$ channels. The present study did not directly test for $K_v3.4$ function in primary CML cells. The similarities between the K_v currents of the primary CML cells and heterelogously expressed $K_v3.4$/MirP2 channels [1] suggest that, likewise K562, $K_v3.4$ contributed to the K_v currents of irradiated primary CML cells. To which extent the K_v channel beta subunit MirP2 participated in the K_v currents of both leukemia cell models was not analyzed in the present study.

The irradiation-induced increase in $K_v3.4$ channel activity was accompanied by a slight hyperpolarization of the membrane potential (Fig. 1a, b) suggesting $K_v3.4$ as a modulator of the membrane potential in K562 cells. $K_v3.4$-mediated hyperpolarization of the plasma membrane has been postulated to contribute to G_1 progression and G_2/M transition in proliferation of vascular smooth muscle cells [45]. $K_v3.4$ might exert similar cell cycle regulatory functions in unirradiated K562 cells as suggested by BDS-I-induced modifications of cell cycle progression (see Fig. 8c). Besides regulating cell proliferation, $K_v3.4$ channels are participating in the stress response of human leukemia cells. This is evident from the present study which discloses a functional significance of $K_v3.4$ channels for the induction of G_2/M cell cycle arrest and clonogenic survival of irradiated leukemia cells.

Irradiation stimulated, in the present study, the $K_v3.4$ currents in K562 without increasing the surface expression of the channel protein indicating radiation-induced modifications of the $K_v3.4$ channel itself or of a putative beta subunit, and/or of the membrane lipid environment of the channel complexes. In this context, irradiation has been reported to result in membrane lipid peroxidation with subsequent activation of tyrosine kinases [15]. Moreover, tyrosine phosphorylation of shaker K_v channels [19] and protein kinase C-dependent phosphorylation of MirP2 have been shown to alter voltage-dependence of K_v channel activation [2].

In the present study, irradiation-induced K_v channel activation stimulated Ca^{2+} entry (see Fig. 4a, b) probably through TRPV5/6 channels. The latter are co-activated in K562 and primary CML cells upon irradiation [21]. Irradiation-induced modulation of K_v and TRPV5/6 channels participates in the generation of Ca^{2+} signals that in turn activate CaMKII isoforms, as deduced from the increased autophosphorylation at Thr286 of this kinase (see Fig. 4c, d and [21]). CaMKII isoforms link biochemical signaling to the Ca^{2+} signalosome and exert multiple functions in cell cycle controls. CaMKII activity results in proteasomal degradation of p27 in colon adenocarcinoma [37], in decreased expression of p21 in osteosarcoma [66], and breast cancer [18] and increased expression of cyclin D1 in breast cancer [61]. Conversely, over-expression of the endogeneous CaMKII inhibitory proteins hCaMKIINalpha and hCaMKIINbeta in human colon adenocarcinoma [64] and ovarian cancer cells [40], respectively, stabilizes p27 or upregulates p21 and downregulates cyclin A, cyclin D1, cyclin E, and Cdk2. Thus, by upregulating cyclin D1 and downregulating the cell cycle inhibitors p21 and p27, CaMKII activity leads to disinhibition of the cyclin-Cdk4 and cyclin-Cdk2 complexes, and thus promotes G_1/S transition and S-G_2/M cell cycle progression. Later on, in cell cycle, CaMKII directly activates cdc25c, triggering G_2/M cell cycle transition [48, 56]. Moreover, CaMKII is required for centrosome duplication [43] and maintenance of the spindle bipolarity during mitosis [23]. Finally, CaMKII regulates M phase exit [13]. In primary CML cells and CML cell lines, cell proliferation specifically depends on activation of the CaMKIIγ isoforms, and CML cells undergoing terminal differentiation or growth arrest display a marked reduction of CaMKIIγ autophosphorylation [54].

In addition to its cell cycle-promoting functions, CaMKII isoforms may also suppress cell cycle progression by inhibition of cdc25c [26], by stabilization of p53 [16], by impairing nuclear translocation of nuclear factor of activated T cells [41], or by inhibiting S phase DNA replication [42]. Moreover, CaMKII induces G_2/M arrest when transiently expressed in a constitutively active form [51]. Thus, CaMKII isoforms appear to interfere with cell cycle control in a complex manner at multiple pathways.

As demonstrated in the present study, IR-induced G_2/M cell cycle arrest of K562 cells is, at least in part, mediated by CaMKII-dependent inactivation of the phosphatase cdc25B and the mitosis-promoting factor. Most importantly, K_v channel inhibition attenuated CaMKII activation and subsequent inactivation of cdc25B and the mitosis promoting factor, and overrode G_2/M cell cycle arrest, increased cell death, and decreased clonogenic survival. This suggests both, that K_v channels, in particular, $K_v3.4$ channels, are key regulators in the stress response of irradiated leukemia cells and that K_v channels might be attractive new targets to overcome therapy resistance of leukemia cells.

Acknowledgments This work was supported by grants from the Wilhelm-Sander-Stiftung and the Deutsche Forschungsgemeinschaft awarded to SH (2011.083.1) and JR (RU 1641/1-1). DP, DK, and ES were supported by the DFG International Graduate School 1302 (TP T9 and T1). We thank Ilka Müller for technical assistance.

Conflict of interest The authors declare that there are no conflicts of interest.

References

1. Abbott GW, Butler MH, Bendahhou S, Dalakas MC, Ptacek LJ, Goldstein SA (2001) MiRP2 forms potassium channels in skeletal muscle with Kv3.4 and is associated with periodic paralysis. Cell 104:217–231
2. Abbott GW, Butler MH, Goldstein SA (2006) Phosphorylation and protonation of neighboring MiRP2 sites: function and pathophysiology of MiRP2-Kv3.4 potassium channels in periodic paralysis. FASEB J 20:293–301
3. Arcangeli A (2005) Expression and role of hERG channels in cancer cells. Novartis Found Symp 266:225–232, discussion 232–224
4. Arcangeli A (2011) Ion channels and transporters in cancer. 3. Ion channels in the tumor cell-microenvironment cross talk. Am J Physiol Cell Physiol 301:C762–C771
5. Barry PH, Lynch JW (1991) Liquid junction potentials and small cell effects in patch-clamp analysis. J Membr Biol 121:101–117
6. Becchetti A (2011) Ion channels and transporters in cancer. 1. Ion channels and cell proliferation in cancer. Am J Physiol Cell Physiol 301:C255–C265
7. Beck EJ, Sorensen RG, Slater SJ, Covarrubias M (1998) Interactions between multiple phosphorylation sites in the inactivation particle of a K+ channel. Insights into the molecular mechanism of protein kinase C action. J Gen Physiol 112:71–84
8. Bielanska J, Hernandez-Losa J, Moline T, Somoza R, Cajal SR, Condom E, Ferreres JC, Felipe A (2012) Increased voltage-dependent K(+) channel Kv1.3 and Kv1.5 expression correlates with leiomyosarcoma aggressiveness. Oncol Lett 4:227–230
9. Bolanz KA, Hediger MA, Landowski CP (2008) The role of TRPV6 in breast carcinogenesis. Mol Cancer Ther 7:271–279
10. Boutros R, Dozier C, Ducommun B (2006) The when and wheres of CDC25 phosphatases. Curr Opin Cell Biol 18:185–191
11. Choi KH, Song C, Shin D, Park S (2011) hERG channel blockade by externally applied quaternary ammonium derivatives. Biochim Biophys Acta 1808:1560–1566
12. Cuddapah VA, Sontheimer H (2011) Ion channels and transporters [corrected] in cancer. 2. Ion channels and the control of cancer cell migration. Am J Physiol Cell Physiol 301:C541–C549
13. D'Angiolella V, Palazzo L, Santarpia C, Costanzo V, Grieco D (2007) Role for non-proteolytic control of M-phase promoting factor activity at M-phase exit. PLoS One 2:e247
14. Diochot S, Schweitz H, Beress L, Lazdunski M (1998) Sea anemone peptides with a specific blocking activity against the fast inactivating potassium channel Kv3.4. J Biol Chem 273:6744–6749
15. Dittmann K, Mayer C, Kehlbach R, Rothmund MC, Peter Rodemann H (2009) Radiation-induced lipid peroxidation activates src kinase and triggers nuclear EGFR transport. Radiother Oncol 92:379–382
16. Duan S, Yao Z, Hou D, Wu Z, Zhu WG, Wu M (2007) Phosphorylation of Pirh2 by calmodulin-dependent kinase II impairs its ability to ubiquitinate p53. EMBO J 26:3062–3074
17. Fiorio Pla A, Avanzato D, Munaron L, Ambudkar IS (2012) Ion channels and transporters in cancer. 6. Vascularizing the tumor: TRP channels as molecular targets. Am J Physiol Cell Physiol 302:C9–C15
18. Glover-Collins K, Thompson ME (2008) Nuclear export of BRCA1 occurs during early S phase and is calcium-dependent. Cell Signal 20:958–968
19. Gu C, Gu Y (2011) Clustering and activity tuning of Kv1 channels in myelinated hippocampal axons. J Biol Chem 286:25835–25847
20. Hadley JK, Noda M, Selyanko AA, Wood IC, Abogadie FC, Brown DA (2000) Differential tetraethylammonium sensitivity of KCNQ1-4 potassium channels. Br J Pharmacol 129:413–415
21. Heise N, Palme D, Misovic M, Koka S, Rudner J, Lang F, Salih HR, Huber SM, Henke G (2010) Non-selective cation channel-mediated Ca2+—entry and activation of Ca2+/calmodulin-dependent kinase II contribute to G2/M cell cycle arrest and survival of irradiated leukemia cells. Cell Physiol Biochem 26:597–608
22. Hemmerlein B, Weseloh RM, Mello de Queiroz F, Knotgen H, Sanchez A, Rubio ME, Martin S, Schliephacke T, Jenke M, Heinz Joachim R, Stuhmer W, Pardo LA (2006) Overexpression of Eag1 potassium channels in clinical tumours. Mol Cancer 5:41
23. Holmfeldt P, Zhang X, Stenmark S, Walczak CE, Gullberg M (2005) CaMKIIgamma-mediated inactivation of the Kin I kinesin MCAK is essential for bipolar spindle formation. EMBO J 24:1256–1266
24. Huber SM (2013) Oncochannels. Cell Calcium. doi:10.1016/j.ceca.2013.01.001
25. Huber SM, Misovic M, Mayer C, Rodemann HP, Dittmann K (2012) EGFR-mediated stimulation of sodium/glucose cotransport promotes survival of irradiated human A549 lung adenocarcinoma cells. Radiother Oncol 103:373–379
26. Hutchins JR, Dikovskaya D, Clarke PR (2003) Regulation of Cdc2/cyclin B activation in *Xenopus* egg extracts via inhibitory phosphorylation of Cdc25C phosphatase by Ca(2+)/calmodulin-dependent protein [corrected] kinase II. Mol Biol Cell 14:4003–4014
27. Jang SH, Kang KS, Ryu PD, Lee SY (2009) Kv1.3 voltage-gated K(+) channel subunit as a potential diagnostic marker and therapeutic target for breast cancer. BMB Reports 42:535–539
28. Jang SH, Choi SY, Ryu PD, Lee SY (2011) Anti-proliferative effect of Kv1.3 blockers in A549 human lung adenocarcinoma in vitro and in vivo. Eur J Pharmacol 651:26–32
29. Kim HJ, Jang SH, Jeong YA, Ryu PD, Kim DY, Lee SY (2010) Involvement of Kv4.1 K(+) channels in gastric cancer cell proliferation. Biol Pharm Bull 33:1754–1757
30. Kunzelmann K (2005) Ion channels and cancer. J Membr Biol 205:159–173
31. Kuo SS, Saad AH, Koong AC, Hahn GM, Giaccia AJ (1993) Potassium-channel activation in response to low doses of gamma-irradiation involves reactive oxygen intermediates in nonexcitatory cells. Proc Natl Acad Sci U S A 90:908–912
32. Lee JM, Davis FM, Roberts-Thomson SJ, Monteith GR (2011) Ion channels and transporters in cancer. 4. Remodeling of Ca(2+) signaling in tumorigenesis: role of Ca(2+) transport. Am J Physiol Cell Physiol 301:C969–C976
33. Lee GW, Park HS, Kim EJ, Cho YW, Kim GT, Mun YJ, Choi EJ, Lee JS, Han J, Kang D (2012) Reduction of breast cancer cell migration via up-regulation of TASK-3 two-pore domain K+ channel. Acta Physiol (Oxf) 204:513–524
34. Lehen'kyi V, Flourakis M, Skryma R, Prevarskaya N (2007) TRPV6 channel controls prostate cancer cell proliferation via Ca(2+)/NFAT-dependent pathways. Oncogene 26:7380–7385
35. Lehen'kyi V, Shapovalov G, Skryma R, Prevarskaya N (2011) Ion channels and transporters in cancer. 5. Ion channels in control of cancer and cell apoptosis. Am J Physiol Cell Physiol 301:C1281–C1289

36. Li H, Liu L, Guo L, Zhang J, Du W, Li X, Liu W, Chen X, Huang S (2008) HERG K+ channel expression in CD34+/CD38-/CD123 (high) cells and primary leukemia cells and analysis of its regulation in leukemia cells. Int J Hematol 87:387–392
37. Li N, Wang C, Wu Y, Liu X, Cao X (2009) Ca(2+)/calmodulin-dependent protein kinase II promotes cell cycle progression by directly activating MEK1 and subsequently modulating p27 phosphorylation. J Biol Chem 284:3021–3027
38. Logsdon NJ, Kang J, Togo JA, Christian EP, Aiyar J (1997) A novel gene, hKCa4, encodes the calcium-activated potassium channel in human T lymphocytes. J Biol Chem 272:32723–32726
39. Lozzio CB, Lozzio BB (1975) Human chronic myelogenous leukemia cell-line with positive Philadelphia chromosome. Blood 45:321–334
40. Ma S, Yang Y, Wang C, Hui N, Gu L, Zhong H, Cai Z, Wang Q, Zhang Q, Li N, Cao X (2009) Endogenous human CaMKII inhibitory protein suppresses tumor growth by inducing cell cycle arrest and apoptosis through down-regulation of the phosphatidylinositide 3-kinase/Akt/HDM2 pathway. J Biol Chem 284:24773–24782
41. MacDonnell SM, Weisser-Thomas J, Kubo H, Hanscome M, Liu Q, Jaleel N, Berretta R, Chen X, Brown JH, Sabri AK, Molkentin JD, Houser SR (2009) CaMKII negatively regulates calcineurin-NFAT signaling in cardiac myocytes. Circ Res 105:316–325
42. Maga G, Mossi R, Fischer R, Berchtold MW, Hubscher U (1997) Phosphorylation of the PCNA binding domain of the large subunit of replication factor C by Ca2+/calmodulin-dependent protein kinase II inhibits DNA synthesis. Biochemistry 36:5300–5310
43. Matsumoto Y, Maller JL (2002) Calcium, calmodulin, and CaMKII requirement for initiation of centrosome duplication in *Xenopus* egg extracts. Science 295:499–502
44. Menendez ST, Rodrigo JP, Allonca E, Garcia-Carracedo D, Alvarez-Alija G, Casado-Zapico S, Fresno MF, Rodriguez C, Suarez C, Garcia-Pedrero JM (2010) Expression and clinical significance of the Kv3.4 potassium channel subunit in the development and progression of head and neck squamous cell carcinomas. J Pathol 221:402–410
45. Miguel-Velado E, Perez-Carretero FD, Colinas O, Cidad P, Heras M, Lopez-Lopez JR, Perez-Garcia MT (2010) Cell cycle-dependent expression of Kv3.4 channels modulates proliferation of human uterine artery smooth muscle cells. Cardiovasc Res 86:383–391
46. Ouadid-Ahidouch H, Chaussade F, Roudbaraki M, Slomianny C, Dewailly E, Delcourt P, Prevarskaya N (2000) KV1.1 K(+) channels identification in human breast carcinoma cells: involvement in cell proliferation. Biochem Biophys Res Commun 278:272–277
47. Patel AJ, Lazdunski M (2004) The 2P-domain K+ channels: role in apoptosis and tumorigenesis. Pflugers Arch 448:261–273
48. Patel R, Holt M, Philipova R, Moss S, Schulman H, Hidaka H, Whitaker M (1999) Calcium/calmodulin-dependent phosphorylation and activation of human Cdc25-C at the G2/M phase transition in HeLa cells. J Biol Chem 274:7958–7968
49. Pillozzi S, Brizzi MF, Balzi M, Crociani O, Cherubini A, Guasti L, Bartolozzi B, Becchetti A, Wanke E, Bernabei PA, Olivotto M, Pegoraro L, Arcangeli A (2002) HERG potassium channels are constitutively expressed in primary human acute myeloid leukemias and regulate cell proliferation of normal and leukemic hemopoietic progenitors. Leukemia 16:1791–1798
50. Pillozzi S, Brizzi MF, Bernabei PA, Bartolozzi B, Caporale R, Basile V, Boddi V, Pegoraro L, Becchetti A, Arcangeli A (2007) VEGFR-1 (FLT-1), beta1 integrin, and hERG K+ channel for a macromolecular signaling complex in acute myeloid leukemia: role in cell migration and clinical outcome. Blood 110:1238–1250
51. Planas-Silva MD, Means AR (1992) Expression of a constitutive form of calcium/calmodulin dependent protein kinase II leads to arrest of the cell cycle in G2. EMBO J 11:507–517
52. Schroter KH, Ruppersberg JP, Wunder F, Rettig J, Stocker M, Pongs O (1991) Cloning and functional expression of a TEA-sensitive A-type potassium channel from rat brain. FEBS Lett 278:211–216
53. Semenova SB, Vassilieva IO, Fomina AF, Runov AL, Negulyaev YA (2009) Endogenous expression of TRPV5 and TRPV6 calcium channels in human leukemia K562 cells. Am J Physiol Cell Physiol 296:C1098–C1104
54. Si J, Collins SJ (2008) Activated Ca2+/calmodulin-dependent protein kinase IIgamma is a critical regulator of myeloid leukemia cell proliferation. Cancer Res 68:3733–3742
55. Smith GA, Tsui HW, Newell EW, Jiang X, Zhu XP, Tsui FW, Schlichter LC (2002) Functional up-regulation of HERG K+ channels in neoplastic hematopoietic cells. J Biol Chem 277:18528–18534
56. Soliman EM, Rodrigues MA, Gomes DA, Sheung N, Yu J, Amaya MJ, Nathanson MH, Dranoff JA (2009) Intracellular calcium signals regulate growth of hepatic stellate cells via specific effects on cell cycle progression. Cell Calcium 45:284–292
57. Spitzner M, Ousingsawat J, Scheidt K, Kunzelmann K, Schreiber R (2007) Voltage-gated K+ channels support proliferation of colonic carcinoma cells. FASEB J 21:35–44
58. Steinhardt RA, Alderton J (1988) Intracellular free calcium rise triggers nuclear envelope breakdown in the sea urchin embryo. Nature 332:364–366
59. Steinle M, Palme D, Misovic M, Rudner J, Dittmann K, Lukowski R, Ruth P, Huber SM (2011) Ionizing radiation induces migration of glioblastoma cells by activating BK K+ channels. Radiother Oncol 101:122–126
60. Taylor JT, Zeng XB, Pottle JE, Lee K, Wang AR, Yi SG, Scruggs JA, Sikka SS, Li M (2008) Calcium signaling and T-type calcium channels in cancer cell cycling. World J Gastroenterol 14:4984–4991
61. Torricelli C, Fortino V, Capurro E, Valacchi G, Pacini A, Muscettola M, Soucek K, Maioli E (2008) Rottlerin inhibits the nuclear factor kappaB/cyclin-D1 cascade in MCF-7 breast cancer cells. Life Sci 82:638–643
62. Voloshyna I, Besana A, Castillo M, Matos T, Weinstein IB, Mansukhani M, Robinson RB, Cordon-Cardo C, Feinmark SJ (2008) TREK-1 is a novel molecular target in prostate cancer. Cancer Res 68:1197–1203
63. Vullhorst D, Jockusch H, Bartsch JW (2001) The genomic basis of K(V)3.4 potassium channel mRNA diversity in mice. Gene 264:29–35
64. Wang C, Li N, Liu X, Zheng Y, Cao X (2008) A novel endogenous human CaMKII inhibitory protein suppresses tumor growth by inducing cell cycle arrest via p27 stabilization. J Biol Chem 283:11565–11574
65. Yeung SY, Thompson D, Wang Z, Fedida D, Robertson B (2005) Modulation of Kv3 subfamily potassium currents by the sea anemone toxin BDS: significance for CNS and biophysical studies. J Neurosci 25:8735–8745
66. Yuan K, Chung LW, Siegal GP, Zayzafoon M (2007) alpha-CaMKII controls the growth of human osteosarcoma by regulating cell cycle progression. Lab Investig J Tech Methods Pathol 87:938–950
67. Zhanping W, Xiaoyu P, Na C, Shenglan W, Bo W (2007) Voltage-gated K+ channels are associated with cell proliferation and cell cycle of ovarian cancer cell. Gynecol Oncol 104:455–460

K^+ channels signaling in irradiated tumor cells

Benjamin Stegen[1]*, Lukas Klumpp[1,3]*, Milan Misovic[1], Lena Edalat[2], Marita Eckert[1], Dominik Klumpp[1], Peter Ruth[2], and Stephan M Huber[1§]

Departments of [1]Radiation Oncology and [2]Pharmacology, Toxicology and Clinical Pharmacy, University of Tübingen, Germany, [3]Dr. Margarete Fischer-Bosch-Institute of Clinical Pharmacology, Stuttgart, and University of Tübingen, Tübingen, Germany

* BS and LK contributed equally to this study and, thus, share first-authorship

§ Correspondence to: Stephan Huber
Department of Radiation Oncology
University of Tübingen
Hoppe-Seyler-Str. 3
72076 Tübingen
Germany
Tel. +49-(0)7071-29-82183
E-mail stephan.huber@uni-tuebingen.de

Abstract

K^+ channels crosstalk with biochemical signaling cascades and regulate virtually all cellular processes by adjusting intracellular K^+ concentration, generating membrane potential, mediating cell volume changes, contributing to Ca^{2+} signaling, and by directly interacting within molecular complexes with e.g., membrane receptors and downstream effectors. Importantly, tumor cells exhibit aberrant expression and activity patterns of K^+ channels. The upregulation of highly "oncogenic" K^+ channels such as the Ca^{2+}-activated IK channel may drive neoplastic transformation, malignant progression, metastasis, or therapy resistance of tumor cells. In particular, ionizing radiation in doses used for fractionated radiotherapy in the clinic has been shown to activate K^+ channels. Radiogenic K^+ channel activity, in turn, contributes to the DNA damage response and promotes survival of the irradiated tumor cells. Tumor-specific overexpression of certain K^+ channel types together with the fact that pharmacological K^+ channel modulators are already in clinical use or well tolerated in clinical trials suggests that K^+ channel targeting alone or in combination with radiotherapy might become a promising new strategy of anti-cancer therapy. The present article aims to review our current knowledge on K^+ channel signaling in irradiated tumor cells. Moreover, it provides new data on molecular mechanisms of radiogenic K^+ channel activation and downstream signaling events.

Key words. Oncochannels, fractionated radiation therapy, electrosignaling, Ca^{2+} signalosome, patch-clamp recording, fura-2 Ca^{2+} imaging

Introduction

Radiotherapy belongs to the standard therapy protocol of many tumor entities. About 50% of all tumor patients undergo radiotherapy often neoadjuvant or adjuvant to surgery and/or combined with chemotherapy (Delaney et al. 2005). Radiation protocols frequently comprise fractionated therapy regimes with single fractions of sublethal radiation doses. Besides damaging the DNA, such doses of ionizing radiation trigger a plethora of cellular signaling events, which in concert with DNA repair mechanisms contribute to the cellular stress response.

Radioresistance of tumor cells often results in failure of local tumor control, metastasis or tumor recurrence. Unexpectedly, ion channels/transporters in the plasma membrane (Stegen et al. 2015), in the inner mitochondrial membrane (Braun et al. 2015; Huang et al. 2015), or in the nucleus/cytoplasma (Kim et al. 2010) have been demonstrated to regulate radioresistance. Specifically, K^+ channels in leukemia (Klumpp et al. 2016; Palme et al. 2013), lung adenocarninoma (Gibhardt et al. 2015; Huber et al. 2012; Roth et al. 2015) and glioblastoma cells (Huang et al.; Stegen et al. 2015; Steinle et al. 2011) are reportedly stimulated by ionizing radiation and exert functions in metabolisms, cell cycle, pro-survival signaling, or stress evasion that improve survival of the irradiated tumor cells. Moreover, preliminary clinical data might hint to a prognostic value of tumor-associated K^+ channels for clinical outcome. In particular, in glioblastoma, a primary brain tumor which is treated with surgery and adjuvant fractionated radiochemotherapy (Stupp et al. 2009), high expression of Ca^{2+}-activated intermediate conductance IK ($K_{Ca}3.1$, KCNN4) K^+ channels (Stegen et al. 2015; Turner et al. 2014) or mitochondrial $_mK_{ATP}$ K^+ channels (Huang et al.) in the tumors has been linked to poor prognosis of the patients.

K^+ channels such as EAG1 are getting more and more in the focus of oncologists due to their pivotal functions in tumor biology (for review see (Pardo and Stühmer 2008) and (Pardo and Stühmer 2014)). However, worldwide, only a handful of groups including our one works on K^+ channel function in irradiated tumor cells. Hence, the available data are very limited and primarily derived from human leukemia or glioblastoma cell lines. The present study aims to give an update of our current knowledge about the functional significance and the signaling upstream and downstream of radiation-induced K^+ channel activation. In addition, new data on radiogenic K^+ channel signaling will be presented. Previous review articles of our group on this topic focus on "oncogenic functions" of ion channels (Huber 2013), on the biophysics of radiogenic modulation of membrane transports and strategies to radiosensitize tumor cells by targeting these transports (Huber et al. 2013), and on the functional significance of ion channels for intrinsic and acquired radioresistance (Huber et al. 2015).

1 Functional significance of radiogenic K^+ channel activity

1.1 Glucose uptake. Many tumor cells metabolize glucose by anaerobic glycolysis and lactic acid fermentation rather than by mitochondrial respiration. This so-called Warburg effect entails high cellular glucose consumption. Low glucose availability in the tumor cell microenvironment of poorly perfused solid tumors, in addition, forces the tumor cells to upregulate highly efficient glucose fuelling pathways in the plasma membrane. Tumor cells have been shown to aberrantly express Na^+-coupled glucose contransporters (SGLTs) which harness the inwardly directed electrochemical Na^+-gradient to take up glucose even against high chemical glucose gradients. Previous work of our group disclosed that irradiated A549 lung adenocarcinoma cells massively increase their SGLT activity in the plasma membrane

(Huber et al. 2012). Notably, elevated Na^+-coupled glucose uptake is preceded by radiogenic K^+ channel activation (Roth et al. 2015) and hyperpolarization of the plasma membrane (Huber et al. 2012), most probably to maintain the electrochemical driving force for Na^+ and to sustain glucose uptake. The latter is required to counteract the cellular energy crises of DNA-damaged cells and to provide carbohydrates for acetyl-CoA synthesis needed for histone acetylation and DNA decondensation as prerequisite for DNA repair (Dittmann et al. 2013).

1.2 Cell cycle control. Cells arrest their cell cycle upon radiogenic DNA damage to prevent entering of mitosis with unfixed DNA double strand breaks. During this arrest cell cycle is halted at several points including G_1/S transition, S phase and G_2/M transition until DNA damages are repaired. Cellular sensors of DNA damage such as ataxia-telangiectasia-and-rad3-related (ATR)-dependent or -independent activation of checkpoint kinases (Chks) and ataxia-telangiectasia-mutated (ATM)-dependent stabilization of p53 arrest the cell cycle via phosphorylation of the phosphatase cdc25 and upregulation of the cyclin-dependent kinase inhibitor p21, respectively. Proteasomal degradation of phosphorylated cdc25 and upregulation of p21, in turn, prevent the formation of or inhibit the cyclin-dependent kinase complexes. Radiogenic electrosignaling by K^+ channels have been demonstrated by our group to crosstalk with this biochemical signaling. Specifically, radiogenic $K_v3.4$ and IK K^+ channel activity in chronic myeloid leukemia (Palme et al. 2013) and glioblastoma (Stegen et al. 2015) cell lines, respectively, has been identified to be required for G_2/M cell cycle arrest.

1.3 Radioresistance. In our studies, pharmacological inhibition of $K_v3.4$ and IK channels did override cell cycle arrest in both tumor entities resulting in entering mitosis despite residual DNA damages (Palme et al. 2013; Stegen et al. 2015). Moreover, IK channel blockade delayed repair of DNA double strand breaks in irradiated glioblastoma cells (Stegen et al. 2015). Premature re-entry of irradiated cells into mitosis, however, is expected to drive the cells in mitotic catastrophe and to decrease the percentage of irradiated tumor cells that maintain their clonogenicity. As a matter of fact, pharmacological inhibition of $K_v3.4$ channels in leukemia cells with TEA, BDS-1, or BDS-2 and IK channels in glioblastoma cells with TRAM-34 radiosensitized these cells as evident from colony formation assays (Palme et al. 2013; Stegen et al. 2015). Importantly, stable knock-down of IK in irradiated glioblastoma cells decreased clonogenic survival and, at the same time, abolished the effect of pharmacological IK channel targeting, indicating the K^+ channel specificity of TRAM-34 (Stegen et al. 2015). *Vice versa*, experimental overexpression of IK channels in a human gliobastoma cell line with low basal IK channel expression rendered the tumor cells radioresistant and sensitive against IK channel blockade by TRAM-34 (Fig. 1). Further *in vitro* evidence for a radioresistance-conferring function of IK channels in glioblastoma has been reported by others (Liu et al. 2010).

Beside cell cycle control, mitochondrial $_{mt}K_{ATP}$ K^+ channels have been demonstrated by a recent report (Huang et al. 2015) to suppress apoptotic cell death in irradiated glioblastoma cells. Knockdown or pharmacological blockage of $_{mt}K_{ATP}$ increased apoptotic death and decreased clonogenic survival of irradiated glioblastoma cells, while opening of $_{mt}K_{ATP}$ with diazoxide suppressed apoptosis and rendered the cells radioresistant.

1.4 Migration and metastasis. Fractionated radiotherapy which applies sublethal single doses of usually 2 Gy may induce migration and metastasis of tumor cells (for review see (Huber et al. 2013)). Specifically, glioblastoma cells responded in our transfilter chemotaxis experiments to ionizing radiation within 1-2 hours with an almost doubling of migration velocity (Steinle et al. 2011). At least in theory, this radiogenic hypermigration during

fractionated radiation therapy (which usually applies a cumulative dose of 60 Gy in 30 fractions á 2 Gy during 6 weeks) might promote evasion of clonogenic glioblastoma cells from the target volume of the radiation beam.

Brain infiltration of glioblastoma cells employs Ca^{2+}-activated BK (SLO1, KCNMA1) K^+ channels which are reportedly required for cell volume decrease during squeezing of glioblastoma cells through smallest interstitial spaces (Sontheimer 2008). Similar to BK, IK K^+ channels have been shown to contribute to the serum- (Catacuzzeno et al. 2011; Catacuzzeno et al. 2012), bradykinin- (Cuddapah et al. 2013) and chemokine-induced glioblastoma cell migration (D'Alessandro et al. 2013) *in vitro* and brain infiltration by *xeno*grafted human glioblastoma cells in orthotopic mouse models (D'Alessandro et al. 2013).

Most importantly, radiogenic BK (Steinle et al. 2011) and IK channel activation (Stegen et al. 2015) are involved in radiogenic hypermigration since BK channel blockade by inhibitors such as paxilline abrogates radiogenic hypermigration of glioblastoma cells *in vitro* and BK as well as IK channel inhibition slows down radiogenic hyperinfiltration of the brain in an orthotopic glioblastoma mouse model (Edalat et al., own unpublished observation). Thus, these results suggest a pivotal function of the Ca^{2+}-activated K^+ channel for radiogenic glioblastoma spreading which - in the worst scenario - might contribute to evasion from the target volume of radiotherapy and tumor relapse.

1.5 Maintenance of "stemness". One might speculate that radiogenic hypermigration might foster homing of glioblastoma cells to perivascular cancer "stem cell" niches (Pajonk and Vlashi 2013). The subsequent reciprocal interaction between endothelial and glioblastoma cells (Rao et al. 2012) within these niches has been demonstrated to induce/maintain "stemness" in glioblastoma cells (Anido et al. 2010; Pietras et al. 2014). Cancer "stem cells", in turn, have been proposed to be more radioresistant than the bulk tumor mass of "differentiated" tumor cells (Pajonk et al. 2010). In this context, a previous report showed that *xeno*grafted $CD133^+$ (prominin-1) stem-like subpopulations of glioblastoma cells exhibited a higher radioresistance than *xeno*grafted $CD133^-$ cells while radiosensitivity of both subpopulations did not differ *in vitro* (Jamal et al. 2012). This clearly indicates a function of the brain microenvironment for radioresistance.

Ionizing radiation has been demonstrated to select cancer "stem"-like cells or even to induce transition of "differentiated" to "stem"-like tumor cells in glioblastoma (Kim et al. 2011; Tamura et al. 2013) and other tumor entities (Lagadec et al. 2012; Pajonk et al. 2010). Noteworthily, up-regulation of "stemness" markers in glioblastoma is reportedly associated with over-expression of IK channels (Ruggieri et al. 2012 and Fig. 2A-C). Moreover, glioblastoma "stem" cells have been proposed to be highly migratory and to be primarily responsible for brain infiltration (Liu et al. 2006a; Nakada et al. 2013). Most importantly, stem cell migration highly depends on IK channels (Ruggieri et al. 2012). Along those lines, IK channels reportedly contribute to the migration of neuronal precursor cells into the olfactory bulb of mouse brain (Turner and Sontheimer 2014).

In summary, K^+ channels might be required for maintenance of "stemness" of tumor cells and radiogenic K^+ channel activity exerts various pro-survival functions. The identified signaling pathways underlying radiogenic K^+ channel activation will be described in the next paragraphs.

2 Upstream signaling

2.1 Radiogenic expression of K^+ channels. Cells receiving fractionated irradiation with sublethal single doses partially recover between the fractions. This recovery is more pronounced in normal tissue than in most tumor entities and, therefore, contributes to the normal tissue protection in radiotherapy. As a consequence of partial recovery between the radiation fractions, cell survival after a certain cumulative total dose of fractionated irradiation is much higher than after a corresponding single dose as shown here in the U251 glioblastoma model (Fig. 2A). Therefore, radiation doses that are assumed to be ablative have to accumulate, e.g. in the case of glioblastoma, within 6 weeks of fractionated radiotherapy. During this time period, however, tumor cells may acquire radioresistance, e.g., by radiation-induced overexpression of the genes involved in DNA repair and cell cycle control (Shimura 2011). In our experiments, 5 fractions of 2 Gy led to a 2-3 fold upregulation of the mRNAs encoding for the proposed "stem"cell marker CD133 (Fig. 2B) and IK (Fig. 2C) in U251 glioblastoma cells. In accordance to elevation of IK mRNA abundance, fractionated radiation induced an increase in plasma membrane IK K^+ currents (Fig. 2D-G). Hence, fractionated radiation may alter the expression of K^+ channels in tumor cells.

2.2 The HIF-1α/SDF-1/CXCR4 axis. Ionizing radiation induces expression and stabilization of the transcription factor hypoxia-inducible-factor-1α (HIF-1α) in several tumor entities. Subsequent gene regulation by HIF-1α has been demonstrated to trigger a metabolic switch from oxidative phosphorylation to anaerobic glycolysis and lactic acid fermentation (Dittmann et al. 2015; Lall et al. 2014), to stimulate angiogenesis (Zagzag et al. 2006), to recruit bone marrow-derived cells resulting in vasculogenesis (Kioi et al. 2010), to induce malignant progression (Kim et al. 2014) and radioresistance (Zhang et al. 2011). Accordingly, HIF-1α overexpression by malignant melanoma or locally advanced squamous cell head-and-neck cancer has been shown to be associated with poor prognosis (Giatromanolaki et al. 2003; Koukourakis et al. 2002)

Radiogenic HIF-1α stabilization may be mediated by hypoxia resulting from the decay of the radiosensitive tumor vasculature, by destabilization of prolyl hydroxylases-2 and HIF-1α-specific E3-ligase (Kim et al. 2014), by S-nitrosylation of the protein via NO release from tumor-associated macrophages (Li et al. 2007). In addition, upregulation of HIF-1α protein expression via complex formation of HIF-1α mRNA with the nuclear epithelial-growth-factor-receptor (EGFR) has been reported (Dittmann et al. 2015). The latter translocates in irradiated cells from the plasma membrane to the nucleus (Dittmann et al. 2009).

The chemokine SDF-1 (stromal cell-derived factor-1, CXCL12) (Kioi et al. 2010) and its receptor CXCR4 (Zagzag et al. 2006) belong to the HIF-1α target genes. In accordance to radiogenic HIF-1α upregulation/stabilization, ionizing radiation has been shown to induce the expression of SDF-1 in different tumor entities including glioblastoma (Kioi et al. 2010; Kozin et al. 2010; Tabatabai et al. 2006; Wang et al. 2013) as well as in normal brain tissue (Zhou et al. 2013). Notably, upregulation of SDF-1 secretion and CXCR4 expression has been proposed to be associated with "stemness" in A549 lung adenocarcinoma cells (Jung et al. 2013). Similarly, glioblastoma "stem" cells markedly upregulate and (Liu et al. 2006a) depend on CXCR4 (Barone et al. 2014). Moreover, formation of the perivascular glioblastoma stem cell niches and reciprocal signaling between glioblastoma stem cells and endothelial cells depend on SDF-1/CXCR4 (Rao et al. 2012; Richardson 2015).

In our yet unpublished experiments, irradiated cells released SDF-1 in the culture medium and conditioned medium from irradiated cells stimulated BK and IK channel activity and migration of glioblastoma cells in a CXCR4-dependent manner (Edalat et al., unpublished). Like conditioned medium, SDF-1 triggers K^+ channel activity (Edalat et al, own unpublished observations) and IK channel-dependent migration of glioblastoma cells (Sciaccaluga et al. 2010). Taken together, it can be concluded that radiogenic HIF-1α stabilization, subsequent SDF-1 formation/secretion and auto-/paracrine SDF-1/CXCR4 signaling contributes to radiogenic IK and BK channel activation in cancer cells.

2.3. Reactive oxygen species (ROS). The majority of radiation energy is absorbed by cellular water molecules resulting in the formation of the short-lived, highly reactive hydroxyl radicals (for review see (Huber et al. 2013)). Hydroxyl radical-mediated lipid peroxidation has been demonstrated to trigger src kinase activity and translocation of EGFR to the nucleus (Dittmann et al. 2009). Nuclear EGFR, in turn, facilitates HIF-1α signaling (see above). In addition, in A549 lung adenocarcinoma cells transfected with reporters of hydrogen peroxide and of glutathione redox potential, ionizing radiation reportedly induces a rapid rise in hydrogen peroxide concentration as a function of both, hydrogen peroxide formation and glutathione buffering capacity (Gibhardt et al. 2015). Hydrogen peroxide signaling stimulates Ca^{2+} entry and eventually activation of IK K^+ channels (Gibhardt et al. 2015; Roth et al. 2015).

2.4 Upstream Ca^{2+} signaling. Reactive oxygen species and ionizing radiation have been demonstrated to activate Ca^{2+}-permeable cation channels of the transient receptor potential (TRP) family such as TRPC6 (Foller et al. 2008) in red blood cells and TRPV5/6 (Heise et al. 2010) as well as TRPM2 (Klumpp et al. 2016) in leukemia cells. Own, yet unpublished data suggest radiogenic up-regulation and activation of the cold receptor TRPM8 in glioblastoma cells (Klumpp et al, unpublished). Glioblastoma cells highly overexpress the cold receptor TRPM8 (Alptekin et al. 2015) and stimulation of TRPM8 with the cooling agent icilin has been shown to induce BK K^+ channel activation and migration of glioblastoma cells via increase in intracellular Ca^{2+} (Wondergem and Bartley 2009).

In addition to Ca^{2+} influx, ionizing radiation may stimulate Ca^{2+} store release via upregulation of SDF-1 (see above) and CXCR4-mediated formation of inositol-trisphosphate (Haribabu et al. 1997). Remarkably, the Ca^{2+}-activated BK channels have been demonstrated to accumulate in lipid rafts which are directly linked to inositol 1,4,5-triphosphate receptors in the ER (Weaver et al. 2007).

Furthermore, the Ca^{2+} effector proteins such as the Ca^{2+}-dependent tyrosine kinase Pyk-2 (protein-tyrosine-kinase-2β or focal-adhesion-kinase-2) (Ling et al. 2004) and the serine/threonine kinase CaMKII (Liu et al. 2006b) reportedly may modulate the function of BK channels. In our experiments, Pyk-2 became activated and phosphorylated in irradiated glioblastoma cells (Fig. 3A) and contributed to radiogenic BK channel activation (Fig. 3B, C) and migration (Fig. 3D, E).

Combined, these data suggest that several radiation-induced pathways converge to Ca^{2+} signaling which either directly or via Ca^{2+}-regulated kinases may alter K^+ channel activity. K^+ channel activity, however, may modulate Ca^{2+} signaling as described in the next paragraph.

3 Downstream signaling

3.1 Downstream Ca^{2+} signaling. Entry of the divalent cation Ca^{2+} depolarizes the plasma membrane, which diminishes the inwardly directed electrochemical gradient for Ca^{2+}. In addition, some Ca^{2+} entry pathways, such as the highly Ca^{2+}-selective TRPV6 channels exhibit strong inward rectification (Voets et al. 2003), i.e., an over-proportional decline of the Ca^{2+} current with depolarizing membrane potential. K^+ channels may form molecular complexes with Ca^{2+} channels as reported for, e.g., mast cells where store-operated Ca^{2+} (ORAI1)- and IK K^+ channels have been demonstrated to physically interact (Duffy et al. 2015). By stabilizing the plasma membrane, voltage-gated or Ca^{2+}-activated K^+ channels counteract Ca^{2+} entry-mediated membrane depolarization, maintain the conductivity of the Ca^{2+} entry and/or the Ca^{2+} driving force and, thus, directly modulate Ca^{2+} signaling. For example, voltage-gated $K_v3.1$ channels have been demonstrated by our group to be required for radiation-induced Ca^{2+} entry in leukemia cells (Palme et al. 2013).

Another example is given by our fura-2 Ca^{2+} imaging experiments (Fig. 4) where we tested the effect of BK and IK K^+ channel blockers on steady state cytosolic free Ca^{2+} concentration of irradiated (0 or 2 Gy) T98G glioblastoma cells. T98G cells responded very heterogeneously to the two blockers. IK channel inhibitor TRAM-34 decreased cytosolic free Ca^{2+} concentration in about half of the cells (Fig. 4 A) while eliciting strong Ca^{2+} oscillations in the other half (data not shown). The response to the BK channel inhibitor paxilline ranged from no change to an instantaneous and long-lasting rise in cytosolic free Ca^{2+} concentration (Fig. 4. B). The latter was unexpected and might hint either to yet unknown off-target effects of paxilline or an speculative effect induced by the blockage of mitochondrial BK channels, or to Ca^{2+}-entry pathways of the plasma membrane that are activated upon BK blockade-associated membrane depolarization. Candidates for such pathways in glioblastoma cells are voltage-gated Ca^{2+} channels or strongly outwardly rectifying cation channels such as TRPM8 (Yudin and Rohacs 2012). Importantly, the effect of both K^+ channel blockers was more pronounced in irradiated than in control T98G cells (compare open circles and closed triangles in Fig. 4A, B) which points to the specific function of IK and BK channels in radiogenic Ca^{2+} signaling.

K^+ channel activity may impact on Ca^{2+} signaling in a complex and mutually interacting manner (for review see (Berridge et al. 2000)). Spatiotemporal and reciprocal activation/deactivation of K^+ and Ca^{2+}-permeable channels may generate complex Ca^{2+} signals such as Ca^{2+} oscillations. In dependence on frequency, amplitude and duration, Ca^{2+} oscillations trigger activation of a vast variety of different Ca^{2+} effector proteins in a highly specific manner. The CaMKIIs are such Ca^{2+} effector proteins (Bayer and Schulman 2001) that reportedly become activated in irradiated tumor cells.

3.2 Activation of CaMKII kinases. The CaMKII isoforms are encoded by four genes and expressed in multiple splice variants, which differ in Ca^{2+} sensitivity and cytoplasma/nuclear distribution. Upon binding of Ca^{2+}/calmodulin, CaMKII kinases become autophosphorylated and remain active in a Ca^{2+} independent manner until dephosphorylation. Hence, CaMKII kinases translate short-lived Ca^{2+} signals in long-lasting biochemical signaling. In our previous studies ionizing irradiation led to CaMKII phosphorylation in leukemia (Palme et al. 2013) and glioblastoma cells (Steinle et al. 2011) in a K^+ channel-dependent manner. Albeit increasing cytosolic free Ca^{2+} (see Fig. 4), inhibition of BK channels by paxilline prevented radiogenic CaMKII activation in glioblastoma cells (Steinle et al. 2011) suggesting complex radiation-induced Ca^{2+} signaling involved in CaMKII activation that requires BK channels. Another piece of evidence for such a sequence of signaling events came from the observation that CaMKII inhibition with KN-93 mimics the effect of BK channel blockade with paxilline on radiogenic hypermigration (Steinle et al. 2011). Similarly to BK, blockage of Kv3.4

channels in leukemia cells blunted radiogenic CaMKII activation (Palme et al. 2013). CaMKII kinases have been reported to regulate ion channels/transporters. Among those are BK channels (Liu et al. 2006b) (see above) hinting to a further possible Ca^{2+}-BK-feedback regulation in glioblastoma. Another CaMKII target is the ClC-3 Cl^- channel/Cl^--proton antiporter.

3.3 ClC-3 Cl^- channel/Cl^--proton antiporter. ClC-3 Cl^- channels/Cl^--proton antiporters reside in intracellular membranes where they contribute to acidification of endosomes/lysosmes by utilizing the V-ATPase-generated outwardly directed proton gradient to transport Cl^- into the endosomes/lysosomes (Stauber et al. 2012). Under oxidative stress, however, ClC-3 may be trafficked to the plasma membrane as shown in leukemia cells (Kasinathan et al. 2007). In glioblastoma, ClC-3 channels/antiporters colocalize with BK channels to lipid rafts in the plasma membrane (Sontheimer 2008), generate an anion current in whole-cell patch-clamp experiments, are activated by CaMKII (Cuddapah and Sontheimer 2010), and are required for cytoplasmic condensation during mitotic cell rounding (Cuddapah et al. 2012) and bradykinin-induced migration (Cuddapah et al. 2013).

In our experiments on glioblastoma cells, CAMKII and ClC-3 were found to co-immunoprecipitate (Fig. 5A). BK channel inhibition by paxilline that prevented CaMKII activation in irradiated cells also blocked radiogenic anion channel activation (Fig. 5B-F). Although not shown directly, one might speculate that radiogenic BK channel activity induces ClC-3 activity via modulation of the Ca^{2+} signaling and subsequent CaMKII activation.

3.4 The cdc25/cdc-2 axis. In addition to modulating ion channels, CaMKII isoforms have been demonstrated to be essential for regulating G_2/M cell cycle transition (for review see (Skelding et al. 2011)). As reported by our group, radiation-induced G_2/M cell cycle arrest of leukemia cells is, at least in part, mediated by CaMKII-dependent proteasomal degradation of cdc25B. Since function of the mitosis promoting factor cdc2 requires cdc25B phosphatase activity, radiogenic CaMKII activation results in inhibition of cdc2 and G_2/M arrest. Most importantly, in our experiments $K_v3.4$ channel inhibition in irradiated leukemia cells compromised CaMKII activation, degradation of cdc25B, and inhibition of cdc2, and overrode G_2/M cell cycle arrest which resulted in increased cell death, and decreased clonogenic survival (Palme et al. 2013).

3.5 *Activation of the MAP kinase pathway*. Glioblastoma cells reportedly overexpress mitochondrial K_{ATP} channels that are required for radiogenic formation of reactive oxygen species (Huang et al. 2015). This K_{ATP}-mediated redox signaling, in turn, confers radioresistance as demonstrated *in vitro* and in an ectopic glioblastoma mouse model. Radioresistance is most probably mediated by suppression of apoptosis and induced by ROS-mediated activation of the MAP kinase kinase MEK (Huang et al. 2015).

Together, these studies demonstrate a close interaction of radiogenic electrosignaling by K^+ channels in plasma and inner mitochondrial membrane with biochemical signaling proteins of the CaMKII/cdc25/cdc2 or the MAP kinase pathways.

Concluding Remarks

Radiation-induced activation of plasma membrane K^+ channels might be a common phenomenon in tumor cells. In glioblastoma, leukemia and lung carcinoma cell lines, radiogenic K^+ channel activity reportedly contributes to radioresistance. The underlying

molecular mechanisms of K^+ channel activation and the K^+ channel functions are largely ill-defined. Radiation-induced cellular lesions may converge to Ca^{2+} signaling upstream of K^+ channel activation. This upstream signaling may involve HIF-1α stabilization, auto-/paracrine chemokine signaling and Ca^{2+} store release, activation of Ca^{2+}-permeable TRP channels, and/or Ca^{2+}-regulated kinases. Radiogenic K^+ channel activation may modulate the Ca^{2+} and redox signaling which modify the activity of biochemical signaling. In this context, activation of CaMKII kinase isoforms seems to be a key event of the signaling downstream of radiogenic K^+ channel activation. Since CaMKII may also act upstream and Ca^{2+} up- and downstream of K^+ channels, radiogenic electrosignaling by K^+ channels may be fine-tuned by several feed-back loops.

Disclose any potential conflicts of interest. The authors declare no conflict of interest.

Acknowledgments. We thank Heidrun Faltin for excellent technical assistance. This work has been supported by a grant from the Wilhelm-Sander-Stiftung awarded to SH and PR (2011.083.1). LE was supported by a grant from the Landesgraduierentenförderungsgesetz, Baden-Württemberg. BS and DK were supported by the DFG International Graduate School 1302 (TP T9 SH) and LK by the ICEPHA program of the University of Tübingen and the Robert-Bosch-Gesellschaft für Medizinische Forschung, Stuttgart.

References

Alptekin M, Eroglu S, Tutar E, Sencan S, Geyik MA, Ulasli M, Demiryurek AT, Camci C (2015) Gene expressions of TRP channels in glioblastoma multiforme and relation with survival. Tumour Biol

Anido J, Saez-Borderias A, Gonzalez-Junca A, Rodon L, Folch G, Carmona MA, Prieto-Sanchez RM, Barba I, Martinez-Saez E, Prudkin L, Cuartas I, Raventos C, Martinez-Ricarte F, Poca MA, Garcia-Dorado D, Lahn MM, Yingling JM, Rodon J, Sahuquillo J, Baselga J, Seoane J (2010) TGF-beta Receptor Inhibitors Target the CD44(high)/Id1(high) Glioma-Initiating Cell Population in Human Glioblastoma. Cancer Cell 18:655-668

Barone A, Sengupta R, Warrington NM, Smith E, Wen PY, Brekken RA, Romagnoli B, Douglas G, Chevalier E, Bauer MP, Dembowsky K, Piwnica-Worms D, Rubin JB (2014) Combined VEGF and CXCR4 antagonism targets the GBM stem cell population and synergistically improves survival in an intracranial mouse model of glioblastoma. Oncotarget 5:9811-9822

Barry PH, Lynch JW (1991) Liquid junction potentials and small cell effects in patch-clamp analysis. J Membr Biol 121:101-117.

Bayer KU, Schulman H (2001) Regulation of signal transduction by protein targeting: the case for CaMKII. Biochem Biophys Res Commun 289:917-923

Berridge MJ, Lipp P, Bootman MD (2000) The versatility and universality of calcium signalling. Nat Rev Mol Cell Biol 1:11-21

Braun N, Klumpp D, Hennenlotter J, Bedke J, Duranton C, Bleif M, Huber SM (2015) UCP-3 uncoupling protein confers hypoxia resistance to renal epithelial cells and is upregulated in renal cell carcinoma. Sci Rep 5:13450

Catacuzzeno L, Aiello F, Fioretti B, Sforna L, Castigli E, Ruggieri P, Tata AM, Calogero A, Franciolini F (2011) Serum-activated K and Cl currents underlay U87-MG glioblastoma cell migration. J Cell Physiol 226:1926-1933

Catacuzzeno L, Fioretti B, Franciolini F (2012) Expression and Role of the Intermediate-Conductance Calcium-Activated Potassium Channel KCa3.1 in Glioblastoma. J Signal Transduct 2012:421564

Cuddapah VA, Habela CW, Watkins S, Moore LS, Barclay TT, Sontheimer H (2012) Kinase activation of ClC-3 accelerates cytoplasmic condensation during mitotic cell rounding. Am J Physiol Cell Physiol 302:C527-538

Cuddapah VA, Sontheimer H (2010) Molecular interaction and functional regulation of ClC-3 by Ca^{2+}/calmodulin-dependent protein kinase II (CaMKII) in human malignant glioma. J Biol Chem 285:11188-11196

Cuddapah VA, Turner KL, Seifert S, Sontheimer H (2013) Bradykinin-induced chemotaxis of human gliomas requires the activation of KCa3.1 and ClC-3. J Neurosci 33:1427-1440

D'Alessandro G, Catalano M, Sciaccaluga M, Chece G, Cipriani R, Rosito M, Grimaldi A, Lauro C, Cantore G, Santoro A, Fioretti B, Franciolini F, Wulff H, Limatola C (2013) KCa3.1 channels are involved in the infiltrative behavior of glioblastoma in vivo. Cell Death Dis 4:e773

Delaney G, Jacob S, Featherstone C, Barton M (2005) The role of radiotherapy in cancer treatment: estimating optimal utilization from a review of evidence-based clinical guidelines. Cancer 104:1129-1137

Dittmann K, Mayer C, Kehlbach R, Rothmund MC, Peter Rodemann H (2009) Radiation-induced lipid peroxidation activates src kinase and triggers nuclear EGFR transport. Radiother Oncol 92:379-382

Dittmann K, Mayer C, Paasch A, Huber S, Fehrenbacher B, Schaller M, Rodemann HP (2015) Nuclear EGFR renders cells radio-resistant by binding mRNA species and

triggering a metabolic switch to increase lactate production. Radiother Oncol 116:431-437
Dittmann K, Mayer C, Rodemann HP, Huber SM (2013) EGFR cooperates with glucose transporter SGLT1 to enable chromatin remodeling in response to ionizing radiation. Radiother Oncol doi:pii: S0167-8140(13)00145-X. 10.1016/j.radonc.2013.03.016.
Duffy SM, Ashmole I, Smallwood DT, Leyland ML, Bradding P (2015) Orai/CRACM1 and KCa3.1 ion channels interact in the human lung mast cell plasma membrane. Cell Commun Signal 13:32
Foller M, Kasinathan RS, Koka S, Lang C, Shumilina E, Birnbaumer L, Lang F, Huber SM (2008) TRPC6 contributes to the Ca^{2+} leak of human erythrocytes. Cell Physiol Biochem 21:183-192
Giatromanolaki A, Sivridis E, Kouskoukis C, Gatter KC, Harris AL, Koukourakis MI (2003) Hypoxia-inducible factors 1alpha and 2alpha are related to vascular endothelial growth factor expression and a poorer prognosis in nodular malignant melanomas of the skin. Melanoma Res 13:493-501
Gibhardt CS, Roth B, Schroeder I, Fuck S, Becker P, Jakob B, Fournier C, Moroni A, Thiel G (2015) X-ray irradiation activates K^+ channels via H_2O_2 signaling. Sci Rep 5:13861
Haribabu B, Richardson RM, Fisher I, Sozzani S, Peiper SC, Horuk R, Ali H, Snyderman R (1997) Regulation of human chemokine receptors CXCR4. Role of phosphorylation in desensitization and internalization. J Biol Chem 272:28726-28731
Heise N, Palme D, Misovic M, Koka S, Rudner J, Lang F, Salih HR, Huber SM, Henke G (2010) Non-selective cation channel-mediated Ca^{2+}-entry and activation of Ca^{2+}/calmodulin-dependent kinase II contribute to G_2/M cell cycle arrest and survival of irradiated leukemia cells. Cell Physiol Biochem 26:597-608
Huang L, Li B, Tang S, Guo H, Li W, Huang X, Yan W, Zou F (2015) Mitochondrial KATP Channels Control Glioma Radioresistance by Regulating ROS-Induced ERK Activation. Mol Neurobiol 52:626-637
Huber SM (2013) Oncochannels. Cell Calcium 53:241-255
Huber SM, Butz L, Stegen B, Klumpp D, Braun N, Ruth P, Eckert F (2013) Ionizing radiation, ion transports, and radioresistance of cancer cells. Front Physiol 4:212
Huber SM, Butz L, Stegen B, Klumpp L, Klumpp D, Eckert F (2015) Role of ion channels in ionizing radiation-induced cell death. Biochim Biophys Acta 1848:2657-2664
Huber SM, Misovic M, Mayer C, Rodemann HP, Dittmann K (2012) EGFR-mediated stimulation of sodium/glucose cotransport promotes survival of irradiated human A549 lung adenocarcinoma cells. Radiother Oncol 103:373-379
Jamal M, Rath BH, Tsang PS, Camphausen K, Tofilon PJ (2012) The brain microenvironment preferentially enhances the radioresistance of $CD133^+$ glioblastoma stem-like cells. Neoplasia 14:150-158
Jung MJ, Rho JK, Kim YM, Jung JE, Jin YB, Ko YG, Lee JS, Lee SJ, Lee JC, Park MJ (2013) Upregulation of CXCR4 is functionally crucial for maintenance of stemness in drug-resistant non-small cell lung cancer cells. Oncogene 32:209-221
Kasinathan RS, Foller M, Lang C, Koka S, Lang F, Huber SM (2007) Oxidation induces ClC-3-dependent anion channels in human leukaemia cells. FEBS Lett 581:5407-5412
Kim JS, Chang JW, Yun HS, Yang KM, Hong EH, Kim DH, Um HD, Lee KH, Lee SJ, Hwang SG (2010) Chloride intracellular channel 1 identified using proteomic analysis plays an important role in the radiosensitivity of HEp-2 cells via reactive oxygen species production. Proteomics 10:2589-2604
Kim MJ, Kim RK, Yoon CH, An S, Hwang SG, Suh Y, Park MJ, Chung HY, Kim IG, Lee SJ (2011) Importance of PKCδ signaling in fractionated-radiation-induced expansion of glioma-initiating cells and resistance to cancer treatment. J Cell Sci 124:3084-3094

Kim YH, Yoo KC, Cui YH, Uddin N, Lim EJ, Kim MJ, Nam SY, Kim IG, Suh Y, Lee SJ (2014) Radiation promotes malignant progression of glioma cells through HIF-1alpha stabilization. Cancer Lett 354:132-141

Kioi M, Vogel H, Schultz G, Hoffman RM, Harsh GR, Brown JM (2010) Inhibition of vasculogenesis, but not angiogenesis, prevents the recurrence of glioblastoma after irradiation in mice. J Clin Invest 120:694-705

Klumpp D, Misovic M, Szteyn K, Shumilina E, Rudner J, Huber SM (2016) Targeting TRPM2 channels impairs radiation-induced cell cycle arrest and fosters cell death of T cell leukemia cells in a Bcl-2-dependent manner. Oxidative Medicine and Cellular Longevity (in press)

Koukourakis MI, Giatromanolaki A, Sivridis E, Simopoulos C, Turley H, Talks K, Gatter KC, Harris AL (2002) Hypoxia-inducible factor (HIF1A and HIF2A), angiogenesis, and chemoradiotherapy outcome of squamous cell head-and-neck cancer. Int J Radiat Oncol Biol Phys 53:1192-1202

Kozin SV, Kamoun WS, Huang Y, Dawson MR, Jain RK, Duda DG (2010) Recruitment of myeloid but not endothelial precursor cells facilitates tumor regrowth after local irradiation. Cancer Res 70:5679-5685

Lagadec C, Vlashi E, Della Donna L, Dekmezian C, Pajonk F (2012) Radiation-induced reprogramming of breast cancer cells. Stem Cells 30:833-844

Lall R, Ganapathy S, Yang M, Xiao S, Xu T, Su H, Shadfan M, Asara JM, Ha CS, Ben-Sahra I, Manning BD, Little JB, Yuan ZM (2014) Low-dose radiation exposure induces a HIF-1-mediated adaptive and protective metabolic response. Cell Death Differ 21:836-844

Li F, Sonveaux P, Rabbani ZN, Liu S, Yan B, Huang Q, Vujaskovic Z, Dewhirst MW, Li CY (2007) Regulation of HIF-1alpha stability through S-nitrosylation. Mol Cell 26:63-74

Ling S, Sheng JZ, Braun AP (2004) The calcium-dependent activity of large-conductance, calcium-activated K^+ channels is enhanced by Pyk2- and Hck-induced tyrosine phosphorylation. Am J Physiol Cell Physiol 287:C698-706

Liu G, Yuan X, Zeng Z, Tunici P, Ng H, Abdulkadir IR, Lu L, Irvin D, Black KL, Yu JS (2006a) Analysis of gene expression and chemoresistance of $CD133^+$ cancer stem cells in glioblastoma. Mol Cancer 5:67

Liu H, Li Y, Raisch KP (2010) Clotrimazole induces a late G1 cell cycle arrest and sensitizes glioblastoma cells to radiation in vitro. Anticancer Drugs 21:841-849

Liu J, Asuncion-Chin M, Liu P, Dopico AM (2006b) CaM kinase II phosphorylation of slo Thr107 regulates activity and ethanol responses of BK channels. Nat Neurosci 9:41-49

Nakada M, Nambu E, Furuyama N, Yoshida Y, Takino T, Hayashi Y, Sato H, Sai Y, Tsuji T, Miyamoto KI, Hirao A, Hamada JI (2013) Integrin alpha3 is overexpressed in glioma stem-like cells and promotes invasion. Br J Cancer 108:2516-2524

Pajonk F, Vlashi E (2013) Characterization of the stem cell niche and its importance in radiobiological response. Semin Radiat Oncol 23:237-241

Pajonk F, Vlashi E, McBride WH (2010) Radiation resistance of cancer stem cells: the 4 R's of radiobiology revisited. Stem Cells 28:639-648

Palme D, Misovic M, Schmid E, Klumpp D, Salih HR, Rudner J, Huber SM (2013) Kv3.4 potassium channel-mediated electrosignaling controls cell cycle and survival of irradiated leukemia cells. Pflugers Arch 465:1209-1221

Pardo LA, Stühmer W (2008) Eag1: an emerging oncological target. Cancer Res. 68:1611-3

Pardo LA, Stühmer W (2014) The roles of K^+ channels in cancer. Nat Rev Cancer 14:39-48

Pietras A, Katz AM, Ekstrom EJ, Wee B, Halliday JJ, Pitter KL, Werbeck JL, Amankulor NM, Huse JT, Holland EC (2014) Osteopontin-CD44 signaling in the glioma perivascular niche enhances cancer stem cell phenotypes and promotes aggressive tumor growth. Cell Stem Cell 14:357-369

Rao S, Sengupta R, Choe EJ, Woerner BM, Jackson E, Sun T, Leonard J, Piwnica-Worms D, Rubin JB (2012) CXCL12 mediates trophic interactions between endothelial and tumor cells in glioblastoma. PLoS One 7:e33005
Richardson PJ (2015) CXCR4 and Glioblastoma. Anticancer Agents Med Chem
Roth B, Gibhardt CS, Becker P, Gebhardt M, Knoop J, Fournier C, Moroni A, Thiel G (2015) Low-dose photon irradiation alters cell differentiation via activation of hIK channels. Pflugers Arch 467:1835-1849
Ruggieri P, Mangino G, Fioretti B, Catacuzzeno L, Puca R, Ponti D, Miscusi M, Franciolini F, Ragona G, Calogero A (2012) The inhibition of KCa3.1 channels activity reduces cell motility in glioblastoma derived cancer stem cells. PLoS One 7:e47825
Sciaccaluga M, Fioretti B, Catacuzzeno L, Pagani F, Bertollini C, Rosito M, Catalano M, D'Alessandro G, Santoro A, Cantore G, Ragozzino D, Castigli E, Franciolini F, Limatola C (2010) CXCL12-induced glioblastoma cell migration requires intermediate conductance Ca^{2+}-activated K^+ channel activity. Am J Physiol Cell Physiol 299:C175-184
Shimura T (2011) Acquired radioresistance of cancer and the AKT/GSK3beta/cyclin D1 overexpression cycle. J Radiat Res 52:539-544
Skelding KA, Rostas JA, Verrills NM (2011) Controlling the cell cycle: the role of calcium/calmodulin-stimulated protein kinases I and II. Cell Cycle 10:631-639
Sontheimer H (2008) An unexpected role for ion channels in brain tumor metastasis. Exp Biol Med (Maywood) 233:779-791
Stauber T, Weinert S, Jentsch TJ (2012) Cell biology and physiology of CLC chloride channels and transporters. Compr Physiol 2:1701-1744
Stegen B, Butz L, Klumpp L, Zips D, Dittmann K, Ruth P, Huber SM (2015) Ca^{2+}-activated IK K^+ channel blockade radiosensitizes glioblastoma cells. Mol Cancer Res 13:1283-1295
Steinle M, Palme D, Misovic M, Rudner J, Dittmann K, Lukowski R, Ruth P, Huber SM (2011) Ionizing radiation induces migration of glioblastoma cells by activating BK K^+ channels. Radiother Oncol 101:122-126
Stupp R, Hegi ME, Mason WP, van den Bent MJ, Taphoorn MJ, Janzer RC, Ludwin SK, Allgeier A, Fisher B, Belanger K, Hau P, Brandes AA, Gijtenbeek J, Marosi C, Vecht CJ, Mokhtari K, Wesseling P, Villa S, Eisenhauer E, Gorlia T, Weller M, Lacombe D, Cairncross JG, Mirimanoff RO (2009) Effects of radiotherapy with concomitant and adjuvant temozolomide versus radiotherapy alone on survival in glioblastoma in a randomised phase III study: 5-year analysis of the EORTC-NCIC trial. Lancet Oncol 10:459-466
Tabatabai G, Frank B, Mohle R, Weller M, Wick W (2006) Irradiation and hypoxia promote homing of haematopoietic progenitor cells towards gliomas by TGF-beta-dependent HIF-1alpha-mediated induction of CXCL12. Brain 129:2426-2435
Tamura K, Aoyagi M, Ando N, Ogishima T, Wakimoto H, Yamamoto M, Ohno K (2013) Expansion of CD133-positive glioma cells in recurrent de novo glioblastomas after radiotherapy and chemotherapy. J Neurosurg 119:1145-1155
Turner KL, Honasoge A, Robert SM, McFerrin MM, Sontheimer H (2014) A proinvasive role for the Ca^{2+} -activated K^+ channel KCa3.1 in malignant glioma. Glia 62:971-981
Turner KL, Sontheimer H (2014) KCa3.1 modulates neuroblast migration along the rostral migratory stream (RMS) in vivo. Cereb Cortex 24:2388-2400
Voets T, Janssens A, Prenen J, Droogmans G, Nilius B (2003) Mg^{2+}-dependent gating and strong inward rectification of the cation channel TRPV6. J Gen Physiol 121:245-260
Wang SC, Yu CF, Hong JH, Tsai CS, Chiang CS (2013) Radiation therapy-induced tumor invasiveness is associated with SDF-1-regulated macrophage mobilization and vasculogenesis. PLoS One 8:e69182

Weaver AK, Olsen ML, McFerrin MB, Sontheimer H (2007) BK channels are linked to inositol 1,4,5-triphosphate receptors via lipid rafts: a novel mechanism for coupling $[Ca^{2+}]_i$ to ion channel activation. J Biol Chem 282:31558-31568

Wolfsperger F, Hogh-Binder SA, Schittenhelm J, Psaras T, Ritter V, Bornes L, Huber SM, Jendrossek V, Rudner J (2016) Deubiquitylating enzyme USP9x regulates radiosensitivity in glioblastoma cells by Mcl-1-dependent and -independent mechanisms. Cell Death Dis 7:e2039

Wondergem R, Bartley JW (2009) Menthol increases human glioblastoma intracellular Ca^{2+}, BK channel activity and cell migration. J Biomed Sci 16:90

Yudin Y, Rohacs T (2012) Regulation of TRPM8 channel activity. Mol Cell Endocrinol 353:68-74

Zagzag D, Lukyanov Y, Lan L, Ali MA, Esencay M, Mendez O, Yee H, Voura EB, Newcomb EW (2006) Hypoxia-inducible factor 1 and VEGF upregulate CXCR4 in glioblastoma: implications for angiogenesis and glioma cell invasion. Lab Invest 86:1221-1232

Zhang GJ, Gao R, Wang JS, Fu JK, Zhang MX, Jin X (2011) Various doses of fractioned irradiation modulates multidrug resistance 1 expression differently through hypoxia-inducible factor 1alpha in esophageal cancer cells. Dis Esophagus 24:481-488

Zhou W, Xu Y, Gao G, Jiang Z, Li X (2013) Irradiated normal brain promotes invasion of glioblastoma through vascular endothelial growth and stromal cell-derived factor 1alpha. Neuroreport 24:730-734

Figures and Legends

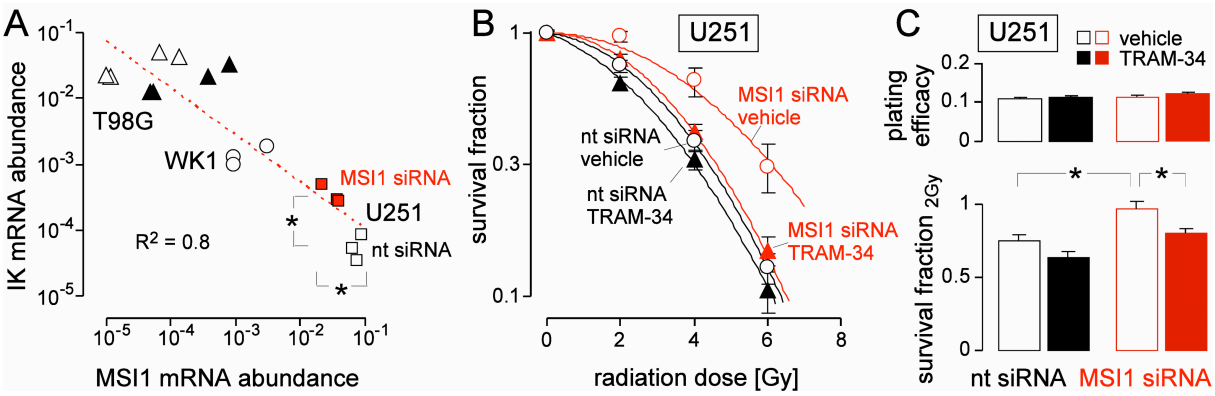

Fig. 1. Upregulation of the Ca^{2+}-activated IK K^+ channels induces radioresistance in human U251 glioblastoma cells. **A.** IK and MSI1 (Musashi-1) mRNA abundances in T98G, WK1, and nt- or MSI1si RNA-transfected U251 cells. MSI1 and IK mRNA abundance negatively correlated (correlation quotient of liner fit $R^2 = 0.8$). MSI1 knockdown was associated with IK upregulation. **B.** Mean survival fractions (± SE, n = 24) of non-targeting (nt)- (black) or MSI1 (Musashi-1) siRNA-transfected U251 cells after irradiation with 0, 2, 4, or 6 Gy and combined treatment with the IK inhibitor TRAM-34 (10 µM, filled triangles) or vehicle alone (0.1% DMSO, open circles) as determined by delayed plating colony formation assay. **C.** Mean (± SE) plating efficacies and **D.** survival fractions after irradiation with 2 Gy (data from (B). * indicates $p \leq 0.05$, two tailed Welch-corrected t-test in (A) and ANOVA in (D). MSI1 knockdown induced radioresistance of U251 cells and rendered the cells sensitive to TRAM-34.

The human WK1 and T98G glioblastoma cell lines were grown in RPMI-1640/10% FCS medium and the U251 cells in DMEM (4500 mg glucose/l)/10% FCS medium. Exponentially growing U251 cells were reversely transfected with stealth MSI1 siRNAs (HSS106732, -33, -34, #1299001, Thermo Fischer Scientific, Waltham, MA, U.S.A) or nt siRNA (*Silencer*® Select Negative Control No. 1 siRNA, #4390844, Ambion™, Thermo Fischer Scientific). Detached cells (250.000 in 2.5 ml RPMI-1640/10% FCS and DMEM (4500 mg glucose/l)/10% FCS medium, respectively) were added to 500 µl of pre-incubated (20 min/RT) Opti-MEM medium containing RNAiMAX lipofectamine (6 µl, Invitrogen Life Technologies, Carlsbad, CA, USA) and siRNA (25 nM final concentration). Messenger RNAs were isolated (Qiagen RNA extraction kit, Hilden, Germany) from parental T98G and WK1 cells and from nt- or MSI1 siRNA-transfected U251 cells (48 h-72 h after transfection) and reversely transcribed in cDNA (Transcriptor First Strand cDNA Synthesis Kit, Roche). IK K^+ channel, MSI1 (Musashi-1) as well as housekeeper β-actin (ACTB)-, pyruvate dehydrogenase beta (PDHB)-, and glyceraldehyde-3-phosphate dehydrogenase (GAPDH)-specific fragments were amplified by the use of SYBR Green-based quantitative real-time PCR (QT00003780, QT00025389, QT00095431, QT00031227, and QT01192646 QuantiTect Primer Assay and QuantiFast SYBR Green PCR Kit, Qiagen) in a Roche LightCycler 480 Instrument (Roche, Mannheim, Germany). To test for clonogenic survival, U251 cells were transfected with nt or MSI1 siRNA. After 24 h, cells were irradiated (0, 2, 4 or 6 Gy) with 6 MV photons by using a linear accelerator (LINAC SL25 Philips) at a dose rate of 4 Gy/min at room temperature in DMEM (4500 mg glucose/l)/10% FCS medium additionally containing TRAM-34 (1-[(2-Chlorophenyl)diphenylmethyl]-1H-pyrazole, 10 µM, Sigma-Aldrich, Taufkirchen, Germany) or vehicle alone (0.1% DMSO). After further 24 h of incubation with the inhibitor/vehicle, cells were detached, 1000-3000 cells were re-seeded in inhibitor-free medium on 6-well plates

and grown for further 2-3 weeks. The plating efficiency was defined by dividing the number of colonies by the number of plated cells. Survival fractions as calculated by dividing the plating efficiency of the irradiated cells by those of the unirradiated controls were fitted by the use of the linear quadratic equation.

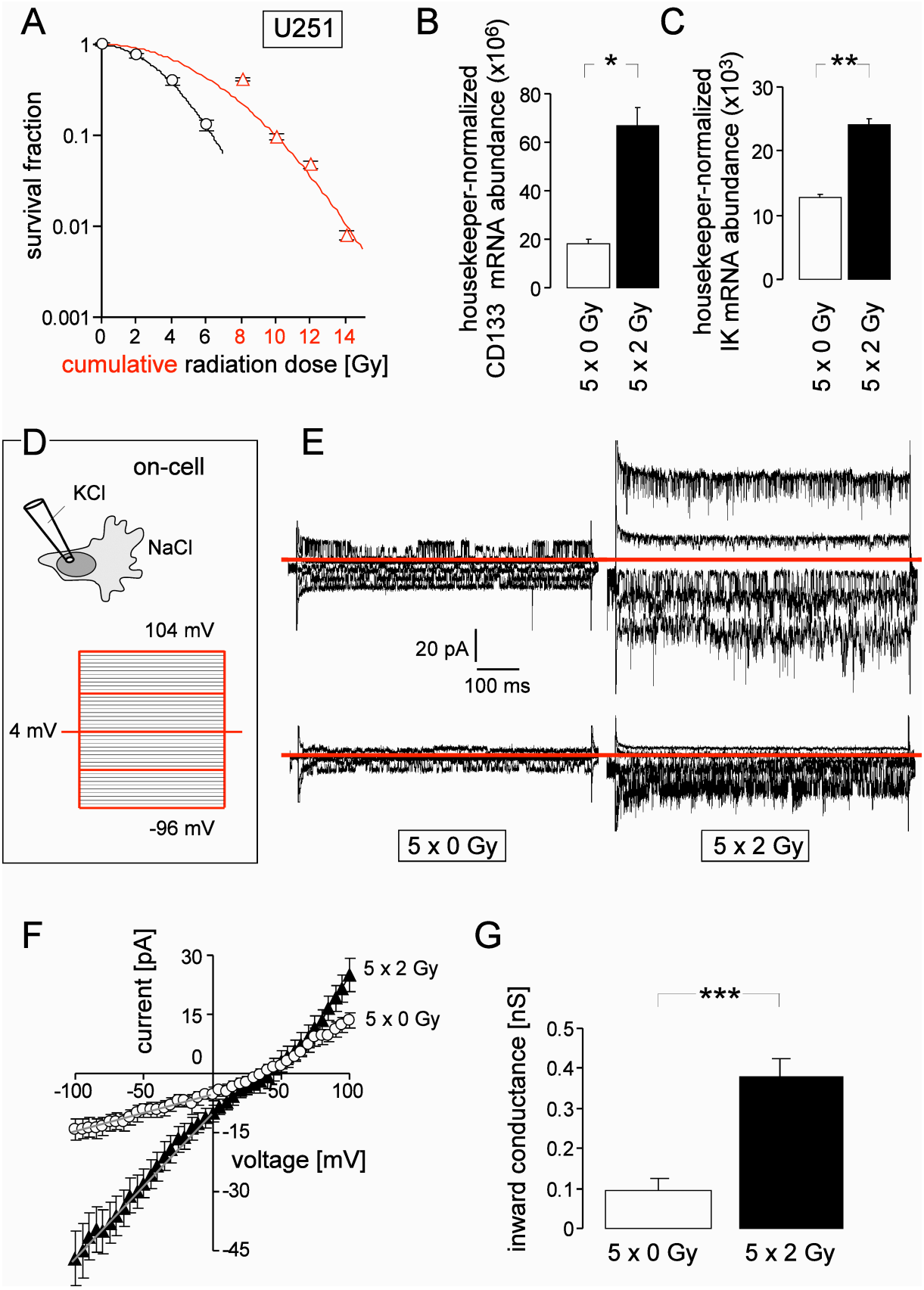

Fig. 2. Fractionated irradiation induces/selects glioblastoma cells with high IK K^+ channel expression. **A.** Mean (± SE, n = 36-48) survival fractions of fractionated irradiated U251 cells (4 x 2 Gy plus 1 x 0, 2, 4, or 6 Gy, red triangles) as plotted against the cumulative dose (red numbers). For comparison, the survival fractions of U251 cells (black circles) irradiated with

a single dose (black numbers) already shown in Fig. 1B are given. **B-C.** Housekeeper-normalized CD133 (B) and IK (C) mRNA abundances in 5 x 0 Gy- (open bars) and 5 x 2 Gy-irradiated (closed bars) U251 glioblastoma cells. **D.** Patch-clamp recording of macroscopic on-cell (cell-attached) currents from semiconfluent U251 cells with KCl and NaCl in pipette and bath solution, respectively. Depicted is the applied voltage pulse protocol. **E.** Macroscopic on-cell current tracings recorded from control (5 x 0 Gy, left) and fractionated irradiated (5 x 2 Gy, right) U251 cells. Shown are representative patches that exhibit BK (prominent upward current deflections at depolarizing voltages) and IK K^+ channel activity or only IK channel activity in the upper and lower line, respectively (only voltage pulses to -96, -46, + 4 +54, and +104 mV are shown as indicated by the red square pulses in A). **F.** Dependence of the mean macroscopic on-cell currents (± SE) on holding potential in control (5 x 0 Gy, open circles) and fractionated irradiated (5 x 2 Gy, closed triangles) U251 cells. **G.** Mean conductance (as calculated for the inward currents in C between-96 mV and +4 mV voltage as indicated by the grey lines) of 5 x 0 Gy- (open bar) and 5 x 2 Gy-irradiated (closed bar) U251 cells. *, ** and *** indicate $p \leq 0.05$, $p \leq 0.01$ and $p \leq 0.001$, respectively, two tailed (Welch-corrected) t-test.

For colony formation assay, U251 cells were irradiated with 2 Gy on days 1, 2, 3, 4, and finally irradiated with 0, 2, 4, or 6 Gy on day 5. On day 6, defined number of cells were reseeded as described in legend to Fig. 1. Survival fractions were fitted by the use of the linear quadratic equation. For RT-PCR, U251 cells were fractionated irradiated on five consecutive days with 5 x 0 Gy or 5 x 2 Gy. Twenty-four hours after the last radiation fraction, mRNA was isolated and CD133 (prominin-1, QT00075586 QuantiTect Primer Assay, Qiagen), IK and housekeepers mRNA abundances were determined as described in legend to Fig. 1. For patch-clamp recording, semiconfluent U251 cells were irradiated with 5 daily fractions of 0 Gy or 2 Gy (T98G). One day after the last fraction, on-cell currents were evoked by 41 voltage square pulses (700 ms each) from 4 mV holding potential to voltages between -96 mV and +104 mV delivered in 5 mV increments. Voltages were corrected for the estimated liquid junction potentials (Barry and Lynch 1991). Cells were superfused at 37°C with NaCl solution (in mM: 125 NaCl, 32 N-2-hydroxyethylpiperazine-N-2-ethanesulfonic acid (HEPES), 5 KCl, 5 D-glucose, 1 MgCl2, 1 CaCl2, titrated with NaOH to pH 7.4). The pipette solution contained (in mM) 130 KCl, 32 HEPES, 5 D-glucose, 1 MgCl2, 1 CaCl2, titrated with KOH to pH 7.4.

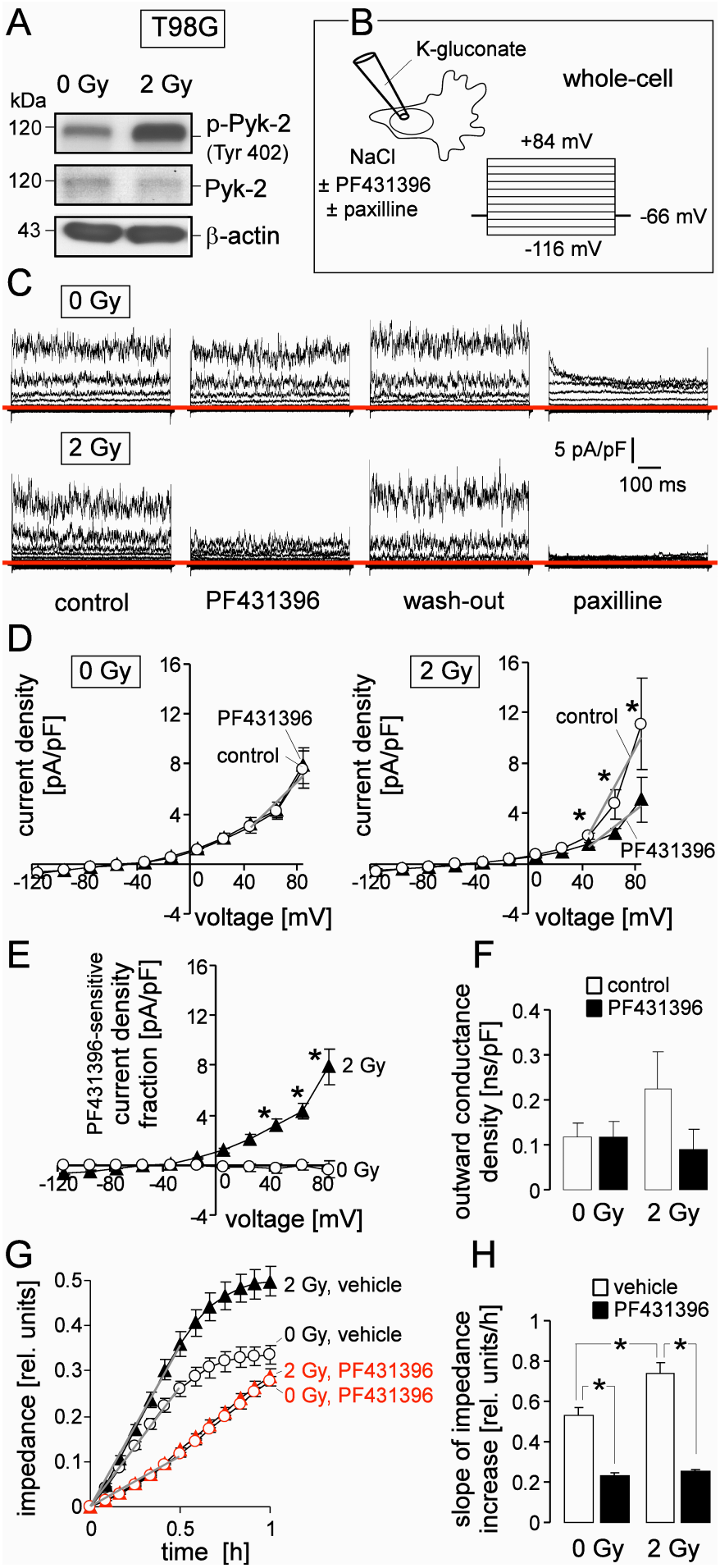
A
T98G
0 Gy
2 Gy
kDa
120
p-Pyk-2
(Tyr 402)
120
Pyk-2
43
β-actin
B
K-gluconate
whole-cell
NaCl
± PF431396
± paxilline
+84 mV
-66 mV
-116 mV
C
0 Gy
2 Gy
5 pA/pF
100 ms
control
PF431396
wash-out
paxilline
D
0 Gy
current density [pA/pF]
PF431396
control
voltage [mV]
2 Gy
control
PF431396
E
PF431396-sensitive current density fraction [pA/pF]
2 Gy
0 Gy
voltage [mV]
F
control
PF431396
outward conductance density [ns/pF]
0 Gy
2 Gy
G
impedance [rel. units]
2 Gy, vehicle
0 Gy, vehicle
2 Gy, PF431396
0 Gy, PF431396
time [h]
H
vehicle
PF431396
slope of impedance increase [rel. units/h]
0 Gy
2 Gy

Fig. 3. Radiogenic activation of the Ca^{2+}-dependent tyrosine kinase Pyk-2 increases BK K^+ channel activity and cell migration in glioblastoma cells. **A.** Immunoblot probed against phospho-(Tyr402)-Pyk-2 (top), total Pyk-2 (middle) and for loading control against β-actin (bottom). Lysates were from an irradiated T98G cell 1 h after irradiation with 0 Gy (left) or 2 Gy (right). **B.** Irradiated T98G cells (0 or 2 Gy, 2-4 h after irradiation) were recorded with the patch-clamp technique applying the whole-cell mode using K-gluconate in the pipette and NaCl in the bath. The voltage-clamp pulse protocol is depicted. **C.** Whole-cell current tracings of a 0 Gy- (upper line) and a 2 Gy (lower line)-irradiated T98G cell recorded before (1^{st} tracings), during application of the Pyk-2 inhibitor PF431396 (1 μM; 2^{nd} tracings), after wash-out (3^{rd} tracings), and after administration of the BK blocker paxilline (5 μM, 4^{th} tracings). **D.** Dependence of the mean (± SE, n = 7-8) whole-cell current densities of 0 Gy (left)- and 2 Gy (right)-irradiated T98G cells on voltage. Records were obtained before (open circles) or during administration of PF431396 (closed triangles, recording as shown in B, C). **E.** Mean (± SE, n = 7-8) PF431396-sensitive current density fractions as calculated by subtracting the current densities of (D) recorded with PF431396 from those obtained under control condition. **F.** Mean (± SE, n = 7-8) conductance densities (as calculated for the outward currents in D between +44 mV and +84 mV voltage as indicated by the grey lines) of 0 Gy- (left) and 2 Gy-irradiated (right) T98G cells recorded in the absence (open bars) or presence (closed bars) of PF431396. **G-H.** Mean (± SE, n = 3-4) impedance (G) as measure of transfilter migration and (H) mean migration velocity (calculated from the data in (G, grey lines) for the first 0.5 h of transfilter migration) of T98G cells irradiated with 0 Gy (open circles/bars) or 2 Gy (closed triangle/bars) and recorded in the absence (black symbols/bars) or presence of PF431396 (1 μM, red symbols/bars. * indicates $p \leq 0.05$, two tailed paired t-test in (D, right) two tailed Welch-corrected t-test in (E) and ANOVA in (H).

For immunoblotting, whole protein lysates were prepared from semiconfluent irradiated (0 or 2 Gy, 1 h after irradiation) T98G cells, proteins were separated by SDS-PAGE and blotted as described (Wolfsperger et al. 2016). Blot membranes were blocked (TBS-Tween/5% milk) and probed overnight at 4°C against Pyk-2 (rabbit polyclonal anti-Pyk-2 antibody, #3292S Cell Signaling Merck-Millipore, Darmstadt, Germany, 1:1000 in TBS-Tween/5% milk), phospho-Pyk2 (rabbit polyclonal anti-phospho (Tyr402)-Pyk-2 antibody, #3291S Cell Signaling, 1:1000 in TBS-Tween/5% milk) and β-actin (mouse anti-β-actin antibody, clone AC-74, Sigma #A2228 1:20,000 in TBS-Tween/5% milk). Antibody binding was detected with a horseradish peroxidase-linked goat anti-rabbit or horse anti-mouse IgG antibody (# 7074 and #7076, respectively; 1:2000 dilution in TBS-Tween/5% milk, Cell Signaling) incubated for 1 h at room temperature and enhanced chemoluminescence (ECL Western blotting analysis system, GE Healthcare/Amersham-Biosciences, Freiburg, Germany). Whole-cell currents were evoked by 11 voltage square pulses (700 ms each) from -66 mV holding potential to voltages between -116 mV and +84 mV delivered in 20 mV increments. Semiconfluent irradiated T98G cells were superfused at 37°C with NaCl solution (see legends to Fig. 2) additionally containing PF431396 (0 or 1 μM), paxilline (0 or 5 μM), and DMSO (0 or 0.1 %). The K-D-gluconate pipette solution contained (in mM): 140 K-D-gluconate, 5 HEPES, 5 $MgCl_2$, 1 K_2-EGTA, 1 K_2-ATP, titrated with KOH to pH 7.4. For transfilter migration, the lower and upper chamber of a CIM-Plate 16 (Roche) were filled with 160 μl (lower chamber) and 100 μl (upper chamber) of RPMI-1640 medium containing 5% and 1% FCS, respectively, equilibrated at 37°C and 5% CO_2 for 30-60 min. The upper and lower chamber additionally contained PF431396 (0 or 1 μM in 0.1% DMSO, Sigma-Aldrich). Irradiated (0 or 2 Gy) T98G cells (40.000) in RPMI-1640/1% FCS were added to the upper chamber. After sedimentation and adherence of the cells (2-3 h after irradiation), migration was analyzed in real-time by measuring the impedance increase between electrodes which

cover the lower surface of the filter membrane and the reference electrode in the lower chamber.

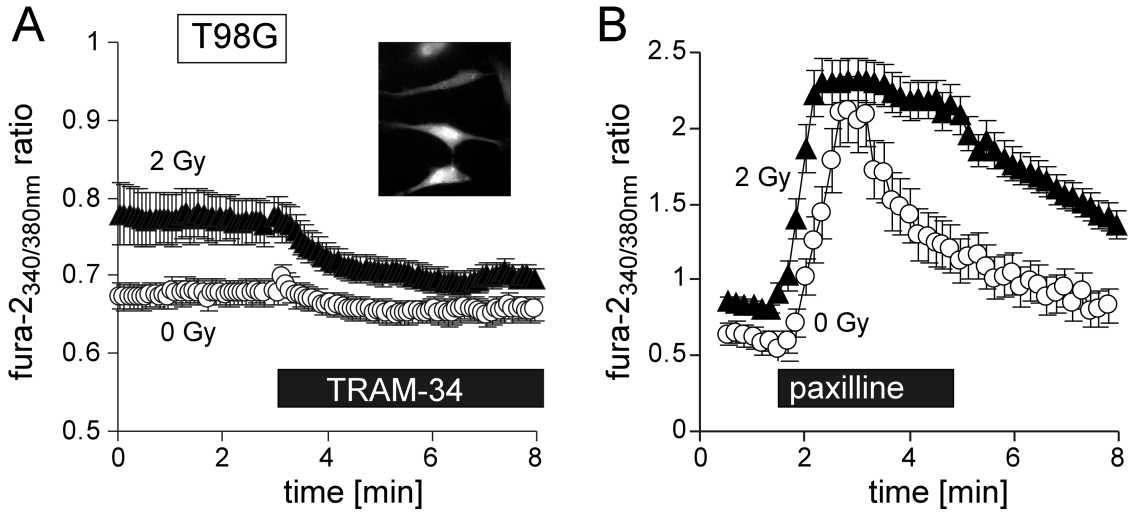

Fig. 4. K^+ channel activity modulates Ca^{2+} signaling in glioblastoma cells. **A-B.** Mean (± SE, n = 24-32 in A and 10-50 in B) fura-2 fluorescence 340/380 nm ratio as measure of cytosolic free Ca^{2+} concentration. Ratios were recorded in 0 Gy (open circles) or 2 Gy (closed triangles)-irradiated semiconfluent T98G cells at 37°C before and during superfusion of the IK K^+ channel blocker TRAM-34 (10 µM in 0.1% DMSO, A) or before, during, and after (wash-out) superfusion of the BK K^+ channel blocker paxilline (2 µM in 0.1% DMSO, B). The insert in (A) shows the immunofluorescence micrograph of fura-2-loaded T98G cells.)

Fura-2 ratiometric Ca^{2+} imaging was performed as described (Klumpp et al. 2016). Semiconfluent T98G cells were superfused at 37 °C with NaCl solution (see legend to Fig. 2) additionally containing the IK K^+ channel inhibitor TRAM-34 (0 or 10 µM in 0.1% DMSO) or the BK channel blocker paxilline (0 or 2 µM in 0.1% DMSO).

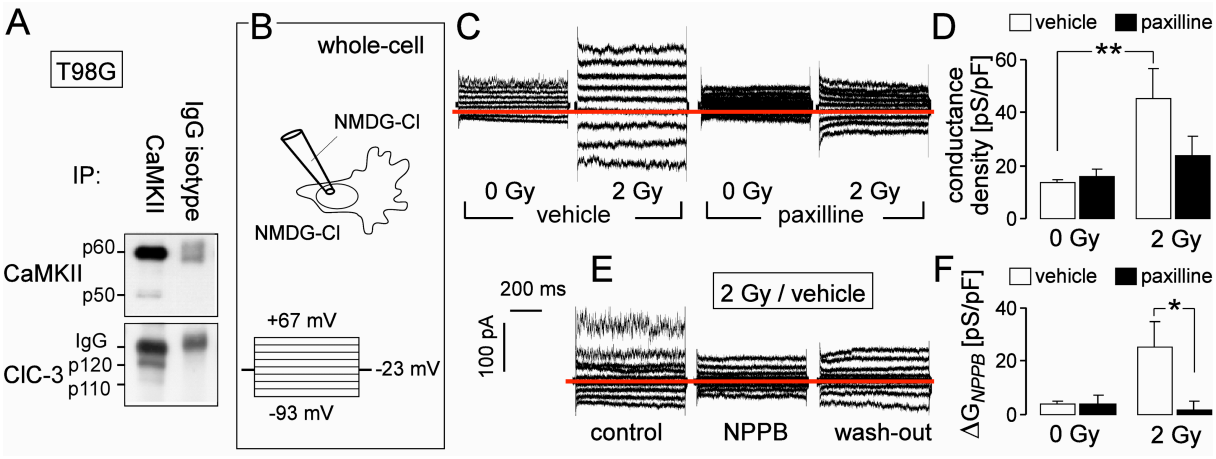

Fig. 5. Radiogenic activation of plasma membrane Cl^- channels in glioblastoma cells depends on BK K^+-channels . **A.** Immunoprecipitation (IP) of CaMKII isoforms co-immunoprecipitates ClC-3 Cl^- channels/Cl^--proton antiporters in T98Gglioblastoma cells. Immunoblots of proteins immunoprecipitated with anti-CaMKII antibody (left lanes) or the respective IgG isotype control (right lanes) probed against CaMKII (upper blot) and ClC-3 (lower blot). **B.** Whole-cell currents of irradiated T98G cells (0 or 2 Gy) were recorded with the impermeable cation N methyl-D-glucamine$^+$ ($NMDG^+$) in bath and pipette solution to isolate Cl^--currents. Cells were irradiated and post-incubated for 3-5 h in cell culture medium containing the BK K^+ channel blocker paxilline (0 or 5 µM in 0.1% DMSO) before recording of the whole-cell currents in the absence of paxilline. Shown is the applied voltage-clamp pulse protocol. **C.** Whole-cell current tracings of a 0 Gy- (1st and 3rd tracings) and a 2 Gy (2nd and 4th tracings)-irradiated T98G cell preincubated with vehicle alone (left) or with paxilline (right). **D.** Mean (± SE, n = 9-27) conductance densities (as calculated for the outward currents between -13 mV and +67 mV) of 0 Gy- (left) and 2 Gy-irradiated (right) T98G cells irradiated and post-incubated in the absence (open bars) or presence (closed bars) of paxilline. **E.** Whole-cell current tracings of a 2 Gy-irradiated vehicle-control cells recorded before (left), during (middle), and after (wash-out, right) superfusion of the anion channel blocker 5-nitro-2-[(3-phenylpropyl)amino]benzoic acid (NPPB, 50 µM). **F.** Mean (± SE, n = 7-17) NPPB-sensitive conductance densities (ΔG_{NPPB}) of 0 Gy- (left) and 2 Gy-irradiated (right) T98G cells irradiated and post-incubated in the absence (open bars) or presence (closed bars) of paxilline. *, and ** indicate $p \leq 0.05$ and $p \leq 0.01$, respectively ANOVA.

For immunopreciptation, cells were lysed and protein (1.6 mg in 800 µl) was precipitated with 5 µg of rabbit polyclonal anti-CaMKII (pan) antibody (3362S, Cell Signaling) or the same amount of rabit IgG isotype antibody (#12-370, Millipore) as described (Wolfsperger et al. 2016). For immunoblotting (non-reducing SDS-PAGE) rabbit polyclonal anti-ClC-3 antibody (ACL-001, Alamone Labs, 1:500 in TBS-Tween/5% milk) and rabbit polyclonal anti-CaMKII (pan) antibody (3362S, Cell Signaling) were used. For patch-clamp recording, T98G cells were irradiated (0 or 2 Gy) and postincubated for 3-5 h in the presence of paxilline (0 or 5 µM in 0.1% DMSO). Whole-currents were evoked by 9 square pulses to voltages from -93 mV to +67 mV delivered in 20 mV increments from a holding potential of -23 mV. A pipette solution containing (in mM) 140 NMDG-Cl (pH 7.4), 40 mannitol, 10 HEPES/NMDG (pH 7.4), 1 MgCl2, 1 Mg-ATP, 0.5 EGTA, was combined with a bath solution containing 180 NMDG-Cl (pH 7.4), 10 HEPES/NMDG (pH 7.4), 1 $CaCl_2$, 1 $MgCl_2$ additionally containing NPPB (0 or 50 µM in 0.1% DMSO, Sigma).

TRPM8-mediated Ca^{2+}-signaling confers radioresistance and promotes migration of glioblastoma cells

Dominik Klumpp[1], Stephanie C. Frank[2,3], Lukas Klumpp[1,4], Marita Eckert[1], Lena Edalat[1,5], Martin Bastmeyer[2,3], Peter Ruth[5], and Stephan M. Huber[1]

[1]Department of Radiation Oncology, University of Tübingen, Tübingen, Germany, [2]Zoological Institute, Department of Cell- and Neurobiology, Karlsruhe Institute of Technology (KIT), Karlsruhe, Germany, [3]Institute of Functional Interfaces, Karlsruhe Institute of Technology (KIT), Eggenstein-Leopoldshafen, Germany, [4]Dr. Margarete Fischer-Bosch-Institute of Clinical Pharmacology, Stuttgart, and University of Tübingen, Tübingen, Germany, [5]Department of Pharmacology, Toxicology and Clinical Pharmacy, University of Tübingen, Tübingen, Germany

Correspondence to:

Stephan Huber
Department of Radiation Oncology
University of Tübingen
Hoppe-Seyler-Str. 3
72076 Tübingen
Germany
Tel.: +49-(0)7071-29-82183
E-mail: stephan.huber@uni-tuebingen.de

Abstract

BACKGROUND: TRPM8 is a Ca^{2+}-permeable nonselective cation channel belonging to the melastatin sub-group of the transient receptor potential (TRP) family. TRPM8 is aberrantly overexpressed in a variety of tumor entities including glioblastoma multiforme where it reportedly may contribute to cancerogenesis, tumor spreading and metastasis, adaptation to hypoxia, or therapy resistance. The present study aimed to disclose the functional significance of TRPM8 in glioma cells in particular upon cell injury by ionizing radiation.

METHODS: TRPM8 channels were stimulated in human glioblastoma cell lines pharmacologically by the cold simulating agents menthol and icilin or inhibited with BCTC or 2-APB. In addition, down- and upregulation of TRPM8 was performed by RNA interference. Glioblastoma cells were irradiated with 0-6 Gy 6 MV photons and TRPM8 channel activity, Ca^{2+} signaling, cell migration, clonogenic survival, apoptotic cell death, and cell cycle control were determined by patch-clamp on-cell recording, fura-2 Ca^{2+} imaging, transfilter migration or wound healing assay, colony formation assay, and flow cytometry, respectively. Moreover, the TCGA data base was queried to expose a dependence of glioma patient survival on TRPM8 mRNA abundance.

RESULTS: TRPM8 channels were required for glioblastoma cell migration and DNA damage response. TRPM8-knock-down slowed-down cell migration, impaired cell cycle regulation, induced apoptotic cell death, and radiosensitized glioblastoma cells. Finally, high TRPM8 abundance in low grade glioma associated with poor patient outcome.

CONCLUSIONS: Combined, our data suggest that TRPM8 channels contribute to malignancy and therapy resistance of glioma and might, therefore, a promising target of future strategies of anti-glioma therapy.

Key words: Radiotherapy, Ca^{2+}-permeable nonselective cation channel, melastatin family of transient-receptor-potential channels, BK Ca^{2+}-activated K^+ channels, patch-clamp recording, transfilter migration, wound healing assay, colony formation assay, CaspACE, propidium iodide, EdU incorporation

Background

The melastatin family member 8 (M8) of the transient receptor potential (TRP) nonselective cation channels has been originally identified as a cancer-associated gene in prostate carcinoma [1]. Meanwhile, there is increasing evidence that many tumor entities such as glioblastoma multiforme [2] highly overexpress TRPM8 channels. Aberrantly expressed TRPM8 channels have been proposed to contribute to epithelial-mesenchymal-transition and metastasis of breast cancer [3], growth and metastasis of pancreatic adenocarcinoma [4], adaptation to hypoxia of prostate cancer [5], metastasis and chemotherapy resistance of osteosarcoma [6], poor prognosis of urothelial carcinoma [7], cancerogenesis of colon carcinoma [8], and migration of glioblastoma cells [9, 10]. Besides these malignancy-associated functions, TRPM8 reportedly suppresses survival of melanoma cells [11]. In addition, TRPM8 is highly upregulated in an early, differentiated stage but downregulated during malignant progression of prostate cancer [1, 12, 13] which might suggest that TRPM8 rather suppresses than promotes malignant progression in these tumor entities. Moreover, overexpression of TRPM8 in glioblastoma has been associated with better clinical outcome [2] again pointing rather to a tumor-suppressing function of TRPM8.

While in normal skin and peripheral neurons TRPM8 functions as a cold sensor (for review see [14]), the functions of TRPM8 in non-temperature-sensing organs such as normal prostate epithelium are not well defined. Reportedly, TRPM8 acts as an ionotropic testosterone receptor in the plasma membrane of prostate epithelium [15, 16] or osmosensor in peripheral neurons [17]. Similarly poorly understood are the mechanisms leading to upregulation of TRPM8 in cancer cells. In prostate cancer, TRPM8 gene [13] and surface expression [18] are up-regulated by androgens, in breast cancer by estrogens [19].

Glioblastoma multiforme infiltrates the brain in a diffuse and net-like manner which confines complete surgical resection and adequate coverage by radiotherapy of the tumor. The highly migrating behavior of glioblastoma cells together with a high intrinsic resistance to radio- and chemotherapy, most probably accounts for therapy failure and bad prognosis of glioblastoma patients (for review see [20]). Glioblastoma migration is reportedly motorized by a local cell volume increase and decrease at the lamellipodium and the opposite cell pole which extrudes the leading edge and retracts the cell rear, respectively. Ca^{2+}-activated IK and BK channels exert a key role in this process pointing to a pivotal function of Ca^{2+} signaling for programming of migration (for review see [21]). Moreover, ionizing radiation at doses used for single fractions of fractionated radiotherapy in the clinic has been shown to induce Ca^{2+} signals that are sufficient to activate BK and IK K^+ channels and to induce migration of glioblastoma cells [22-24]. In addition, radiation-induced activation of IK channels has been demonstrated to be required for cell cycle arrest and DNA repair since inhibition of IK radiosensitizes glioblastoma cells [23].

Activation of TRPM8 channels by menthol reportedly stimulates BK channel activity and migration of glioblastoma cells [9, 10] suggesting that TRPM8 functions as Ca^{2+} entry pathway in glioblastoma cells. Therefore, the present study aimed to define *in vitro* the functional significance of TRPM8 for the Ca^{2+} signaling in glioblastoma cells involved on the one hand in cell migration and chemotaxis and on the other in the stress response to DNA damage by ionizing radiation. Our data strongly suggest that TRPM8 contributes to both, migration and radioresistance of glioblastoma cells.

Methods

Cell Culture. Human WK1, T98G, U373, A172, U-87MG, and DBTRG glioblastoma cells were grown in 10% fetal calf serum (FCS)-supplemented RPMI-1640 medium, human U251 glioblastoma cells in DMEM (4500 mg glucose/l)/10% FCS medium. Exponential growing T98G, U251 and U-87MG-Katushka cells were irradiated with 6 MV photons (IR, single dose of 0, 2, 4 and 6 Gy) or five daily fractions of 0 or 2 Gy (fractionated IR) by using a linear accelerator (LINAC SL25 Philips) at a dose rate of 4 Gy/min at room temperature. Following IR, cells were post-incubated in the respective cell culture media for 1.5-3 h (fura-2 Ca^{2+}-imaging), 24 h (RT-PCR, CaspACE flow cytometry), 48 h (flow cytometry, Nicoletti protocol), 54 h (EdU incorporation), or 2-3 weeks (colony formation assay).

Querying The-Cancer-Genome-Atlas (TGCA) data sets. Via the cBIOportal Web resource [25, 26], the provisional Glioblastoma-Multiforme and Lower-Grade-Glioma TCGA databases (http://cancergenome.nih.gov/) were queried for TRPM8 mRNA abundance of the tumor specimens and progression free and overall survival of the glioma patients. Statistical analysis was performed with log-rank test. To assess TRPM8- , CXCR4- and IK mRNA abundances in low grade and high grade gliomas, RNA sequencing data (Illumina HiSeq 2000 RNA Sequencing platform) were received from the file TCGA_KIRC_exp_HiSeqV2-2015-02-24, downloaded on 2015-10-20 via the Cancer Genomics Browser. The file contained log2(x+1)-transformed data for n (low grade) and N (high grade) gliomas on 20,530 genes. Here, x are RSEM (RNA-Seq by Expectation Maximization) expression estimates, which were normalized to set the upper quartile count at 1000 (for details, vide http://cancergenome.nih.gov/ and https://genome-cancer.soe.ucsc.edu/proj/site/hgHeatmap.

Patch-clamp recording. On-cell currents of semi-confluent T98G cells were elicited by 41 voltage square pulses (700 ms each) delivered in 5 mV increments from 0 mV holding potential to voltages between -100 mV and +100 mV. Voltages refer to the intracellular face of the plasma membrane. Flow of positive charge out of the cells (or the counter flow of anions) is defined as positive current and depicted as upward deflection of the current tracings. Cells were superfused at 37°C. with NaCl solution (in mM: 125 NaCl, 32 N-2-hydroxyethylpiperazine-N-2-ethanesulfonic acid (HEPES), 5 KCl, 5 D-glucose, 1 $MgCl_2$, 1 $CaCl_2$, titrated with NaOH to pH 7.4). This NaCl solution was also used for the pipette solution further containing 0 or 10 µM icilin (in 0.1% DMSO). Macroscopic on-cell currents were analyzed by averaging the currents between 100 and 700 ms of each square pulse.

Transfection. Exponentially growing U251 and T98G cells were reversely transfected with stealth siRNAs (Thermo Fischer Scientific, Waltham, MA, U.S.A) specific for TRPM8 (HSS128188, HSS128189, HSS128190) and MSI1 (Musashi-1, HSS106732, HSS106733, HSS106734), or with nt siRNA (*Silencer*® Select Negative Control No. 1 siRNA, #4390844, Ambion™, Thermo Fischer Scientific). Detached T98G and U251 cells (250.000 in 2.5 ml RPMI-1640/10% FCS and DMEM (4500 mg glucose/l)/10% FCS medium, respectively) were added to 500 µl of pre-incubated (20 min/RT) Opti-MEM medium containing RNAiMAX lipofectamine (6 µl, Invitrogen Life Technologies, Carlsbad, CA, USA) and siRNA (25 nM final concentration).

Migration assays. For cell migration during wound healing, control (T98G, U-87MG) and TRPM8- or nt siRNA-treated (T98G) glioblastoma cells were plated in 35 mm dishes (120.000 cells per insert) with culture inserts (Ibidi, Martinsried, Germany). After monolayer formation, cells were pretreated (30 min) with TRPM8 activator icilin or inhibitor N-(4-tert-butylphenyl)-4-(3-chloropyridin-2-yl)piperazine-1-carboxamide (BCTC, both 0 or 10 µM in

0.1% DMSO) in phenol red-free 20 mM HEPES (pH 7.4)-supplemented RPMI-1640 medium. Migration assay was started by removing the inserts to create a wound of approximately 500 µm in width. Thereafter (0 -18 h), 3 fields of the wound were photographed with an inverse light microscope every 30 min (Axio Observer.Z1, 10x, Zeiss, Jena). For each field 5 cells were tracked (Manual Tracking, ImageJ) and the velocity was calculated.

For transfilter migration, the lower and upper chamber of a CIM-Plate 16 (Roche, Mannheim, Germany) were filled with 160 µl (lower chamber) and 100 µl (upper chamber) of RPMI-1640 medium containing 5% and 1% FCS, respectively, equilibrated at 37°C and 5% CO_2 for 30-60 min. After CO_2 equilibration and resetting the impedance to zero, 100 µl of cell suspension containing 40.000 of control (U251 or T98G) or TRPM8- or nt siRNA-treated (T98G) cells in RPMI-1640/1% FCS were added to the upper chamber. After sedimentation and adherence of the cells (2-3 h after IR), migration was analyzed. The upper and lower chamber additionally contained icilin, 2-aminoethoxydiphenyl borate (2-APB) and BCTC (all 0 or 10 µM in 0.1% DMSO). Transfilter migration was assessed by measuring the electrical impedance increase between electrodes which cover the lower surface of the filter membrane (i.e., the bottom of the upper chamber) and the reference electrode at the bottom of the lower chamber. Upon transfilter migration, cells adhere to the electrode at the lower surface of the filter membrane and, thereby, increase the impedance.

Quantitative RT-PCR. Messenger RNAs of WK1, T98G, U373, A172, U-87MG, DBTRG and U251 cells, of fractionated irradiated (5 x 0 Gy or 5 x 2 Gy) T98G, U251 and U-87MG cells (24 h after the last IR fraction), as well as of TRPM8 siRNA-, MSI1 siRNA- or nt siRNA-transfected U251 and T98G cells (48-72 h after transfection) were isolated (Qiagen RNA extraction kit, Hilden, Germany) and reversely transcribed in cDNA (Transcriptor First Strand cDNA Synthesis Kit, Roche, Mannheim, Germany). TRPM8-, TRPV1-, TRPV2-, TRPC6-, and housekeeper glyceraldehyde-3-phosphate dehydrogenase (GAPDH)-specific fragments were amplified by the use of SYBR Green-based quantitative real-time PCR (QT00038906, QT00046109, QT00035987, QT00037660, and QT00079247 QuantiTect Primer Assay and QuantiFast SYBR® Green PCR Kit, Qiagen) in a Roche LightCycler Instrument. Abundances of the individual mRNAs were normalized to the GAPDH housekeeper mRNA.

Colony formation assay. To test for clonogenic survival, TRPM8-, MSI1-, or nt siRNA-transfected U251 and T98G cells (24 h (MSI1) and 48 h (TRPM8)) were irradiated (0, 2, 4 or 6 Gy) in the respective cell culture media. Twenty-four h after IR, 400 and 600 (T98G) or 1200 (U251) cells were re-seeded on 6-well plates and grown for further 2-3 weeks. The plating efficiency was defined by dividing the number of colonies by the number of plated cells. Survival fractions as calculated by dividing the plating efficiency of the irradiated cells by those of the unirradiated controls were fitted by the use of the linear quadratic equation.

Fura-2 fluorescence imaging of $_{free}[Ca^{2+}]_i$. Fluorescence measurements were performed at 37°C using an inverted phase-contrast microscope (Axiovert 100; Zeiss, Oberkochen, Germany). Fluorescence was evoked by a filter wheel (Visitron Systems, Puchheim, Germany)-mediated alternative excitation at 340/26 or 387/11 nm (AHF, Analysentechnik, Tübingen, Germany). Excitation and emission light was deflected by a dichroic mirror (409/LP nm beam splitter, AHF) into the objective (Fluar x40/1.30 oil; Zeiss) and transmitted to the camera (Visitron Systems), respectively. Emitted fluorescence intensity was recorded at 587/35 nm (AHF). Excitation was controlled and data acquired by Metafluor computer software (Universal Imaging, Downingtown, PA, USA). The 340/380-nm fluorescence ratio was used as a measure of cytosolic free Ca^{2+} concentration ($_{free}[Ca^{2+}]_i$). Irradiated (0 or 2 Gy, 1.5-3 h after IR) T98G cells and TRPM8- , MSI1- or nt siRNA-transfected U251 cells (24 h

(MSI1) and 48 h (TRPM8)) were incubated with fura-2/AM (2 µM for 30 min at 37°C; Molecular Probes, Goettingen, Germany) in RPMI-1640/10% FCS and DMEM/10% FCS medium, respectively. In irradiated T98G cells, fura-2 fluorescence ratios were measured during superfusion with EGTA-buffered Ca^{2+}-free NaCl (in mM: 125 NaCl, 32 HEPES, 5 KCl, 5 D-glucose, 1 $MgCl_2$, 0.5 EGTA, titrated with NaOH to pH 7.4) solution and upon wash-in of Ca^{2+} in NaCl ringer (in mM: 125 NaCl, 32 HEPES, 5 KCl, 5 D-glucose, 1 $MgCl_2$, 2 $CaCl_2$, titrated with NaOH to pH 7.4) additionally containing menthol (100 µM). In transfected U251 cells, steady state ${}_{free}[Ca^{2+}]_i$ was recorded in Ca^{2+}-containing NaCl solution before and during superfusion of icilin (10 µM).

Flow cytometry. To determine the caspase activity after irradiation T98G and U251 cells were transfected with TRPM8- or nt-siRNA, irradiated (48 h after transfection, 0 or 4 Gy) and incubated for further 24 h in the respective cell culture media. CaspACE ^{TM} FITC-VAD-FMK *In Situ* Marker was added directly to the medium (5 µM) and incubated for 30 min at room temperature. CaspaACE-specific fluorescence was measured by flow cytometry (FACS Calibur, Becton Dickinson, Heidelberg, Germany, 488 nm excitation wavelength) in fluorescence channel FL-1 (log scale, 515-545 nm emission wavelength).

For cell cycle analysis, irradiated TRPM8- or nt-siRNA transfected T98G and U251 cells (0 or 4 Gy, 48 h afer IR and 96 h after transfection) were permeabilized and stained (30 min at room temperature) with propidium iodide (PI) according to the Nicoletti protocol (containing 0.1% Na-citrate, 0.1% triton X-100, 10 µg/ml PI in phosphate-buffered saline, PBS), and the DNA amount was analyzed by flow cytometry in fluorescence channel FL-3 (>670 nm, linear scale). Data were analyzed with the FCS Express 3 software (De Novo Software, Los Angeles, CA, USA).

For EdU incorporation, , irradiated TRPM8- or nt-siRNA transfected T98G and U251 cells (0 or 4 Gy, 48 h afer IR and 96 h after transfection) were incubated for further 6 h in the respective cell culture media additionally containing the base analogon 5-ethynyl-2'-deoxyuridine (EdU, 5 µM). EdU incorporation was analyzed by the use of a EdU flow cytometry kit (BCK-FC488, baseklick, Tutzing, Germany) after fixing the cells and co-staining the DNA with propidium iodide (PI, Sigma-Aldrich) according the manufacturer's instructions. EdU- PI specific fluorescence were recorded by flow cytometry in fluorescence channel FL-1 (log scale) and FL-3 (linear scale), respectively.

Results

Glioma overexpress TRPM8. Glioblastoma reportedly upregulate TRPM8 channels [2]. The present study queried The-Cancer-Genome-Atlas (TCGA) to expose the dependence of TRPM8 mRNA abundance on disease-free (DS) and overall survival (OS) of low grade glioma and glioblastoma patients. Moreover, TCGA TRPM8 mRNA abundances were compared between low grade glioma and glioblastoma and associated with those of the Ca^{2+}-activated IK K^+ channel and the chemokine receptor CXCR4. IK [23] and CXCR4 [27, 28] have been associated with therapy resistance and poor prognosis in glioblastoma. As a result, high TRPM8 mRNA abundance in low grade glioma was associated with shorter DS and OS of the patients ($p \leq 0.0000001$, log rank test, Fig. 1A, B). In particular, low grade glioma without mutations in isocitrate dehydrogenas-1 (IDH1) exhibit significant higher TRPM8 mRNA abundance as compared to low grade glioma with IDH1 mutations (Fig. 1C). In glioblastoma specimens (n = 528), in contrast, which exhibited TRPM8 upregulation similarly to the low grade gliomas without IDH1 mutations (Fig. 1C), no dependence of patient DS or OS on TRPM8 mRNA abundance was evident (data not shown). However, TRPM8 mRNA expression by the glioblastoma specimens seemed to be weakly but significantly ($p \leq 0.05$) associated with that of CXCR4 and moderately associated with that of IK ($p \leq 0.01$). The associations with these proposed malignancy markers were in particular higher (reaching Pearson coefficients of 0.33 and 0.51 for CXCR4 and IK, respectively) in glioblastoma patients treated with the standard therapy protocol [29] (Fig. 1D).

TRPM8 generates a Ca^{2+} entry pathway and promotes cell migration. We started our experiments by determining the TRPM8 mRNA expression in different human glioblastoma cell lines by real time RT-PCR. Among TRPV1 and -V2 mRNA (Fig. 1E), TRPM8 mRNA could be detected in human glioblastoma lines at different abundances (Fig. 1F). Cell lines with relatively high (U251 and U-87MG) and low (T98G) TRPM8 mRNA abundance were chosen for further studies. First, we tested for functional expression of TRPM8 by on-cell patch-clamp recording.

To this end, glioblastoma cells were stimulated with the TRPM8 agonist icilin and activation of the Ca^{2+}-activated BK K^+-channels was used as a surrogate marker for TRPM8-mediated Ca^{2+} entry into the cells. As shown in Fig. 2A-D, icilin induced a macroscopic outward current in T98G cells when recorded with NaCl in pipette and bath solution. This current was generated by channels with a unitary conductance of about ~200 pS (Figs. 3A-C). The negative reversal potential of the current amplitude which can be extrapolated from the current amplitude-voltage relationship in Fig 3C indicated K^+ selectivity of the 200 pS channels. Under control conditions, channel activity occurred at depolarized voltages (Fig 3A, D) and open probability increased with increasing positive clamp-voltage (Fig 3D, open circles). The high unitary conductance, the K^+-selectivity, and the typical voltage-dependence proved the channels as BK K^+ channels.

Icilin induced channel activity already at negative voltages (Fig 3B), a left shift of the open probability voltage relationship (Fig 3D, closed triangles) and changed the mean voltage of activation from +30 mV (control) to -15 mV clamp-voltage (Fig 4E). Stimulation by icilin did not affect the unitary conductance of the channels (Fig 3F). Together, these data indicate icilin-induced activation of Ca^{2+}-dependent BK K^+ channels suggestive of functional expression of TRPM8 channels in the plasma membrane of T98G cells.

Experimental TRPM8-upregulation and TRPM8 knock-down. In U251 cells, transfection with siRNA specific for the mRNA-binding protein MSI1 (Musashi-1) was paralleled by an

increase in TRPM8 mRNA abundance (Fig.4A), a phenomenon which could not be defined mechanistically. Nevertheless, MSI1 knock-down was harnessed for experimental upregulation of TRPM8 in further functional studies. In addition, U251 and T98G were transfected with TRPM8 siRNA which reduced TRPM8 mRNA abundance by more than (U251) and below (T98G) 50% (Fig. 4B, C). In U251 cells, the functional significance of TRPM8 up- and downregulation for icilin-stimulated Ca^{2+} entry was confirmed by fura-2 Ca^{2+} imaging. TRPM8 upregulation and knock-down significantly in- and decreased menthol (100 μM)-induced rise in intracellular free Ca^{2+} concentration indicating both, effectiveness of the transfection protocols and functional expression of TRPM8 in the plasma membrane of glioblastoma cells (Fig. 4D, E).

TRPM8 promotes cell migration. TRPM8 agonists have been reported previously to stimulate migration of glioblastoma cells [9, 10]. Therefore, we tesed in our glioblastoma models whether cell migration and chemotaxis depend on TRPM8 channel activity. As shown in Fig. 5A-D, TRPM8 activation by icilin tended to increase (U-87MG) or significantly (T98G) increased the migration speed in wound healing assays while TRPM8 inhibition by BCTC (U-87MG and T98G) or downregulation by RNA interference (T98G) significantly reduced the migration velocity. Similarly, TRPM8 channel activation by icilin tended to increase and TRPM8 channel inhibition by 2-APB and BCTC or downregulation by RNA interference significantly decreased transfilter chemotaxis as induced by a fetal calf serum (FCS) gradient (Fig. 5E-H). Combined, these data clearly indicated a cell migration-stimulating role of TRPM8 channels in the human glioblastoma lines.

Ionizing radiation induces TRPM8 upregulation. In order to characterize any function of TRPM8 for radioresistance, T98G and U251 glioblastoma cells were fractionated irradiated with single doses of 2 Gy photons as used in the standard radiotherapy of glioblastoma patients. Radiation-induced changes in expression and function of TRPM8 were assessed by real time PCR and fura-2 Ca^{2+} imaging, respectively. As shown in Fig. 6A-D, fractionated irradiation (5 x 2 Gy) induced a significant increase in TRPM8 mRNA abundance in T98G and U251 cells and a not quite significant increase in U-87MG cells. The latter cell line showed highest basal TRPM8 mRNA abundance (see Fig. 1F). Moreover, a single dose (2Gy) of ionizing radiation already evoked within 2 h an increase in menthol-stimulated Ca^{2+} influx into T98G cells as recorded by fura-2 imaging applying a Ca^{2+}-depletion/repletion protocol (Fig. 6E, F). Together, these data suggest that ionizing radiation may stimulate TRPM8 expression and function in glioblastoma cells.

TRPM8 confers radioresistance. To discriminate, whether this radiation-induced TRPM8 stimulation is an epiphenomenon of DNA damage response or has functional significance for the survival of irradiated glioblastoma cells, TRPM8 was knocked-down in U251 and T98G cells by RNA silencing. Moreover, TRPM8 was upregulated in U251 cells by MSII knock-down (see Fig. 4). Cells with unchanged (non-targeting siRNA) and down-regulated TRPM8 activity (U251, T98G) as well as up-regulated TRPM8 expression (U251) were then tested for clonogenic survival and radioresistance in colony formation assays. For the latter, 0 - 6 Gy-irradiated cells were delayed-plated 24 h after irradiation. Notably, TRPM8 knock-down radaisensitized both glioblastoma lines (Fig. 7A, B). In particular, TRPM8 knock-down diminished the survival fraction at 2 Gy by some 30% in U251 (Fig. 7C) and 10% in T98G cells (Fig. 7D). Moreover, TRPM8 knock-down lowered the plating efficiency of U251 and T98G cells by 30% (Fig. 7E) and 60% (Fig. 7F), respectively. *Vice versa*, TRPM8-upregulated U251 cells (MSI1 knock-down) exhibited higher radioresistance (Fig. 7A, C) but lower plating efficiency (Fig. 7E) than non-targeting siRNA-transfected U251 control cells. In

summary, these experiments strongly suggest a pivotal function of TRPM8 channels for the clonogenicity and radioresistance of glioblastoma cells.

TRPM8 knock-down results in caspase activation. To test whether TRPM8 activity is required for cell survival, caspase activity was determined upon TRPM8 knock-down in T98G and U251 cells 24 h after irradiation with 0 or 4 Gy by measuring the active-caspase-dependent caspACE fluorescence intensity in flow cytometry (Fig. 8A). TRPM8 knock-down increased the fraction of cells with detectable caspase activity by a factor of three in both cell lines (Fig. 8B, C) suggesting a survival function of TRPM8. Importantly, effects of irradiation and TRPM8 knock-down on caspase activation were only (T98G, Fig. 8B) or not even (U251, Fig. 8C) additive suggesting that further mechanisms probably underlie the observed TRPM8-conferred radioresistance (see Fig. 7). We, therefore, characterized the effect of TRPM8 knock-down in irradiated T98G and U251 on cell cycle control as analyzed 48 h after irradiation.

TRPM8 function is required for S phase progression and mitosis. To this end, the cellular DNA content was measured in permeabilized glioblastoma cells by flow cytometry using the fluorescence dye propidium iodide (Nicoletti protocol, Fig. 9A). In both cell lines, irradiation increased the G_2 and S and decreased the G_1 population (compare 1st and 2nd bars of the first three diagrams in Fig 5B, C). Combined, these results suggest a radiation-induced S- and G_2/M arrest in both glioblastoma cell lines.

Although not always reaching significance, TRPM8 knock-down exerted in both glioblastoma lines similar effects on cell cycle: TRPM8 knock-down showed the tendency to augment both, the radiation-induced rise of the G_2 and the shrinkage of the G1 population. At the same time, TRPM8 knock-down blunted (U251) or abolished (T98G) the radiation-induced accumulation in S phase (Fig. 9B, C, first three diagrams) and increased the hyper G population exclusively (U251) or in a pronounced manner (T98G) in irradiated cells (Fig. 9B, C, last diagrams). The hyper G population presents cells with elevated DNA content. An increase in this population, therefore, hints to an impairment of mitosis or cytokinesis upon TRPM8 knock-down. Such impairment might be consistent with the observed pronounced increase in G_2 and decrease in G_1 population that was associated with TRPM8 knock-down. To directly test for a function of TRPM8 for the re-entry in mitosis and cell division upon radiation-induced cell cycle arrest, T98G and U251 cells were irradiated (0 or 4 Gy) and post-incubated for 48 h. Thereafter, 5-ethynyl-2′-deoxyuridine (EdU) was incubated for 8 h before EdU incorporation into the DNA and DNA content was determined by flow cytometry (Fig. 10A).

Irradiation (1st and 2nd bars in Fig. 10B, C) resulted in both cell lines in an increase in EdU-negative S and G_2 phase cells and in a decrease of EdU-negative G_1 cells (Fig. 10B, C, 1st-3rd diagrams) while having no effect on the S and G_2 phase cells that incorporated EdU (Fig. 10B, C, 4th-5th diagrams). The latter observation suggests that G_1/S transition and S phase progression (i.e., DNA replication) seemed to be restored to levels of unirradiated cells already 48-56 h after irradiation with 4 Gy. In both cell lines TRPM8 knock-down further increased the EdU-negative S and G_2 phase cells and decreased the EdU-negative G_1 population mostly in both, irradiated and unirradiated cells (compare 1st with 3rd and 2nd with 4th bars in Fig. 10B, C, 1st-3rd diagrams). This parallel increase and decrease in EdU-negative G_2 and G_1 population, respectively, again (see Fig. 9) points to a role of TRPM8 in mitosis. Moreover, the TRPM8 knock-down-associated increase in EdU-negative S cells hints to an additional function of TRPM8 in S phase progression.

Consistent with elevated EdU negative populations, TRPM8 knock-down diminished the EdU-positive S and G_2 populations (Fig. 10B, C, 4th and 5th diagrams). Computing the ratio between EdU-positive and EdU-negative cells revealed that irradiation alone did not alter this ratio in U251 and T98G cells (compare 1st and 2nd bar in Fig. 10D, E) again pointing to a restored DNA replication 48-56 h after irradiation. TRPM8 knock-down, in contrast, decreased the ratio between EdU-positive and EdU-negative cells (compare 1st and 3rd bars in Fig. 10D, E). In U251, but not in T98G cells, combined irradiation and TRPM8 knock-down further decreased this ratio (compare 3rd and 4th bar in Fig. 10D, E). In summary, these data suggest a functional significance of TRPM8 channels in cell cycle control of unirradiated glioblastoma cells. At least in U251 cells, TRPM8 knock-down increased the hyperG population specifically in irradiated cells (see Fig. 9 B, 4th diagram) and exerted supra-additive effects with irradiation on EdU incorporation into the DNA (see Fig. 10D) further suggesting TRPM8 function in the cell cycle management of irradiated cells.

Discussion

The present study confirms previous data showing that TRPM8 channels constitute a Ca^{2+} entry pathway in glioblastoma cells and that TRPM8 channel activity stimulates glioblastoma cell migration. The new findings of our study are that ionizing radiation in doses used in the clinic for fractionated radiation therapy of glioblastoma patients induces upregulation of TRPM8 and that elevated TRPM8 channel function, in turn, confers radioresistance. The latter might result from the observed dependence of cell cycle control during DNA damage response on TRPM8-mediated Ca^{2+} signaling.

Radiation-induced Ca^{2+} signaling. In addition to glioblastoma, chronic myeloid and T cell leukemia cells have been reported to respond to ionizing radiation with Ca^{2+} signaling that utilizes Ca^{2+}-permeable TRP channels [30, 31]. These TRP channels have been suggested to regulate cell cycle progression and contribute to survival in concert with voltage-gated Kv3.4 [32] or Ca^{2+}-activated IK K^+ channels [31]. By re- or hyperpolarizing the plasma membrane, voltage-gated or Ca^{2+}-activated K^+ channels counteract Ca^{2+} entry-generated membrane depolarization. By doing so, these K^+ channels maintain locally in close vicinity to a Ca^{2+} entry pathway a high inwardly directed electrochemical Ca^{2+} gradient across the plasma membrane and regulate the activity of voltage-gated or voltage-dependent Ca^{2+} entry pathways. Therefore, these K^+ channels are important players of the Ca^{2+}-signalosome (for review see [20]).

Interaction between TRPM8, IK and BK channels. In glioblastoma, ionizing radiation has been shown to activate BK [22] and IK Ca^{2+}-activated K^+ channels [23]. Activities of both channels signal back to Ca^{2+} or biochemical signaling. For instance, radiation-induced BK electrosignaling has been demonstrated to be pivotal for the activation of downstream Ca^{2+} effector proteins such as the Ca^{2+}/calmodulin kinase-II isoforms and glioblastoma cell migration [22]. Radiation-induced IK electrosignaling, on the other hand, is reportedly required for cell cycle control, DNA damage repair and clonogenic survival [23]. Since TRPM8 function - as suggested by the present study - seems to be needed for both, migration and survival of irradiated cells it is tempting to speculate that IK and BK closely interact with TRPM8 in glioblastoma cells. The cation permeability of the strongly outwardly rectifying TRPM8 channels (for review see [14]) decreases with hyperpolarizing voltages. Therefore, a plausible scenario might be that IK and BK channel activities hyperpolarize the plasma membrane and shut down TRPM8 channel-mediated Ca^{2+} influx. Decrease of Ca^{2+} influx, however, deactivates the Ca^{2+}-activated BK and IK channels resulting in membrane re-depolarization. Depolarization again increases TRPM8-mediated Ca^{2+}-entry and reactivation of the K^+ channels. Thus, reciprocal and interdependent activity of IK, BK, and TRPM8 may generate membrane voltage and Ca^{2+} oscillations specifically recognized by certain Ca^{2+} effector proteins such as CaMKII isoforms (for review see [20]). CaMKIIs reportedly regulate glioblastoma cell migration [22, 33, 34] and mitosis [35].

TRPM8 activation in glioblastoma cells. In brain tumors, TRPM8 channels are not exposed to low temperature. In addition, our experimental settings (e.g, migration, colony formation assays) did not subject the cells to any changes in osmolarity, suggesting that the documented osmosensing function of TRPM8 [17] can also not account for the observed TRPM8 activity in glioblastoma cells. TRPM8 channel function is reportedly modulated by G-protein coupled receptors [36], phosphoinosites [14], serine/threonine [37] and tyrosine kinases/phosphatases [38], as well as UBA1-dependent ubiquitination [18]. Moreover, protein-protein interactions with the two-transmembrane domain protein Pirt [39] and the TRP channel-associated factors (TCAFs) [40] reportedly promote trafficking and/or modulate activity of TRPM8. Finally,

picomolar concentrations of testosterone have been shown to stimulate openings of the purified TRPM8 channel protein in planar lipid bilayers [15]. Combined, these data suggest a highly complex regulation of TRPM8 surface expression and activity which might shift the set point of temperature-dependent activation towards body temperature. The exact molecular mechanisms leading to activation of TRPM8 in glioblastoma, however, are far from being understood.

Upregulation of TRPM8 expression by glioblastoma cells. Reportedly, TRPM8 is a target gene of the androgen receptor and p53 [13, 18]. The documented upregulation of the androgen receptor in glioblastoma [41] might therefore contribute to TRPM8 overexpression in the brain tumor. In U251 glioblastoma cells, downregulation of musashi-1 (MSI1) was associated with upregulation of TRPM8 (see Fig. 4A). This might hint to a possible negative regulation of TRPM8 by the RNA binding protein musashi-1. Querying the Cancer-Genome-Atlas for MSI1 and TRPM8 mRNA abundances, however, did not confirm such an association in glioblastoma patient specimens (data not shown) suggesting that this phenomenon is restricted to U251 cells. In the present study, TRPM8 mRNA abundance increased significantly in T98G and U251 glioblastoma cells and not quite significantly in U-87MG cells during fractionated radiation (see Fig. 6A-D). This suggests either selection of TRPM8 overexpressing and resistant glioblastoma cell clones or an adaptative response. The latter might in theory result from stabilization of p53. U251, which are p53-mutated, however, show similar fractionated radiation-induced increase in TRPM8 as heterogeneous p53 wildtype/mutated T98G cells and a higher increase than p53 wildtype U-87MG cells, an observation which does not support a p53-mediated TRPM8 upregulation.

Possible TRPM8 functions in malignant progression of glioma. TRPM8 knock-down radiosensitized the T98G and U251 cells in our colony formation assays which might classify TRPM8 as resistance factor. In addition, glioblastoma migration required in the present study TRPM8 function. Since the spreading of glioblastoma in the brain contributes to the high malignancy of the tumor, TRPM8 might also be thought of a malignancy factor. As a matter of fact, high TRPM8 abundance in specimens of low grade glioma associated with bad prognosis (see Fig. 1A, B). Although neither subgroup analysis of the patients, nor multivariate testing nor validation by a second patient cohort could be performed, these data might hint to a possible prognostic value of TRPM8. Such value might be supported by the observation that low grade glioma specimens with wildtype IDH1 showed significant higher TRPM8 mRNA expression than those with IDH1 mutations (but similar high TRMP8 abundances as glioblastoma specimens. see Fig. 1C) since IDH1 mutations in low grade gliomas are associated with better prognosis than non-IDH1-mutated low grade gliomas [42].

Association of TRPM8 with CXCR4 chemokine receptor and IK K^+ channels. In patient-derived glioblastoma specimens, TRPM8 mRNA abundance positively correlated with those of the IK K^+ channel and the CXCR4 chemokine receptor (see Fig. 1D). Reportedly, IK confers radioresistance [23] and is required for glioblastoma brain infiltration [34, 43, 44]. CXCR4 has been proposed as biomarker of radioresistant cancer stem cells and is associated with poor prognosis (for review see [27, 28]). Thus, one might speculate that TRPM8 expression possibly is associated with a highly migratory and therapy-resistant glioblastoma phenotype. In sharp contrast to this assumption, a recent study enrolling 33 glioblastoma patients suggests that longer overall survival associates with high TRPM8 mRNA abundance in the glioblastoma specimens [2]. In the present study, querying TCGA data from 528 glioblastoma specimens did not confirm such an association (data not shown).

Conclusions

The present *in vitro* study proposes a possible functional significance of Ca^{2+}-permeable TRPM8 nonselective cation channels for glioblastoma brain spreading and radioresistance. Targeting TRPM8 alone or in combination with radiotherapy might, therefore, become a promising new strategy for future anti-glioblastoma therapy. New and more specific pharmacological TRPM8 inhibitors are available [45, 46], antagonizing antibodies binding to extracellular TRPM8 protein have been developed [47] suggesting that TRPM8-targeting therapy is theoretically feasible. Whether or not TRPM8-targeting alone or in combination with radiotherapy has tolerable side effects and does effectively prolong survival has to await future preclinical studies in orthotopic glioblastoma animal models.

Declarations

Ethics approval and consent to participate. Not applicable
Competing interests. The authors declare no conflict of interest.
Funding. This work has been supported by a grant from the Wilhelm-Sander-Stiftung awarded to SH and PR (2011.083.1). DK was supported by the DFG International Graduate School 1302 (TP T9 SH), LK by the ICEPHA program of the University of Tübingen and the Robert-Bosch-Gesellschaft für Medizinische Forschung, Stuttgart, and LE by the Landesgraduiertenförderungsgesetz, Baden-Württemberg.
Authors' contributions. D.K., S.M.H., P.R. and M.B. designed the study, analyzed the data, did the statistics and wrote the manuscript. D.K. performed patch-clamp recordings, colony formation assay and flow cytometry, and did part of the Ca^{2+}-imaging, transfilter migration and wound healing experiments. L.K. and M.E. queried The-Cancer-Genome-Atlas, did TRPM8 and MSI1 knockdown and real-time RT-PCR and part of the Ca^{2+} imaging, S.C.F. and L.E. performed part of the wound healing and transfilter migration experiments.
Acknowledgments. We thank Heidrun Faltin and Ilka Müller for excellent technical assistance. We acknowledge support by Deutsche Forschungsgemeinschaft and Open Access Publishing Fund of Tübingen University.

References

[1] Tsavaler L, Shapero MH, Morkowski S, Laus R. Trp-p8, a novel prostate-specific gene, is up-regulated in prostate cancer and other malignancies and shares high homology with transient receptor potential calcium channel proteins. Cancer Res. 2001;61:3760-9.

[2] Alptekin M, Eroglu S, Tutar E, Sencan S, Geyik MA, Ulasli M, et al. Gene expressions of TRP channels in glioblastoma multiforme and relation with survival. Tumour Biol. 2015.

[3] Liu J, Chen Y, Shuai S, Ding D, Li R, Luo R. TRPM8 promotes aggressiveness of breast cancer cells by regulating EMT via activating AKT/GSK-3beta pathway. Tumour Biol. 2014;35:8969-77.

[4] Yee NS, Li Q, Kazi AA, Yang Z, Berg A, Yee RK. Aberrantly Over-Expressed TRPM8 Channels in Pancreatic Adenocarcinoma: Correlation with Tumor Size/Stage and Requirement for Cancer Cells Invasion. Cells. 2014;3:500-16.

[5] Yu S, Xu Z, Zou C, Wu D, Wang Y, Yao X, et al. Ion channel TRPM8 promotes hypoxic growth of prostate cancer cells via an O2 -independent and RACK1-mediated mechanism of HIF-1alpha stabilization. J Pathol. 2014;234:514-25.

[6] Wang Y, Yang Z, Meng Z, Cao H, Zhu G, Liu T, et al. Knockdown of TRPM8 suppresses cancer malignancy and enhances epirubicin-induced apoptosis in human osteosarcoma cells. Int J Biol Sci. 2013;10:90-102.

[7] Xiao N, Jiang LM, Ge B, Zhang TY, Zhao XK, Zhou X. Over-expression of TRPM8 is associated with poor prognosis in urothelial carcinoma of bladder. Tumour Biol. 2014;35:11499-504.

[8] Borrelli F, Pagano E, Romano B, Panzera S, Maiello F, Coppola D, et al. Colon carcinogenesis is inhibited by the TRPM8 antagonist cannabigerol, a Cannabis-derived non-psychotropic cannabinoid. Carcinogenesis. 2014;35:2787-97.

[9] Wondergem R, Ecay TW, Mahieu F, Owsianik G, Nilius B. HGF/SF and menthol increase human glioblastoma cell calcium and migration. Biochem Biophys Res Comm. 2008;372:210-5.

[10] Wondergem R, Bartley JW. Menthol increases human glioblastoma intracellular Ca^{2+}, BK channel activity and cell migration. J Biomed Sci. 2009;16:90.

[11] Yamamura H, Ugawa S, Ueda T, Morita A, Shimada S. TRPM8 activation suppresses cellular viability in human melanoma. Am J Physiol Cell Physiol. 2008;295:C296-301.

[12] Bidaux G, Flourakis M, Thebault S, Zholos A, Beck B, Gkika D, et al. Prostate cell differentiation status determines transient receptor potential melastatin member 8 channel subcellular localization and function. J Clin Invest. 2007;117:1647-57.

[13] Bidaux G, Roudbaraki M, Merle C, Crepin A, Delcourt P, Slomianny C, et al. Evidence for specific TRPM8 expression in human prostate secretory epithelial cells: functional androgen receptor requirement. Endocr Relat Cancer. 2005;12:367-82.

[14] Yudin Y, Rohacs T. Regulation of TRPM8 channel activity. Mol Cell Endocrinol. 2012;353:68-74.

[15] Asuthkar S, Demirkhanyan L, Sun X, Elustondo PA, Krishnan V, Baskaran P, et al. The TRPM8 protein is a testosterone receptor: II. Functional evidence for an ionotropic effect of testosterone on TRPM8. J Biol Chem. 2015;290:2670-88.

[16] Asuthkar S, Elustondo PA, Demirkhanyan L, Sun X, Baskaran P, Velpula KK, et al. The TRPM8 protein is a testosterone receptor: I. Biochemical evidence for direct TRPM8-testosterone interactions. J Biol Chem. 2015;290:2659-69.

[17] Quallo T, Vastani N, Horridge E, Gentry C, Parra A, Moss S, et al. TRPM8 is a neuronal osmosensor that regulates eye blinking in mice. Nat Commun. 2015;6:7150.

[18] Asuthkar S, Velpula KK, Elustondo PA, Demirkhanyan L, Zakharian E. TRPM8 channel as a novel molecular target in androgen-regulated prostate cancer cells. Oncotarget. 2015;6:17221-36.

[19] Chodon D, Guilbert A, Dhennin-Duthille I, Gautier M, Telliez MS, Sevestre H, et al. Estrogen regulation of TRPM8 expression in breast cancer cells. BMC Cancer. 2010;10:212.
[20] Huber SM. Oncochannels. Cell calcium. 2013;53:241-55.
[21] Huber SM, Butz L, Stegen B, Klumpp L, Klumpp D, Eckert F. Role of ion channels in ionizing radiation-induced cell death. Biochim Biophys Acta. 2015;1848:2657-64.
[22] Steinle M, Palme D, Misovic M, Rudner J, Dittmann K, Lukowski R, et al. Ionizing radiation induces migration of glioblastoma cells by activating BK K^+ channels. Radiother Oncol. 2011;101:122-6.
[23] Stegen B, Butz L, Klumpp L, Zips D, Dittmann K, Ruth P, et al. Ca^{2+}-activated IK K^+ channel blockade radiosensitizes glioblastoma cells. Mol Cancer Res. 2015;13:1283-95.
[24] Edalat L, Stegen B, Klumpp L, Haehl E, Schilbach K, Lukowski R, et al. BK K+ channel blockade inhibits radiation-induced migration/brain infiltration of glioblastoma cells. Oncotarget. 2016;(in press).
[25] Cerami E, Gao J, Dogrusoz U, Gross BE, Sumer SO, Aksoy BA, et al. The cBio cancer genomics portal: an open platform for exploring multidimensional cancer genomics data. Cancer Discov. 2012;2:401-4.
[26] Gao J, Aksoy BA, Dogrusoz U, Dresdner G, Gross B, Sumer SO, et al. Integrative analysis of complex cancer genomics and clinical profiles using the cBioPortal. Sci Signal. 2013;6:pl1.
[27] Chatterjee S, Behnam Azad B, Nimmagadda S. The intricate role of CXCR4 in cancer. Advances in cancer research. 2014;124:31-82.
[28] Trautmann F, Cojoc M, Kurth I, Melin N, Bouchez LC, Dubrovska A, et al. CXCR4 as biomarker for radioresistant cancer stem cells. Int J Radiat Biol. 2014;90:687-99.
[29] Stupp R, Hegi ME, Mason WP, van den Bent MJ, Taphoorn MJ, Janzer RC, et al. Effects of radiotherapy with concomitant and adjuvant temozolomide versus radiotherapy alone on survival in glioblastoma in a randomised phase III study: 5-year analysis of the EORTC-NCIC trial. Lancet Oncol. 2009;10:459-66.
[30] Heise N, Palme D, Misovic M, Koka S, Rudner J, Lang F, et al. Non-selective cation channel-mediated Ca^{2+}-entry and activation of Ca^{2+}/calmodulin-dependent kinase II contribute to G_2/M cell cycle arrest and survival of irradiated leukemia cells. Cell Physiol Biochem. 2010;26:597-608.
[31] Klumpp D, Misovic M, Szteyn K, Shumilina E, Rudner J, Huber SM. Targeting TRPM2 channels impairs radiation-induced cell cycle arrest and fosters cell death of T cell leukemia cells in a Bcl-2-dependent manner. Oxid Med Cell Longev. 2016;(in press).
[32] Palme D, Misovic M, Schmid E, Klumpp D, Salih HR, Rudner J, et al. Kv3.4 potassium channel-mediated electrosignaling controls cell cycle and survival of irradiated leukemia cells. Pflugers Arch. 2013;465:1209-21.
[33] Cuddapah VA, Sontheimer H. Molecular interaction and functional regulation of ClC-3 by Ca^{2+}/calmodulin-dependent protein kinase II (CaMKII) in human malignant glioma. J Biol Chem. 2010;285:11188-96.
[34] Cuddapah VA, Turner KL, Seifert S, Sontheimer H. Bradykinin-induced chemotaxis of human gliomas requires the activation of KCa3.1 and ClC-3. J Neurosci. 2013;33:1427-40.
[35] Cuddapah VA, Habela CW, Watkins S, Moore LS, Barclay TT, Sontheimer H. Kinase activation of ClC-3 accelerates cytoplasmic condensation during mitotic cell rounding. Am J Physiol Cell Physiol. 2012;302:C527-38.
[36] Bavencoffe A, Gkika D, Kondratskyi A, Beck B, Borowiec AS, Bidaux G, et al. The transient receptor potential channel TRPM8 is inhibited via the alpha 2A adrenoreceptor signaling pathway. J Biol Chem. 2010;285:9410-9.

[37] Mandadi S, Armati PJ, Roufogalis BD. Protein kinase C modulation of thermo-sensitive transient receptor potential channels: Implications for pain signaling. J Nat Sci Biol Med. 2011;2:13-25.
[38] Morgan K, Sadofsky LR, Crow C, Morice AH. Human TRPM8 and TRPA1 pain channels, including a gene variant with increased sensitivity to agonists (TRPA1 R797T), exhibit differential regulation by SRC-tyrosine kinase inhibitor. Biosci Rep. 2014;34.
[39] Tang M, Wu GY, Dong XZ, Tang ZX. Phosphoinositide interacting regulator of TRP (Pirt) enhances TRPM8 channel activity in vitro via increasing channel conductance. Acta Pharmacol Sin. 2015.
[40] Gkika D, Lemonnier L, Shapovalov G, Gordienko D, Poux C, Bernardini M, et al. TRP channel-associated factors are a novel protein family that regulates TRPM8 trafficking and activity. J Cell Biol. 2015;208:89-107.
[41] Yu X, Jiang Y, Wei W, Cong P, Ding Y, Xiang L, et al. Androgen receptor signaling regulates growth of glioblastoma multiforme in men. Tumour Biol. 2015;36:967-72.
[42] Wick W, Hartmann C, Engel C, Stoffels M, Felsberg J, Stockhammer F, et al. NOA-04 randomized phase III trial of sequential radiochemotherapy of anaplastic glioma with procarbazine, lomustine, and vincristine or temozolomide. J Clin Oncol. 2009;27:5874-80.
[43] Catacuzzeno L, Fioretti B, Franciolini F. Expression and Role of the Intermediate-Conductance Calcium-Activated Potassium Channel KCa3.1 in Glioblastoma. J Signal Transduct. 2012;2012:421564.
[44] D'Alessandro G, Catalano M, Sciaccaluga M, Chece G, Cipriani R, Rosito M, et al. KCa3.1 channels are involved in the infiltrative behavior of glioblastoma in vivo. Cell Death Dis. 2013;4:e773.
[45] Ohmi M, Shishido Y, Inoue T, Ando K, Fujiuchi A, Yamada A, et al. Identification of a novel 2-pyridyl-benzensulfonamide derivative, RQ-00203078, as a selective and orally active TRPM8 antagonist. Bioorg Med Chem Lett. 2014;24:5364-8.
[46] Lehto SG, Weyer AD, Zhang M, Youngblood BD, Wang J, Wang W, et al. AMG2850, a potent and selective TRPM8 antagonist, is not effective in rat models of inflammatory mechanical hypersensitivity and neuropathic tactile allodynia. Naunyn Schmiedebergs Arch Pharmacol. 2015;388:465-76.
[47] Miller S, Rao S, Wang W, Liu H, Wang J, Gavva NR. Antibodies to the extracellular pore loop of TRPM8 act as antagonists of channel activation. PLoS One. 2014;9:e107151.

Figures and Figure Legends

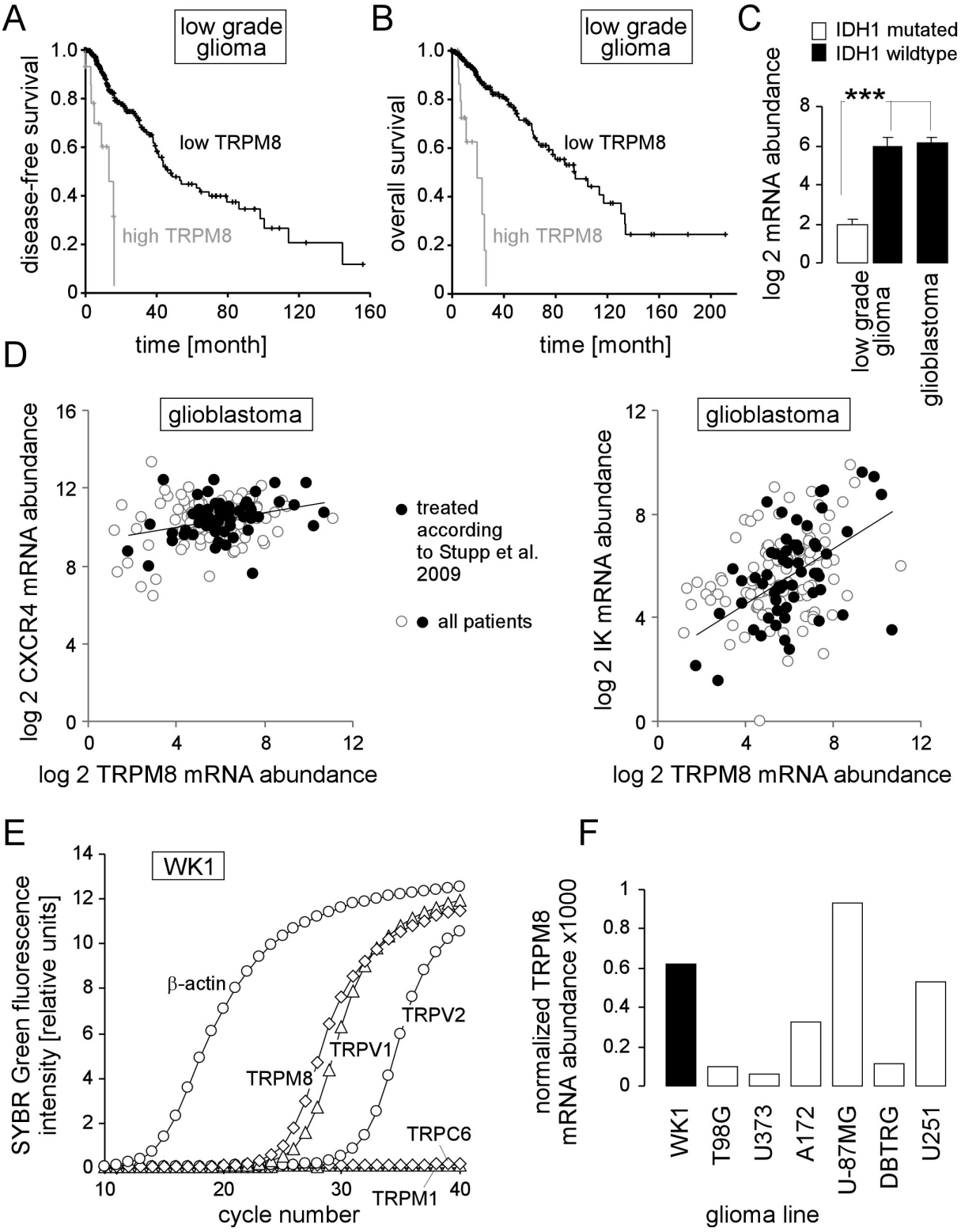

Fig. 1. TRPM8 as prognostic marker in glioma. **A.** Disease-free and **B.** overall survival of patients with low grade glioma with high (n = 15-17, grey) and low (n = 335-352, black) expression of TRPM8 mRNA in the tumor (data from TCGA). **C.** Mean (± SE) TRPM8 mRNA abundance in human IDH1-mutated low grade glioma (n = 30, left), IDH1 wildtype low grade glioma (n = 19, middle) and IDH1 wildtype glioblastoma (n = 48, right) specimens.

$Log2^{x+1}$-transformed RNA sequencing data (Illumina HiSeq 2000 RNA Sequencing platform) were received from the The-Cancer-Genome-Atlas (TCGA). **D.** Association between TRPM8 and CXCR4 (left), and between TRPM8 and IK mRNA expression (right) by primary glioblastoma of patients treated according to [29] (n = 58, closed circles) and of other patients (n = 100, open circles, data from TCGA). **E.** PCR cycle-dependent increase in SYBR green fluorescent specific for β-actin, TRPM8, TRPV1, TRPV2, TRPC6 and TRPM1 in WK1 human glioblastoma cells. **F.** GAPDH housekeeper-normalized TRPM8 mRNA abundance in the human glioma lines WK1, T98G, U373, A172, U-87MG, DBTRG, and U251. *** indicates $p \leq 0.001$, ANOVA.

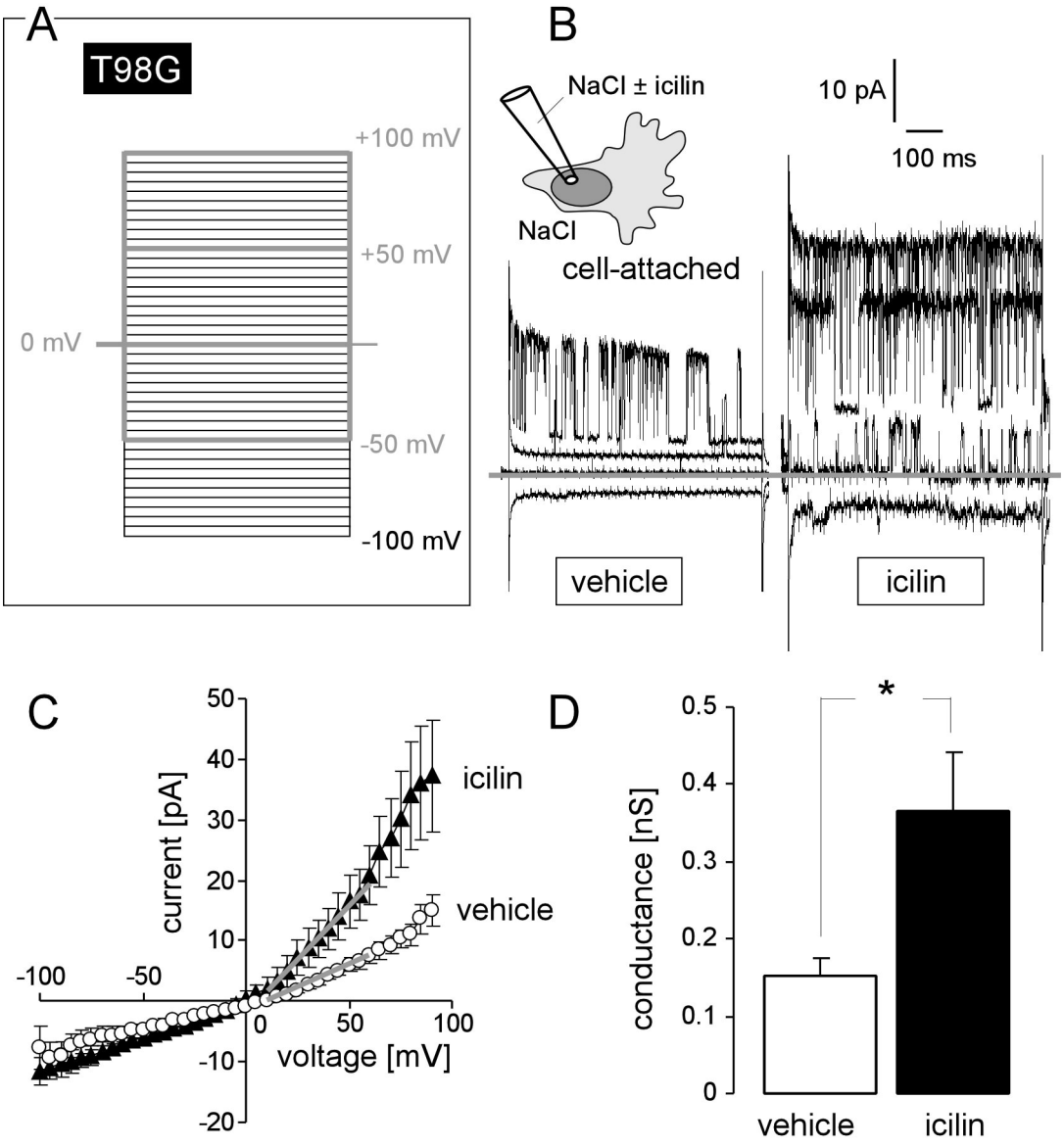

Fig. 2. TRPM8 agonist icilin stimulates outward currents in glioblastoma cells. **A, B.** Recording of macroscopic on-cell currents in human T98G glioblastoma cells. Depicted are the applied voltage-clamp pulse protocol (A) and (B) tracings recorded with NaCl bath and NaCl pipette solution further containing 0 µM (vehicle, left) or 10 µM (right) of the TRPM8 agonist icilin. In (B) only the currents evoked by voltage sweeps to -50, 0, +50 and +100 mV are shown. **C.** Dependence of the mean macroscopic on-cell currents (± SE, n = 8-10) on the voltage recorded as in (A, B) from 0 µM (open circles) or 10 µM icilin-stimulated T98G cells (closed triangles). **D.** Mean (± SE, n = 8-10) macroscopic on-cell conductance as determined for the outward currents in (C) of icilin (0, open bar, or 10 µM, closed bar)-stimulated T98G cells. Conductances were calculated between +10 and +60 mV voltage as shown by the grey lines in (C). * indicates $p \leq 0.05$, two-tailed Welch-corrected t-test.

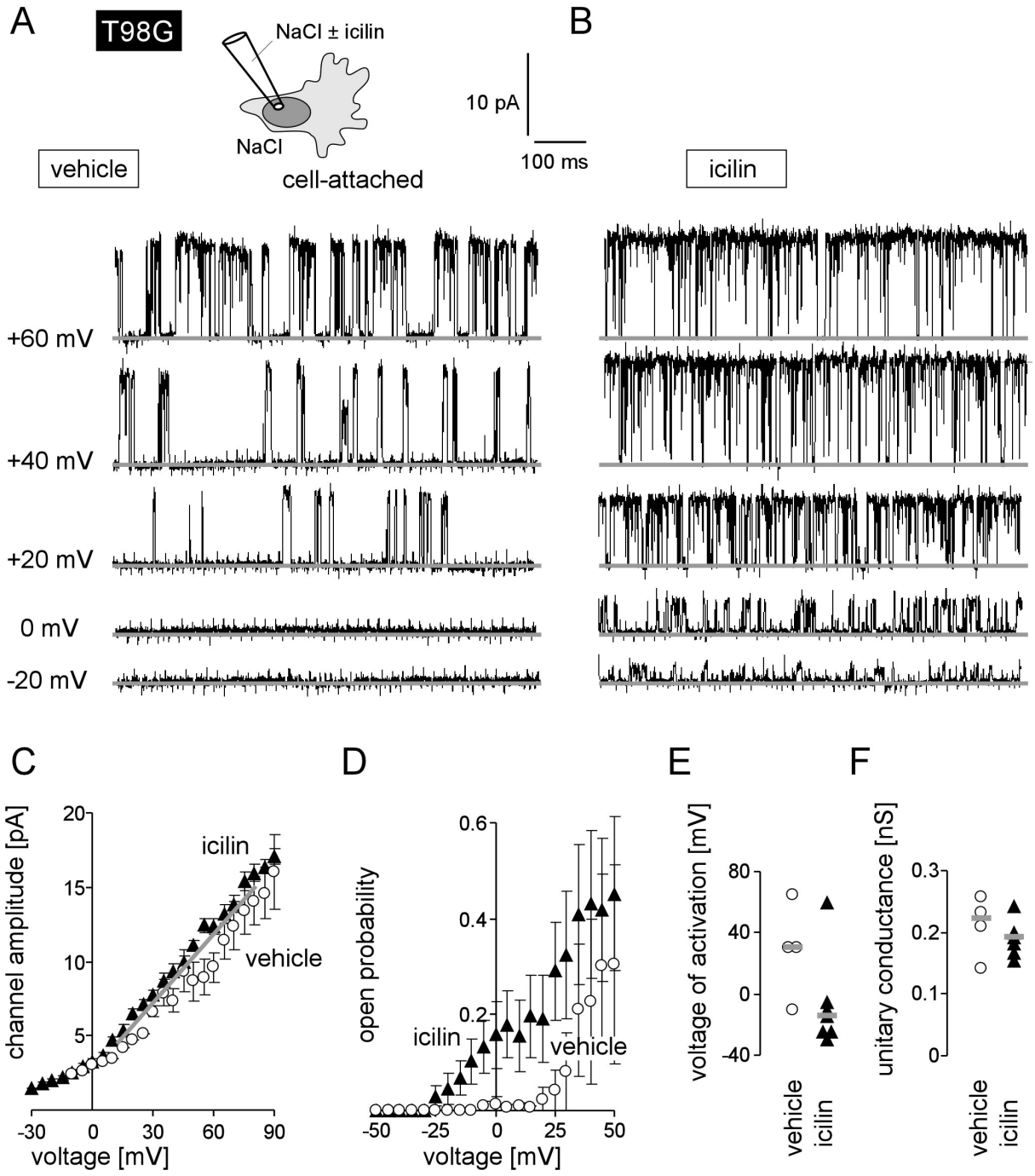

Fig. 3. Icilin induces activity of BK K^+ channels at physiological membrane potential. **A, B.** Single channel current transitions recorded from T98G glioblastoma cells in on-cell mode at different holding potentials (as indicated) with NaCl bath and NaCl pipette solution further containing 0 µM (vehicle, A) or 10 µM icilin (B). Note, that the voltage-dependent increase in open probability is shifted towards more negative potentials in the icilin-stimulated (B) as compared to the vehicle-treated cells (A). **C, D.** Dependence of the mean (± SE) unitary current transition (C, n = 7) and open probability (P_o, D, n = 4-7) on the voltage of the channels recorded as in (A, B) in the absence (open circles) or presence of icilin (closed triangle). **E, F**. Activation voltage (E) and unitary conductance (F) of channels in vehicle- (open circles, n = 4) and icilin-treated (closed triangle, n = 7) T98G cells (given are individual recordings and the median values as grey lines).

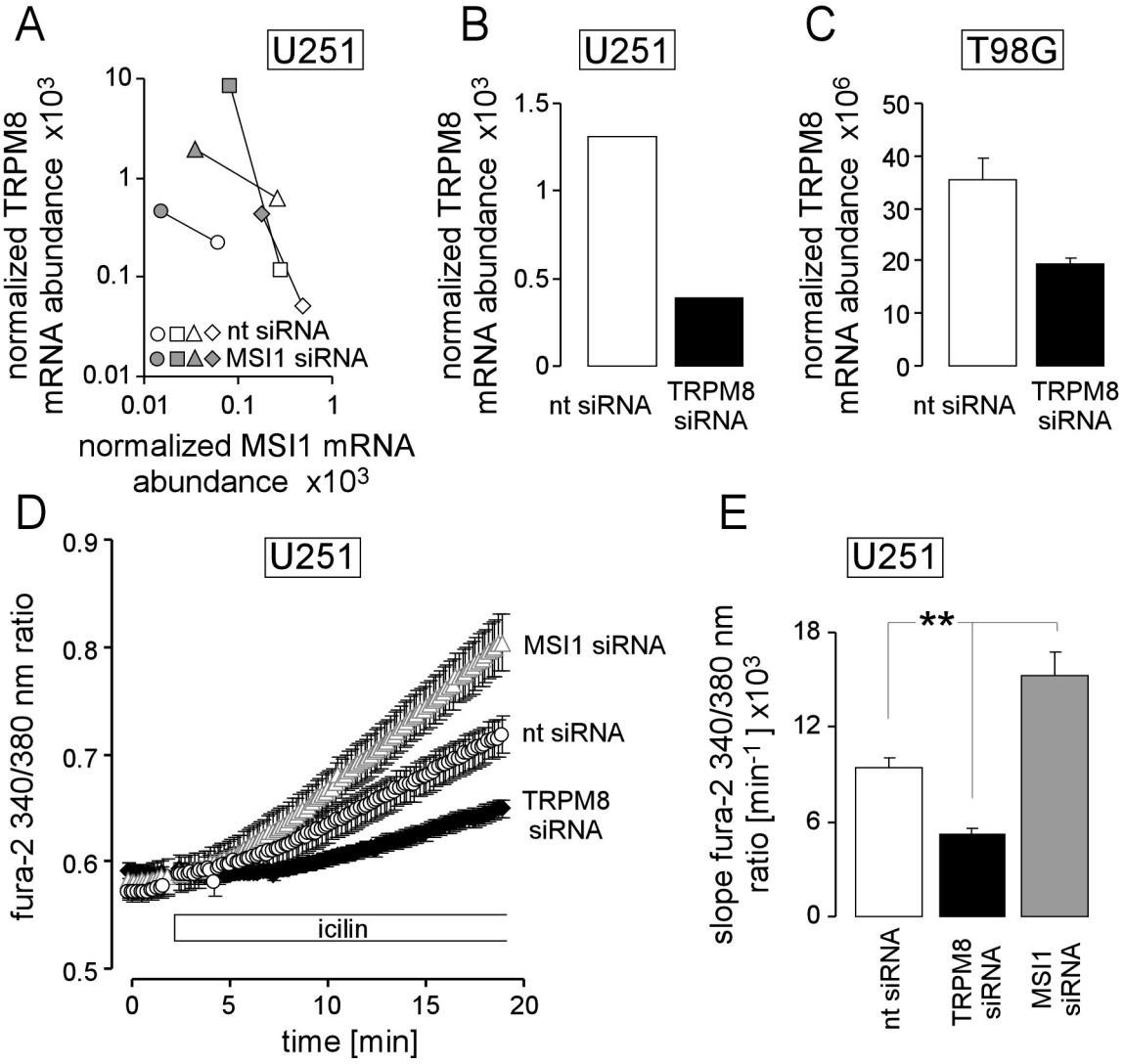

Fig. 4. Transfection with TRPM8- and MSI1-specific siRNA decreases and increases TRPM8 mRNA abundance and icilin-stimulated Ca^{2+}-entry in glioblastoma cells, respectively. **A.** Silencing of MSI1 mRNA in U251 glioblastoma cells was associated with an increase in TRPM8 mRNA abundances (four independent experiments are depicted). MSI1 knock-down, therefore, was harnessed to upregulate TRPM8. **B, C.** TRPM8 mRNA abundance in U251 (B) and T98G cells (C) transfected with nontargeting (nt siRNA, open bars) or TRPM8 siRNA (closed bars). Shown are means of n = 2 (B) or means (± SE) of n = 3 experiments. **D.** Mean (± SE, n = 16-19) fura-2 340/380 nm fluorescence ratio recorded in nontargeting- (nt siRNA open circles), TRPM8 siRNA- (closed triangles) or MSI1 siRNA-transfected (open triangles) U251 glioblastoma cells before and during superfusion with the TRPM8 agonist icilin (10 µM). **E.** Mean (± SE, n = 16-19) slope of the ratio increase following icilin wash-in as calculated for nt siRNA- (open bar), TRPM8 siRNA- (black bar) or MSI1 siRNA-transfected (grey bar) U251 cells (data from (D)). ** indicates $p \leq 0.01$, ANOVA. Knock-down and fura-2 Ca^{2+}-imaging experiments were performed as described in the main article.

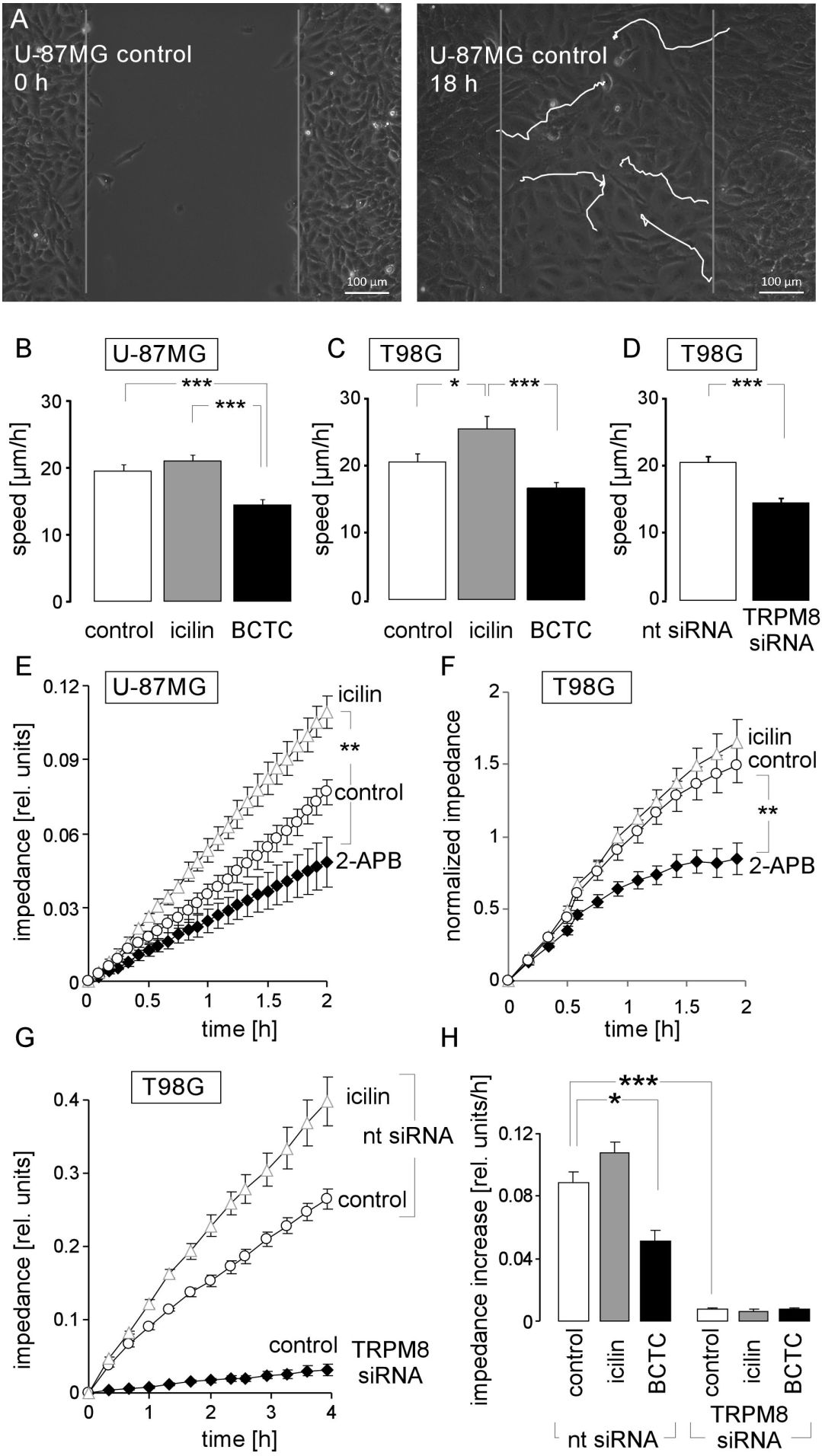
A
U-87MG control
0 h
100 µm
U-87MG control
18 h
100 µm
B
U-87MG
speed [µm/h]
control
icilin
BCTC
C
T98G
speed [µm/h]
control
icilin
BCTC
D
T98G
speed [µm/h]
nt siRNA
TRPM8 siRNA
E
U-87MG
impedance [rel. units]
time [h]
icilin
control
2-APB
F
T98G
normalized impedance
time [h]
icilin
control
2-APB
G
T98G
impedance [rel. units]
time [h]
icilin
nt siRNA
control
control
TRPM8 siRNA
H
impedance increase [rel. units/h]
control
icilin
BCTC
control
icilin
BCTC
TRPM8 siRNA
nt siRNA

Fig. 5. TRPM8 function is required for cell migration. **A.** Light Micrographs showing wound healing of the human glioblastoma cell line U-87MG at time 0 h (left) and 18 h (right) after scratching the monolayer. The white lines indicate the migration routes of 5 selected cells as recorded by time lapse microscopy. **B-D.** Mean (± SE) migration speed during wound healing of U-87MG (B, n = 15-15) and T98G glioblastoma cells (C, D, n = 15-45). Wound healing was performed either in the absence (open bars) or presence of the TRPM8 agonist icilin (10 μM, grey bars) or the TRP channel inhibitor BCTC (10 μM, black bars, B, C) as well as upon transfecting the cells with nt- (open bar) or TRPM8 siRNA (closed bar, D). **E-G.** Time dependence of the mean impedance (± SE,) as a real-time measure of transfilter migration in U-87MG (E, n = 4-15) and T98G cells (F, G, n = 4-7). Transfilter migration was performed either in the absence (open circles in E, F, G, closed diamonds in G) or presence of the TRPM8 agonist icilin (10 μM, open triangles in E, F, G) or the TRP channel inhibitor 2-APB (10 μM, closed diamonds in E, F) as well as upon transfecting the cells with nt- (open symbols in G) or TRPM8 siRNA (closed diamonds in G). **H.** Mean (± SE, n = 4-8) impedance increase in T98G cells as a measure of transfilter migration velocity. Transfilter migration velocity was calculated for nt- (left) or TRPM8 siRNA-transfected (right) cells in the absence (open bars) or presence of icilin (10 μM, grey bars) or BCTC (10 μM, black bars). *, **, and *** indicate $p \leq 0.05$, $p \leq 0.01$, and $p \leq 0.001$, ANOVA (B, C and E-H) or two-tailed t-test (D), respectively.

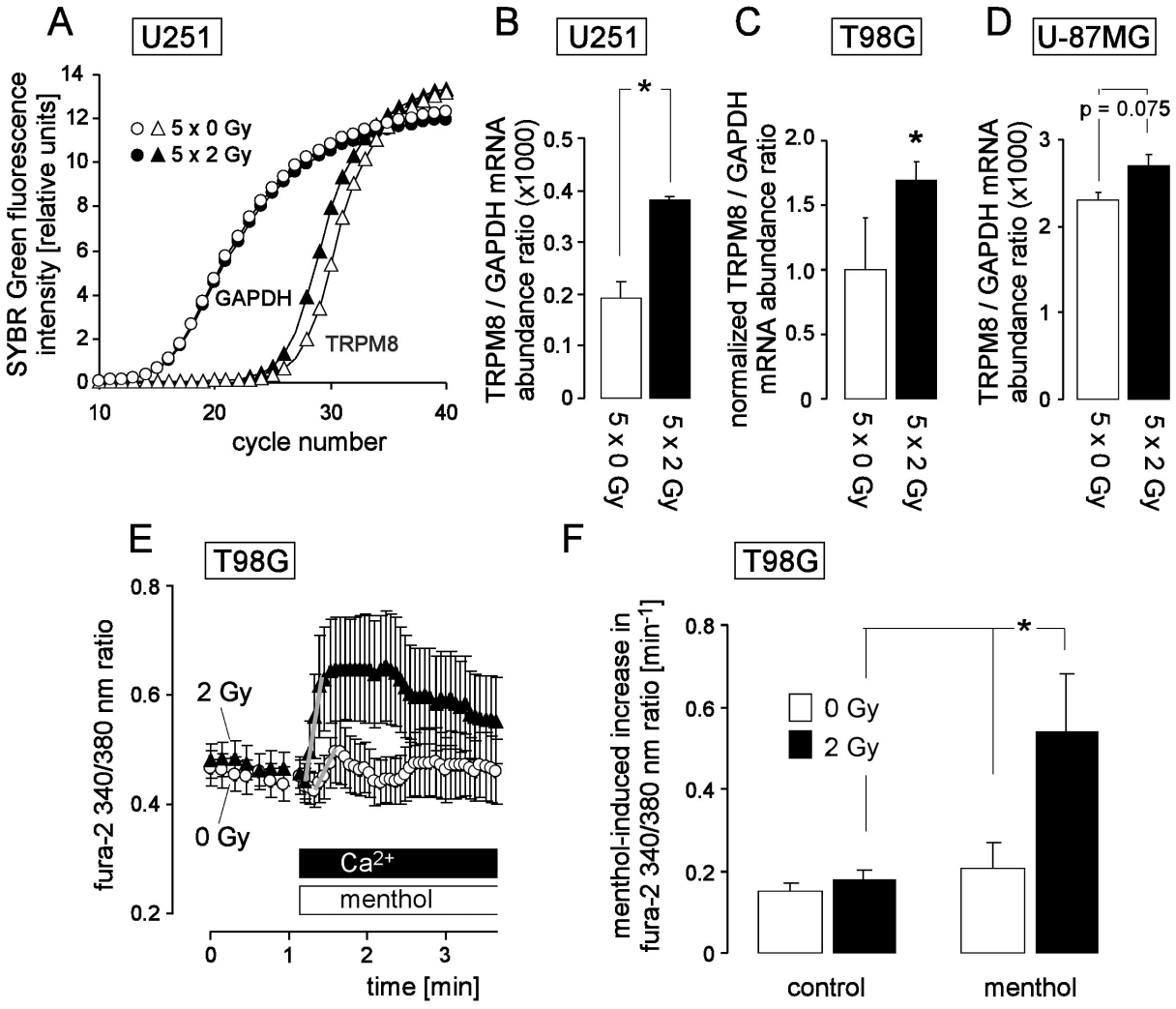

Fig. 6. Ionizing radiation stimulates TRPM8 mRNA abundance and TRPM8 agonist menthol-induced Ca^{2+} entry in glioblastoma cells. **A.** Dependence of the GAPDH- (circles) and TRPM8 (triangles) mRNA-specific SYBR green fluorescence on PCR cycle. mRNAs were extracted from cells irradiated with 5 fractions of 0 Gy (open symbols) or 2 Gy (closed symbols) **B-D.** Mean (± SE, n = 3) GAPDH housekeeper-normalized abundance of TRPM8-specific mRNA in U251 (B), T98G (C), and (D) U-87MG cells fractionated irradiated with 5 x 0 Gy (open bars) or 5 x 2 Gy (closed bar, mRNA was extracted 24 h after the last IR fraction; in (C) mRNA abundances were normalized to those of the respective control (5 x 0 Gy) cells). **E.** Mean (± SE, n = 24-32) fura-2 340/380 nm fluorescence ratio as measure of cytosolic free Ca^{2+} concentration ($_{free}[Ca^{2+}]_i$) recorded in 0 Gy- (open circles) or 2 Gy-irradiated (1.5-3 h after IR, closed triangles) T98G cells. Ratios were measured during superfusion with EGTA-buffered Ca^{2+}-free NaCl solution and upon wash-in of Ca^{2+}- and menthol (100 µM). **F.** Mean (± SE, n = 58-72) increase in $_{free}[Ca^{2+}]_i$ as determined by the slope (grey lines in D) of the rise in the 340/380 nm ratio following Ca^{2+} wash-in. Slopes were determined from 0 Gy- (open bars) or 2 Gy-irradiated T98G cells in the absence (control, left) or presence of menthol (right). * indicates $p \leq 0.05$, respectively, two-tailed (Welch-corrected) t-test in (B, D), one-sample two-tailed t-test (significant difference from 1.0) in (C), and ANOVA in (F).

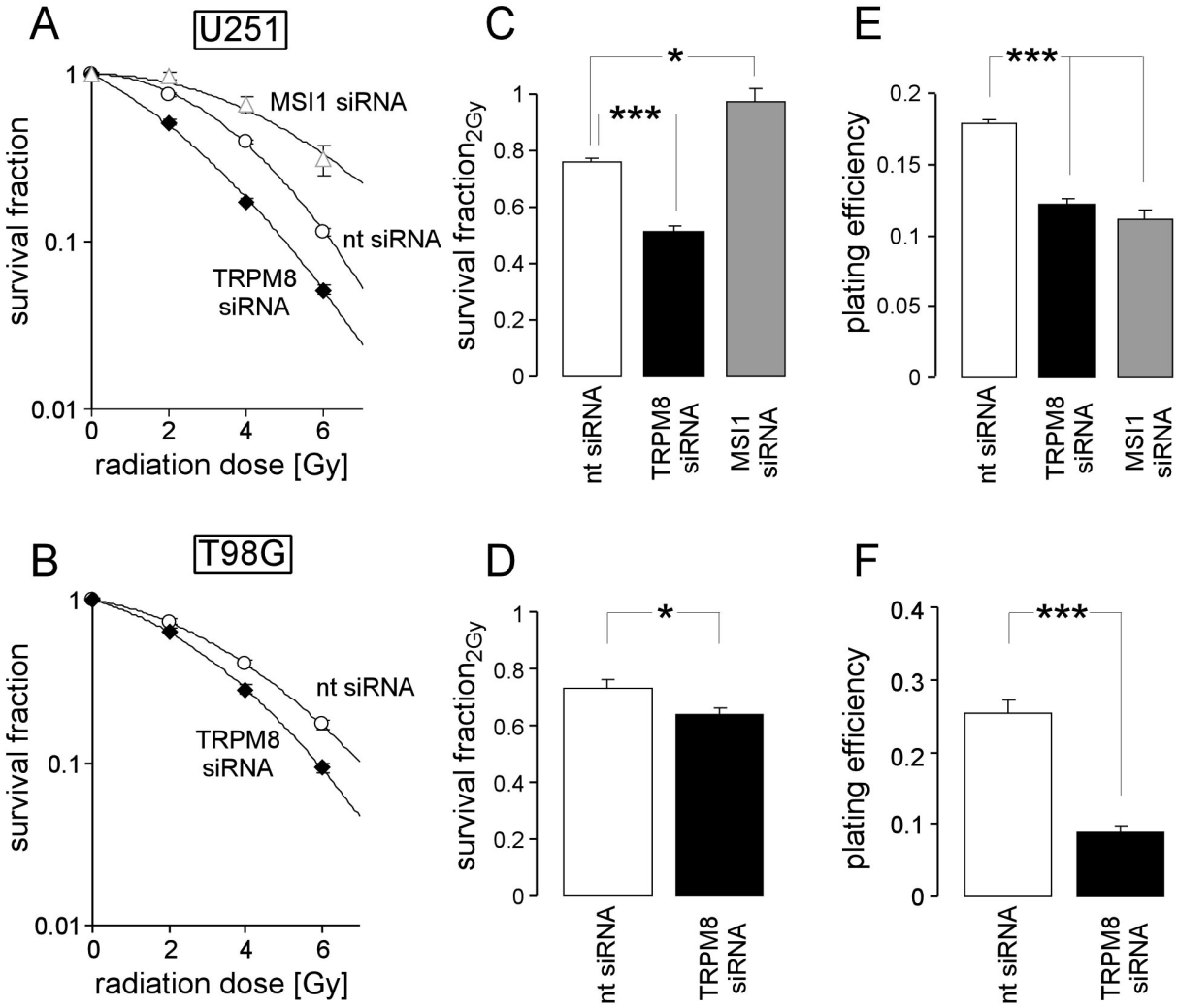

Fig. 7. MSI1- and TRPM8 RNA interference increase and decrease radioresistance, respectively, and diminish clonogenic survival in glioblastoma cells. **A, B.** Mean survival fractions (± SE, n = 24-36) of non targeting siRNA- (nt siRNA, open circles), TRPM8 siRNA- (closed triangles), or MSI1 siRNA-transfected (open triangles) U251 (A) and T98G (D) glioblastoma cells after irradiation with 0, 2, 4, or 6 Gy as determined by delayed plating colony formation assay. **C-F.** Mean (± SE, n = 24-36) survival fractions at 2 Gy (C, D) and mean plating efficiencies (± SE, n = 24-36 E, F) of nt- (open bars), TRPM8- (closed bar), or MSI1 (grey bar) siRNA-transfected U251 cells (C, E) and T98G cells (D, F). * and *** indicate $p \leq 0.05$ and $p \leq 0.001$, respectively, ANOVA (C, E) or two tailed (Welch-corrected) t-test (D, F).

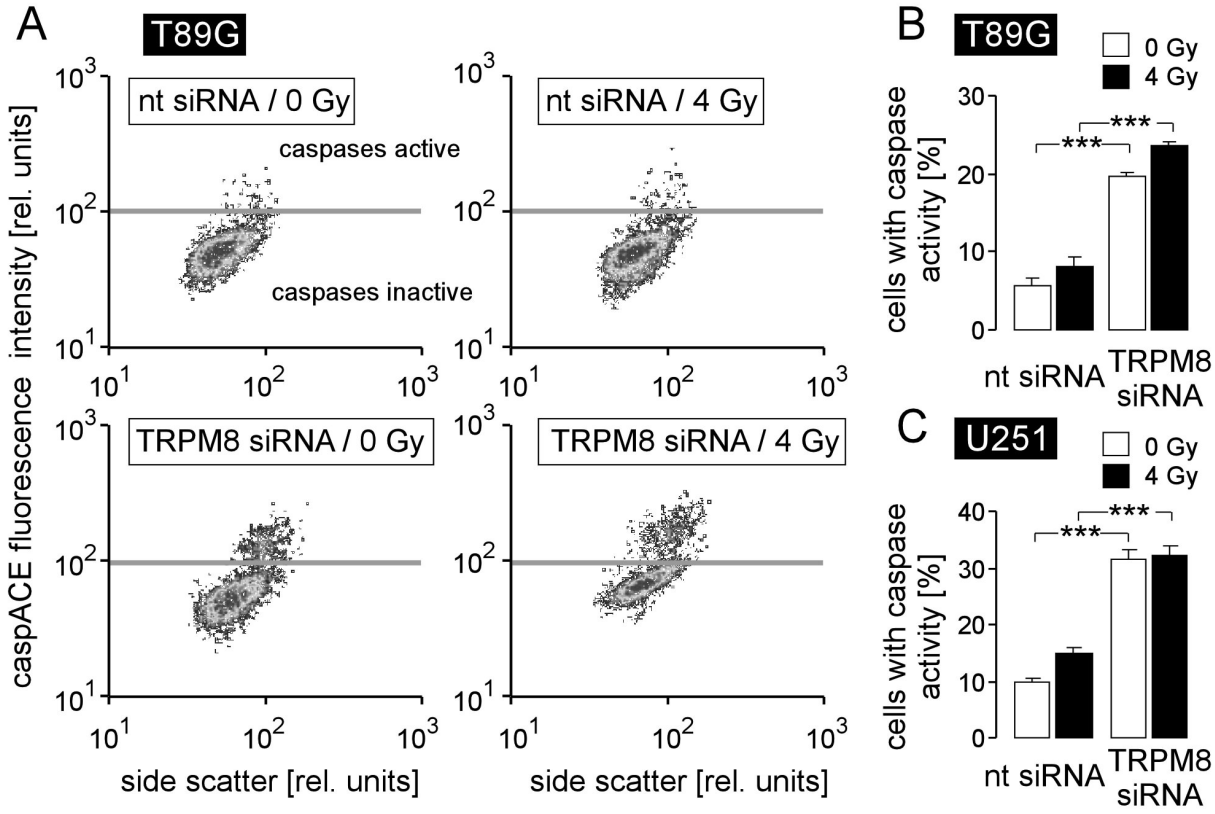

Fig. 8. TRPM8 RNA silencing induces caspase activation in glioblastoma cells. **A.** Dot blots recorded by flow cytometry showing the caspACE fluorescence intensity as a measure of caspase activity in nt- (top) or TRPM8 (bottom) siRNA-transfected T89G cells 24 h after irradiation with 0 Gy (left) or 4 Gy (right). **B, C.** Mean percentage (± SE, n = 17-18) of nt- (left) or TRPM8 (right) siRNA-transfected T98G (B) and U251 cells (B) cells 24 h after irradiation with 0 Gy (open bars) or 4 Gy (closed bars). *** indicates $p \leq 0.001$, ANOVA.

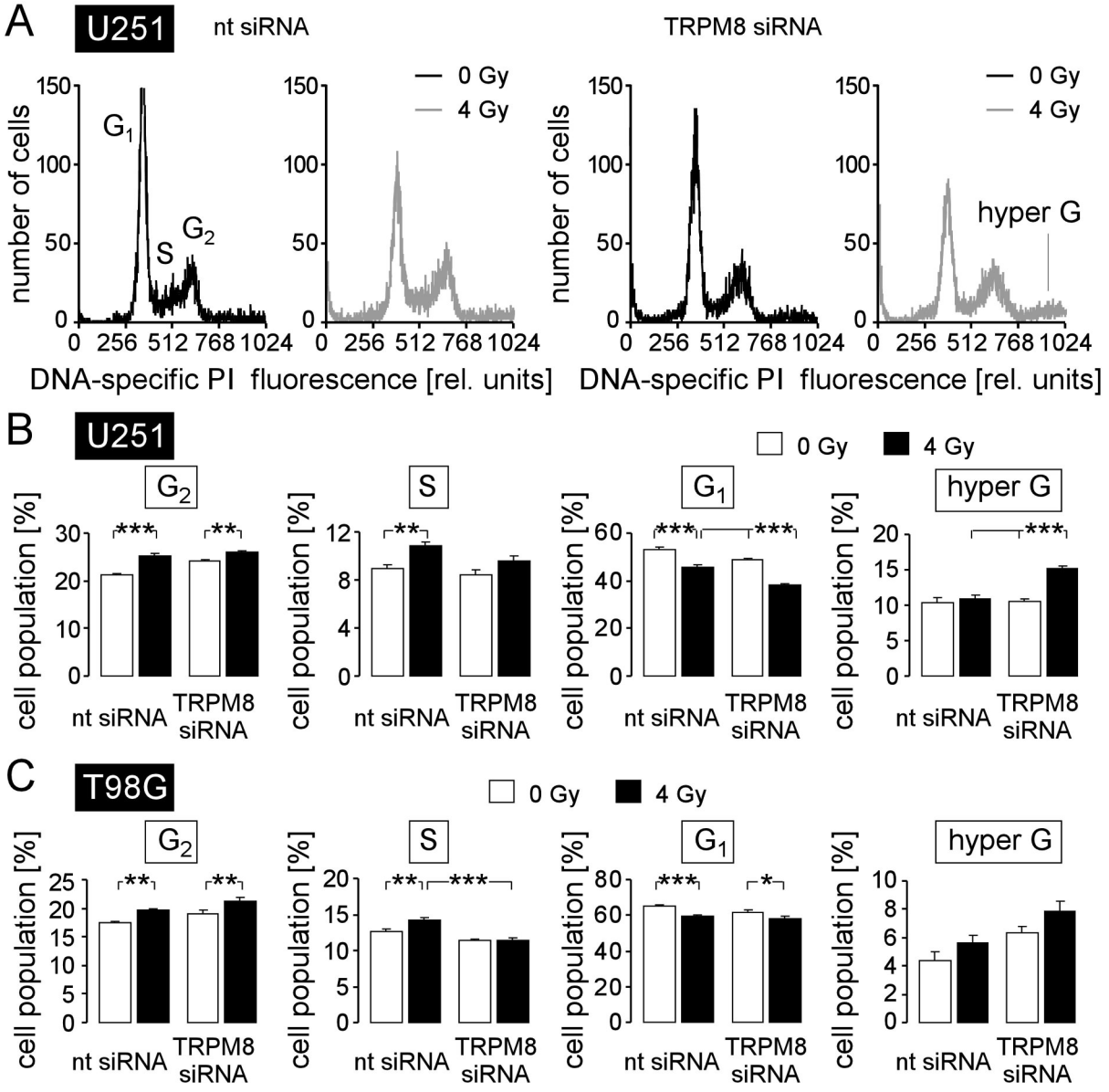

Fig. 9. TRPM8 RNA silencing impairs cell cycle control in irradiated glioblastoma cells. A. Histograms showing the cellular DNA content of nt- (left) or TRPM8 (right) siRNA-transfected U251 cells 48 h after irradiation with 0 Gy (black) or 4 Gy (grey) as determined by flow cytometry using propidium iodide as DNA-specific fluorescence dye. **B, C.** Mean percentage (± SE, n = 17-18) of nt- (left) or TRPM8 (right) siRNA-transfected and 0 Gy- (open bars) or 4 Gy-irradiated (closed bars) U251 (B) and T98G cells (C) belonging to the G_2, S, G_1, or hyper G population. *, **, and *** indicate $p \leq 0.05$, $p \leq 0.01$, and $p \leq 0.001$, respectively, ANOVA.

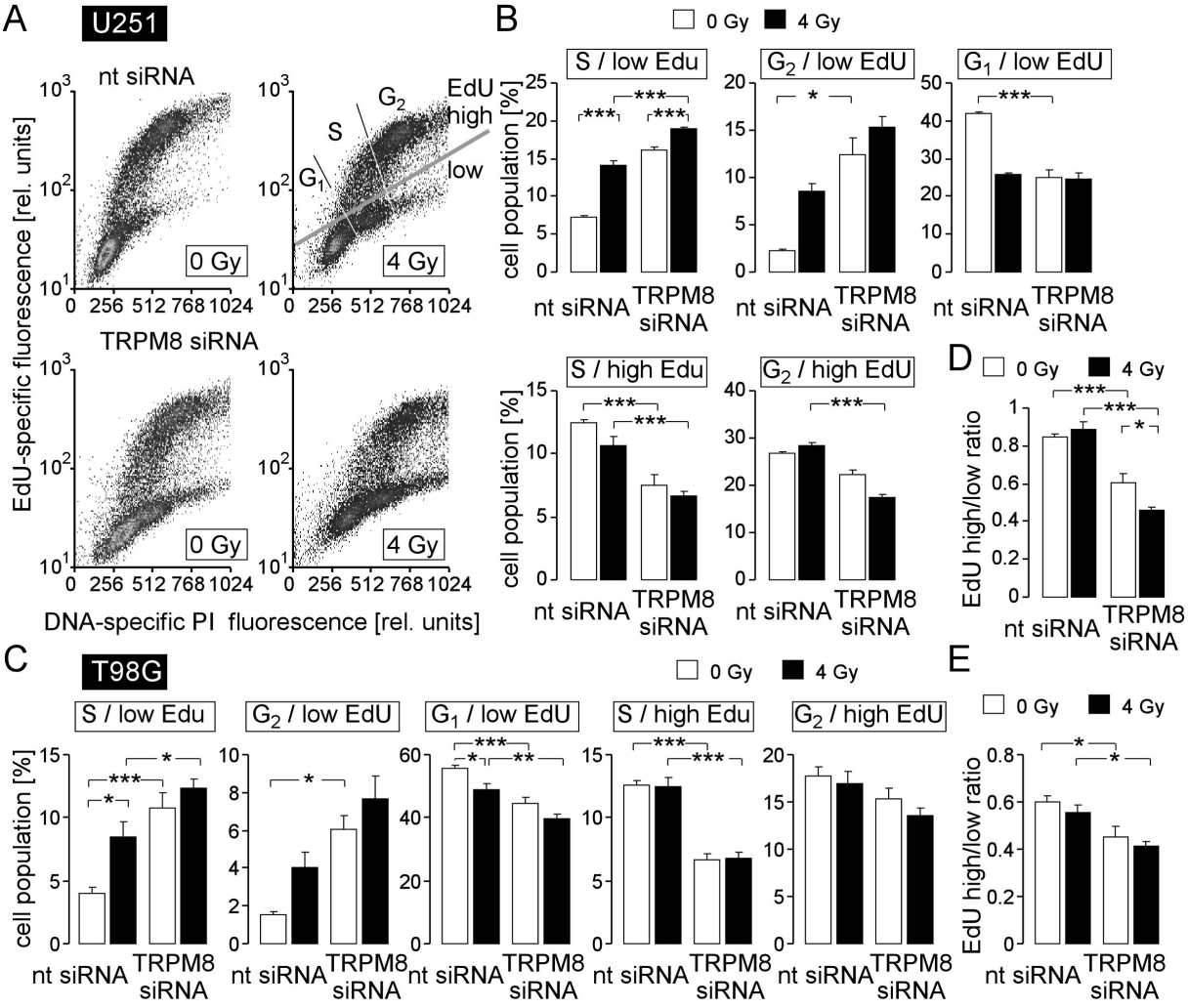

Fig. 10. TRPM8 RNA silencing impairs DNA replication and mitosis in control and irradiated glioblastoma cells. **A**. Dot blots showing 5-ethynyl-2'-deoxyuridine (EdU) incorporation by nt- (left) or TRPM8 siRNA-transfected (right) and irradiated (0 or 4 Gy as indicated) U251 cells. Forty-eight h after irradiation cells were incubated for 6 h with EdU (5 μM) before co-staining with propidium iodide and analysis by flow cytometry**.** Gray gates show the different cell populations. **B, C**. Mean percentage (± SE, n = 6) of nt- (left) or TRPM8 siRNA-transfected (right) and 0 Gy- (open bars) or 4 Gy-irradiated (closed bars) EdU-negative (1st-3rd diagram) and EdU-positive (4th-5th diagram) U251 (B) and T98G (C) cells residing in S, G_1, or G_2 phase of cell cycle. **D, E.** Ratios between EdU-positive and EdU-negative cells in U251 (D) and T98G (E) cells in dependence on TRPM8 knock-down and irradiation. *, **, and *** indicate $p \leq 0.05$, $p \leq 0.01$, and $p \leq 0.001$, respectively, ANOVA.